University of Granada

Department of Civil Engineering

Environmental Technology Area

Title:

Treatment of variable-salinity urban wastewater using submerged membrane bioreactors with and without moving bed

Alejandro Rodriguez Sanchez

Universidad de Granada

Departmento de Ingeniería Civil

Área de Tecnologías del Medio Ambiente

Título:

Tratamiento de agua residual urbana con salinidad variable en biorreactores de membrana sumergida con y sin lecho en suspensión

Alejandro Rodriguez Sanchez

Editor: Universidad de Granada. Tesis Doctorales
Autor: Alejandro Rodríguez Sánchez
ISBN: 978-84-1306-156-6
URI: http://hdl.handle.net/10481/55483

I would like to acknowledge the help of God Father Almighty, Creator of all that exists, and the support of the Lord Jesus Christ who, fitting to the topic of this Ph.D., is the Spring of Life-Giving Water.

I would like to acknowledge the unbreaking support of my lovely wife, Angelica, who is the perfect companion and the ideal help through my life.

I would also like to acknowledge the unfailing support of my dedicated parents, Jose and Maria Jose, who always believed in me and pushed me onward in times of difficulty.

I would also like to acknowledge my brilliant twin, Julio, who is the best brother and friend that I could ever imagine.

Also, I would like to acknowledge the support given by my caring aunt Manoli, my charming uncle Bartolome and his cheerful family, Rosalia, Diego and Mario.

This Ph.D. would have never been possible without the excellent guidance of my two directors, Prof. Dr. Jesus Gonzalez Lopez and Prof. Dr. Jose Manuel Poyatos Capilla, whose wisdom in the fields of environmental microbiology and bioreactor engineering has helped me so much.

I would like to acknowledge the fundamental support given by Prof. Dr. Jesus Gonzalez Lopez, for his trust in me and his undying passion for research has given me opportunity and guidance into the important first steps of the scientific career.

I would also like to acknowledge the crucial support given by Prof. Dr. Jose Manuel Poyatos Capilla, for his endless dedication to this Ph.D. thesis has given me example and guidance to become an honest and keen professional.

Also, I would like to mention the valuable tutoring provided by Juan Carlos, who greatly contributed to this Ph.D. thesis.

It is of importance to acknowledge the support given to me by Alejandro, Barbara and Miguel, who besides partners I consider friends. The support in training my skills given by Alejandro and the time Barbara and Miguel helped me with my tasks at the laboratory have been very important for the consecution of this Ph.D.

Also, I would like to mention the help given by Julia, Lorenz, Ines, Leone and Philip.

Also, there are many friends in Paterna del Campo and Granada who have been supporting me all this time, to which I acknowledge.

It is necessary to acknowledge the Department of Civil Engineering and the Institute of Water Research of the University of Granada for their support during this Ph.D.

[1] The Pharisees heard that Jesus was winning and baptizing more disciples than John. ([2] Actually, Jesus himself did not baptize anyone; only his disciples did.) [3] So when Jesus heard what was being said, he left Judea and went back to Galilee; [4] on his way there he had to go through Samaria.

[5] In Samaria he came to a town named Sychar, which was not far from the field that Jacob had given to his son Joseph. [6] Jacob's well was there, and Jesus, tired out by the trip, sat down by the well. It was about noon.

[7] A Samaritan woman came to draw some water, and Jesus said to her, “Give me a drink of water.” ([8] His disciples had gone into town to buy food.)

[9] The woman answered, “You are a Jew, and I am a Samaritan—so how can you ask me for a drink?” (Jews will not use the same cups and bowls that Samaritans use.)

[10] Jesus answered, “If you only knew what God gives and who it is that is asking you for a drink, you would ask him, and he would give you life-giving water.”

[11] “Sir,” the woman said, “you don't have a bucket, and the well is deep. Where would you get that life-giving water? [12] It was our ancestor Jacob who gave us this well; he and his children and his flocks all drank from it. You don't claim to be greater than Jacob, do you?”

[13] Jesus answered, “Those who drink this water will get thirsty again, [14] but those who drink the water that I will give them will never be thirsty again. The water that I will give them will become in them a spring which will provide them with life-giving water and give them eternal life.”

Gospel of John, 4, 1:13 (GNT)

Index

Summary

This Ph.D. thesis is based on the operation of a membrane bioreactor and hybrid moving bed biofilm reactor-membrane bioreactor for the treatment of constant- and variable-salinity urban wastewater, which results have been published in several papers. The bioreactors were operated under 6, 9.5 and 12 h of hydraulic retention time, and 2500 and 3500 mg L^{-1} total solids. The bioreactors were operated under constant salinity conditions of 6.5 mS cm^{-1} electric conductivity and under salinity cycles consisting on: 6 hours of salinity-amended urban wastewater - 4.5, 6.5 and 8.5 mS cm^{-1} electric conductivity -, followed by 6 hours of regular-salinity urban wastewater - around 1 mS cm^{-1}. The analyses conducted to investigate the bioreactors could be classified in four different categories: physicochemical performance, microbial kinetics, microbial ecology, and biofouling communities and biomineralization studies.

The start-up of the bioreactors under saline influents was successful but resulted in the lack of substantial biofilm attached to carriers (<50 mg L^{-1}) in the hybrid moving bed biofilm reactor-membrane bioreactor systems under both constant- and variable salinity-conditions. This fact showed that hybrid moving bed biofilm reactor-membrane bioreactor systems started-up treating saline wastewater under the conditions tested did not show any improvements over the membrane bioreactor system.

In relation to this finding, the performances in terms of organic matter and nitrogen removal were similar for the membrane bioreactor and hybrid moving bed biofilm reactor-membrane bioreactors, as occurred with the heterotrophic and autotrophic kinetics and microbial community structures. High influent maximum salinity drastically decreased the total nitrogen removal while the organic matter removal was overall similar for all salinity conditions. In this way, mean removal of BOD5 and COD was of 97-99% and 71-99%, respectively, for variable salinity at 4.5 and 6.5 mS cm^{-1}. However, slightly lower mean removal performances were found for 8.5 mS cm-1 (83-98% and 74-99). Removal of nitrogen was sensitive for maximum influent salinity, showing values of 27-85%, 15-50% and 24-38% for 4.5, 6.5 and 8.5 mS cm^{-1}. Decrease in

nitrogen removal with increasing maximum salinity was found to be related to deficiency in ammonium oxidation caused by salinity increase.

Autotrophic and heterotrophic kinetics slowed with increasing hydraulic retention time and solids concentration. This was shown by the trends of the rate of substrate utilization for autotrophic and heterotrophic substrates. Even though the rate of substrate utilization for the heterotrophic biomass showed similar values for the three technological configurations used, the membrane bioreactor had faster kinetics under 2500 mg L^{-1} total solids and the hybrid moving bed biofilm reactor-membrane bioreactor without carriers in the anoxic zone had faster kinetics at 3500 mg L^{-1} total solids. However, the values of the rates of substrate utilization were higher for the 6.5 mS cm^{-1} scenario than for the 4.5 and 8.5 mS cm^{-1} scenario. For the autotrophic biomass, the membrane bioreactor had the slowest kinetics and both hybrid moving bed biofilm reactor-membrena bioreactor systems were very similar.

The microbial communities in the bioreactors studied showed to be influenced primarily by the maximum influent salinity and loading (constant vs variable), then by the total solids, hydraulic retention time and in the last place by technological configuration. The microbial communities found were unique for each set of operational conditions tested, but *Rhodanobacter*, *Nitrobacter*, *Ottowia*, *Mizugakiibacter* and *Gemmatimonadaceae* members were represented in all salinity scenarios and operational conditions in all bioreactors. In this sense, these phylotypes may develop important ecological roles for the treatment of saline wastewater in membrane-based technologies.

Finally, the different maximum influent salinities severely selected for biofouling communities and for strains with capacity to mediate the precipitation of calcium and magnesium crystals. *Bacillus* genus was the only phylotype with biomineralization capacity found in at all conditions.

Esta tesis doctoral se centra en el estudio del funcionamiento de sistemas de biorreactores de membrana y de biorreactor de lecho fluidificado-bioreactor de membrana híbridos para el tratamiento de agua residual urbana con salinidad constante y variable, cuyos resultados se han publicados en varios artículos científicos. Las condiciones de operación de los biorreactores fueron establecidas en 6, 9.5 y 12 h de tiempo de retención hidráulico y 2500 y 3500 mg L^{-1} de sólidos totales. Los biorreactores se operaron bajo influentes de salinidad constante a 6.5 mS cm^{-1} de conductividad eléctrica y bajo ciclos de salinidad de: 6 h de agua residual urbana con salinidad modificada - a 4.5, 6.5 y 8.5 mS cm^{-1} de conductividad eléctrica - seguidas de 6 h de agua residual urbana con salinidad convencional - alrededor de 1 mS cm^{-1}. Los análisis realizados para determinar el comportamiento de los bioreactores se dividieron en: rendimiento físicoquímico, cinética microbiana, ecología microbiana, y y comunidades en el biofouling junto con estudios de biomineraliación.

La puesta en marcha de los biorreactores bajo influentes salinios fue satisfactorio, pero resultó en la escasa formación de biopelícula adherida a los carriers (< 50 mg L^{-1}) en los reactores de lecho fluidificado-bioreactor de membrana híbridos bajo condiciones de salinidad constante y variable. Este hecho demostró que los sistemas de lecho fluidificado-bioreactor de membrana híbridos puestos en marcha bajo influentes salinos en las condiciones operacionales analizadas no presentaron ventajas con respecto a los sistemas de biorreactores de membrana.

En relación a este hallazgo, el rendimiento de los biorreactores de membrana y de lecho fluidificado-bioreactor de membrana híbridos fue similar en términos de eliminación de materia orgánica y de nitrógeno total, tal y como ocurrió también con las cinéticas de comunidades heterotrófica y autotróficas y la estructura de comunidades microbianas. La salinidad máxima en el influente hizo caer el rendimiento de eliminación de nitrógeno mientras que la eliminación de materia orgánica fue similar para todas las condiciones de salinidad. De este modo, la eliminación promedio de BOD_5 y de COD fue de 97-99% y 71-99%, respectivamente, para las

salinidades variables de 4.5 y 6.5 mS cm^{-1}. Sin embargo, valores ligeramente menores fueron registrados para el escenario de salinidad de 8.5 mS cm^{-1} (83-98% y 71-99%). La eliminación de nitrógeno se vio afectada por la salinidad máxima en el influente, mostrando valores del 27-85%, 15-50% y 24-38% para 4.5, 6.5 y 8.5 mS cm^{-1}. El descenso de la eliminación de nitrógeno con el incremento de la salinidad máxima fue relacionado con una deficiencia en la oxidación de amonio causada por el incremento de salinidad.

La cinética de autotrofos y heterótrofos se hizo más lenta con el incremento del tiempo de retención hidráulico y de la concentración de sólidos. Esto fue mostrado por la tendencia de la tasa de utilización de sustratos autotróficos y heterotróficos. Aunque la tasa de utilización de sustrato por la biomasa heterotrófica mostró valores similares para las tres configuraciones tecnológicas usadas, el biorreactor de membrana mostró valores más altos para concentraciones de sólidos totales de 2500 mg L^{-1} y el bioractor de lecho fluidificado-bioreactor de membrana híbrido sin carriers en la zona anóxica para sólidos totales de 3500 mg L^{-1}. Sin embargo, los valores de tasa de utilización de sustrato autotrófico fueron mayores para el escenario de 6.5 mS cm^{-1} que para los escenarios de 4.5 y 8.5 mS cm^{-1}. El biorreactor de membrana mostró la cinética autotrófica más lenta mientras que los bioreactores de lecho fluidificado-bioreactor de membrana híbridos tenían valores muy similares.

Las comunidades microbianas en los bioreactores estudiados se vio influenciada principalmente por la salinidad máxima del influente y su tipo de carga (constante o variable), seguidamente por los sólidos totales, el tiempo de retención hidráulico y en último lugar por la configuración tecnológica. Las comunidades microbianas encontradas fueron características para cada combinación de condiciones operacionales analizadas, si bien *Rhodanobacter*, *Nitrobacter*, *Ottowia*, *Mizugakiibacter* y miembros de la familia *Gemmatimonadaceae* fueron hallados en todos los escenarios de salinidad y condiciones de operación. Por lo tanto, estos filotipos podrían

desarrollar importantes roles ecológicos para el tratamiento de agua residual salina en tecnologías de membrana.

Por ultimo, las diferentes salinidades máximas en el influente determinaron las comunidades en el biofouling y las cepas con capacidad para mediar la precipitación de critales de calcio y magnesio. El género *Bacillus* fue el único filotipo con capacidad de biomineralización encontrado en todas las condiciones analizadas.

Objectives

According to the explanations given in the introduction section, research on saline wastewater treatment has always been constrained under two main points: adaptation to saline wastewater after operation under no-salinity wastewater; and use of influents with constant salinity. Therefore, there is a lack of understanding about the operation of bioreactors subjected to variable salinity conditions and about the start-up process under saline wastewater. The effect that variable salinity loadings could have over the performance, kinetics, microbial communities and biofouling in bioreactors has largely been understudied, but it can pose a serious threat for the remediation of wastewater in multitudinous economic sectors and areas. The same principles can be applied to start-up under saline wastewater. Moreover, the negative effects of salinity for wastewater treatment bioprocesses could be minimized using membrane technologies.

Following this rationale, the main objective of this Ph.D. is the analysis of the treatment of variable-salinity urban wastewater using membrane processes with and without moving bed.

In order to achieve the main objective, the following secondary objectives were proposed:

1) Study of the start-up of MBR and hybrid MBBR-MBR systems treating saline urban wastewater: effect over the performance, microbial kinetics and microbial communities
2) Analyze of the performance, microbial kinetics and microbial communities of MBR and hybrid MBBR-MBR systems treating variable-salinity urban wastewater: effect of maximum influent salinity, hydraulic retention time and total solids concentration
3) Analyze of the biofouling communities of hybrid MBBR-MBR systems treating constant- and variable-salinity urban wastewater: effect of maximum influent salinity
4) Analyze of the biomineralization capacity of bacterial strains isolated from biofouling of MBR and hybrid MBBR-MBR systems treating constant- and variable-salinity urban wastewater: effect of maximum influent salinity

General Introduction

1. The environmental concerns arising from discharge of wastewater

Human activities all around the world have had, have and will have a negative impact over the Earth's environment, polluting the biosphere. One of the most important activities that pollute the environment is the discharge of wastewater. Wastewater can be defined as the combination of several types of liquid effluents, which are: domestic effluents, names as blackwater and greywater; effluents from commercial places and institutions, including hospitals; effluents from industrial facilities, rain run-off and stormwater; effluents used in agriculture, aquaculture or horticulture (Gomes, 2009).

The discharge of wastewater has been linked to the deterioration of water bodies, with detrimental consequences for these aquatic environments and the use of these waters for human activities such as drinking water supply or recreation (Ntengwe, 2005). The World Health Organization has reported that about 1 billion people can't get access to clean water and other governmental health association declared that around 4000 children die every day due to waterborne illnesses (Dharupaneedi et al., 2019).

Indeed, wastewater contamination of water bodies can pose serious threats to human health. In addition to pathogenic bacteria contamination, novel studies have found that wastewater discharge increases the numbers of human, animal and plant pathogenic enteroviruses in receiving waters (Farkas et al., 2018; Masachessi et al., 2018), that microbial communities subjected to wastewater discharge develop antibiotic resistance, which in turn may severely complicate treatment of bacterial infections (Inyinbor et al., 2018), and that numerous contaminants of emerging concern are not removed in wastewater treatment systems and thus released to the environment (Krzeminski et al., 2018).

With the previous facts into account and joined to the growth of urban population and cities and to the climate change undergoing on Earth in the recent decades, there is an increasing need for water supply, which in turn makes water reserves scarcer. For this reason, wastewater

is becoming a possible resource of water and nutrients, and hence water reclamation process has been developed during the last decades (Angelakis et al., 2018). In this sense, modern wastewater treatment systems are in need of technologies that enable reuse of the treated wastewater, in addition to removal of nutrients and organic pollutants.

2. Technologies for the decontamination of wastewater: the membrane bioreactor and the moving bed biofilm reactor

To avoid environmental damage or human health concerns with respect to polluted water, governmental agencies have imposed wastewater discharge standards to control the concentration of contaminants discharged in wastewaters. The control over such contaminants led to the popularization of wastewater treatment systems.

The most used technology for the decontamination of wastewater in the 20th century has been the activated sludge process (Gonzalez-Martinez et al., 2016). This bioprocess is more than 100 years old (Ardern & Locket, 1914a; 1914b; 1915) and has been proficiently and successfully used for the removal of organic matter, nitrogen and phosphorus from wastewater.

In spite of its wide application, the activated sludge technology has to deal with several operational problems such as excess foam, high effluent suspended solids, high effluent biological oxygen demand or ammonia, or low effluent pH, among others (Marshall & Shimoto, 2004).

On the other hand, different technologies which surpasses the limitations of the activated sludge processes, also offering some advantages with respect to them, have been developed in the last few decades. Among them it is of relevance to cite the membrane bioreactor (MBR) technology.

The MBR is prominently based on a solids/liquid separation process mediated by a membrane. The principle is that a membrane with a small pore size will allow the liquid to pass while it will

impede the pass of solids. According to membrane pore size, the membrane filtration processes have been named as microfiltration (0.1-5 μm), ultrafiltration (0.01-0.1 μm), nanofiltration (0.001-0.01 μm) and reverse osmosis (0.0001-0.001 μm). The different sizes of membrane pore have been designed in order to remove a certain variety of particles. Microfiltration can remove microorganisms of big size such as *Bacteria* or *Eukarya* members. Ultrafiltration, however, can remove polymers, viruses, colloidal particles and macromolecules. Nanofiltration membranes can remove metallic salts and most of organics and biomacromolecules. On the smallest side of the spectrum, the reverse osmosis membranes are used to separate ions such as chlorine and sodium from water.

For the functioning of the membrane separation process, a generation of pressure inside the membrane is needed. This is accomplished by the means of pumping. Thus, pumping operation creates a transmembrane differential pressure which forces the liquid to pass through the membrane pores while the solids are kept outside. Pore size is of importance for the purpose of membrane filtration since smaller membrane pore size leads to higher transmembrane pressure needed. Given that ultrafiltration can effectively remove particles up to virus size, it has been widely used for the reclamation of water from urban wastewater treatment systems (Cailean et al., 2014). In this sense, MBR systems with ultrafiltration membranes have been used for the reuse of urban wastewater at full-scale (Deowan et al., 2015).

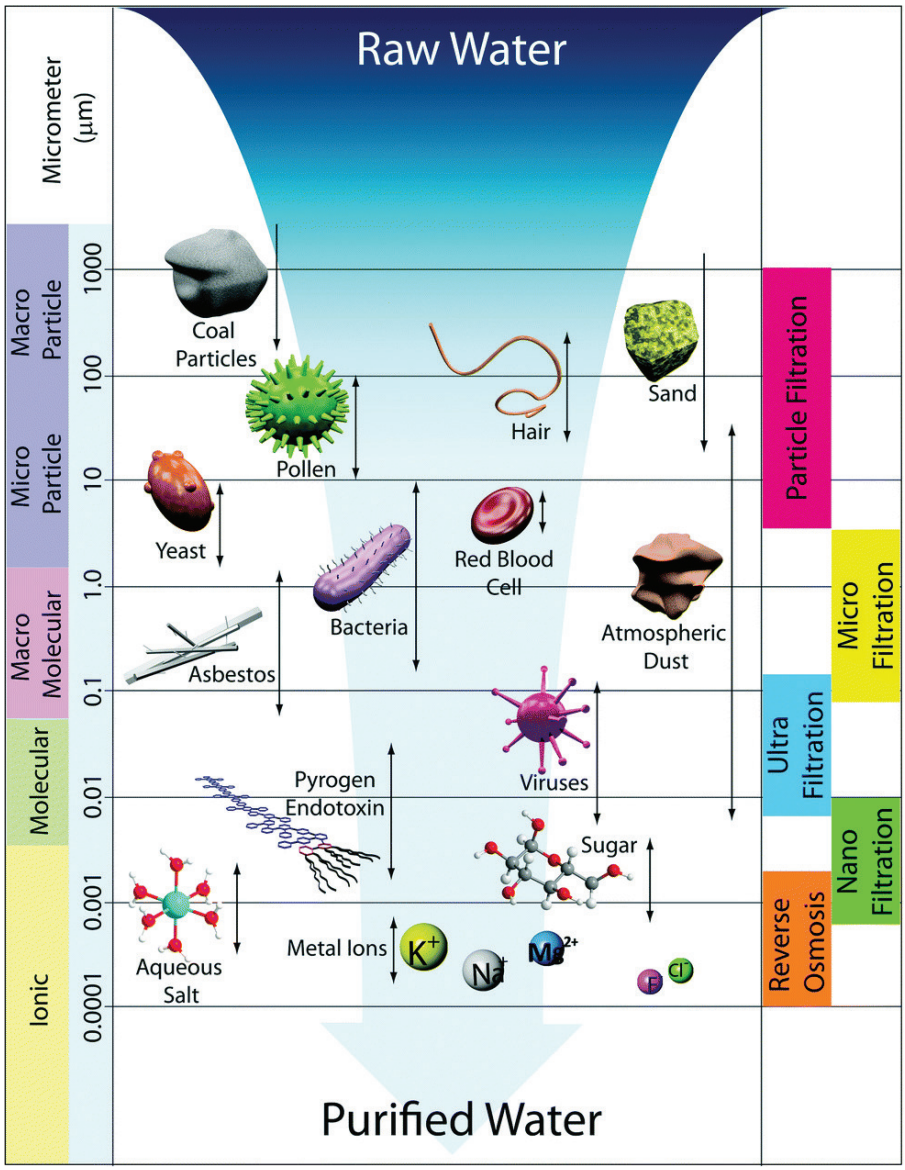

Figure 1 – Distribution of particle size and membrane filtration technology (Source: Lee et al., 2016)

The advantages of the MBR over the activated sludge system are very important. First, the efficient solids-water separation offers the possibility of working at higher suspended solids concentrations, which impacts the capacity of the system for bioremediation. Consequently, the MBR system requires less footprint than the activated sludge system for the same treatment performance. Also, high-efficiency separation of solids allows to dispense with the secondary sedimentation processes after the bioreactor. The efficient solids-liquid separation also enhances the biomass retention in the bioreactor, which permits longer solids retention times

in MBR than in the activated sludge. As a consequence, the excess sludge produced in the MBR is significantly lower than that produced in the activated sludge process (Leyva-Diaz et al., 2014; 2015). Moreover, the MBR system is less susceptible than the activated sludge to the influent wastewater composition, can remove the totality of solids, and has a much better capacity for disinfection of the treated water (Bertanza et al., 2017). However, there are disadvantages associated with the MBR system, such as high capital and operational costs, more complex management and control, the need of extensive aeration, and the unavoidable degradation of the filtration properties of the membrane caused by deposition of materials on its surface known as membrane fouling (Makisha & Nesterenko, 2018).

The major problem that MBR systems have to face is the apparition of membrane fouling, which is the inevitable process of clogging of membrane pores, resulting in higher demands of transmembrane pressure, lower flux rates and, eventually, irreversible deterioration of the membrane (Bagheri & Mirbagheri, 2017; Oh & Lee, 2018). Membrane biofouling occurs due to attachment of microbial products and/or growth of microbial biofilm over the surface or pores of the membrane (Aslam et al., 2018). One of the controlling factors affecting the membrane fouling is the suspended solids concentration in the bioreactor, thus operation at high solids concentration become problematic for the MBR systems due to high risks of fouling (Le-Clech et al., 2006).

An alternative to the activated sludge technology is the submerged biological filter or biofilter. In a submerged biofilter, a bioreactor is filled with immobile media over which the wastewater is poured. The media grows attached biofilm over it, providing enough biomass to perform the treatment of the wastewater. This technology is compact and feasible for the removal of organic matter and nitrogen. However, the immobile media systems are prone to clogging when treating wastewater with high particulate matter concentrations, which imposes a stringent regulation on the flow rate under which they can be operated (Leiknes & Ødegaard, 2007). In order to solve

the clogging of submerged biofilter media, the moving bed biofilm reactor (MBBR) was developed (Hem et al., 1994). In the MBBR a floating media is introduced, over which attached biofilm grows while the media moves freely, avoiding the clogging mechanisms occurring in the case of immobile media.

The addition of floating media offers several advantages with respect to submerged biofilters. A major advantage is the development of attached biofilm to floating media, which increases the concentration of total solids in the bioreactor without the increase in suspended solids. Other beneficial advantages are also lower head loss, the need of no backwashing, low residual sludge production, high resistance to shock loadings and high nitrification rates (Leyva-Diaz et al., 2017; Zhang et al., 2017a). Moreover, it also offers advantages over the activated sludge process, such as higher biomass concentration within the same bioreactor, smaller footprints required for the same effluent quality, the growth of slow growth rate microorganisms in the attached biomass in continuous flow conditions or lower sludge production (Barwal & Chaudhary, 2014; Leyva-Diaz et al., 2017). However, the development of attached biofilm within the system also had the negative effect of reducing the settleability of suspended solids generated in the MBBR process (Zhang et al., 2017a). The MBBR systems have been distinguished between pure or hybrid depending on the absence or presence of a biomass recycling flow (Leyva-Diaz et al., 2017).

The operation of MBR systems becomes difficult at high suspended solids concentrations due to quicker apparition of membrane fouling. However, higher biomass concentrations in the bioreactor enhance the capability of the MBR to treat wastewater. In this sense, operation of MBR systems is in constant trade-off between the suspended solids concentration and the membrane fouling. On the other hand, the operation of MBBR yields poor settling biomass which is difficult to remove by settling processes (Luo et al., 2015). In order to partially solve these two operational problems, the MBBR and the MBR technologies have been merged to develop a new process named as MBBR-MBR.

The MBBR-MBR system proposes a bioreactor with floating media followed by a membrane separation process (Leiknes & Ødegaard, 2007). The combination offers the operation of the membrane process under lower suspended solids, since an important fraction of the biomass will be attached to the floating media, thus mitigating biofouling (Bagheri & Mirbagheri, 2017) and decreasing energy consumption while increasing the efficiency of the separated systems (Zhang et al., 2017b). In addition, the poor-settling biomass obtained from the operation of the MBBR is efficiently removed from the effluent water by the MBR process. The MBBR-MBR configuration has proven higher efficiency that activated sludge and MBR systems in terms of complex organic matter removal (Jiang et al., 2018). Similarly to the MBBR systems, the MBBR-MBR systems are named as pure or hybrid if there is absence or presence of a recycling flow.

In the field of wastewater engineering today, the MBR and MBBR-MBR systems have gained attention as technologies that offer important advantages over the activated sludge systems (Leyva-Diaz & Poyatos, 2017). These technologies have been proven in pilot-scale for the treatment of urban wastewater (Leyva-Diaz et al., 2013) and there are numerous examples of these implemented at full-scale (Yang et al., 2006; Wang et al., 2008; GE Water & Process Technologies, 2014).

3. Salinity in wastewater: effect over the performance and the microbial communities of bioreactors

Salt is used in many industry sectors, such as agro-food, chemical, petrochemical, textile and leather, as well as in other human activities, such as road de-icing strategies and softening of hard water, with an estimated consumption of 30 million tons per year in the European Union (Lefebvre & Moletta, 2006). Due to all these processes, high salinity wastewaters are generated. It has been reported that influent of saline and hypersaline wastewater accounts for the 5% of all wastewater streams worldwide (Lefebvre et al., 2007). Regarding saline wastewater

influents, the intrusion of saline wastewater in wastewater treatment systems is increasingly becoming a concern. In fact, it has been reported that seawater intrusion in wastewater treatment systems affects the performance and microbial communities in these bioprocesses (Wu et al., 2013; Hao et al., 2014; Welles et al., 2015).

The presence of salinity in wastewater is detrimental for the treatment bioprocesses, since salinity decreases the microbial degradation efficiency of microorganisms (Castillo-Carvajal et al., 2014). The affection of microbes by high salinities includes increasing cell death due to higher cell wall osmotic pressure, the inhibition of metabolism and accumulation of harmful metabolites, or the biounavailability of metabolism-needed compounds (Bassin et al., 2012; He et al., 2017). It has also been reported that high salinities in wastewater decreases sludge settleability and microbial growth, thus decreasing the treatment capacity of floc biomass bioprocesses (He et al., 2017). On the other hand, salinity decreases microbial community diversity and the removal performances of COD, NH_4^+ and TN in wastewater treatment systems (Chen et al., 2018).

Concerning the membrane systems, it has been observed that punctual increase in salinity is related to more rapid membrane fouling and to lower biomass activity expresses as oxygen uptake rate (Di Bella et al., 2013). Similar results have been found for MBBR-MBR systems (Sun et al., 2010), showing the detrimental effect of salinity shocks over membrane processes. In spite of the operational problems that saline influents may have over membrane processes, it has been reported that their performance is higher than that of activated sludge systems subjected to similar saline loads in terms of nitrification (Jang et al., 2013). Acclimation of MBR and MBBR-MBR systems to saline influent suggested that the MBBR-MBR system has advantages over the MBR in terms of performance, caused by the presence of attached biomass in the MBBR-MBR which also showed higher biomass activity as observed by kinetics measurement (Di Bella et al., 2015a; Di Bella et al., 2015b).

i) Influence of salinity over microbial communities

Salt concentrations is detrimental for microbial communities in bioreactors. First, when salinity increases past the 1-2% concentrations, the death of no-halotolerant microorganisms is observed, as well as an increase in cell lysis and a decrease in cell activity (Wang et al., 2015). Moreover, the increase in water density due to higher salinity might enhance the flotation of biomass, which may eventually be washed out of the bioreactor (Reid et al., 2006). Under high salinity conditions (>1%), halotolerant microbial communities will be promoted thus gaining importance in the bioreactor. As well, the activities of microorganisms will change. This has been reported previously in many occasions (Cortes-Lorenzo et al., 2012; 2014).

ii) Influence of salinity over sludge structure

It has been shown that salinity affects the sludge structure in wastewater treatment processes. The loss in settleability of flocs under saline conditions has been linked to the higher water density at high salt concentrations (Wang et al., 2015). On the other hand, increasing salinity triggers the washout of filamentous bacteria, leading to better settleability of the biomass (Moussa et al., 2006). Therefore, the effect of salinity over the settling capacity of biomass is dependent on the acclimatization of the microbial communities to the influent salinity conditions. For the salinity shock the effect on biomass is detrimental, promoting its rupture and reduction in size, decreasing its settling capacity (Wang et al., 2015). However, when the biomass is adapted to salinity, better settling capacity than under no-salinity conditions is observed (Moussa et al., 2006).

iii) Influence of salinity over microbial respiration

It has been reported that the addition of salt to activated sludge biomass caused a decrease in its specific oxygen uptake rate, showing a detrimental effect over the activity of microorganisms (Di Bella et al., 2013). However, it has also been theorized that adaptation of halo-tolerant

microorganisms to salinity conditions might enhance the specific oxygen uptake rate to similar levels of biomass under no-salinity conditions (Ferrer-Polonio et al., 2016).

iv) Influence of salinity over osmotic pressure

It has been reported that addition of inorganic salts to activated sludge increased the osmotic pressure over its microbial communities, leading to cell death and lower performance in terms of organic matter removal (Ozalp et al., 2003). However, it has been found that halo-tolerant microorganisms can endure such osmotic pressures (Uygur, 2006). In this sense, the effect of influent salinity wastewater over the osmotic pressure becomes of less importance with acclimatization of the biomass.

The data above suggested that it is indeed possible to attain high removal performances in wastewater treatment bioprocesses treating wastewater with high salinity after the biomass has been acclimatized. In fact, successful researches have demonstrated this (Di Trapani et al., 2014; Di Bella et al., 2015a; Di Bella et al., 2015b; Mannina et al., 2016). However, there are two limitations with respect to the majority of researches aiming to observe the effect of salinity over the performance and microbial communities of bioprocesses treating salinity wastewater. One of these is that, in most cases, the bioreactors are started-up and operated under regular wastewater, which is changed to saline wastewater afterwards. This procedure therefore selects halotolerant microorganisms from the previous biomass but is not valid to observe the start-up of the systems using saline wastewater. The second limitation is that most of these researches used constant salinity conditions rather than variable influent salinity. The constant salinity conditions in the influent are more beneficial for a long-term adaptation of the microbial communities in the bioreactor to salinity, but nevertheless it has been observed that salinity shocks are more detrimental than constant salinities, as discussed above.

In this sense, it is needed to analyze the performance of bioprocesses subjected to variable salinity conditions, as these would be harmful for the microbial communities living within possibly resulting in lower treatment performances.

4. Membrane fouling process: importance of biologically-induced minerals

Membrane systems are subjected to fouling along their operation. Membrane fouling is the process of attachment of materials to membrane surface, blocking the membrane pores and thus reducing the efficiency of the water-liquid separation process. During practical operation of membrane-based systems, membrane fouling can be observed in two different ways: by a loss in permeate flux if operating at constant transmembrane pressure; or by an increase in transmembrane pressure if operating at constant flux (Guo et al., 2012). Membrane fouling has such importance for the performance of the membrane process that much research has been done over its characterization (Judd, 2017) and over the many possibilities to mitigate it: use of microbial quorum quenching, design of novel materials for membranes and development of novel dynamic membrane systems (Oh & Lee, 2018; Quin et al., 2018).

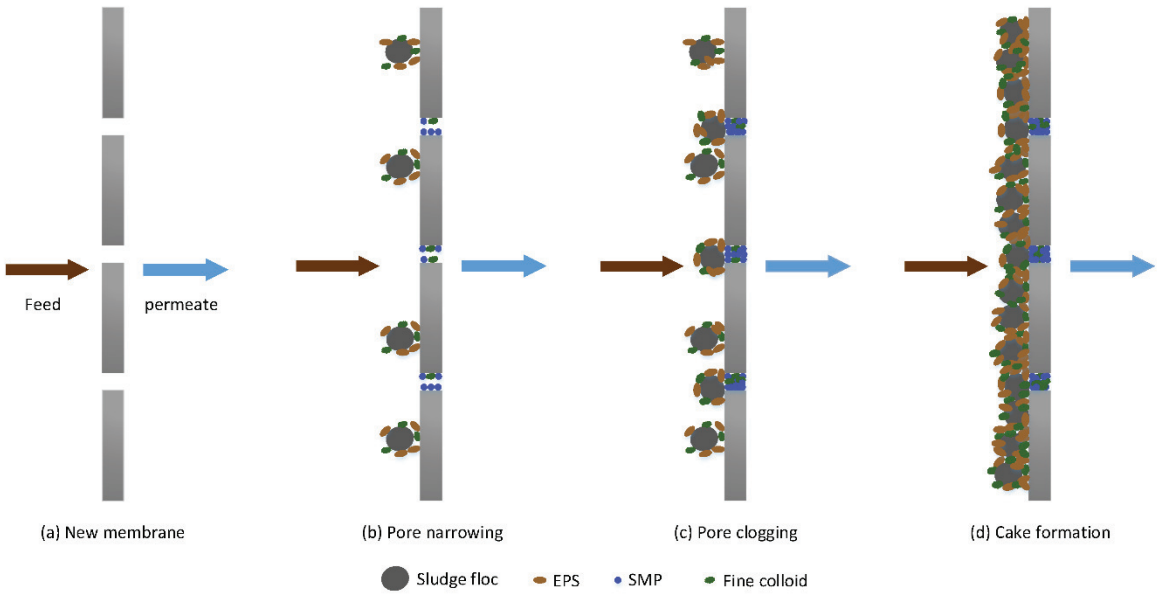

Figure 2 - Process of membrane fouling (Source: Iorhemen et al., 2016)

Membrane fouling can be classified into reversible and irreversible. Reversible fouling can be mitigated using backwashing procedures or membrane cleaning protocols, recovering the filtration capability of the membrane. However, irreversible fouling damages the filtration capacity of the membrane and could lead to the replacement of the equipment, with the consequential costs involved. According to this classification, reversible fouling is created by generation of a cake layer over the membrane surface. The formation of cake layer over the membrane surface is a process driven by continuous accumulation of inorganic matter, biopolymers and microorganisms (Iorhemen et al., 2016). On the contrary, irreversible biofouling is generated by pore clogging or chemisorption mechanisms (Rezakazemi et al., 2018). It has been reported that pore clogging is dependent on the membrane pore size and the particle size causing it (Iorhemen et al., 2016).

It has been widely accepted that fouling in membrane processes are related to three essential components in these systems: polysaccharides, proteins and humic substances, referred as organic foulants; microorganisms, referred as biofoulants; and inorganic materials with capability to precipitate inside membrane pores, referred as inorganic foulants (Iorhemen et al., 2016; Meng et al., 2017). Research on membrane fouling has identified six fouling mechanisms, which are pore blocking, cake formation, concentration polarization, organic adsorption, inorganic precipitation, and biofouling, with the former being considered the most important of them all (Deng et al., 2016).

Biofouling can be described as a process of microbial biomass accumulation in the interface of a membrane, which occurs by biomass deposition or microbial biofilm growth over the membrane surface. The susceptibility of membrane-based technologies for biofouling can affect the feasibility of these processes for the treatment of wastewater in coordination with other microbial-based technologies (Guo et al., 2012). In relation to this, it has been stated that the

apparition of biofouling is related to higher operational costs in membrane-based technologies (Aslam et al., 2018).

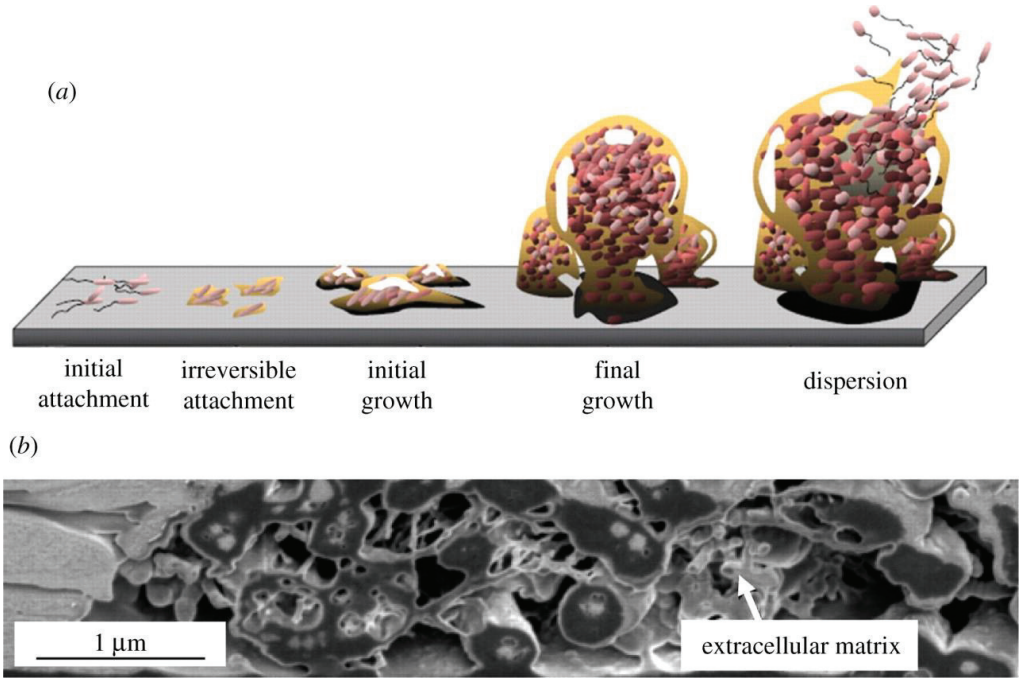

Figure 3 - Process of membrane biofouling (Source: Bixler & Bhushan 2012)

The formation of biofouling over a membrane is a process that requires several steps. First, the membrane surface should develop a conditioning film, which is composed of organic and inorganic materials and which sets a proper environment for microbial adhesion. Second, planktonic cells become displaces over the membrane surface and start to generate extracellular polymeric substances for adhesion to the membrane surface. The pioneer microbes will then grow, developing a mature biofilm from which, after enough time, microbial material will detach to colonize other areas (Aslam et al., 2018).

Being membrane biofouling such a complex process, there are many factors influencing it in wastewater treatment operations. These factors can be divided into four categories: characteristics of the mixed liquor (concentrations of extracellular polymeric substances and soluble microbial products, concentration of mixed liquor suspended solids, sludge viscosity, floc

size), operational conditions (solids retention time, hydraulic retention time, dissolved oxygen concentration, temperature), influent wastewater characteristics (organic loading rate, carbon to nitrogen and carbon to phosphorus ratios, salinity), and membrane characteristics (material, zeta potential, hydrophobicity, pore size, morphology) (Deng et al., 2016).

Biofouling problems have been reported to increase specially under treatment of saline wastewater (Shi et al., 2014). In this manner, salt shocks caused an increase of soluble microbial products within MBR systems leading to increase in both reversible and irreversible biofouling (De Temmerman et al., 2014). Moreover, it has been reported that increasing salinity accelerated membrane biofouling (Jang et al., 2013). Therefore, biofouling operational issues become of higher concern when treating saline wastewater.

Among the many microbial products that can trigger biofouling in membrane systems, one of the most harmful reported are biologically-induced minerals. It has been reported that minerals in membrane cake layer, joining extracellular polymeric substances due to electrostatic interactions, generate macro structures that favor biofouling and that are very difficult to clean, which makes the cake layer stiffer and could lead to irreversible fouling damage (Herrera-Robledo et al., 2011a; Herrera-Robledo et al., 2011b; Herrera-Robledo & Noyola, 2015).

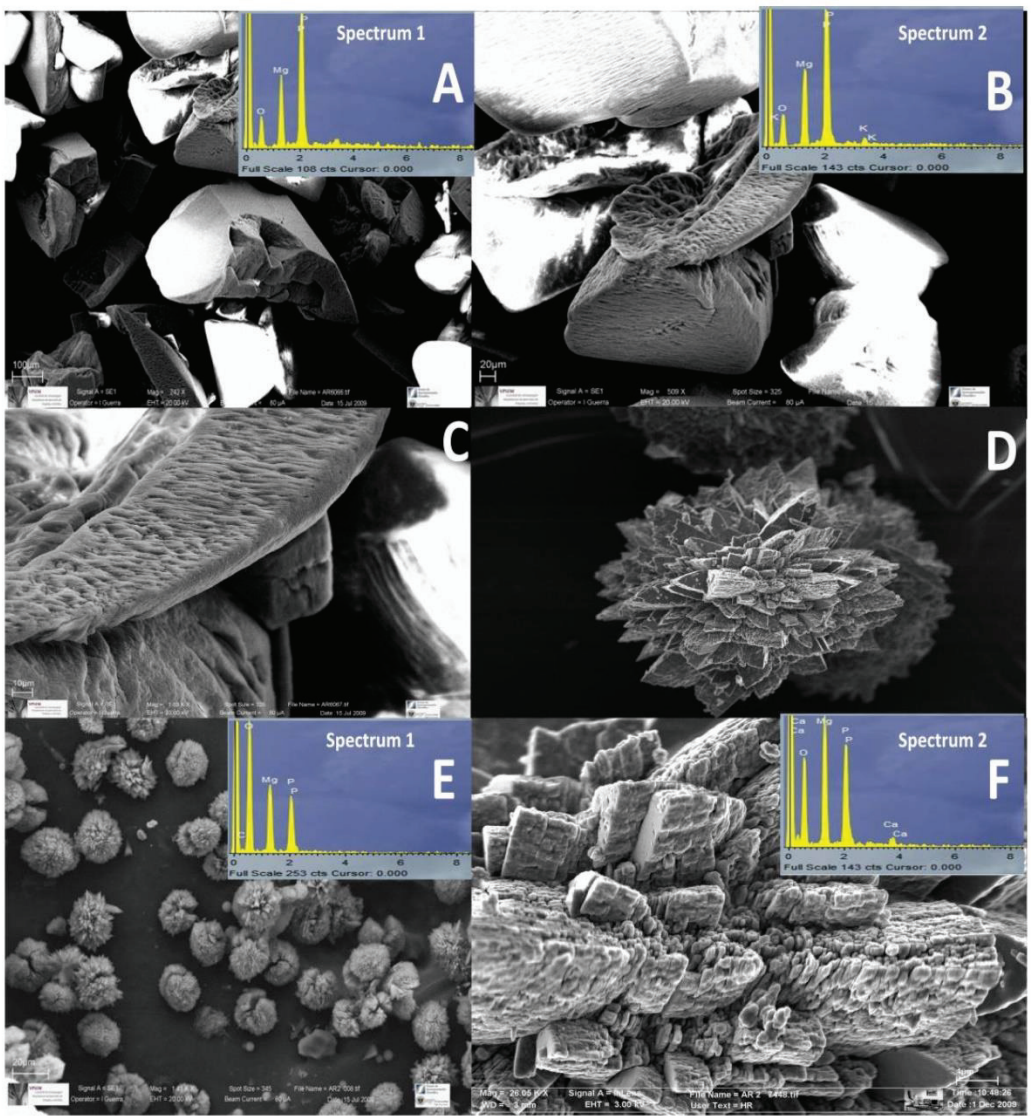

Figure 4 - Examples of minerals whose precipitation was mediated by microorganisms isolated from a wastewater treatment system (Source: Rivadeneyra et al., 2014a)

It has been discovered in the last two decades that microorganisms play a very important role in the formation of fine-grained minerals within a wide variety of environments (Lloyd et al., 2008). These are produced through a process named as biomineralization, in which living beings such as microorganisms are involved in the formation of minerals. The formation of the mineral can be controlled by the microorganism or induced by a microorganism's metabolism (Dhami et al., 2013). One important aspect of the biomineralization process is that the diversity of minerals formed is dependent on the living organism involved in its creation as well as in the

environmental conditions under which the mineral is created (Gonzalez-Martinez et al., 2017; Perez-Huerta et al., 2018).

It has been found that biomineralization is a common process occurring in wastewater treatment systems, especially concerning the precipitation of calcium carbonates and struvite, and several species isolated from activated sludge systems have been found to mediate the precipitation of such minerals (Rivadeneyra et al., 2013; Rivadeneyra et al., 2014b). Moreover, it has been found that many halophilic microorganisms have the capability to form biominerals (Sanchez-Roman et al., 2007).

Calcium carbonate minerals, usually calcite, vaterite and aragonite, are formed by many microorganisms living in aquatic environments. Formation of these minerals has been claimed as feasible solutions to sequestrate CO_2 and thus reduce its release to the atmosphere, mitigating the emission of this greenhouse gas (Sheik et al., 2014). It is though that the cell wall acts as nucleation site for the formation of calcium carbonate minerals, leading to calcification of the cell (Kumar et al., 2018).

On the other hand, the formation of phosphate minerals such as struvite has been regarded as a promising pathway for the recovery of phosphorus from wastewater (Sinha et al., 2014). However, precipitation of struvite in wastewater treatment systems causes operational problems (Arias et al., 2017). The formation of struvite is thought to be related with the combination of ammonium, magnesium and phosphate ions in the immediate vicinity of the microorganism (Li et al., 2014; Sinha et al., 2014).

In addition, it has been observed that bacterial strains isolated from the biofouling of membrane systems treating urban wastewater have the capability to precipitate carbonates and phosphate minerals, showing the risk of membrane fouling derivate from microbial-mediated mineralization processes (Gonzalez-Martinez et al., 2015b).

However, the capability of biofouling acclimatized to saline wastewater conditions has never been tested, nor under constant or variable salinity conditions. The halotolerant microbial communities, as well as the different environmental conditions for the formation of minerals (e.g.: higher presence of Cl^- and Na^+ ions under salinity conditions) could lead to high capacity of biomineral formation and, therefore, to high risk of membrane fouling by precipitated minerals.

5. Molecular biology techniques for characterization of bioreactors

The biological nature of bioprocesses for the treatment of wastewater imposes the microbial communities developing within them as crucial factors for its performance (Saunders et al., 2015). However, the lack of complete understanding of microbial communities in these systems makes that, in practice, design of bioprocesses is considered from an engineering point of view only, without regards of their intrinsic microbiological nature (Cydzik-Kwiatkowska & Zielinska, 2016). Indeed, the microbiological aspects of the biological wastewater treatment processes have been regarded as important for the design and operation of these bioprocesses (Gonzalez-Martinez et al., 2014) and today are deemed as essential in order to obtain successful exploitation of these facilities (Rodriguez et al., 2015).

The techniques available for the exploration of microbial ecology in any given environment can be divided in two groups: culture-dependent techniques and culture-independent techniques. Culture-dependent techniques are based on controlled growth of microorganisms in specific growth media. However, it has been reported that culture-dependent techniques cannot effectively capture the whole diversity of environmental microbial communities, given our inability to grow the majority of microorganisms under controlled conditions (Rappé & Giovanonni, 2003). Therefore, in the last decades, culture-independent techniques have been used to unravel environmental microbial ecology (Ferrara & Sanchez, 2016). The dominant culture-independent techniques are based on the polymerase chain reaction (PCR) and

sequencing. With the development of high throughput sequencing techniques, the number of sequences obtained from an environmental sample has increased exponentially, allowing for the successful characterization of its microbial community. In practice, high throughput characterization of environmental microbial communities has been implemented by targeted amplification of marker genes, with 16S rRNA gene being the most popular.

However, high throughput sequencing can be biased due to failures dependent on PCR approach. These failures are related to primer mismatches during the amplification process (Shokralla et al., 2012). Among these parameters, annealing temperature has been shown to greatly affect the diversity of an environmental sample when studied by high throughput sequencing (Gonzalez-Martinez et al., 2015a).

In spite of the intrinsic limitations to the high throughput sequencing methodology, its usage for the investigation of environmental microbial communities has become popularized in the last decade, being used to analyze microbiota from humans and animals (Dovretski et al., 2018; Hayes et al., 2018), deep-sea sediments (Quiao et al., 2018), hot springs (Ghilamicael et al., 2018), Arctic environments (Rapp et al., 2018), and many more environments. With respect to wastewater treatment bioprocesses, many examples of high throughput sequencing analyses of their microbial communities can be cited (Narciso-da-Rocha et al., 2018; Wang et al., 2018).

The microbial communities involved in the urban wastewater treatment in MBR and MBBR-MBR systems have been previously studied by the means of temperature gradient gel electrophoresis fingerprinting and high throughput sequencing (Gomez-Silvan et al., 2014; Calderon et al., 2012; Leyva-Diaz et al., 2015). The microbial communities in membrane systems treating saline wastewater have been timidly explored in the last years, with the analyses being restricted to constant salinity wastewater (Luo et al., 2016). However, no insights on the microbial communities in membrane systems treating variable saline wastewater have been attempted to this date.

The microbial communities involved in the membrane biofouling have been extensively studied. It has been defended that biofouling in membrane systems is caused by the activity of a certain group of microbial genera (Matar et al., 2017). In accordance to this result, it was also found that certain genera develop in the inner cake layer over the membrane surface, linking their activity with the biofouling formation (Choi et al., 2017). In addition, it has been observed that the microbial communities growing on the membrane surface change during the different stages of development of biofouling (Luo et al., 2017; Takada et al., 2018). Moreover, the bacterial members in the biofouling of MBBR-MBR systems with capability for mediation of mineral formation were identified using high throughput sequencing procedures (Gonzalez-Martinez et al., 2015b). However, none of these studies has been used for the description of biofouling communities in variable saline wastewater treatment by MBR or MBBR-MBR.

In spite of the high screening capacity of ecosystem's diversity of high throughput sequencing techniques, these cannot offer insights into taxonomic affiliation of microorganisms found, leading to community composition where many phylotypes involved are not properly identified. Moreover, the metabolic capabilities of these now-well-known phylotypes cannot be determined by high throughput sequencing techniques when they share the environment with many other microorganisms. In this sense, the wide application of high throughput sequencing for the characterization of the environmental microbial ecology in the last decade increases the importance of the cultivation-dependent techniques (Gutleben et al., 2017). One of the specific microbial abilities that scape the screening of usual high throughput sequencing techniques used in environmental microbiology in the biomineralization capacity. In this sense, for the whole characterization of environmental microbial communities and their metabolic capabilities, both culture-dependent and culture-independent techniques are needed.

Cultivation and isolation techniques have been previously used for the identification of bacterial strains with capacity to mediate carbonate and phosphate mineral formations present in

wastewater treatment systems (Rivadeneyra et al., 2013; Rivadeneyra et al., 2014b). Also, many bacterial isolates with biomineralization capacity for carbonate and phosphate were retrieved from saline soils and marine sediments (Sanchez-Roman et al., 2007; Delgado et al., 2008; Silva-Castro et al., 2013; Silva-Castro et al., 2014). Regarding biofouling in membrane systems, some effort has been spent on identifying bacterial strains in the biofouling with capacity for the formation of carbonate and phosphate minerals (Gonzalez-Martinez et al., 2015b). Nevertheless, no investigation on the biomineral-mediating strains in biofouling of membrane systems treating saline wastewater has been done to this date.

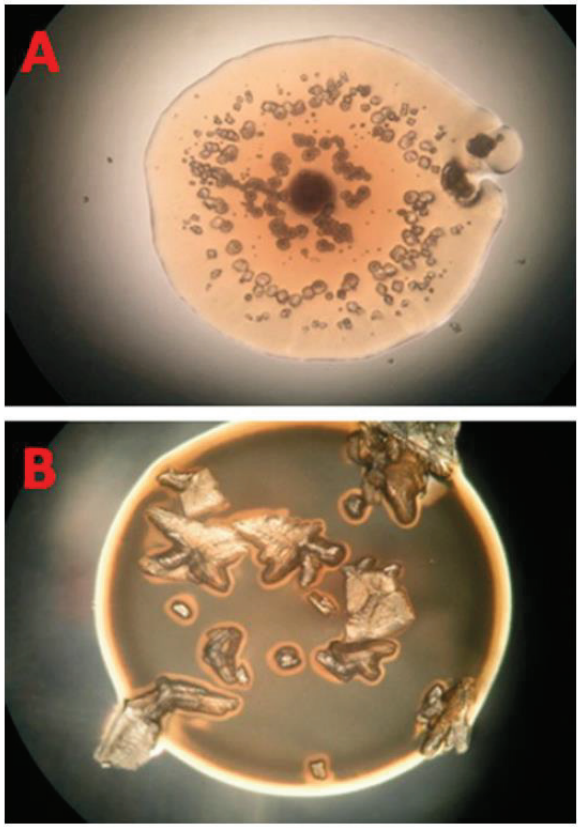

Figure 5 - Bacterial strains isolated from membrane biofouling with capacity to mediate the formation of calcite and struvite minerals (Source: Gonzalez-Martinez et al., 2015b)

References

Angelakis AN, Asano T, Bahri A, Jimenez BE, Tchobanoglous G. (2018). Water Reuse: From Ancient to Modern Times and the Future. Front Environ Sci 6. e-pub ahead of print, doi: 10.3389/fenvs.2018.00026.

Ardern E, Lockett WT (1914a) Experiments on the Oxidation of Sewage without the Aid of Filters. J Soc Chem Ind 33: 523.

Ardern E, Lockett WT (1914b) Experiments on the Oxidation of Sewage without the Aid of Filters, Part II. J Soc Chem Ind 33: 1122.

Ardern E, Lockett WT (1915) Experiments on the Oxidation of Sewage without the Aid of Filters, Part III. J Soc Chem Ind 34: 937.

Arias D, Cisternas L, Rivas M. (2017). Biomineralization Mediated by Ureolytic Bacteria Applied to Water Treatment: A Review. Crystals 7: 345.

Aslam M, Ahmad R, Kim J. (2018). Recent developments in biofouling control in membrane bioreactors for domestic wastewater treatment. Sep Purif Technol 206: 297–315.

Bagheri M, Mirbagheri SA. (2018). Critical review of fouling mitigation strategies in membrane bioreactors treating water and wastewater. Bioresour Technol 258: 318–334.

Barwal A, Chaudhary R. (2014). To study the performance of biocarriers in moving bed biofilm reactor (MBBR) technology and kinetics of biofilm for retrofitting the existing aerobic treatment systems: A review. Rev Environ Sci Biotechnol 13: 285–299.

Bassin JP, Kleerebezem R, Muyzer G, Rosado AS, Van Loosdrecht MCM, Dezotti M. (2012). Effect of different salt adaptation strategies on the microbial diversity, activity, and settling of nitrifying sludge in sequencing batch reactors. Appl Microbiol Biotechnol 93: 1281–1294.

Bertanza G, Canato M, Laera G, Vaccari M, Svanström M, Heimersson S. (2017). A comparison between two full-scale MBR and CAS municipal wastewater treatment plants: techno-economic-environmental assessment. Environ Sci Pollut Res 24: 17383–17393.

Bixler GD, Bhushan B. (2012). Review article: Biofouling: Lessons from nature. Philos Trans R Soc A Math Phys Eng Sci 370: 2381–2417.

Căilean D, Barjoveanu G, Teodosiu C, Pintilie L, Dăscălescu IG, Păduraru C. (2015). Technical performances of ultrafiltration applied to municipal wastewater treatment plant effluents. Desalin Water Treat 56: 1476–1488.

Calderón K, Martín-Pascual J, Poyatos JM, Rodelas B, González-Martínez A, González-López J. (2012). Comparative analysis of the bacterial diversity in a lab-scale moving bed biofilm reactor (MBBR) applied to treat urban wastewater under different operational conditions. Bioresour Technol 121: 119–126.

Castillo-Carvajal LC, Sanz-Martin JL, Barragan-Huerta BE. (2014). Biodegradation of organic pollutants in saline wastewater by halophilic microorganisms: A review. Environ Sci Pollut Res 21: 9578–9588.

Chen Y, He H, Liu H, Li H, Zeng G, Xia X, et al. (2018). Effect of salinity on removal performance and activated sludge characteristics in sequencing batch reactors. Bioresour Technol 249: 890–899.

Choi J, Kim ES, Ahn Y. (2017). Microbial community analysis of bulk sludge/cake layers and biofouling-causing microbial consortia in a full-scale aerobic membrane bioreactor. Bioresour Technol 227: 133–141.

Cortes-Lorenzo C, Rodriguez-Diaz M, Lopez-Lopez C, Sanchez-Peinado M, Rodelas B, Gonzalez-Lopez J. (2012). Effect of salinity on enzymatic activities in a submerged fixed bed biofilm reactor for municipal sewage treatment. Bioresour Technol 121: 312–319.

Cortes-Lorenzo C, Sipkema D, Rodriguez-Diaz M, Fuentes S, Juarez-Jimenez B, Rodelas B, et al. (2014). Microbial community dynamics in a submerged fixed bed bioreactor during biological treatment of saline urban wastewater. Ecol Eng 71: 126–132.

Cydzik-kwiatkowska A, Zielin M. (2016). Bacterial communities in full-scale wastewater treatment systems. World J Microbiol Biotechnol 32: 66, doi: 10.1007/s11274-016-2012-9.

De Temmerman L, Maere T, Temmink H, Zwijnenburg A, Nopens I. (2014). Salt stress in a membrane bioreactor: Dynamics of sludge properties, membrane fouling and remediation through powdered activated carbon dosing. Water Res 63: 112–124.

Delgado G, Delgado R, Párraga J, Rivadeneyra MA, Aranda V. (2008). Precipitation of carbonates and phosphates by bacteria in extract solutions from a semi-arid saline soil. Influence of Ca2+and Mg2+concentrations and Mg2+/Ca2+molar ratio in biomineralization. Geomicrobiol J 25: 1–13.

Deng L, Guo W, Ngo HH, Zhang H, Wang J, Li J, et al. (2016). Biofouling and control approaches in membrane bioreactors. Bioresour Technol 221: 656–665.

Deowan SA, Bouhadjar SI, Hoinkis J. (2015). Membrane bioreactors for water treatment. Advances in membrane technology for water treatment. Woodhead Publishing. 155-184.

Dhami NK, Reddy MS, Mukherjee MS. (2013). Biomineralization of calcium carbonates and their engineered applications: A review. Front Microbiol 4: 1–13.

Dharupaneedi SP, Nataraj SK, Nadagouda M, Reddy KR, Shukla SS, Aminabhavi TM. (2019). Membrane-based separation of potential emerging pollutants. Sep Purif Technol 210: 850–866.

Di Bella G, Di Prima N, Di Trapani D, Freni G, Giustra MG, Torregrossa M, et al. (2015). Performance of membrane bioreactor (MBR) systems for the treatment of shipboard slops: Assessment of hydrocarbon biodegradation and biomass activity under salinity variation. J Hazard Mater 300: 765–778.

Di Bella G, Di Trapani D, Torregrossa M, Viviani G. (2013). Performance of a MBR pilot plant treating high strength wastewater subject to salinity increase: Analysis of biomass activity and fouling behaviour. Bioresour Technol 147: 614–618.

Di Trapani D, Di Bella G, Mannina G, Torregrossa M, Viviani G. (2014). Comparison between moving bed-membrane bioreactor (MB-MBR) and membrane bioreactor (MBR) systems: Influence of wastewater salinity variation. Bioresour Technol 162: 60–69.

Di G, Di D, Freni G, Torregrossa M. (2014). Analysis of Biomass Characteristics in MBR and MB-MBR Systems Fed with Synthetic Wastewater: Influence of a Gradual Salinity Increase. 38: 445–450.

Drovetski S V., O'Mahoney M, Ransome EJ, Matterson KO, Lim HC, Chesser RT, et al. (2018). Spatial Organization of the Gastrointestinal Microbiota in Urban Canada Geese. Sci Rep 8: 1–10.

Farkas K, Cooper DM, McDonald JE, Malham SK, de Rougemont A, Jones DL. (2018). Seasonal and spatial dynamics of enteric viruses in wastewater and in riverine and estuarine receiving waters. Sci Total Environ 634: 1174–1183.

Ferrera I, Sánchez O. (2016). Insights into microbial diversity in wastewater treatment systems: How far have we come? Biotechnol Adv 34: 790–802.

Ferrer-Polonio E, Mendoza-Roca JA, Iborra-Clar A, Alonso-Molina JL, Pastor-Alcañiz L. (2016). Biological treatment performance of hypersaline wastewaters with high phenols concentration from table olive packaging industry using sequencing batch reactors. J Ind Eng Chem 43: 44–52.

Fusco V, Quero GM. (2014). Culture-dependent and culture-independent nucleic-acid-based methods used in the microbial safety assessment of milk and dairy products. Compr Rev Food Sci Food Saf 13: 493–537.

Garcı PA, Stams AJM, Maphosa F, Sousa DZ. (2015). Meta-omics approaches to understand and improve wastewater treatment systems. 385–406.Ghilamicael AM, Boga HI, Anami SE, Mehari T, Budambula NLM. (2018). Potential human pathogenic bacteria in five hot springs in Eritrea revealed by next generation sequencing. PLoS One 13: 1–12.

GE Water & Process Technologies (2014). MBR with MACarrier technology targets tough-to-treat wastewater. Membr Technol July 2014.

Gomes K. (2009). Wastewater management: A UN-Water Analytical Brief. UN Water 55.

Gómez-Silván C, Arévalo J, González-López J, Rodelas B. (2014). Exploring the links between population dynamics of total and active bacteria and the variables influencing a full-scale membrane bioreactor (MBR). Bioresour Technol 162: 103–114.

Gonzalez-Martinez A, Pesciaroli C, Martinez-Toledo M V., Hontoria E, Gonzalez-Lopez J, Osorio F. (2014). Study of nitrifying microbial communities in a partial-nitritation bioreactor. Ecol Eng 64: 443–450.

Gonzalez-Martinez A, Rodriguez-Sanchez A, Rivadeneyra MA, Rivadeneyra A, Martin-Ramos D, Vahala R, et al. (2017). 16S rRNA gene-based characterization of bacteria potentially associated with phosphate and carbonate precipitation from a granular autotrophic nitrogen removal bioreactor. Appl Microbiol Biotechnol 101: 817-829 , doi: 10.1007/s00253-016-7914-9.

Gonzalez-Martinez A, Rodriguez-Sanchez A, Rodelas B, Abbas BA, Martinez-Toledo MV, Van Loosdrecht MCM, et al. (2015). 454-Pyrosequencing Analysis of Bacterial Communities from Autotrophic Nitrogen Removal Bioreactors Utilizing Universal Primers: Effect of Annealing Temperature. Biomed Res Int 892013, 1-12, doi: 10.1155/2015/892013.

Gonzalez-Martinez a, Leyva-Díaz JC, Rodriguez-Sanchez A, Muñoz-Palazon B, Rivadeneyra A, Poyatos JM, et al. (2015). Isolation and metagenomic characterization of bacteria associated with calcium carbonate and struvite precipitation in a pure moving bed biofilm reactor-membrane bioreactor. Biofouling 31: 333–348.

Gonzalez-Martinez A, Rodriguez-Sanchez A, Lotti T, Garcia-Ruiz MJ, Osorio F, Gonzalez-Lopez J, et al. (2016). Comparison of bacterial communities of conventional and A-stage activated sludge systems. Sci Rep 6: 18786.

Guo W, Ngo HH, Li J. (2012). A mini-review on membrane fouling. Bioresour Technol 122: 27–34.

Gutleben J, Chaib De Mares M, van Elsas JD, Smidt H, Overmann J, Sipkema D. (2018). The multi-omics promise in context: from sequence to microbial isolate. Crit Rev Microbiol 44: 212–229.

Hao T wei, Xiang P yu, Mackey HR, Chi K, Lu H, Chui H kwong, et al. (2014). A review of biological sulfate conversions in wastewater treatment. Water Res 65: 1–21.

Hayes CL, Dong J, Galipeau HJ, Jury J, McCarville J, Huang X, et al. (2018). Commensal microbiota induces colonic barrier structure and functions that contribute to homeostasis. Sci Rep 8: 1–14.

He H, Chen Y, Li X, Cheng Y, Yang C, Zeng G. (2017). Influence of salinity on microorganisms in activated sludge processes: A review. Int Biodeterior Biodegrad 119: 520–527.

Hem LJ, Rusten B, Ødegaard H. (1994). Nitrification in a moving bed biofilm reactor. Water Res 28: 1425–1433.

Herrera-Robledo M, Cid-León DM, Morgan-Sagastume JM, Noyola A. (2011). Biofouling in an anaerobic membrane bioreactor treating municipal sewage. Sep Purif Technol 81: 49–55.

Herrera-Robledo M, Arenas C, Morgan-Sagastume JM, Castaño V, Noyola A. (2011). Chitosan/albumin/CaCO3 as mimics for membrane bioreactor fouling: Genesis of structural mineralized-EPS-building blocks and cake layer compressibility. Chemosphere 84: 191–198.

Herrera-Robledo M, Noyola A. (2015). The evolution of pore-blocking during the ultrafiltration of anaerobic effluent-like mixtures. Sep Purif Technol 147: 172–178.

Inyinbor AA, Bello OS, Fadiji AE, Inyinbor HE. (2018). Threats from antibiotics: A serious environmental concern. J Environ Chem Eng 6: 784–793.

Iorhemen OT, Hamza RA, Tay JH. (2016). Membrane bioreactor (Mbr) technology for wastewater treatment and reclamation: Membrane fouling. Membranes (Basel) 6: 13–16.

Jang D, Hwang Y, Shin H, Lee W. (2013). Effects of salinity on the characteristics of biomass and membrane fouling in membrane bioreactors. Bioresour Technol 141: 50–56.

Jiang Q, Ngo HH, Nghiem LD, Hai FI, Price WE, Zhang J, et al. (2018). Effect of hydraulic retention time on the performance of a hybrid moving bed biofilm reactor-membrane bioreactor system for micropollutants removal from municipal wastewater. Bioresour Technol 247: 1228–1232.

Judd SJ. (2017). Membrane technology costs and me. Water Res 122: 1–9.

Krzeminski P, Tomei MC, Karaolia P, Langenhoff A, Almeida CMR, Felis E, et al. (2019). Performance of secondary wastewater treatment methods for the removal of contaminants of emerging concern implicated in crop uptake and antibiotic resistance spread: A review. Sci Total Environ 648: 1052–1081.

Kumar M, Sundaram S, Gnansounou E, Larroche C, Thakur IS. (2018). Carbon dioxide capture, storage and production of biofuel and biomaterials by bacteria: A review. Bioresour Technol 247: 1059–1068.

Le-Clech P, Chen V, Fane TAG. (2006). Fouling in membrane bioreactors used in wastewater treatment. J Memb Sci 284: 17–53.

Lee A, Elam JW, Darling SB. (2016). Membrane materials for water purification: Design, development, and application. Environ Sci Water Res Technol 2: 17–42.

Lefebvre O, Quentin S, Torrijos M, Godon JJ, Delgenès JP, Moletta R. (2007). Impact of increasing NaCl concentrations on the performance and community composition of two anaerobic reactors. Appl Microbiol Biotechnol 75: 61–69.

Lefebvre O, Moletta R. (2006). Treatment of organic pollution in industrial saline wastewater: A literature review. Water Res 40: 3671–3682.

Leiknes T, Ødegaard H. (2007). The development of a biofilm membrane bioreactor. Desalination 202: 135–143.

Leyva-díaz JC, Calderón K, Rodríguez FA, González-lópez J. (2013). Comparative kinetic study between moving bed biofilm reactor-membrane bioreactor and membrane bioreactor systems and their influence on organic matter and nutrients removal. Biochem Eng J 77: 28–40.

Leyva-díaz JC, González-martínez A, González-lópez J, Muñío MM, Poyatos JM. (2015). Kinetic modeling and microbiological study of two-step nitrification in a membrane bioreactor and hybrid moving bed biofilm reactor – membrane bioreactor for wastewater treatment. Chem Eng J 259: 692–702.

Leyva-Díaz JC, Martín-Pascual J, Poyatos JM. (2017). Moving bed biofilm reactor to treat wastewater. Int J Environ Sci Technol 14: 881–910.

Leyva-Díaz JC, Poyatos JM. (2017). Modeling and Optimization of Membrane Bioreactors and Moving Bed Biofilm Reactor-Membrane Bioreactors. Chem Eng Technol 40: 1726–1735.

Li H, Yao QZ, Wang YY, Li YL, Zhou GT. (2015). Biomimetic synthesis of struvite with biogenic morphology and implication for pathological biomineralization. Sci Rep 5: 1–8.

Lloyd JR, Pearce CI, Coker VS, Pattrick RAD, Van Der Laan G, Cutting R, et al. (2008). Biomineralization: Linking the fossil record to the production of high value functional materials. Geobiology 6: 285–297.

Luo J, Lv P, Zhang J, Fane AG, McDougald D, Rice SA. (2017). Succession of biofilm communities responsible for biofouling of membrane bioreactors (MBRs). PLoS One 12: 1–23.

Luo W, Phan H V., Hai FI, Price WE, Guo W, Ngo HH, et al. (2016). Effects of salinity build-up on the performance and bacterial community structure of a membrane bioreactor. Bioresour Technol 200: 305–310.

Luo Y, Jiang Q, Ngo HH, Nghiem LD, Hai FI, Price WE, et al. (2015). Evaluation of micropollutant removal and fouling reduction in a hybrid moving bed biofilm reactor-membrane bioreactor system. Bioresour Technol 191: 355–359.

Makisha N, Nesterenko A. (2018). Wastewater treatment in membrane bioreactors. Features and application. IOP Conf Ser Mater Sci Eng 365: 022046.

Mannina G, Capodici M, Cosenza A, Di Trapani D, Viviani G. (2016). Sequential batch membrane bio-reactor for wastewater treatment: The effect of increased salinity. Bioresour Technol 209: 205–212.

Matar GK, Bagchi S, Zhang K, Oerther DB, Saikaly PE. (2017). Membrane biofilm communities in full-scale membrane bioreactors are not randomly assembled and consist of a core microbiome. Water Res 123: 124–133.

Marshall & Shimoto. (2004). Troubleshooting Activated Sludge Processes. Maine Dep Environ Prot 1–12.

Massachessi G, pisano MB, Prez VE, Martinez LC, Michelena JF, Martinez-Wassaf M, Giordano MO, Isa MB, Pavan JV, Welter A, Nates SV, Re V. (2018). Enteric viruses in surface waters in Argentina: molecular and viable-virus detection. Appl Environ Microbiol 84: 1–12.

Moussa MS, Sumanasekera DU, Ibrahim SH, Lubberding HJ, Hooijmans CM, Gijzen HJ, et al. (2006). Long term effects of salt on activity, population structure and floc characteristics in enriched bacterial cultures of nitrifiers. Water Res 40: 1377–1388.

Narciso-da-Rocha C, Rocha J, Vaz-Moreira I, Lira F, Tamames J, Henriques I, et al. (2018). Bacterial lineages putatively associated with the dissemination of antibiotic resistance genes in a full-scale urban wastewater treatment plant. Environ Int 118: 179–188.

Ntengwe FW. (2005). An overview of industrial wastewater treatment and analysis as means of preventing pollution of surface and underground water bodies - The case of Nkana Mine in Zambia. Phys Chem Earth 30: 726–734.

Oh HS, Lee CH. (2018). Origin and evolution of quorum quenching technology for biofouling control in MBRs for wastewater treatment. J Memb Sci 554: 331–345.

Ozalp G, Gomec CY, Ozturk I, Gonuldinc S, Altinbas M. (2004). Effect of high salinity on anerobic treatment of low strength effluents. Water Sci Technol 48: 207–212.

Pérez-Huerta A, Coronado I, Hegna TA. (2018). Understanding biomineralization in the fossil record. Earth-Science Rev 179: 95–122.

Qiao Y, Liu J, Zhao M, Zhang XH. (2018). Sediment depth-dependent spatial variations of bacterial communities in mud deposits of the Eastern China marginal seas. Front Microbiol 9: 1–12.

Qin L, Zhang Y, Xu Z, Zhang G. (2018). Advanced membrane bioreactors systems: New materials and hybrid process design. Bioresour Technol 269: 476–488.

Rapp JZ, Fernández-Méndez M, Bienhold C, Boetius A. (2018). Effects of ice-algal aggregate export on the connectivity of bacterial communities in the central Arctic Ocean. Front Microbiol 9. 1035, doi: 10.3389/fmicb.2018.01035.

Rappé MS, Giovannoni SJ. (2003). The Uncultured Microbial Majority. Annu Rev Microbiol 57: 369–394.

Reid E, Liu X, Judd SJ. (2006). Effect of high salinity on activated sludge characteristics and membrane permeability in an immersed membrane bioreactor. J Memb Sci 283: 164–171.

Rezakazemi M, Dashti A, Riasat Harami H, Hajilari N, Inamuddin. (2018). Fouling-resistant membranes for water reuse. Environ Chem Letters 16: 715-763.

Rivadeneyra Torres A, Martinez-Toledo M V., Gonzalez-Martinez A, Gonzalez-Lopez J, Martín-Ramos D, Rivadeneyra MA. (2013). Precipitation of carbonates by bacteria isolated from wastewater samples collected in a conventional wastewater treatment plant. Int J Environ Sci Technol 10: 141–150.

Rivadeneyra A, Gonzalez-Martinez A, Gonzalez-Lopez J, Martin-Ramos D, Martinez-Toledo MV, Rivadeneyra MA. (2014). Precipitation of phosphate minerals by microorganisms isolated from a fixed-biofilm reactor used for the treatment of domestic wastewater. Int J Environ Res Public Health 11: 3689–3704.

Sánchez-Román M, Rivadeneyra MA, Vasconcelos C, McKenzie JA. (2007). Biomineralization of carbonate and phosphate by moderately halophilic bacteria. FEMS Microbiol Ecol 61: 273–284.

Saunders AM, Albertsen M, Vollertsen J, Nielsen PH. (2015). The activated sludge ecosystem contains a core community of abundant organisms. 10: 11–20.

Sheikh, Afeefa Qayoom, Skinder, Bhat Mohd, Pandit, Ashok K, Ganai BA. (2014). Terrestrial carbon sequestration as a climate change mitigation activity. J Pollut Eff Control 0–8.

Shi X, Tal G, Hankins NP, Gitis V. (2014). Fouling and cleaning of ultrafiltration membranes: A review. J Water Process Eng 1: 121–138.

Shokralla S, Spall JL, Gibson JF, Hajibabaei M. (2012). Next-generation sequencing technologies for environmental DNA research. Mol Ecol 21: 1794–1805.

Silva-Castro GA, Uad I, Gonzalez-Martinez A, Rivadeneyra A, Gonzalez-Lopez J, Rivadeneyra MA. (2015). Bioprecipitation of calcium carbonate crystals by bacteria isolated from saline environments grown in culture media amended with seawater and real brine. Biomed Res Int 816102: 1-12 e-pub ahead of print, doi: 10.1155/2015/816102.

Silva-Castro GA, Uad I, Rivadeneyra A, Vilchez JI, Martin-Ramos D, González-López J, et al. (2013). Carbonate Precipitation of Bacterial Strains Isolated from Sediments and Seawater: Formation Mechanisms. Geomicrobiol J 30: 840–850.

Sinha A, Singh A, Kumar S, Khare SK, Ramanan A. (2014). Microbial mineralization of struvite: A promising process to overcome phosphate sequestering crisis. Water Res 54: 33–43.

Sun C, Leiknes TO, Weitzenböck J, Thorstensen B. (2010). Salinity effect on a biofilm-MBR process for shipboard wastewater treatment. Sep Purif Technol 72: 380–387.

Takada K, Shiba T, Yamaguchi T, Akane Y, Nakayama Y, Soda S, et al. (2018). Cake layer bacterial communities during different biofouling stages in full-scale membrane bioreactors. Bioresour Technol 259: 259–267.

Uygur A. (2006). Specific nutrient removal rates in saline wastewater treatment using sequencing batch reactor. Process Biochem 41: 61–66.

Wang X, Jiang L, Gai Z, Tao F, Tang H, Xu P. (2018). The plasticity of indigenous microbial community in a full-scale heavy oil-produced water treatment plant. J Hazard Mater 358: 155–164.

Wang Z, Wu Z, Mai S, Yang C, Wang X, An Y, et al. (2008). Research and applications of membrane bioreactors in China: Progress and prospect. Sep Purif Technol 62: 249–263.

Wang Z, Gao M, She Z, Wang S, Jin C, Zhao Y, et al. (2015). Effects of salinity on performance, extracellular polymeric substances and microbial community of an aerobic granular sequencing batch reactor. Sep Purif Technol 144: 223–231.

Warsinger DM, Chakraborty S, Tow EW, Plumlee MH, Bellona C, Loutatidou S, et al. (2018). A review of polymeric membranes and processes for potable water reuse. Prog Polym Sci 81: 209–237.

Welles L, Lopez-Vazquez CM, Hooijmans CM, van Loosdrecht MCM, Brdjanovic D. (2015). Impact of salinity on the aerobic metabolism of phosphate-accumulating organisms. Appl Microbiol Biotechnol 99: 3659–3672.

Wu YJ, Whang LM, Fukushima T, Chang SH. (2013). Responses of ammonia-oxidizing archaeal and betaproteobacterial populations to wastewater salinity in a full-scale municipal wastewater treatment plant. J Biosci Bioeng 115: 424–432.

Yang W, Cicek N, Ilg J. (2006). State-of-the-art of membrane bioreactors: Worldwide research and commercial applications in North America. J Memb Sci 270: 201–211.

Zhang W, Tang B, Bin L. (2017). Research Progress in Biofilm-Membrane Bioreactor: A Critical Review. Ind Eng Chem Res 56: 6900–6909.

Results

Chapter 1

Performance and kinetics of membrane and hybrid moving bed biofilm-membrane bioreactors treating salinity wastewater

This chapter has been published in its current form in AIChE Journal. The complete citation is the following:

Alejandro Rodríguez-Sanchez, Juan Carlos Leyva-Diaz, José Manuel Poyatos, Jesus Gonzalez-Lopez. 2017. Performance and kinetics of membrane and hybrid moving bed biofilm-membrane bioreactors treating salinity wastewater. AIChE Journal. 63(8), 3329-3342. doi: 10.1002/aic.15694

Abstract

A pilot-plant membrane bioreactor (MBR) and two pilot-plant hybrid moving bed biofilm reactor–membrane bioreactors (MBBR–MBRs), divided into three aerobic and one anoxic chambers, were started up for the treatment of salinity-amended urban wastewater. The MBBR–MBR systems worked with and without carriers in the anoxic zone (MBBR–MBRanox and MBBR-MBRn/anox, respectively). The systems were operated from start-up to stabilization, showing high removal of organic matter—a maximum of 90% chemical oxygen demand and 98% biochemical oxygen demand on the fifth day for MBBR–MBRn/anox in the stabilization phase—but low nitrogen elimination—30% maximum for MBBR– MBRn/anox in the stabilization phase. Biofilm attached to carriers reached less than 50 mg L^{-1} in the hybrid system. MBR showed faster kinetics than the two MBBR–MBR systems during start-up, but the opposite occurred during stabilization. Maximum specific growth rates for heterotrophic and autotrophic biomass were 0.0500 and 0.0059 h^{-1} for MBBR–MBRn/anox in the stabilization phase.

1. Introduction

One of the most important environmental problems in our world is the discharge of industrial and urban wastewater, which affects both the environment and human health. To remediate the impacts associated with this practice, wastewater treatment systems have been designed and operated during the last century to meet discharge standard policies (Leyva-Diaz et al., 2015a). Many technologies have been developed during this time.

Biological wastewater treatment processes can be divided into suspended growth or attached growth processes (Metcalf & Eddy, 2003). In suspended growth processes, microbial communities within a bioreactor spontaneously form amalgamations of biomass called flocs or granules (Wang et al., 2015). Among suspended growth processes, one of the most popular is the activated sludge (AS) system. On the other hand, in attached growth processes, an inert medium is used to facilitate the attachment of microbial communities to its surface (Muhamad et al., 2015). One of the most used attached growth processes is the moving bed biofilm reactor (MBBR) system. MBBR system can be compared with an AS system in which a floating medium, denominated as carrier, is introduced into the system and maintained in continuous movement by means of aeration and/or mechanical stirring. MBBR offers advantages over the AS process, such as less space required for the bioreactor, easier handling of biomass separation from the effluent, and higher specialization of active biomass (Ødegaard, 2006). Also, MBBR is not subject to clogging of the media, which implies an advantage over other attached growth processes such as trickling filters (Leiknes & Ødegaard, 2007).

One of the most efficient technologies in terms of wastewater treatment performance is membrane bioreactor (MBR) technology (Visvanathan & Parameshwaran, 2015). MBR has several advantages over other wastewater treatment systems such as lower footprint required for implementation, complete biomass retention, possibility of operation under higher suspended solids concentrations, higher solids retention times, low sludge production, and very

high disinfection capacity (Le-Clech et al., 2006; Leiknes & Ødegaard, 2007). Nevertheless, fouling of the membrane is the major drawback of MBR processes (Leiknes & Ødegaard, 2007). MBR processes have led to new technologies that are being of importance for both scientific research and industrial applications. Among these, some of the most novel comprises electrochemical MBRs, osmotic MBRs, and membrane aerated biofilm reactors (Li et al., 2016; Nerenberg, 2016; Luo et al., 2017).

The use of a biological system combining MBBR and MBR has led to the development of the MBBR–MBR process. In these technical applications, an MBBR process is followed by an MBR (Leiknes & Ødegaard, 2007; Leyva-Diaz et al., 2015b). The MBBR–MBR process offers advantages over the MBR process in terms of lower membrane biofouling and improved settleability issues regarding MBBR processes (Leyva-Diaz et al., 2014). MBBR–MBR processes are denominated pure or hybrid depending on the absence or presence of recycling flow from the MBR to the MBBR, respectively.

The regular salinity of urban wastewater is measured in the range of 0.7–3.0 mS cm^{-1} electrical conductivity (Norton-Brandao et al., 2013). Many industrial processes (e.g., seafood processing, milk processing, petroleum refining, and textile manufacturing) result in high salinity of the wastewater they produce (Mines & Robertson, 2003; Yang et al., 2013). The use of salt for cooking, snow melting activities, and utilization of marine water for toilet flushing, among others, could also generate high-salinity wastewater (Cortes-Lorenzo et al., 2012). It has been shown that salinity is an environmental parameter that can affect microbial communities in wastewater treatment due to the reduction of bioavailability of compounds, microbial mortality caused by differential osmotic pressure across cell membranes, or inhibition of biodegradation of potentially harmful intermediates and, thus, their accumulation in the bioreactor (Bassin et al., 2012; Castillo-Carvajal et al., 2014).

The purpose of this study was to analyze the start-up and operation of an MBR and two different configurations of hybrid MBBR-MBR fed with salinity-amended (6.5 mS cm^{-1}) wastewater in terms of process performance and microbial kinetics. Thus, an MBR and two hybrid MBBR– MBR working in parallel and fed with the same 6.5 mS cm^{-1} (3.5 g L^{-1} of NaCl) salinity-amended urban wastewater were started up and operated for 84 days. The effect of salinityon the growth of both suspended and attached biomass inside the bioreactors was analyzed during the start-up and stabilization phases. Moreover, the influence of salinity on the performance of the three processes, in terms of organic matter and nitrogen removal, and heterotrophic and autotrophic microbial kinetics was evaluated. The results were compared with bioreactors with the same configurations operating in parallel with the same urban wastewater under unmodified salinity conditions.

2. Materials and Methods

2.1 Experimental setup

Overview of Pilot-Scale Plants. The experiment was carried out by using three different pilot-scale plants working in parallel and fed with the same wastewater. A storage tank was filled with municipal wastewater taken from the WWTP located in Puente de Los Vados (Granada, Spain). According to the method of Ramos et al. (2007) 3.5 g L^{-1} of NaCl was added to the storage tank in order to achieve salinity-amended urban wastewater with 6.50 6 0.30 mS cm^{-1} of electrical conductivity. The bioreactors were not inoculated prior to saline wastewater feeding, so the salinity-amended urban wastewater was the only source of biomass for the bioreactors. Each of the pilot-scale plants was fed with wastewater coming from the storage tank using 323S Watson-Marlow peristaltic pumps (Watson Marlow Pumps Group, USA). These systems were configured into four zones: one anoxic zone and three aerobic zones, followed by a membrane tank with a submerged membrane module. The bioreactor effluent was then discharged to the membrane

tank, from which permeate was extracted through the ultrafiltration membrane using a 323U suction-backwashing peristaltic pump (Watson-Marlow Pumps Group). One of the pilot plants consisted of an MBR (Figure 1 top), another was a hybrid with carriers in the aerobic zones only (MBBR–MBRanox) (Figure 1 middle), and the last one consisted of a hybrid MBBR–MBR with carriers in all aerobic and anoxic zones (MBBR–MBRn/anox).

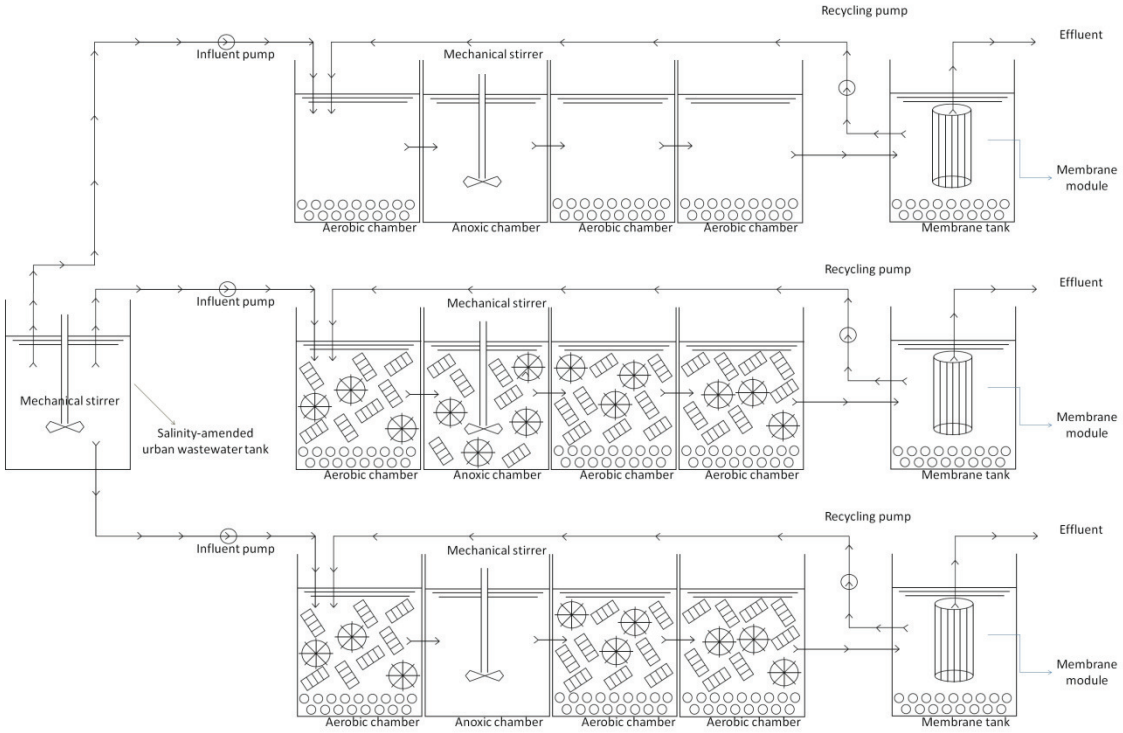

Figure 1 - Scheme of the three pilot-scale plants used in the study. with the MBR on top. hybrid MBBR-MBRanox in the middle and hybrid MBBR-MBRn/anox on the bottom.

In light of this, the use of three pilot plants in parallel allowed for determining the effect of the attached biomass in MBBR-MBR systems on the efficiencies of organic matter and nitrogen removal compared with the MBR. Moreover, the influence of attached biomass in the anoxic zone of MBBRMBRn/anox was analyzed concerning the nitrogen removal performance.

2.2 Description of the bioreactors

The MBR (Figure 1A) included a bioreactor divided into four zones: three aerobic zones and one anoxic zone and was followed by a membrane tank with a hollow-fiber membrane module. The four compartments of the MBR had 12 cm length, 12 cm width, and 60 cm height. Thus, the bioreactor volume was 36 L. However, operational security mechanisms were installed to work with a reduction of 33% of the total volume. Therefore, the total operational volume of the MBR was 24 L. Salinity-amended urban wastewater was pumped into the first aerobic chamber of the bioreactor. Then, it passed through the anoxic chamber and two more aerobic chambers. Wastewater passed through chambers by a communicating vessel system. Finally, salinity-amended urban wastewater was discharged into the membrane tank. A recycling flow was imposed from the membrane tank to the first aerobic chamber using a 323S Watson-Marlow peristaltic pump (Watson-Marlow Pumps Group). The recycling flow rate was set to 14.9 L h^{-1}, making it 500% of the influent flow.

The placement of the anoxic chamber after the first aerobic chamber was decided in order to provide an anoxic environment for denitrification within the configuration of the bioreactor while also avoiding excessive input of aeration in that chamber coming with the recycling flow.

The anoxic zones were mixed by means of Multi Mixer MM-1000 stirrers (Biosan Laboratories Inc, USA) to avoid settling of suspended biomass and to promote movement of carriers within the anoxic chamber. In this regard, the mixing of the aerobic chambers was achieved by means of AFD 270 fine bubble diffusers (ECOTEC SA, Spain) located at the bottom of the aerobic chambers. Moreover, this aeration was controlled to satisfy the requirements of microorganisms for their aerobic metabolism. The aeration was provided by the working of an ACO-500 air compressor (Hailea, China). The air flow in the aerobic chambers was regulated using a valve and was measured continuously using a 2100 Model rotameter (Tecfluid SA, Spain).

The membrane tank consisted of an external unit with submerged configuration. The membrane tank had a cylindrical shape with 10 cm diameter and 65 cm height. Therefore, the total volume

of the membrane tank was 6.7 L, but it was operated at 4.32 L. The membrane module of the membrane tank consisted of an ultrafiltration hollow-fiber membrane module (Micronet Porous Fibers SL, Spain) displaced vertically. Wastewater flow entered from the exterior of the membrane and passed to the interior using a suction peristaltic pump. The total membrane area was 0.20 m^2. Hollow fibers were made of polyvinylidene fluoride and had a core reinforcement of polyester. The fibers were 2.45 mm external diameter and 1.10 mm internal diameter, with 0.04 µm pore diameter. Aeration in the membrane tank was exerted by a CAP 3 coarse bubble diffuser (ECOTEC SA). The membrane module operated under continuous aeration with tangential air flow to avoid deposition of solids onto the membrane surface. Aeration was provided by the working of an ACO-500 air compressor (Hailea). The air flow in the membrane tank was regulated through a valve and was measured continuously using a 2100 Model rotameter (Tecfluid SA). The air flow was provided at 500 L h^{-1} and at constant pressure and temperature of 0.5 bar and 20 °C, respectively. The permeate was extracted using a suction-backwashing peristaltic pump and collected in the permeate tank. The operation of the membrane was cyclical and consisted of permeate extraction and backwashing of 9 and 1 min, respectively. The MBR was operated at a constant flow of 14.9 L m^{-2} h^{-1}, with transmembrane pressure varying between 0.1 and 0.5 bar. The membranes were cleaned chemically using NaClO every 2 weeks to maintain transmembrane pressure in that range. The bioreactors used in this study were also analyzed under the same conditions, with the exception of salinity-amended influent, by other authors.[12]

The three pilot-scale plant configurations used in this study were an MBR system and two hybrid MBBR–MBR systems (hybrid MBBR–MBRanox and hybrid MBBR–MBRn/anox). The differences in the three bioreactors used in this study resided in the use of carriers among them. K1 carriers (AnoxKaldnes AS, Norway), used in this research, have a specific biofilm surface area in bulk of 500 m^2 m^{-3} and a density of 0.92–0.96 g cm^{-3} (Martin-Pascual et al., 2016). The use of carriers was as follows: no carriers in the MBR configuration (MBR); 35% chamber volume in the three

aerobic compartments in the hybrid MBBR–MBRanox configurations; and 35% chamber volume in the three aerobic chambers and in the anoxic chamber for the hybrid MBBR–MBRn/anox configuration. The different configurations are shown in Figure 1.

2.3 Experimental procedure

The pilot-scale plants operated at a constant flow rate of 2.98 L h^{-1} and at a hydraulic retention time (HRT) of 9.5 h. The recycling flow rate was five times the influent flow rate. Influent flow rate was controlled in each of the pilot-scale plants by a water-level sensor connected to the feeding pump, ensuring that the working volume of each pilot-scale plant was suitable. The sludge retention time (SRT) of the systems was set to 58.3 days.

Samples were taken from the influent consisting of salinity-amended municipal wastewater and from the three effluents of the pilot-scale plants. Furthermore, mixed liquor samples were taken from the anoxic and aerobic zones of each pilot-scale plant. The three systems were monitored for a period of 84 days. Monitoring of system performance was done by dividing the operation period into four phases, each 21 days long. Thus, Phase 1 comprised operational days 1–21, Phase 2 days 22–42, Phase 3 days 43–63, and Phase 4 days 64–84. This division was done to evaluate the start-up and stabilization phases in the three systems. The Phases 1, 2, and 3 corresponded to the start-up of the systems, in which the adaptability of the microbiota was analyzed for each of the bioreactors operated. Once the desired biomass concentration (2500 mg L^{-1}) was reached in each of the systems Phase 4 started, in which the analysis of the system under stabilization conditions was done.

2.4 Physicochemical determination and statistical analysis

Temperature, electrical conductivity, and pH were measured in the influent, the three effluents and in the anoxic and aerobic zones of the three pilot-scale plants each working day using a PCE-PHD 1 multimeter (PCE Ibérica SL, Spain). Additionally, dissolved oxygen concentration was measured with a PCE-PHD 1 multimeter (PCE Ibérica SL) in each of the anoxic and aerobic zones on each day of operation.

Chemical oxygen demand (COD), biochemical oxygen demand on the fifth day (BOD_5), total suspended solids (TSS), fixed suspended solids (FSS), and volatile suspended solids (VSS) were measured according to established standard protocols (APHA, 2012). Ammonium, nitrite, nitrate, and total nitrogen (TN) were measured by ionic chromatography using an electrical conductivity detector (Metrohm®, Metrohm AG, Switzerland).

Carrier samples were collected from each anoxic zone and from one of the aerobic zones of each of the three pilot-scale plants to evaluate their attached biomass concentration following the procedure developed previously for hybrid MBBRMBR systems (Martin-Pascual et al., 2012; Leyva-Diaz et al., 2014; 2015a; 2015b), except that the number of carrier samples taken was higher for a better measurement of the low attached biofilm observed. This evaluation was done as follows: 10 representative carriers were extracted at random from a given chamber; later, these carriers were submerged into Tween 80 solution; then, the carriers were sonicated for 3 min at 3000 rpm to ensure the separation of fixed biofilm from the carriers; finally, the samples were centrifuged, filtered using a 0.45 μm filter, dehydrated at 105 °C and measured. Attached biofilm concentration was extrapolated to that for the given chamber, as the total number of carriers per chamber was known.

Data from physicochemical monitoring of COD, BOD_5, TN, and TSS were used to develop analysis of variance (ANOVA) tests in order to define statistically significant differences between the three bioreactors during the whole experiment period and in every bioreactor through the

different phases of operation. The ANOVA tests were performed using R-Project statistical software.

2.5 Respirometric tests

Respirometric tests to characterize the kinetics of heterotrophic and autotrophic biomass were carried out for each of the pilot-scale plants. They were used to analyze the consumption of organic matter and nitrogen within the systems, respectively. These tests were conducted using a BMAdvance Multipurpose (SURCIS SL, Spain) gas flux/static liquid respirometer (Spanjers et al., 1998). Dissolved oxygen concentration was continuously measured during the test in order to infer the oxygen consumption of the microorganisms while biodegrading a given quantity of added metabolic substrate. Prior to the respirometric test, a mixed liquor sample containing suspended biomass and carriers (if any) from one of the aerobic chambers of each pilot-scale plant was collected and kept under continuous aeration for 18–24 h at 20 °C in order to consume all substrates available in the sample. This sample was collected to provide a 1 L representation of the bioreactor's conditions for the respirometric tests and, thus, contained 1 L volume of mixed liquor or 1 L volume of mixed liquor and 35% carriers. The sample was placed into a Peltier thermostat (Dinko Instruments, Spain) which was maintained at a constant temperature of 20.0± 0.1 °C during all respirometric tests. Complete mixing of the sample was achieved using a mechanical stirrer (Dinko Instruments) and continuous recycling from the bottom to the top of the respirometer that was imposed by means of a peristaltic pump. The tested sample was aerated using an air pump, which provided a constant air flow rate of 0.906± 0.001 L min^{-1}. Characterization of the heterotrophic biomass was done using a 500 mg L^{-1} solution of sodium acetate, which was inoculated as substrate under 35%, 70%, and 100% dilutions. In light of this, the total nitrification capacity of autotrophic biomass was characterized using a 150 mg L^{-1} ammonium chloride solution, which was inoculated in the bioreactor under 35%, 70%, and 100% dilutions. Moreover, bacterial

cell decay was characterized by observation of oxygen consumption when the sample was stripped of aeration until dissolved oxygen dropped to 0 mg L^{-1}. During the respirometric tests, the pH of the sample was controlled in the range of 7.75±0.75. The dissolved oxygen concentration was continuously measured using an oxygen sensor (Hamilton Company, USA). Temperature, aeration and recycling flow rate were directly controlled by BM-Advance software (SURCIS SL). An illustrative figure of a respirometric test is shown in Figure 2.

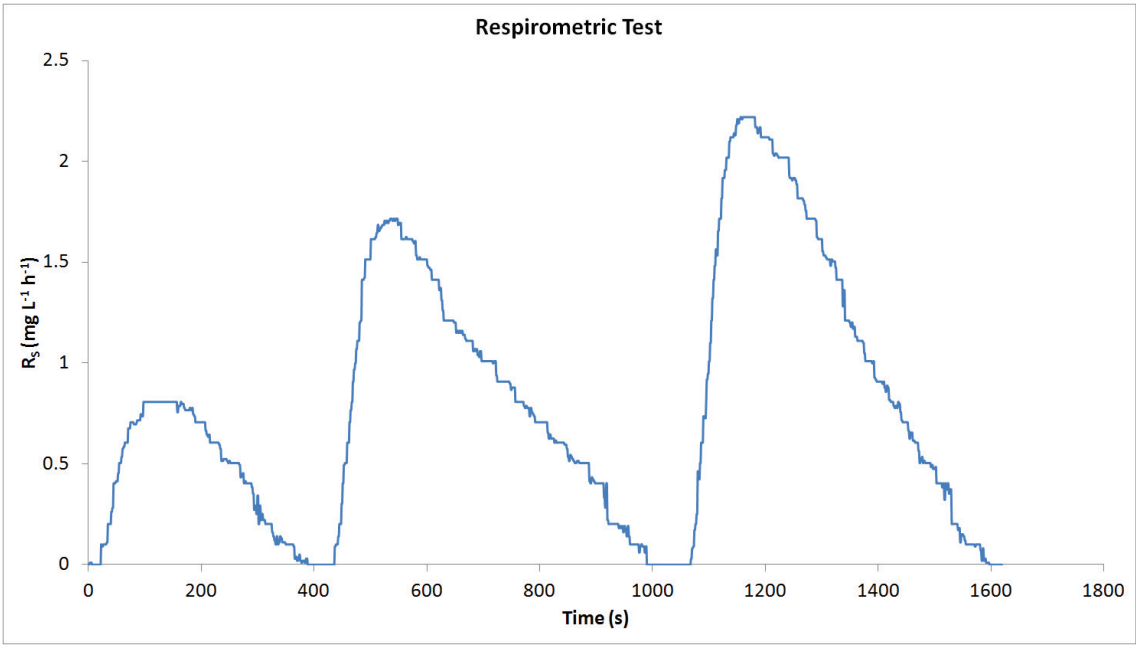

Figure 2 - Example of a respirometric test for the heterotrophic biomass from the MBR working with 6.5 mS cm^{-1} (3.5 g L^{-1} of NaCl) salinity-amended urban wastewater.

2.6 Kinetic parameter estimation

Acquisition and visualization of the respirometric tests was done using BM-Advance software (SURCIS SL). These data were used to assess a number of kinetic parameters for the characterization of the heterotrophic and autotrophic biomass contained in the sample. The calculation procedure was carried out following the one described by Leyva-Diaz et al. (2013a).

3. Results and Discussion

3.1 Biofilm formation and mixed liquor suspended solids concentration

The biomass developed inside the pilot-scale plants was achieved by the feeding of influent wastewater and the recycling of membrane tank wastewater. The biomass inside the pilot-scale plants was monitored during the whole experiment period. A representation of the biomass concentration in the three pilot-scale plants is shown in Figures 3A–C for MBR, hybrid MBBR–MBRanox, and hybrid MBBR–MBRn/anox, respectively. Moreover, the evolution of the fixed biofilm in the hybrid MBBR–MBRanox and hybrid MBBR–MBRn/anox is shown in Figures 3E, D, respectively. In this regard, the suspended solid concentrations in aerobic and anoxic chambers during the experimentation period are given in Table 1.

Table 1 - Suspended solids concentration and biofilm density during experiment time

Parameter	MBR		Hybrid MBBR-MBRanox		Hybrid MBBR-MBRn/anox	
	Aerobic	Anoxic	Aerobic	Anoxic	Aerobic	Anoxic
Phase 1 (Day 1 - Day 21)						
MLSS (mg L^{-1})	541.2±212.82	520.36±2	688.33±275.51	674.24±270.00	608.87±268.3	602.84±265.64
MLVSS (mg L^{-1})	367.13±158.9	352.55	444.6±161.88	458.32±178.2	389.47±183.47	385.28±199.23
BD (mg L^{-1})	-	-	3.47±2.9	2.85±1.9	6.87±3.56	-
VBD (mg L^{-1})	-	-	2.6±2.17	2.31±2.14	5.15±2.67	-
Phase 2 (Day 22 - Day 42)						
MLSS (mg L^{-1})	1269.4±251.9	1215.24±	1478±249.24	1508.16±246.7	1342.93±316.1	1369.70±310.81
MLVSS (mg L^{-1})	877.13±246.9	850.68	950.93±254.22	965.12±170.26	884.93±294.63	944.61±280.20
BD (mg L^{-1})	-	-	20.4±8.35	19.68±8.94	19.13±9.9	-
VBD (mg L^{-1})	-	-	15.3±6.26	13.90±6.34	14.35±7.42	-
Phase 3 (Day 43 - Day 63)						
MLSS (mg L^{-1})	1997.8±334.4	1906±32	2132.07±187.1	2046.79±182.1	2042.53±264.2	2032.32±256.27
MLVSS (mg L^{-1})	1393.47±257.	1002.93±	1371.8±225.64	1370.82±223.4	1295.33±297.0	1288.68±288.30
BD (mg L^{-1})	-	-	13.53±11.58	11.48±10.74	12.27±10.87	-
VBD (mg L^{-1})	-	-	11.73±9.37	9.4±8.65	11.07±9.3	-
Phase 4 (Day 64 - Day 84)						
MLSS (mg L^{-1})	2597.83±64.1	2508.50±	2414.11±87.94	2541.50±144.7	2527.78±127.8	2591.44±88.70
MLVSS (mg L^{-1})	1772.33±211.	1524.61±	1677.78±332.5	1708.39±272.9	1748.22±252.2	1890.72±236.27
BD (mg L^{-1})	-	-	21.11±11.80	17.38±10.21	17.27±14.31	-
VBD (mg L^{-1})	-	-	17.38±10.21	13.68±8.49	14.72±12.73	-

In the pilot-plant MBR, the biomass concentration was provided only for suspended biomass measured as mixed liquor suspended solids (MLSS), given that no carriers were provided in any of the bioreactor's chambers. The evolution of MLSS inside the aerobic chambers of the MBR showed a slow constant increase in biomass concentration.

The most important characteristic of the hybrid MBBR– MBRanox and hybrid MBBR–MBRn/anox with respect to their biomass concentration was the low concentration of attached biomass in both aerobic and anoxic chambers, with biofilm density (BD) always lower than 50 mg L^{-1}. These values were low in comparison with suspended biomass, with mean values in the range of 500–2500 mg L^{-1} during the whole experiment period (Figure 3). However, Leyva-Diaz et al.[12] reported that, in hybrid MBBR–MBRanox and hybrid MBBR–MBRn/anox treating unmodified-saline urban wastewater, the attached biomass was in the range of 1500 mg L^{-1} after 60 days of operation; thus, fixed biofilm concentrations were 30 times higher for the regular salinity operation than for the amended-salinity operation developed in the present study. As a result, under our experimental conditions, the biomass concentration in the three bioreactors was provided mainly by the suspended biomass. It is possible that feeding of the bioreactors with saline wastewater could have reduced the formation of attached biomass to the plastic carriers during the startup of the systems. Salinity inhibition of biofilm formation has been observed in different attachment media and different bacterial species, such as *Pseudomonas aeruginosa*, *Halomonas meridiana*, *Halomonas aquamarina*, *Kushneria indalinina*, and *Aeromonas hydrophila*, under salinity conditions as low as 3 g L^{-1} (Bazire et al., 2007; Qurashi et al., 2012; Jahid et al., 2015). In light of this, colonization of carriers by planktonic bacteria could be affected by the salinity levels in the three pilot plants. Furthermore, the evolution of bacterial biomass in the three pilot plants was slower than that in the three pilot plants operated under an unmodified salinity scenario, in which a concentration of 2500 mg L^{-1} was achieved after approximately 30 days of operation (Leyva-Diaz et al., 2015b), while the time needed to achieve solids concentrations of around 2500 mg L^{-1} was of about 80 days under salinity-amended wastewater.

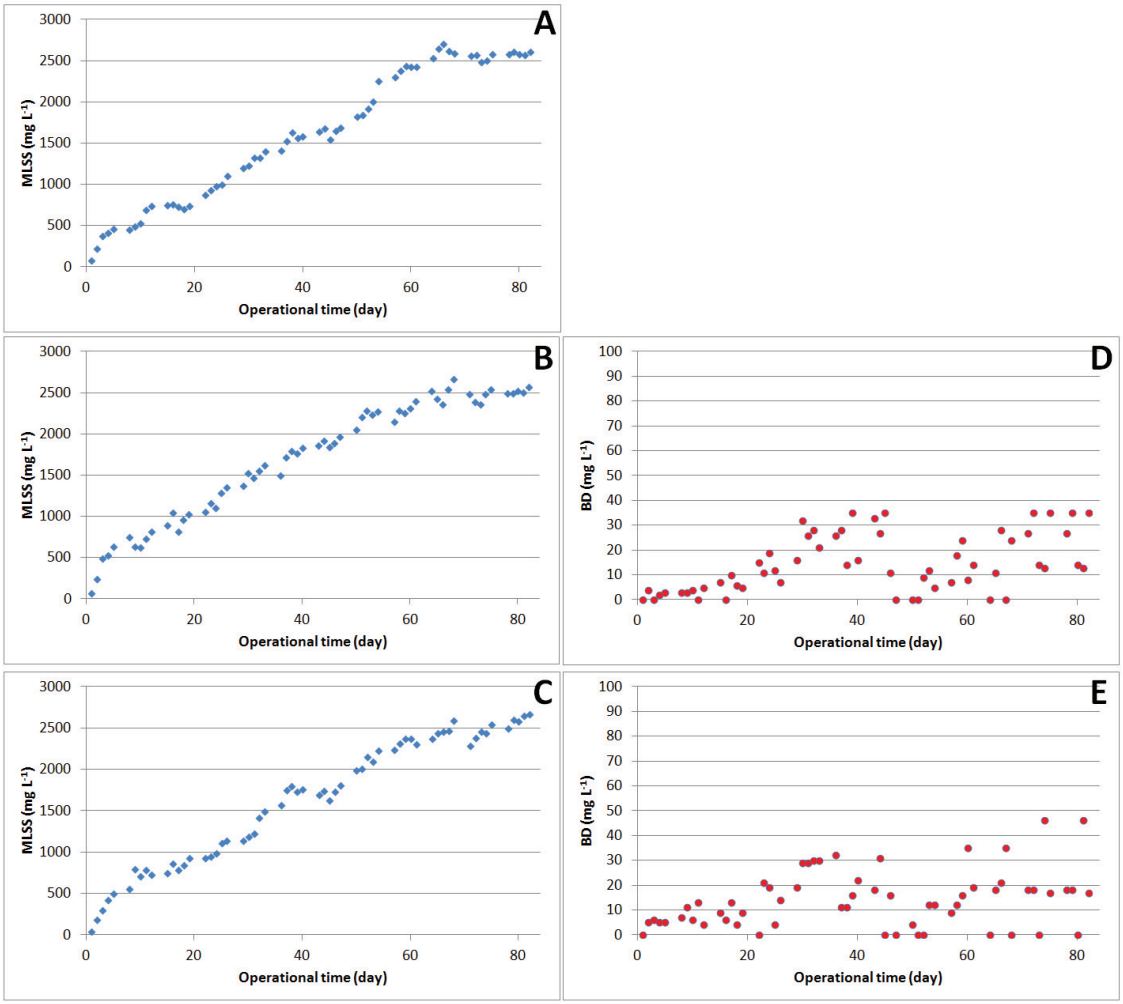

Figure 3 - Mixed liquor suspended solids concentration in the three bioreactors during the whole experiment time for the MBR (A). hybrid MBBR-MBRanox (B) and hybrid MBBR-MBRn/anox (C) and biofilm density for the hybrid MBBR-MBRanox (D) and hybrid MBBR-MBRn/anox (E). Mixed liquor suspended solids concentration is represented by blue diamonds (◆) and biofilm density by red circle (●).

The experiment conducted at 6.5 mS cm^{-1} (3.5 g L^{-1} of NaCl) salinity showed that growth of biomass was affected by salinity. In this regard, salinity slowed down the growth of biomass within the three pilot plants, and decreased the growth of attached biomass. These results are in accordance with previous research (Li et al., 2015) and will be of importance regarding the operation of MBBR for treating high-salinity wastewater. The startup of the systems under salinity-amended urban wastewater seemed to negatively affect the formation of attached biomass in the hybrid MBBR-MBR configurations. Extensive detachment of biomass on carriers of around 0.8 g L^{-1} was found for MBBR-MBR systems subjected to a salinity shock (Di Trapani et al.,

2014a). In light of this, even though biofilms are capable to adapt to saline conditions (Sun et al., 2010), it is possible that microorganisms responsible for attached biomass formation could not develop biofilms on carriers in presence of certain concentrations of NaCl.

3.2 Physical and chemical parameters

The mean values, along with their standard deviation, of the parameters pH, temperature, conductivity, and dissolved oxygen in the influent and the aerobic and anoxic chambers of the three pilot plants during the experiment period are shown in Figure 4. The electrical conductivity was close to 6.5 mS cm^{-1} (3.5 g L^{-1} of NaCl) in the influent and all chambers, which was done to replicate a high-salinity wastewater scenario. A significant drop in pH values was clearly detected in all chambers with respect to the influent (Figure 4). Probably, as Leyva-Diaz et al. (2015b) have previously described, this important decrease in the pH values could be driven by the nitrification process taking place within the pilot plants. In this way, biological nitrification would increase the concentrations of nitrite and nitrate, which decreases pH. The pH was slightly higher in the anoxic chambers than in the aerobic chambers. This could have been caused by a denitrification process being developed in the anoxic chambers, in which nitrite and nitrate concentrations decrease and the pH is increased. The experimental procedure was carried out during the months of May–July, with a constant temperature in the influent and chambers of 21 °C. The dissolved oxygen level was adjusted between 1.6 and 2.4 mg O_2 L^{-1} in the aerobic chambers and provided sufficient oxygen for mineralization of organic matter and oxidation of ammonium to nitrite and nitrate. Low dissolved oxygen concentrations were achieved in the aerobic chambers in order to minimize the entrance of oxygen in the anoxic chamber. Extensive aeration was used in the membrane tank in order to avoid deposition of biofilm on the surface of membrane fibers. This caused the existence of low dissolved oxygen in the anoxic chamber—means between 0.4 and 0.7 mg O_2 L^{-1} (Figure 4)—as the aerated mixed liquor was pumped from the membrane tank

to the bioreactor. However, in order to reduce this effect, an intermediate aerobic chamber was placed between the membrane tank and the anoxic chamber.

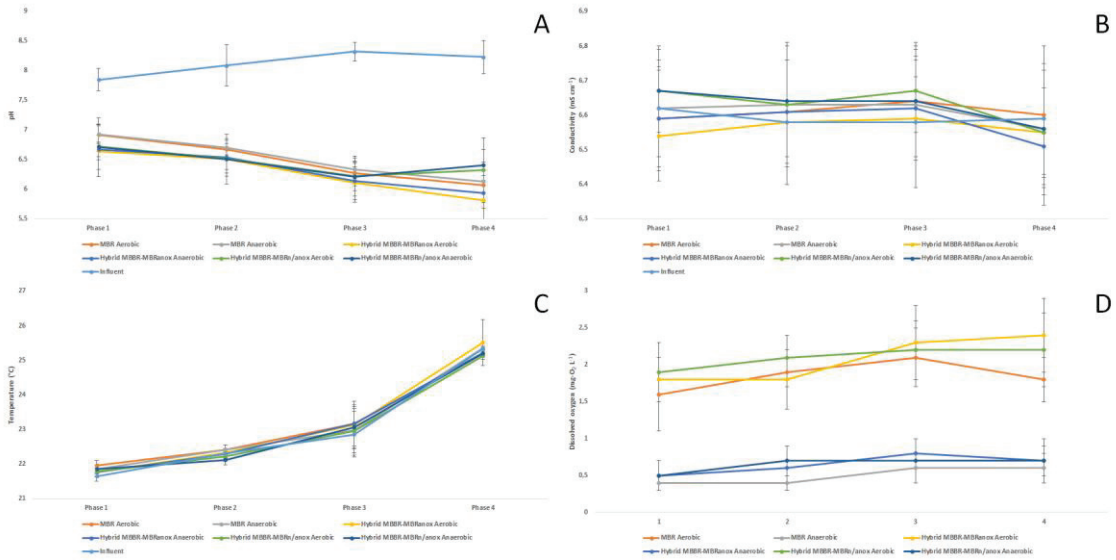

Figure 4 - Average values of pH (A), conductivity (B), temperature (C) and dissolved oxygen (D) in the three pilot-plants during the experiment time

3.3 Organic matter, suspended solids, and nitrogen removal

The performance of the three pilot plants working under salinity conditions was analyzed for the purpose of organic matter and nitrogen removal (Figure 5). The mean values of the COD, BOD_5, and ammonium, nitrite, nitrate, and TN concentrations in the influent and effluent of each pilot plant during the experiment period are shown in Table 2. In addition, the performance of the three pilot plants in terms of TSS, COD, BOD_5, and TN removal for the experiment period is shown in Table 2. Results are given for each of the four phases. In Table 3, the *P* values given by the ANOVA tests comparing the three configurations in each of the operational phases and comparing the transitions between phases are shown.

The removal of TSS by the membrane was very good during the total experimental period. TSS removal rates decreased slightly with the passing of operational days, dropping from the range of 98% to 99% in the first phase to the range of 97– 98% during the mineralization phase. As

expected, differences were not statistically significant ($P > 0.05$) as shown by ANOVA tests comparing the three technologies during the whole experiment period, given that a 0.04 µm pore diameter membrane was used in the experimentation. On the other hand, other parameters such as COD, BOD_5, and TN showed significant statistical differences during the experiment time.

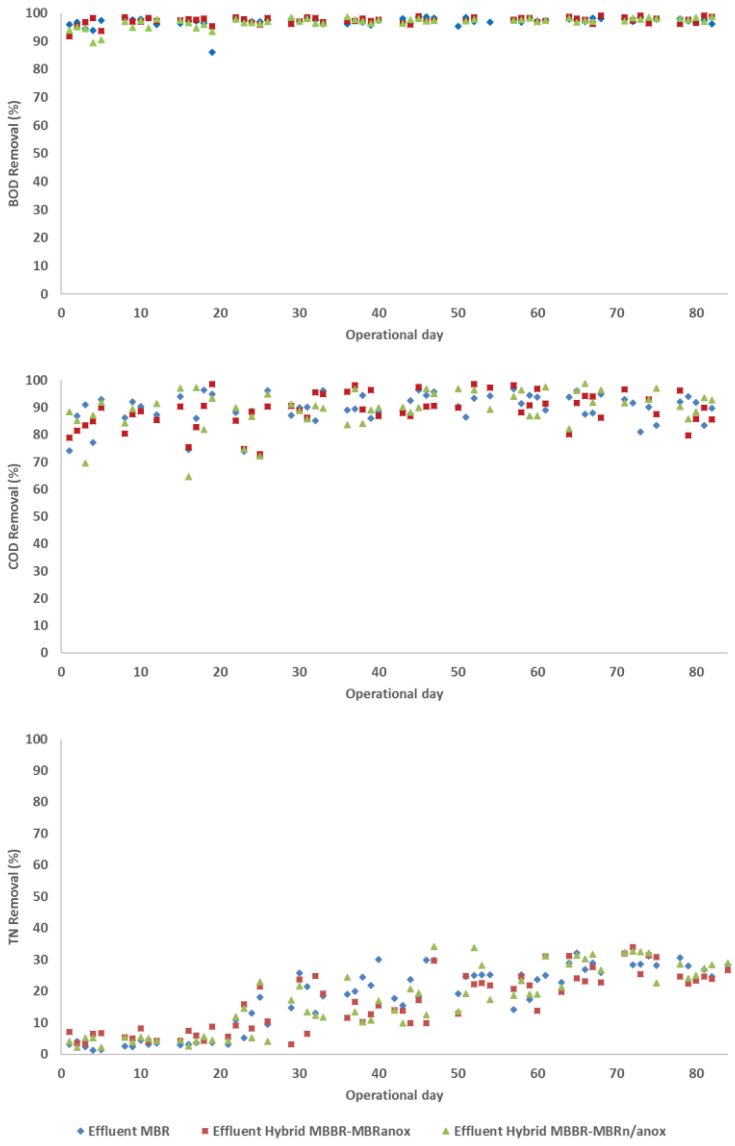

Figure 5 – Removal performances of BOD_5, COD and TN for the MBR and the two hybrid MBBR-MBR systems during the operational time

Table 2 - Organic matter and nitrogenous compounds concentrations, as well as organic matter and total nitrogen removal efficiencies, during the experiment time

Parameter	Performance				Parameter	Removal rate		
	Influent	MBR	Hybrid MBBR-MBRanox	Hybrid MBBR-MBRn/anox		MBR	Hybrid MBBR-MBRanox	Hybrid MBBR-MBRn/anox
Phase 1 (Day 1 - Day 21)								
COD (mg O_2 L^{-1})	663.63±253.23	86.06±53.14	97.20±44.74	85.74±57.58	COD (%)	84.13±15.25	82.47±14.22	83.08±19.76
BOD_5 (mg O_2 L^{-1})	335.33±82.97	10.93±4.68	10.53±4.09	10.00±4.86	BOD_5 (%)	96.23±3.02	96.88±1.91	95.13±2.42
TSS (mg SS L^{-1})	343.27±176.67	5.46±2.66	2.88±1.80	2.74±1.67	TSS (%)	98.23±1.54	99.16±0.79	99.51±0.76
TN (mg-TN L^{-1})	112.14±23.35	109.10±17.21	105.42±24.56	107.41±10.47	TN (%)	2.71±2.30	5.99±2.96	3.96±1.91
NH_4^+-N (mg-TN L^{-1})	72.93±2.62	26±9.49	25.14±9.49	34.6±9.49	-	-	-	-
NO_2^--N (mg-TN L^{-1})	0.11±0.49	50.64±15.22	12.87±18.2	21.81±9.49	-	-	-	-
NO_3^--N (mg-TN L^{-1})	0.02±0.1	1.34±0.92	30.47±42.18	0.38±0.05	-	-	-	-
Phase 2 (Day 22 - Day 42)								
COD (mg O_2 L^{-1})	703.67±179.48	79.93±31.73	67.98±34.49	79.28±25.96	COD (%)	87.09±9.05	89.17±7.33	87.46±6.61
BOD_5 (mg O_2 L^{-1})	363.33±46.39	9.27±2.55	8.60±3.18	9.40±3.38	BOD_5 (%)	97.42±0.78	97.62±0.85	97.46±0.78
TSS (mg SS L^{-1})	262.4±80.60	7.60±3.87	6.79±3.05	7.85±3.45	TSS (%)	97.10±1.49	97.41±0.61	97.00±1.23
TN (mg-TN L^{-1})	182.64±15.98	149.51±10.41	153.57±8.59	154.49±10.04	TN (%)	18.14±13.20	14.96±12.29	15.41±13.01
NH_4^+-N (mg-TN L^{-1})	116.44±14.13	48.12±5.24	50.44±3.77	47.31±5.08	-	-	-	-
NO_2^--N (mg-TN L^{-1})	1.4±0.43	74.42±60.54	90.73±69.96	75.34±61.07	-	-	-	-
NO_3^--N (mg-TN L^{-1})	3.46±1.03	0.94±0.35	1.08±14.7	3.91±2.00	-	-	-	-
Phase 3 (Day 43 - Day 63)								
COD (mg O_2 L^{-1})	719.98±212.76	52.15±22.77	60.06±37.03	65.07±49.93	COD (%)	91.63±5.77	89.97±8.77	88.025±14.83
BOD_5 (mg O_2 L^{-1})	418.00±52.26	8.00±3.23	11.40±6.17	10.60±2.82	BOD_5 (%)	98.09±0.72	97.13±2.03	97.43±0.79
TSS (mg SS L^{-1})	271.07±125.87	8.33±2.39	7.65±3.38	7.87±2.45	TSS (%)	96.92±1.12	97.18±1.05	97.10±0.45
TN (mg-TN L^{-1})	183.21±49.34	140.70±21.14	143.00±17.36	147.44±4.05	TN (%)	21.92±9.49	20.33±11.98	20.19±16.81
NH_4^+-N (mg-TN L^{-1})	115.62±41.03	57.29±15.02	50.83±25.47	52.68±0.56	-	-	-	-
NO_2^--N (mg-TN L^{-1})	0.06±0.26	23.85±13.47	7.76±9.43	1.91±1.28	-	-	-	-
NO_3^--N (mg-TN L^{-1})	0.29±0.32	33.65±15.53	57.69±20.35	65.21±3.98	-	-	-	-
Phase 4 (Day 64 - Day 84)								
COD (mg O_2 L^{-1})	654.07±154.57	59.21±32.07	66.87±32.56	51.00±25.11	COD (%)	90.50±4.57	88.55±6.62	91.36±4.43
BOD_5 (mg O_2 L^{-1})	408.33±46.18	9.33±2.40	9.66±4.03	9.22±5.07	BOD_5 (%)	97.69± 0.67	98.09±1.03	97.78±1.04
TSS (mg SS L^{-1})	354.50±22.13	8.84±2.92	6.65±3.74	8.47±3.77	TSS (%)	97.50±0.41	98.12±0.33	97.60±0.34
TN (mg-TN L^{-1})	181.14±28.59	135.99±15.74	138.18±22.19	125.88±43.35	TN (%)	24.29±7.88	22.97±12.76	29.34±7.00
NH_4^+-N (mg-TN L^{-1})	113.45±23.94	49.98±12.41	50.93±18.01	36.92±25.1	-	-	-	-
NO_2^--N (mg-TN L^{-1})	0.03±0.19	11.93±15.82	3.88±7.05	0.96±1.33	-	-	-	-
NO_3^--N (mg-TN L^{-1})	0.55±1.49	48.78±20.04	70.05±19.21	64.28±11.94	-	-	-	-

Table 3 - Results of ANOVA tests for the performance parameters of the three pilot plants during the same operational phase and of performance parameters for each of the pilot plants for transitions between operational phases (*:p-values that indicate statistically significant differences).

		Phase 1			Phase 2			Phase 3			Phase 4			Transition 1 (Phase 1-Phase 2)	Transition 2 (Phase 2-Phase 3)	Transition 3 (Phase 3-Phase 4)
Parameter	Configuration	MBR	Hybrid MBBR-MBR	Hybrid MBBR-MBR	MBR	Hybrid MBBR-MBR	Hybrid MBBR-MBR	MBR	Hybrid MBBR-MBR	Hybrid MBBR-MBR	MBR	Hybrid MBBR-MBR	Hybrid MBBR-MBR			
COD	MBR	-	0.760	0.871	-	0.495	0.899	-	0.545	0.388	-	0.263	0.426	0.524	0.112	0.482
	Hybrid	0.760	-	0.923	0.495	-	0.509	0.545	-	0.665	0.263	-	0.091	0.116	0.787	0.463
	Hybrid	0.871	0.923	-	0.899	0.509	-	0.388	0.665	-	0.426	0.091	-	0.423	0.894	0.375
BOD	MBR	-	0.483	0.284	-	0.510	0.895	-	0.094	0.025*	-	0.428	0.959	0.151	0.021*	0.193
	Hybrid	0.483	-	0.036*	0.510	-	0.592	0.094	-	0.590	0.428	-	0.539	0.185	0.394	0.146
	Hybrid	0.284	0.036*	-	0.895	0.592	-	0.025*	0.590	-	0.959	0.539	-	0.001*	0.934	0.347
TN	MBR	-	0.855	0.552	-	0.242	0.372	-	0.158	0.364	-	0.897	0.776	0.760	0.868	0.498
	Hybrid	0.855	-	0.712	0.242	-	0.337	0.158	-	0.946	0.897	-	0.851	0.372	0.813	0.701
	Hybrid	0.552	0.712	-	0.372	0.337	-	0.364	0.946	-	0.776	0.851	-	0.400	0.887	0.493

The performance of the systems in terms of COD and BOD_5 removal were very high during the whole experimental period. Minimal COD and BOD_5 removal performance was found during the first phase and reached 82.47% and 95.13% for the hybrid MBBR-MBRanox and hybrid MBBR-MBRn/anox, respectively (Table 2). ANOVA tests performed for COD and BOD_5 removal percentage data demonstrated that mean removal values throughout the whole experimental period were not different in terms of statistical significance ($P < 0.05$), which showed the capacity of the three different configurations to eliminate organic matter from saline urban

wastewater. Differences between phases for COD were not significantly detected, as shown by ANOVA tests. On the other hand, transitions from Phase 1 to Phase 2 for the hybrid MBBR–MBRn/anox and Phase 2 to Phase 3 for the MBR had significant statistical differences ($P < 0.05$), but all other values did not. These results suggest that the performance of the

three bioreactors in terms of organic matter removal was not affected by the different bioreactor configurations. This similarity could be linked to the low attached biomass concentrations found in the two hybrid MBBR–MBR systems.

In the mineralization phase, the values for COD and BOD_5 removal, around 87% and 98%, respectively, were similar to those obtained previously by Leyva-Diaz et al.[12] for the three pilot plants operated under unmodified salinity (around 84% for COD and 95% for BOD_5). In this regard, results from this study suggested that the pilot-scale plants could attain similar levels of performance with respect to organic matter removal operating under different salinity scenarios—6.5 mS cm^{-1} (3.5 g L^{-1} of NaCl) in comparison with values around 1.0 mS cm^{-1}. These results are in accordance with those reported by other authors, in which performance in organic matter removal was not affected by the addition of NaCl up to 5 g L^{-1} (Di Trapani et al., 2014a; 2014b; Luo et al., 2015), which is higher than the salinity addition in this experiment (3.5 g L^{-1}).

However, the performance of the system regarding TN removal was inefficient. TN removal was very low in Phase 1 and increased over time. Nitrogen removal could not reach more than 40% in any of the operational phases. The ANOVA tests showed no differences ($P < 0.05$) for the three bioreactors during the whole experimental period but showed significant statistical differences for the bioreactors at different stages. Unlike organic matter and TSS, removal of nitrogen within the systems was inefficient. The reasons for the low TN removal could be the high aeration detected in the anoxic chamber or the slow adaptation of nitrifying communities to the salinity conditions.

In this regard, TN removal in the mineralization phase did not reach 35% for any of the pilot plants during the experiment period—24.29%, 22.97%, and 29.34% removal for MBR, hybrid MBBR–MBRanox, and hybrid MBBR–MBRn/anox pilot-scale plants, respectively. The same pilot plants achieved more than 50% removal of TN working in the unmodified salinity scenario—58.03%, 54.84%, and 56.58% for MBR, hybrid MBBR–MBRanox, and hybrid MBBR–MBRn/anox systems, respectively (Leyva-Diaz et al., 2015b). The loss in TN removal efficiency with respect to an unmodified salinity scenario could be caused by the higher salinity in this experiment. In light of this, a negative effect on nitrogen removal exerted by high-salinity wastewater has been observed. A decrease in TN removal from 23% to 2.5% was observed in MBR systems when influent wastewater changed from 0 to 3 g L^{-1} NaCl addition (Luo et al., 2015). Also, the high dissolved oxygen concentration in the anoxic chambers—0.6–0.7 mg O_2 L^{-1}—could have reduced the efficiency of denitrification, leading to accumulation of nitrate. Dissolved oxygen concentrations in the anoxic chamber were caused by intrusion of oxygen from the previous aerobic chamber. In this experiment, the oxygen intrusion could have been caused by a scale problem, as differences in operational parameters have been observed in MBBR-MBR systems operated at lab- and pilot-scale configurations (Leyva-Diaz et al., 2013b).

Ionic chromatography data showed that ammonium could not be fully oxidized within the pilot plants working at 6.5 mS cm^{-1} (3.5 g L^{-1} of NaCl) salinity in all phases. In addition, data suggested that efficient complete oxidation of ammonium to nitrate was not accomplished until Phase 3, starting at day 43. In the previous phases, significant amounts of nitrite were found in the effluent. Complete oxidation of ammonium to nitrate was achieved working under unmodified salinity (Leyva-Diaz et al., 2014; Di Trapano et al., 2014a). In accordance with these results, ammonium oxidation in MBR showed a decrease with the addition of NaCl (Luo et al., 2015). In fact, it has been shown that the most adverse effect of salinity increase in MBR and hybrid MBBR–MBR systems exposed to a gradual increase in salinity was reported around 2 g L^{-1} NaCl (Di Trapani et al., 2014b). Moreover, other authors reported that 2.5 g L^{-1} NaCl inhibited nitrification activity (Li et al., 2015). On the other hand, concentrations of nitrite were low in the pilot plants, so all oxidized ammonium was found in the form of nitrate.

3.4 Kinetic parameters for autotrophic and heterotrophic biomass

The kinetic parameters of the three pilot plants concerning yield coefficient, maximum specific growth rate, Monod half-saturation constant, and decay coefficient for heterotrophic and autotrophic biomass during the experimental period are shown in Table 4. The values reported for the kinetic characterization of heterotrophic and autotrophic biomass for the unmodified salinity scenario were taken from Leyva-Diaz et al. (2015b).

Table 4 - Kinetic parameters during experiment time

Parameters	Sampling zone		
	MBR	Hybrid MBBR-MBRanox	Hybrid MBBR-MBRn/anox
Phase 1			
Y_H (mg-VSS mg-COD^{-1})	0.6267	0.6228	0.6256
$\mu_{m,H}$ (h^{-1})	0.2149	0.1198	0.2680
K_M (mg-O_2 L^{-1})	535.8944	1047.0272	983.7572
Y_A (mg-VSS mg-N^{-1})	n.d.	n.d.	0.6082
$\mu_{m,A}$ (h^{-1})	n.d.	n.d.	0.0001
K_A (mg-N L^{-1})	n.d.	n.d.	526.1619
k_d (d^{-1})	0.0031	0.0097	0.0072
Phase 2			
Y_H (mg-VSS mg-COD^{-1})	0.5781	0.6121	0.6511
$\mu_{m,H}$ (h^{-1})	0.0843	0.0399	0.0179
K_M (mg-O_2 L^{-1})	497.9114	54.8534	232.4718
Y_A (mg-VSS mg-N^{-1})	n.d.	0.6091	0.6415
$\mu_{m,A}$ (h^{-1})	n.d.	0.0050	0.0399
K_A (mg-N L^{-1})	n.d.	5.4063	150.0080
k_d (d^{-1})	0.0051	0.0080	0.0050
Phase 3			
Y_H (mg-VSS mg-COD^{-1})	0.6744	0.4787	0.4188
$\mu_{m,H}$ (h^{-1})	0.0444	0.0045	0.0100
K_M (mg-O_2 L^{-1})	64.3820	7.8355	46.0155
Y_A (mg-VSS mg-N^{-1})	0.6756	0.6421	0.3289
$\mu_{m,A}$ (h^{-1})	0.0517	0.0031	0.0015
K_A (mg-N L^{-1})	488.3461	6.2660	54.8534
k_d (d^{-1})	0.0081	0.0081	0.0718
Phase 4			
Y_H (mg-VSS mg-COD^{-1})	0.5135	0.4526	0.5034
$\mu_{m,H}$ (h^{-1})	0.0036	0.0018	0.0050
K_M (mg-O_2 L^{-1})	7.8833	7.8386	5.9808
Y_A (mg-VSS mg-N^{-1})	0.5947	0.5947	0.4932
$\mu_{m,A}$ (h^{-1})	0.0031	0.0041	0.0059
K_A (mg-N L^{-1})	6.2660	5.7192	4.7404
k_d (d^{-1})	0.0532	0.0702	0.0870

n.d.: not detected

3.5 Kinetic parameters for heterotrophic biomass

The microbial kinetics of heterotrophic biomass growth in the three pilot plants showed evident differences. During Phases 1–3 (start-up), the MBR showed higher maximum growth rates than

those of the two hybrid MBBR–MBR systems. Thus, the MBR appeared to have the fastest kinetics during the start-up period of the system. Nevertheless, this trend ceased during the stabilization phase, in which the kinetics for the MBBR–MBRn/anox system were faster than that of the MBR. This is reflected in the substrate consumption rate (r_{su}) values for the three configurations during the four operational phases (Figure 4). In general, the r_{su} values were higher for the start-up phases than for the stabilization phase. This behavior of microbial kinetics during the start-up of pilot plants with MBR and MBBR-MBR configurations operating under an unmodified salinity scenario was also found by other authors (Leyva-Diaz et al., 2015c) and could be related to the adaptation of the microbial communities during the start-up period, which in the case of this study would be more critical than in previous experiments regarding the same systems due to operation with salinity-amended wastewater. The low concentrations of biomass in Phases 1–3 caused incomplete consumption of the substrate added during the respirometric tests, which led to high K_M values and to slow kinetics of heterotrophs.

Capodici et al. (2016) also studied the heterotrophic kinetics of an MBR treating salinity wastewater that operated at a constant flux of 19 L m^{-2} h^{-1} and an HRT of 12 h, with a heterotrophic biomass concentration of 2–3 g VSS L^{-1} for the respirometric tests. These authors obtained similar values of K_M regarding those got in the stabilization phase of this study, although the values of $l_{m,H}$ were higher than those obtained in this work. This was probably due to the higher HRT considered by Capodici et al. (2016).

For the stabilization phase, the highest yield coefficients belonged to the MBR pilot plant while the fastest Monod parameters (higher maximum growth rate and lowest half-saturation constant) belonged to the hybrid MBBR–MBRn/anox pilot plant. Regarding previous studies performed in an unmodified salinity scenario, the hybrid MBBR–MBR configuration showed the fastest microbial kinetics in terms of Monod growth model (Leyva-Diaz et al., 2014; Di Trapani et al., 2014a; 2014b).

In this regard, the results suggested that the relation of system configuration and microbial kinetics were not changed by increased salinity.

Differences among the different salinity scenarios in terms of Monod growth model parameters were substantial. Maximum specific growth rate coefficients obtained for the amended salinity scenario—0.0036, 0.0018, and 0.0050 h^{-1} for MBR, hybrid MBBR–MBRanox, and hybrid MBBR–MBRn/anox systems, respectively—were 10-fold lower compared to those reported (Leyva-Diaz et al., 2015b) for the unmodified salinity scenario—0.0191, 0.0214, and 0.02665 h^{-1} for MBR, hybrid MBBR–MBRanox, and hybrid MBBR–MBRn/anox, respectively. However, values for half-saturation constant and yield coefficient were similar in both cases—7.88, 7.84, and 5.98 for the salinity amendment case and 16.47, 9.82, and 8.88 for the regular case.

When the r_{su} of the heterotrophic biomass for the three pilot-scale plants working under salinity amendment was compared with similar experiments (Leyva-Diaz et al., 2015b) at no salinity amendment, it can be observed that the three configurations were more similar in terms of heterotrophic kinetics under salinity conditions. In terms of r_{su}, the hybrid MBBR–MBRn/anox configuration had the fastest kinetics under salinity conditions, while hybrid MBBR–MBRanox had the slowest. The hybrid configuration MBBR–MBRn/anox showed similar values of heterotrophic kinetics working under amended and unamended salinity, while MBR and hybrid MBBR–MBRanox configurations showed much faster kinetics with no NaCl addition. Therefore, it could be suggested that different system configurations did not much affect the heterotrophic kinetics working at 6.5 mS cm^{-1} electrical conductivity (3.5 g L^{-1} of NaCl), while they were a driving parameter for r_{su} with no salinity addition.

3.6 Kinetic parameters for autotrophic biomass

The evolution of kinetics for the autotrophic biomass in the three pilot plants showed the same behavior as that of heterotrophic biomass (Table 4): microbial kinetics was faster for the MBR system than for the two MBBR–MBR systems, which changed in the stabilization phase (Figure 6). This pattern of autotrophic biomass kinetics was also reported for MBR and MBBR–MBR pilot plants with identical configurations to those used in this study during the process of start-up treating regular urban wastewater. (Leyva-Diaz et al., 2015c) The high values of K_A could have been caused by the inability of autotrophic biomass to utilize the whole substrate added during the respirometric tests due to the low biomass concentrations during Phases 1–3.

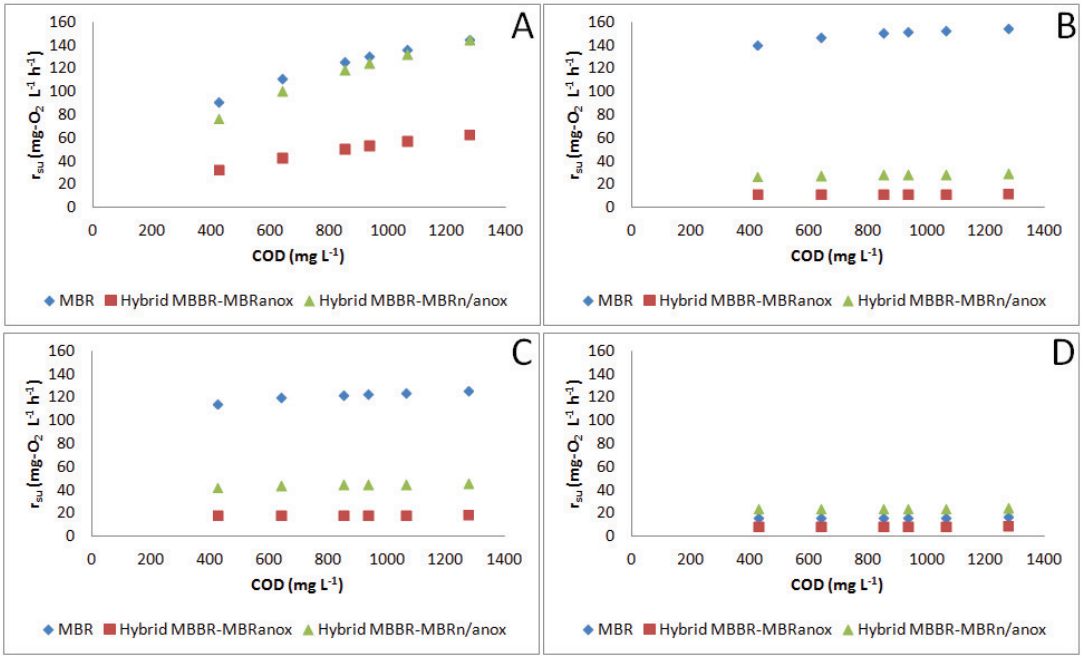

Figure 6 - Rate of substrate utilization (r_{su}) values for the three systems during the experimentation time. A: heterotrophic kinetics in phase 1; B: heterotrophic kinetics in phase 2; C: heterotrophic kinetics in phase 3; D: heterotrophic kinetics in phase 4.

Possibly, the failure to determine autotrophic activity in the early phases of the MBR and hybrid MBBR–MBRn/anox was caused by the low concentration of biomass. The data from Figure 7 show

that autotrophic biomass was favored in the MBBR–MBR systems, which might imply a positive influence of carriers over autotrophic activity under salinity conditions even though attached biofilm concentration was very low in comparison with suspended biomass concentration. The decrease in r_{su} in the stabilization phase compared with the start-up phases could be explained by the salinity adaptation process that the microbiota was subject to. The microbial kinetics of autotrophs in the three pilot plants showed that the hybrid MBBR–MBRn/anox pilot plant, which had carriers only in the three aerobic chambers (see Figure 1), achieved the fastest kinetics. As occurred with heterotrophic microbial kinetics, the hybrid MBBR–MBRn/anox was the configuration that showed the fastest kinetics in salinity conditions. Similar results were obtained by other authors in unmodified salinity scenarios (Leyva-Diaz et al., 2014; Di Trapani et al., 2014a; 2014b).

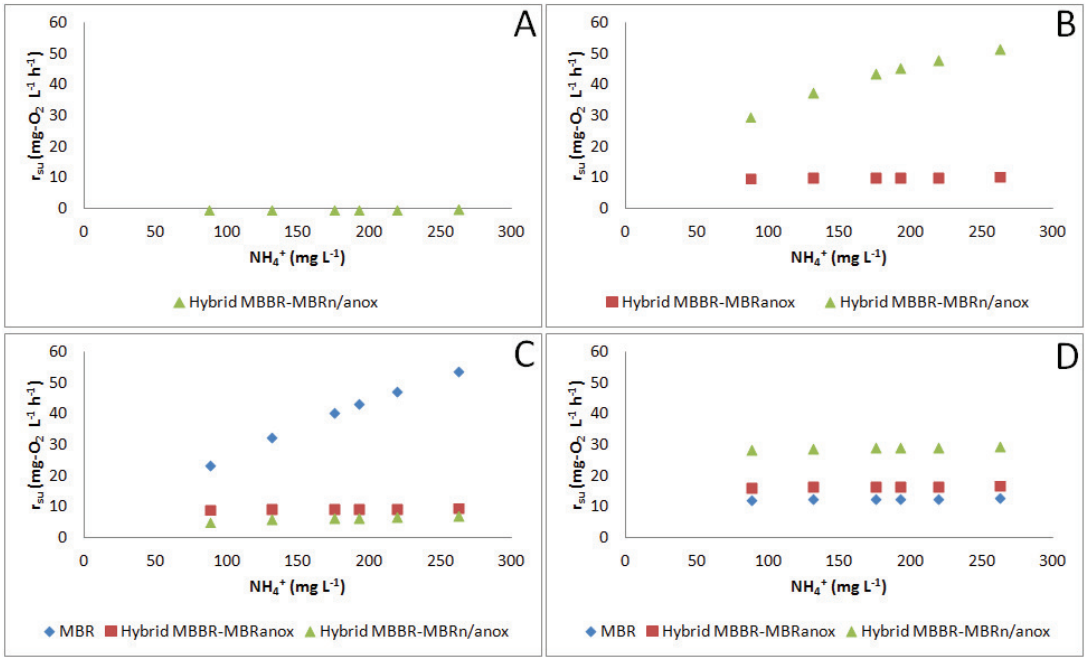

Figure 7 - Rate of substrate utilization (r_{su}) values for the three systems during the experimentation time. A: autotrophic kinetics in phase 1; B: autotrophic kinetics in phase 2; C: autotrophic kinetics in phase 3; D: autotrophic kinetics in phase 4.

In the case of autotroph kinetics, the differences between amended and unamended salinity scenarios in terms of Monod growth model parameters were sharper than for heterotrophic biomass. Maximum specific growth rates for the amended salinity scenario—0.0031, 0.0041, and 0.0059 h^{-1} for MBR, hybrid MBBR–MBRanox, and hybrid MBBR–MBRn/anox,respectively—were 50- to 100-fold lower than those previously reported under unmodified salinity conditions—0.2719, 0.0804, and 0.0928 for MBR, hybrid MBBR–MBRanox, and hybrid MBBR–MBRn/anox systems, respectively. On the other hand, half-saturation constants and yield coefficients were higher for the amended salinity scenario—6.26, 5.72, and 4.74 mg N L^{-1} in comparison with similar experiments performed in unmodified salinity conditions—0.93, 1.08, and 1.11 mg N L^{-1}. Thus, microbial kinetics under salinity was expressed in a lower maximum growth rate and higher half-saturation constant with respect to base salinity.

Data from this research were also compared with previous results obtained in unmodified salinity conditions (Leyva-Diaz et al., 2015b). It can be seen that, for the salinity-amendment scenario, all the configurations showed similar r_{su} values, hybrid MBBR–MBRn/anox being the fastest and MBR the slowest in autotrophic kinetics. Nevertheless, system configuration showed an impact over the autotrophic r_{su} values under unmodified salinity, with MBR attaining much higher values than the other configurations. Moreover, the hybrid MBBR–MBRn/anox configuration in this case showed values close to those at salinity. The hybrid MBBR–MBRanox configuration was faster in terms of microbial kinetics than the hybrid MBBR–MBRn/anox with no salinity addition. As previously described, the hybrid MBBR– MBR was the configuration that showed the fastest kinetics for autotrophic biomass (Leyva-Diaz et al., 2014; Di Trapani et al., 2014a; 2014b). The absence of carriers in the anoxic zone of the hybrid MBBR–MBRn/anox suggests the suppression of competition of suspended biomass vs. attached biofilm for ammonium and nitrite substrates, leading to faster

oxidation of these compounds than in the hybrid MBBR–MBRanox. However, more experimental work will be necessary in order to confirm these preliminary results.

3.7 Decay coefficient for heterotrophic and autotrophic biomass

The highest decay coefficient belonged to the hybrid MBBR–MBRn/anox system, even though they were of similar value in the three cases—5.32%, 7.02%, and 8.70% for MBR, hybrid MBBR–MBRanox, and hybrid MBBR–MBRn/anox pilot-scale plants, respectively. This implies that around 5–9% of the total biomass was lost every day of operation under salinity conditions. In this regard, decay coefficients for the amended salinity scenario were higher than for the unmodified salinity scenario—3.04%, 3.39%, and 3.62% loss of biomass per day for MBR, hybrid MBBR–MBRanox, and hybrid MBBR–MBRn/anox systems, respectively (Leyva-Diaz et al., 2015b). Salinity has been reported as the cause of cell lysis due to an increment in cell transmembrane pressure (Bassin et al., 2012; Castillo-Carvajal et al., 2014). Therefore, a higher decay coefficient for the higher salinity scenario might be directly related to salt pressure over the microbial communities in the bioreactors. On the other hand, hybrid MBBR–MBRn/anox was the configuration with the higher decay coefficient in both cases.

With respect to microbial kinetics of the pilot plants working under base salinity concentration, decay coefficients showed similar values except for the hybrid MBBR–MBRn/ anox bioreactor (Leyva-Diaz et al., 2015b). In this way, salinity seems to little affect microbial kinetics in terms of decay coefficient.

4. Conclusions

MBR and hybrid MBBR–MBR pilot plants were operated in parallel treating urban wastewater with amended salinity, 6.5 mS cm^{-1} (3.5 g L^{-1} of NaCl). Hybrid MBBR–MBR showed a reduction in attached biofilm formation on carriers. The three systems showed similar performance under salinity conditions and an HRT of 9.5 h. Nevertheless, the hybrid MBBR-MBRn/anox had slightly higher efficiencies than the others concerning COD, BOD_5, and TN, with values of 88.68%, 97.78%, and 26.83–33.26% for COD, BOD_5, and TN removals, respectively. This was related to the highest substrate degradation rate for hybrid MBBR–MBRn/anox for heterotrophic and autotrophic biomass, involving maximum growth rates with values of 0.050 and 0.006 h^{-1} for heterotrophic and autotrophic biomass, respectively. Hybrid MBBR– MBR systems showed no superior performance than MBR under salinity conditions.

Acknowledgments

The authors acknowledge the support given by the Department of Civil Engineering and the Institute of Water Research, both part of the University of Granada, as well as the support of the Los Vados WWTP personnel and EMASAGRA, SA. This research was supported by the Ministry of Education, Culture and Sports of Spain in the “Ayudas para contratados predoctorales para la formación de doctores 2014” training plan (BES-2014-067852), by the University of Granada in the “Programa de Ayudas Puente” training plan, and by the “Convocatoria de ayudas a Proyectos de I 1 D Excelencia 2013 program” (CTM2013-48154-P).

Conflict of interest*:* The authors declare that no conflicts of interest are present in this work.

Literature Cited

APHA, AWWA, WEF. (2012) Standard Methods for the Examination of Water and Wastewater, 22nd ed. Washington, DC: American Public Health Association.

Bassin JP, Kleerebezem R, Muyzer G, Rosado AS, Van Loosdrecht MCM, Dezotti M (2012) Effect of different salt adaptation strategies on the microbial diversity, activity, and settling of nitrifying sludge in sequencing batch reactors. *Appl Microbiol Biotechnol* 93: 1281–1294.

Bazire A, Diab F, Jebbar M, Haras D (2007) Influence of high salinity on biofilm formation and benzoate assimilation by *Pseudomonas aeruginosa*. *J Ind Microbiol Biotechnol* 34: 5–8.

Capodici M, Di Bella G, Di Trapani D, Torregrossa M, Viviani G (2016) Respirometry for the characterization of heterotrophic biomass activity: application to a MBR pilot plant operated with two different start-up strategies. *J Environ Eng* 142: 06015009.

Castillo-Carvajal LC, Sanz-Martín JL, Barragán-Huerta BE (2014) Biodegradation of organic pollutants in saline wastewater by halophilic microorganisms: a review. *Environ Sci Pollut Res* 21: 9578–9588.

Cortés-Lorenzo C, Rodriguez-Diaz M, Lopez-Lopez C, SanchezPeinado M, Rodelas B, Gonzalez-Lopez J (2012) Effect of salinity on enzymatic activities in a submerged fixed bed biofilm reactor for municipal sewage treatment. *Biores Technol* 121: 312–319.

Di Trapani D, Di Bella G, Mannina G, Torregrossa M, Viviani G (2014a) Comparison between moving bed-membrane bioreactor (MB-MBR) and membrane bioreactor (MBR) systems: influence of wastewater salinity variation. *Bioresour Technol* 162: 60–69.

Di Trapani G, Di Bella D, Freni G, Torregrossa M (2014b) Analysis of biomass characteristics in MBR and MB-MBR systems fed with synthetic wastewater: influence of a gradual salinity increase. *Chem Eng Trans* 38: 445–450.

Jahid KI, Mizan MFR, Ha AJ, Ha S-D (2015) Effect of salinity and incubation time of planktonic cells on biofilm formation, motility, exoprotease production, and quorum sensing of *Aeromonas hydrophila*. *Food Microbiol* 49: 142–151.

Le-Clech P, Chen V, Fane TAG (2006) Fouling in membrane bioreactors used in wastewater treatment. *J Membrane Sci* 284: 17–53.

Leiknes T, Ødegaard H (2007) The development of a biofilm membrane reactor. *Desalination* 202: 135–143.

Leyva-Diaz JC, Calderon K, Rodriguez FA, Gonzalez-Lopez J, Hontoria E, Poyatos JM (2013a) Comparative kinetic study between moving bed biofilm reactor-membrane bioreactor and membrane bioreactor systems and their influence of organic matter and nutrients removal. *Biochem Eng J* 77: 20–40.

Leyva-Diaz JC, Martin-Pascual J, Gonzalez-Lopez J, Hontoria E, Poyatos JM (2013b) Effects of scale-up on a hybrid moving bed biofilm reactor-membrane bioreactor for treating urban wastewater. *Chem Eng Sci* 104: 808–816.

Leyva-Díaz JC, Martín-Pascual J, Muñío MM, González-López J, Hontoria E, Poyatos JM (2014) Comparative kinetics of hybrid and pure moving bed reactor-membrane bioreactors. *Ecol Eng* 70: 227– 234.

Leyva-Díaz JC, López-López C, Martín-Pascual J, Muñío MM (2015a) Kinetic study of the combined processes of a membrane bioreactor and a hybrid moving bed biofilm reactor-membrane bioreactor with advanced oxidation processes as a post-treatment stage for wastewater treatment. *Chem Eng Process Process Intensif* 91: 57–66.

Leyva-Díaz JC, González-Martínez A, González-López J, Muñío MM, Poyatos JM (2015b) Kinetic modeling and microbiological study of two-step nitrification in a membrane bioreactor and hybrid moving bed biofilm reactor-membrane bioreactor for wastewater treatment. *Chem Eng J* 259: 692–702.

Leyva-Diaz JC, Poyatos JM (2015c) Start-up of membrane bioreactor and hybrid moving bed biofilm reactor-membrane bioreactor: kinetic study. *Water Sci Technol.* 72: 1948–1953.

Li K, Xu J, Yun G, Zhao Y, Dong Z, Liu J, Wang K (2015) Treatment of high salt wastewater in MBBR process strengthened by complex salt-tolerant microorganism. *Chinese J Environ Eng* 9: 2829–2834.

Li H, Zuo W, Tian Y, Zhang J, Di S, Li L, Su X (2017) Simultaneous nitrification and denitrification in a novel membrane bioelectrochemical reactor with low membrane fouling tendency. *Environ Sci Pollut Res* 24: 5106-5117. doi:10.1007/s11356-016-6084-8.

Luo W, Hai FI, Kang J, Price WE, Guo W, Ngo HH, Yamamoto K, Nghiem LD (2015) Effects of salinity build-up on biomass characteristics and trace organic chemical removal: implications on the development of high retention membrane bioreactors. *Bioresour Technol* 177: 274–281.

Luo W, Phan HV, Xie M, Hai FI, Price WE, Elimelech M, Nghiem LD (2017) Osmotic versus conventional membrane bioreactors integrated with reverse osmosis for water reuse: biological stability, membrane fouling, and contaminant removal. *Water Res* 109: 122–134.

Martin-Pascual J, Lopez-Lopez C, Cerdá A, Gonzalez-Lopez J, Hontoria E, Poyatos JM (2012) Comparative kinetic study of carrier type in a moving bed system applied to organic matter removal in urban wastewater treatment. *Water Air Soil Pollut* 223: 1699–1712.

Martin-Pascual J, Reboleiro-Rivas P, Munio MM, Gonzalez-Lopez J, Poyatos JM (2016) Membrane fouling of a hybrid moving bed membrane bioreactor plant to treat real urban wastewater. *Chem Eng Process* 104: 112–119.

Metcalf & Eddy (2003) *Wastewater Engineering: Treatment and Reuse*, 4th ed. Boston: McGraw Hill.

Mines RO Jr, Robertson RR II (2003) Treatability study of a seafoodprocessing wastewater treatability study of a seafood-processing wastewater. *Toxic/Hazard Subst Environ Eng* 9: 1927–1937.

Muhamad MH, Abdullah SRS, Hasan HA, Rahim ARA (2015) Comparison of the efficiencies of attached versus suspended-growth SBR systems in the treatment of recycled paper mill wastewater. *J Environ Manage* 163: 115–124.

Nerenberg R (2016) The membrane-biofilm reactor (MBfR) as a counterdiffusional biofilm process. *Curr Opin Biotechnol.* 38: 131–136.

Norton-Brandão D, Scherrenberg SM, Van Lier JB (2013) Reclamation of used urban waters for irrigation purposes—A review of treatment technologies. *J Environ Manage* 22: 85–98.

Ødegaard H (2006) Innovations in wastewater treatment: the moving bed biofilm process. *Water Sci Technol* 7491: 17–33.

Qurashi AW, Sabri AN (2012) Biofilm formation in moderately halophilic bacteria. *J Basic Microbiol* 52: 566–572.

Ramos AF, Gómez MA, Hontoria E, González-López J (2007) Biological nitrogen and phenol removal from saline industrial wastewater by submerged fixed-film reactor. *J Hazard Mater* 142: 175–183.

Spanjers H, Vanrolleghem P, Olsson G, Doldt P (1998) Respirometry in control of the activated sludge process. In: *Water Quality International'96, Part 2*. Singapore: Selected Proceedings of the 18th Biennial Conference of the International Association on Water Quality, Water Science and Technology.

Sun C, Leiknes TO, Weitzenböck J, Thorstensen B (2010) Salinity effect on a biofilm-MBR process for shipboard wastewater treatment. *Sep Pur Technol* 72: 380–387.

Visvanathan C, Aim RB, Parameshwaran K (2015) Membrane separation bioreactors for wastewater treatment. *Crit Rev Environ Sci Technol* 30: 1–48.

Yang J, Spanjers H, Jeison D, Van Lier JB (2013) Impact of Na^1 on biological wastewater treatment and the potential of anoxic membrane bioreactors: A review. *Crit Rev Environ Sci Technol* 43: 2722–2746.

Wang Y, Jiang X, Wang H, Guo G, Guo J, Qin J, Zhou S (2015) Comparison of performance, microorganism populations, and biophysiochemical properties of granular and flocculent sludge from denitrifying phosphorus removal reactors. *Chem Eng J* 62: 49–58.

Chapter 2

Linkage of microbial kinetics and bacterial community structure of MBR and hybrid MBBR–MBR systems to treat salinity-amended urban wastewater

This chapter has been published in its current form in Biotechnology Progress. The complete citation is the following:

Alejandro Rodriguez-Sanchez, Juan Carlos Leyva-Diaz, Alejandro Gonzalez-Martinez, Jose Manuel Poyatos. 2017. Linkage of microbial kinetics and bacterial community structure of MBR and hybrid MBBR–MBR systems to treat salinity-amended urban wastewater. Biotechnology Progress. 33(6), 1483-1495. doi: 10.1002/btpr.2513

Abstract

Three pilot-scale bioreactors were started up and operated under salinity-amended urban wastewater feeding. The bioreactors were configured as membrane bioreactor and two different hybrid, moving bed biofilm reactor-membrane bioreactor and operated with a hydraulic retention time of 9.5 h, a solid residence time of 11.75 days and a total solids concentration of 2500 mg L^{-1}. The three systems showed excellent performance in sus pended solids, BOD_5, and COD removal (values of 96–100%, 97–99%, and 88–90%, respectively), but poor nitrogen removal (values of 20–30%). The bacterial community structure during the start-up phase and the stabilization phase were different, as showed by b diversity analyses. The differences between aerobic and anoxic biomass—and between suspended and attached biomass—were higher at the start-up phase than at the stabilization phase. The start-up phase showed high abundances of *Chiayiivirga* (mean values around 3– 12% relative abundance) and *Luteimonas* (5–8%), but in the stabilization phase, the domination belonged to *Thermomonas* (3–14%), *Nitrobacter* (3–7%), *Ottowia* (3–11.5%), and *Comamonas* (2–6%), among others. Multivariate redundancy analyses showed that *Thermomonas* and *Nitrosomonas* were positively correlated with fast autotrophic kinetics, while *Caulobacter* and *Ottowia* were positively correlated with fast heterotrophic kinetics. *Nitrobacter*, *Rhodanobacter*, and *Comamonas* were positively correlated with fast autotrophic and heterotrophic kinetics.

1. Introduction

Wastewater treatment is usually carried out by bioprocesses in which microbes in general, and especially bacteria, play a very important role. An efficient utilization of microbes for wastewater treatment can be difficult due to characteristics of wastewater, such as salinity. It has been found that salinity affects microbial communities in wastewater treatment bioreactors in different ways, such as increasing mortality rate due to differential osmotic pressure across cell membranes, inhibition of biodegradation of toxic metabolic intermediate compounds, and reduction of bioavailability of substrates, among others (Bassin et al., 2012; Castillo-Carvajal et al., 2014). Urban wastewater usually has a salinity level between the 0.7 and 3.0 mS cm^{-1} measured as electric conductivity (Norton-Brandao et al., 2013). Nevertheless, there are many industrial processes and human activities that produce wastewater of higher salinity, such as seafood processing, utilization of seawater for toilet flushing, snow-melting strategies in human settlements, or legal or illegal disposal of flowback from gas drilling procedures (Cortes-Lorenzo et al., 2012; Yang et al., 2013; Rosenblum et al., 2017). In this regard, the effect of salinity over microbial communities performing wastewater treatment must be investigated to develop more efficient salinity-wastewater treatment bioprocesses.

One of the most important parameters for activated sludge systems is the mixed liquor suspended solids (MLSS) concentration in the bioreactor, as higher concentrations of solids yield higher concentrations of microbes in the system. Therefore, several technologies have been developed to maximize the solids concentration of activated sludge processes. One of those is the membrane bioreactor (MBR), which uses a membrane with a small pore size for the filtering and cleaning of wastewater. MBR can achieve high MLSS concentrations due to its very efficient separation of water and solids (Visvanathan & Parameshwaran, 2000). In addition, it offers several advantages over conventional activated sludge technology, such as lower footprint required, high sludge retention

time, low sludge production, and high disinfection of effluents; on the other hand, biofouling of membrane is a problem related to the MBR (Visvanathan & Parameshwaran, 2000; Ødegaard, 2006; Le-Clech et al., 2006; Leiknes & Ødegaard, 2007). To solve this, the moving-bed-biofilm reactor (MBBR) technology, in which floating media-denominated carriers are introduced in the bioreactor, was developed. The presence of carriers mitigates the effect of membrane clogging operating under high solids concentrations (Visvanathan & Parameshwaran, 2000). Moreover, the combination of these two technologies has created the MBBR–MBR technology, in which an MBBR is followed by an MBR, yielding lower biofouling of the membrane and faster settleability of the solids with respect to the MBBR and the MBR, respectively (Leyva-Diaz et al., 2015a). An MBBR–MBR system operated with a recycling flow from the membrane tank to the bioreactor is called as hybrid MBBR–MBR (Leyva-Diaz et al., 2014). The utilization of these technologies is very suitable for the treatment of salinity wastewater, as higher solids concentration might mitigate the problems caused by salinity over the growth and kinetics of bioreactor's biomass.

Kinetic modeling of a biological process has been developed to obtain a useful tool for the design and control of these processes, and to evaluate and predict their behavior, from a process engineering point of view (Leyva-Diaz et al., 2014). On the other hand, the characterization of microbial communities in bioreactors through molecular biology techniques has been done to investigate the species of microorganisms present in these engineered systems and as a tool to elucidate the potential ecological roles of these species with respect to wastewater treatment (Gonzalez-Martinez et al., 2016). The combined use of both tools can yield valuable information for the design, operation, and control of bioreactors with diverse affections, such as salinity wastewater.

The main objective of this research was to characterize the bacterial communities developing in the MBR and hybrid MBBR–MBR systems treating salinity wastewater and their relationship with the

microbial kinetics of the biomass under this feeding condition. Three pilot-scale plants with different configurations of MBR and hybrid MBBR–MBR were operated in parallel and fed with the same 6.5 mS cm^{-1} electric conductivity salinity-amended urban wastewater. The bacterial community structure of these technologies treating salinity wastewater was determined during the start-up and stabilization phases, and the microbial kinetics of the biomass present in the systems.

2. Materials and Methods

2.1 Pilot plants description

The experiment consisted in three bioreactors working in parallel and fed with the same wastewater. These bioreactors had three different technological configurations: an MBR system (bioreactor #1), a hybrid MBBR–MBR system with carriers in aerobic and anoxic zones (bioreactor #2), and a hybrid MBBR–MBR system with carriers in the aerobic zone only (bioreactor #3). Each bioreactor was configured with 4 compartments and a membrane tank. Each compartment had 6 L volume. The influent wastewater was introduced in the systems through the first compartment and extracted by membrane filtration from the membrane tank. The influent flow rate was of 2.98 L h^{-1}, which set a hydraulic retention time (HRT) of 9.5 h. The solids retention time (SRT) was of 11.75 days. The system operated with around 2500 mg L^{-1} total solids concentration (TSS) during the stabilization phase. The membrane tank was of 4.32 L. The second compartment of each bioreactor had no aeration to achieve anoxic conditions for nitrogen removal. All other three compartments were aerated using fine bubble diffusers AFD 270 displaced at the bottom of the compartments. The aeration was provided by an air compressor ACO-500 (Guangdong Hailea Group Co., Ltd, Guangdong, China), and the air flow was continuously measured and controlled. For the purpose of complete mixing of the anoxic compartments, mechanical stirrers Multi-Mixer MM-100 were placed in the anoxic compartments. The carriers used were called K1 (AnoxKaldnes

AS, Norway).[11] The filling ratio with carriers was 35% in the anoxic and aerobic compartments for hybrid MBBR–MBRanox, and 35% in the aerobic zone for hybrid MBBR–MBRn/anox. The effective surface area for biomass growth was 500 m^2/m^3 for this kind of carrier. The membrane consisted on a vertical module of ultrafiltration hollow fiber membranes with fibers of 0.04 µm pore size, 2.45 mm external diameter, and 1.10 mm internal diameter. The permeate was forced from the exterior of the fibers to the interior using a peristaltic pump. The membrane tank was aerated by means of a coarse bubble diffuser CAP 3. A schematic flowchart of the bioreactors is shown in Figure 1.

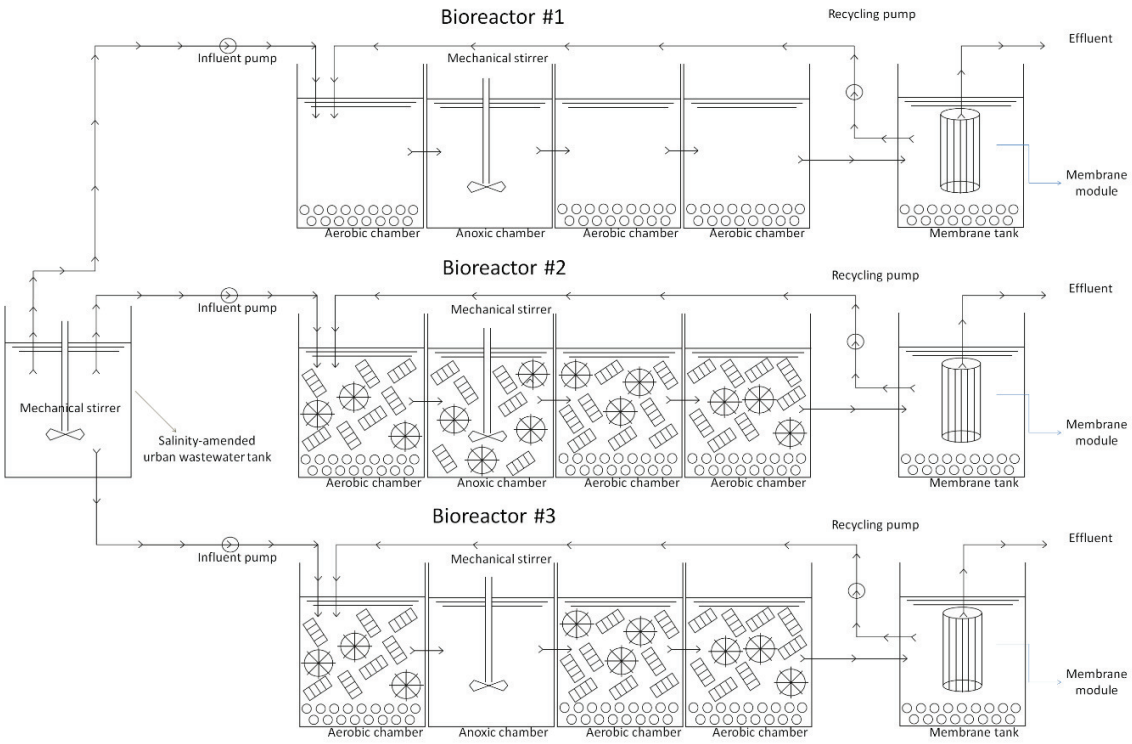

Figure 1 – Schematic of the three pilot plant bioreactors.

2.2 Experimental procedure

The urban wastewater used in the experiment was collected from the Los Vados WWTP (Granada, Spain). Wastewater salinity was then amended using NaCl to achieve an electric conductivity of 6.5 mS cm^{-1} (~3.5 mg L^{-1}) prior feeding to the systems. A recycling flow was set from the membrane tank into the first compartment with a flow rate of 14.9 L h^{-1}. The system was operated during 84 days. The operation was differentiated in start-up (from Day 0 to Day 63) and stabilization phase (from Day 64 to Day 84). The start-up was divided into three phases: phase 1 (Day 0 to Day 21), phase 2 (Day 22 to Day 42), and phase 3 (Day 43 to Day 63). The stabilization phase was named as Phase 4.

2.3 Physicochemical and microbial kinetics analyses

The physicochemical characterization of the performance and the operational system variables was monitored daily. The biochemical oxygen demand at day 5 (BOD_5), chemical oxygen demand (COD), total suspended solids (TSS), attached biofilm density (BD), and volatile suspended solids (VSS) were measured according to the standard protocols (APHA, 2012; Gonzalez-Martinez et al., 2014). The concentrations of ammonium, nitrite, nitrate, and total nitrogen were measured by the means of ionic chromatography (Metrohm AG, Switzerland).

The respirometric tests were developed using a gas/flux static liquid respirometer BM_Advance Multipurpose (SURCIS SL, Spain). For the respirometric tests, a sample of 1 L of mixed liquor (with or without carriers, depending on the bioreactor analyzed) was extracted from the aerobic zone of the corresponding bioreactor and aerated for 18 h at 20 °C. The sample was then introduced into a Peltier thermostat that maintained the temperature of the mixed liquor at 20 °C during the whole respirometric test. The mixed liquor was completely mixed using a mechanical stirrer, continuous aeration, and recycling, and the pH was controlled at 7.00. The characterization of the heterotrophic

and autotrophic biomass was done by addition of 35%, 70%, and 100% dilutions of 500 mg L^{-1} sodium acetate for the heterotrophic biomass and of 150 mg L^{-1} NH_4Cl for the autotrophic biomass, respectively. The characterization of the biomass decay rate was measured by oxygen consumption under no-aeration conditions until the dissolved oxygen of the sample decreased to 0 mg L^{-1}. The calculation of the kinetic parameters was done following the methods of Leyva-Diaz et al. (2014).

2.4 Biological samples collection, DNA extraction, and iTag sequencing process

Samples for microbiological analysis were collected from the three pilot plants in the aerobic zone (first compartment) and in the anoxic zone (second compartment), both in the form of mixed liquor and fixed biofilm, if applicable. For the collection of the mixed liquor samples, 100 mL of mixed liquor was taken from 5 different points evenly distributed in the compartment's volume. For the collection of fixed biofilm samples, a volume of 100 mL of carriers (~90 carriers) was taken from the compartment, avoiding the collection of mixed liquor, from 5 different and evenly distributed points in the compartment's volume. The collection was done at operational days 60 (Phase
3) and 80 (Phase 4), yielding a total of 90 samples.

The collected samples were immediately taken to the laboratory. There the biomass was separated from the water or the carriers, respectively. For the mixed liquor, the samples were centrifuged at 3500 rpm during 10 min at room temperature, then the supernatant was discarded and the remaining pelleted biomass was kept at -20 °C for further DNA extraction. For the fixed biofilm, the carriers were submerged in saline solution (0.9% NaCl) and subjected to 3 min of sonication for biomass detachment. Detached biomass in saline solution was then separated by centrifugation similarly to the mixed liquor samples. The pelleted biomass was kept at -20 °C while the supernatant was also discarded.

The pelleted biomass was then subjected to a DNA extraction procedure using the FastDNA SPIN Kit for Soil (MP Biomedicals, Solon, OH, USA) following the instructions given by the manufacturers. The five DNA extracts obtained from samples with the same biomass type (e.g., mixed liquor or fixed biofilm), collected in the same compartment and in the same date were then merged into a DNA pool. Therefore, 18 DNA pools were obtained. These were kept at -20 °C at all times until further *iTag* sequencing procedure.

The DNA pools were sent to Research & Testing Laboratory (Lubock, TX, USA) to complete an *iTag* sequencing procedure using the Illumina MiSeq equipment and the Illumina MiSeq Reagent Kit v3. The primer pair 28F (5'-GAGTTTGATCNTGGCTCAG-3')-519R (5'-GTNTTACNGCGGCKGCTG-3') was used in the tag-encoded paired-end *iTag* sequencing process for the parallel massive sequencing of DNA fragments corresponding to the hypervariable regions V1–V2–V3 of the 16S rRNA gene of the domain *Bacteria*. The PCR conditions used for the *iTag* sequencing process were preheating at 94 °C during 120 s; 32 cycles of 94 °C during 30 s, 40 °C during 40 s, and 72 °C during 60 s; and elongation at 72 °C for 300 s.

2.5 iTag sequencing postprocess

The 18 DNA pools sequenced by the Illumina MiSeq process yielded 18 paired-end samples (Table 1). The *iTag* sequencing postprocess was done for each of the paired-end samples separately using mother v1.40 software (Schloss et al., 2009). First, the paired-end reads of the same sample were merged into contigs, minimizing the appearance of ambiguous bases in the overlap region, as recommended by Unno (2015). Then, a quality screening was done to eliminate sequences with more than 0 ambiguous bases and/or more than 8 homopolymers. Subsequently, the remaining sequences were aligned against the release 123 of the SiLVA SEED database. Sequences that failed to align properly were discarded. Alignment failures were decided as (1) sequences that did not start in the position of the 28F primer and (2)

sequences that ended further than the 95% of all aligned sequences. The remaining sequences were then preclustered (Huse et al., 2010) into a 2difference threshold, and then subjected to chimera detection and removal using UCHIME 4.2 software (Edgar et al., 2011). After chimera removal, the remanent sequences were classified using the release 123 of the SiLVA SEED database, and those that failed to classify inside the domain *Bacteria* were eliminated. After this process, only high-quality sequences remained. The minimum number of reads among all samples was of 11882, and therefore all samples were rarefied and cut to 11882 reads to conduct a proper ecological analysis. For this purpose, a Phylip distance matrix was calculated for the sequences of each subsample. The distance matrix was then used to cluster the sequences in a 97% similarity threshold OTUs. Then the representative sequence of each OTU was identified and taxonomically classified using the release 123 of the SiLVA SEED database. Finally, the taxonomically classified OTUs were used to develop a consensus taxonomy in an 80% cutoff.

Table 1 – Code names for the biological samples

Sample	Description	Sample	Description
ML1A	Bioreactor #1 mixed liquor of aerobic zone during phase 3	ML1A2	Bioreactor #1 mixed liquor of aerobic zone during phase 4
ML1X	Bioreactor #1 mixed liquor of anoxic zone during phase 3	ML1X2	Bioreactor #1 mixed liquor of anoxic zone during phase 4
ML2A	Bioreactor #2 mixed liquor of aerobic zone during phase 3	ML2A2	Bioreactor #2 mixed liquor of aerobic zone during phase 4
ML2X	Bioreactor #2 mixed liquor of anoxic zone during phase 3	ML2X2	Bioreactor #2 mixed liquor of anoxic zone during phase 4
FB2A	Bioreactor #2 fixed biofilm of aerobic zone during phase 3	FB2A2	Bioreactor #2 fixed biofilm of aerobic zone during phase 4
FB2X	Bioreactor #2 fixed biofilm of anoxic zone during phase 3	FB2X2	Bioreactor #2 fixed biofilm of anoxic zone during phase 4
ML3A	Bioreactor #3 mixed liquor of aerobic zone during phase 3	ML3A2	Bioreactor #3 mixed liquor of aerobic zone during phase 4
ML3X	Bioreactor #3 mixed liquor of anoxic zone during phase 3	ML3X2	Bioreactor #3 mixed liquor of anoxic zone during phase 4
FB3A	Bioreactor #3 fixed biofilm of aerobic zone during phase 3	FB3A2	Bioreactor #3 fixed biofilm of aerobic zone during phase 4

BD: Biofilm Density; VBD: Volatile Biofilm Density

2.6 Analyses of diversity coverage of iTag sequencing subsamples

Following Rodriguez-R & Konstantinidis (2014a), the coverage of each *iTag* sequencing subsample used for the ecological analysis was evaluated using two different methods: complexity curves and redundancy abundance-weighted coverage analysis. The complexity curves were calculated using the aRarefactWin software. The redundancy abundance-weighted coverage analysis was calculated using NonPareil software (Rodriguez-R & Konstantinidis, 2014b) allowing for a 50% sequence overlap and a 95% sequence identity with query set size of 1000 sequences.

2.7 α and β-diversity analyses of the iTag sequencing samples

The *α*-diversity analysis of each subsample was conducted by the calculation of the Hill diversity indices of order 1 and order 2, as they have been defended as the more robust *α*-diversity indices of microbial communities (Haegeman et al., 2013). The Hill diversity indices were calculated using the vegan 2.0 package implemented in R statistical software. The *β*-diversity analysis of pairs of subsamples of interest was done by the calculation of the Morisita–Horn and symmetric indices, reported as the most accurate *b*-diversity estimators for dominant and rare phylotypes, respectively (Barwell et al., 20145. The Morisita–Horn and symmetric indices were calculated using the vegan 2.0 and vegetarian packages implemented in R statistical software, respectively.

2.8 Multivariate redundancy analyses of iTag sequencing samples: linkage of communities with operational conditions and respirometric parameters

Two multivariate redundancy analyses (RDA) were done to link the bacterial communities in the pilot-plant bioreactors with the operational conditions and the respirometric parameters of their biomass. The bacterial communities considered were those with >1% relative abundance in at least one of the 18 *iTag* sequencing subsamples. The data from the operational conditions were COD

removal, BOD removal, TN removal, dissolved oxygen concentration, temperature, conductivity, and pH. The data from the respirometric tests considered for the RDA were the autotrophic and heterotrophic yield coefficients, Monod maximum growth rate, Monod half-saturation constant, and cell decay coefficient. The RDAs were calculated using the CANOCO 4.5 for Windows software with 499 unconstrained Monte-Carlo simulations under a full permutation model.

2.9 Comparison with regular salinity scenario

For the purpose of comparison between the regular and salinity-amended scenarios, the three bioreactors analyzed in this research were also started up and operated for the treatment of regular salinity urban wastewater. The operational conditions were the same for the two cases of regular and amended salinities. The collection of suspended and attached biomass, the DNA extraction procedure, the massive parallel sequencing of the extracted DNA, and the ecological analysis of the massive parallel sequencing samples were done in similar manner as those at the amended-salinity scenario for proper comparison.

3. Results and Discussion

3.1 Physicochemical parameters

The operational parameters and the physicochemical performance of the three bioreactors during Phases 3 and 4 are shown in Tables 2 and 3, respectively. The operational parameters of pH, conductivity, and dissolved oxygen were similar during both phases, while the temperature was slightly higher for the Phase 4. The MLSS concentration was also higher in Phase 4. In this sense, as higher MLSS and higher temperatures have been usually related to higher physicochemical performance and faster kinetics, the values of these parameters were expected to be higher during

Phase 4 than Phase 3. Interestingly, the concentration of fixed biofilm (FB) density was very low compared to the MLSS concentration during all the experiment time, with mean values between 15 and 20 mg L^{-1}. In light of this, it seemed that the ecological relevance of the attached biomass was very low in relation to that of the suspended biomass. The low attached biomass concentration could be caused by the startup of the system under salinity-amended wastewater feeding, as other researches using the same bioreactors configuration under regular salinity wastewater had achieved much higher attached biofilm concentrations, in the range of 1500 mg L^{-1} (Leyva-Diaz et al., 2015a).

Table 2 – Operational parameters of the three bioreactors during phases 3 and 4

Parameter	Sampling zone						
	Influent	Bioreactor #1		Bioreactor #2		Bioreactor #3	
		Aerobic	Anoxic	Aerobic	Anoxic	Aerobic	Anoxic
Phase 3 (Day 43 - Day 63)							
pH	8.32 ± 0.16	6.27 ± 0.29	6.33 ± 0.15	6.11 ± 0.33	6.14 ± 0.32	6.22 ± 0.16	6.21 ± 0.32
Conductivity (mS cm^{-1})	6.58±0.19	6.64±0.16	6.63±0.16	6.59±0.12	6.62±0.14	6.67±0.12	6.64±0.17
Temperature (°C)	22.86±0.65	23.17±0.65	22.97±0.64	23.14±0.67	23.17±0.65	22.96±0.70	23.07±0.64
Dissolved oxygen (mg-O_2 L^{-1})	-	2.1 ± 0.4	0.6 ± 0.2	2.3 ± 0.5	0.8 ± 0.2	2.2 ± 0.4	0.7 ± 0.3
MLSS (mg L^{-1})	-	1997.8±334.42	1906±321.04	2132.07±187.14	2046.79±182.11	2042.53±264.23	2032.32±256.274
MLVSS (mg L^{-1})	-	1393.47±257.94	1002.93±243.99	1371.8±225.64	1370.82±223.49	1295.33±297.09	1288.68±288.30
BD (mg L^{-1})	-	-	-	13.53±11.58	11.48±10.74	12.27±10.87	-
VBD (mg L^{-1})	-	-	-	11.73±9.37	9.4±8.65	11.07±9.3	-
Phase 4 (Day 64 - Day 84)							
pH	8.23 ± 0.28	6.07 ± 0.39	6.13 ± 0.19	5.81 ± 0.42	5.94 ± 0.14	6.32 ± 0.55	6.41 ± 0.26
Conductivity (mS cm^{-1})	6.59 ± 0.16	6.60 ± 0.20	6.56 ± 0.17	6.55 ± 0.18	6.51 ± 0.17	6.55 ± 0.13	6.56 ± 0.19
Temperature (°C)	25.34 ± 0.06	25.19± 0.02	25.36 ± 0.05	25.51 ± 0.66	25.21 ± 0.09	25.13 ± 0.11	25.19 ± 0.09
Dissolved oxygen (mg-O_2 L^{-1})	-	1.8 ± 0.3	0.6 ± 0.2	2.4 ± 0.5	0.7 ± 0.2	2.2 ± 0.5	0.7 ± 0.3
MLSS (mg L^{-1})	-	2597.83±64.11	2508.50±83.71	2414.11±87.94	2541.50±144.75	2527.78±127.80	2591.44±88.70
MLVSS (mg L^{-1})	-	1772.33±211.21	1524.61±279.12	1677.78±332.50	1708.39±272.92	1748.22±252.23	1890.72±236.27
BD (mg L^{-1})	-	-	-	21.11±11.80	17.38±10.21	17.27±14.31	-
VBD (mg L^{-1})	-	-	-	17.38±10.21	13.68±8.49	14.72±12.73	-

MLSS: Mixed Liquor Suspended Solids; MLVSS: Mixed Liquor Volatile Suspended Solids

Table 3 – Performance of the bioreactors during phases 3 and 4

Parameter	Performance				Parameter	Removal rate		
	Influent	Bioreactor #1	Bioreactor #2	Bioreactor #3		Bioreactor #1	Bioreactor #2	Bioreactor #3
Phase 3 (Day 43 - Day 63)								
COD (mg O_2 L^{-1})	719.98±212.76	52.15±22.77	60.06±37.03	65.07±49.93	COD (%)	91.63±5.77	89.97±8.77	88.025±14.83
BOD_5 (mg O_2 L^{-1})	418.00±52.26	8.00±3.23	11.40±6.17	10.60±2.82	BOD_5 (%)	98.09±0.72	97.13±2.03	97.43±0.79
TSS (mg SS L^{-1})	271.07±125.87	8.33±2.39	7.65±3.38	7.87±2.45	TSS (%)	96.92±1.12	97.18±1.05	97.10±0.45
TN (mg-TN L^{-1})	183.21±49.34	140.70±21.14	143.00±17.36	147.44±4.05	TN (%)	21.92±9.49	20.33±11.98	20.19±16.81
NH_4^+-N (mg-TN L^{-1})	115.62±41.03	57.29±15.02	50.83±25.47	52.68±0.56	-	-	-	-
NO_2^--N (mg-TN L^{-1})	0.06±0.26	23.85±13.47	7.76±9.43	1.91±1.28	-	-	-	-
NO_3^--N (mg-TN L^{-1})	0.29±0.32	33.65±15.53	57.69±20.35	65.21±3.98	-	-	-	-
Phase 4 (Day 64 - Day 84)								
COD (mg O_2 L^{-1})	654.07±154.57	59.21±32.07	66.87±32.56	51.00±25.11	COD (%)	90.50±4.57	88.55±6.62	91.36±4.43
BOD_5 (mg O_2 L^{-1})	408.33±46.18	9.33±2.40	9.66±4.03	9.22±5.07	BOD_5 (%)	97.69± 0.67	98.09±1.03	97.78±1.04
TSS (mg SS L^{-1})	354.50±22.13	8.84±2.92	6.65±3.74	8.47±3.77	TSS (%)	97.50±0.41	98.12±0.33	97.60±0.34
TN (mg-TN L^{-1})	181.14±28.59	135.99±15.74	138.18±22.19	125.88±43.35	TN (%)	24.29±7.88	22.97±12.76	29.34±27.00
NH_4^+-N (mg-TN L^{-1})	113.45±23.94	49.98±12.41	50.93±18.01	36.92±25.1	-	-	-	-
NO_2^--N (mg-TN L^{-1})	0.03±0.19	11.93±15.82	3.88±7.05	0.96±1.33	-	-	-	-
NO_3^--N (mg-TN L^{-1})	0.55±1.49	48.78±20.04	70.05±19.21	64.28±11.94	-	-	-	-

With respect to the influent, Phase 3 had higher COD and BOD_5 and lower TSS than the influent in Phase 4. The influent total nitrogen (TN) concentrations were very similar during both phases. For COD, BOD_5, TN, and TSS removal efficiencies, all values were similar at both phases but for TN, which was better during phase 4. This suggested that the heterotrophic communities in the system could successfully mineralize organic matter during both phases, but that nitrifying and/or denitrifying communities were still developing during Phase 3 in comparison to Phase 4. With respect to previous research under regular-salinity wastewater feeding, the values of COD and BOD_5 removal were similar at both salinity scenarios (Leyva-Diaz et al., 2015a). Nevertheless, the removal of nitrogen was much lower at the salinity-amended scenario. In this sense, loss in total nitrogen removal followed by a recovery due to adaptation of biomass was observed in MBR and hybrid MBBR–MBR systems when influent wastewater salinity was gradually increased from regular salinity to 10–16 mg L^{-1} NaCl concentration (Di Trapani et al., 2014; Luo et al., 2015). In these experiments, the systems were operated under steady-state conditions treating regular

urban wastewater prior to the feeding with salinity wastewater. Therefore, it is possible that the presence of sufficient biomass before salinity feeding could lead to a final adaptation under salinity conditions coupled to efficient nitrogen removal, while start-up under salinity conditions would not.

In terms of organic matter and nitrogen removal, the three configurations attained similar performance. Nevertheless, the low concentrations of fixed biofilm in the hybrid MBBR–MBR systems showed problems in biofilm formation during the start-up and stabilization of the bioreactors under salinity wastewater feeding. This suggested that the addition of carriers was not relevant for the performance of the hybrid MBBR–MBR systems, which in practice performed as MBR systems.

3.2 Respirometric parameters

The respirometric parameters of the three bioreactors during Phases 3 and 4 are shown in Table 4. As well, a graphical representation of the rate of substrate utilization during Phases 3 and 4 for all bioreactors is shown in Figure 2. The bioreactor #3 showed similar respirometric values in Phases 3 and 4. On the other hand, the bioreactor #1 had higher substrate utilization ratios at Phase 3 than at Phase 4. The results showed that the MBR had faster kinetics during the start-up phase, but that the bioreactor #2 was the fastest during the stabilization phase. This has also been found by other authors in the start-up of MBR and hybrid MBBR–MBR systems under regular salinity urban wastewater (Leyva-Diaz et al., 2015b). Higher substrate utilization ratios during start-up phase in comparison with stabilization phase have been found previously in MBR and hybrid MBBR–MBR operating under regular salinity wastewater feeding (Leyva-Diaz et al., 2015b). The differences in terms of kinetics were more pronounced for the autotrophic biomass than for the heterotrophic biomass. This is linked to the physicochemical performance of the system, which showed a higher

stability in organic matter mineralization for all bioreactors between Phases 3 and 4 and a slight increase in nitrogen removal between the phases. The respirometric parameters for the heterotrophic biomass showed that maximum growth rates were 10 times lower under salinity wastewater than under regular wastewater (Leyva-Diaz et al., 2015a); also, the respirometric parameters for the autotrophic biomass had up to 100 lower maximum growth rate values and 10 times higher half saturation coefficient values compared to those obtained in the systems working under regular salinity wastewater (Leyva-Diaz et al., 2015a).

Table 4 – Respirometric parameters of the bioreactors during phases 3 and 4

Parameters	Sampling zone		
	Bioreactor #1	Bioreactor #2	Bioreactor #3
Phase 3			
Y_H (mg-VSS mg-COD^{-1})	0.6744	0.4787	0.4188
$\mu_{m,H}$ (h^{-1})	0.0444	0.0045	0.0100
K_M (mg-O_2 L^{-1})	64.3820	7.8355	46.0155
Y_A (mg-VSS mg-N^{-1})	0.6756	0.6421	0.3289
$\mu_{m,A}$ (h^{-1})	0.0517	0.0031	0.0015
K_A (mg-N L^{-1})	488.3461	6.2660	54.8534
k_d (d^{-1})	0.0081	0.0081	0.0718
Phase 4			
Y_H (mg-VSS mg-COD^{-1})	0.5135	0.4526	0.5034
$\mu_{m,H}$ (h^{-1})	0.0036	0.0018	0.0050
K_M (mg-O_2 L^{-1})	7.8833	7.8386	5.9808
Y_A (mg-VSS mg-N^{-1})	0.5947	0.5947	0.4932
$\mu_{m,A}$ (h^{-1})	0.0031	0.0041	0.0059
K_A (mg-N L^{-1})	6.2660	5.7192	4.7404
k_d (d^{-1})	0.0532	0.0702	0.0870

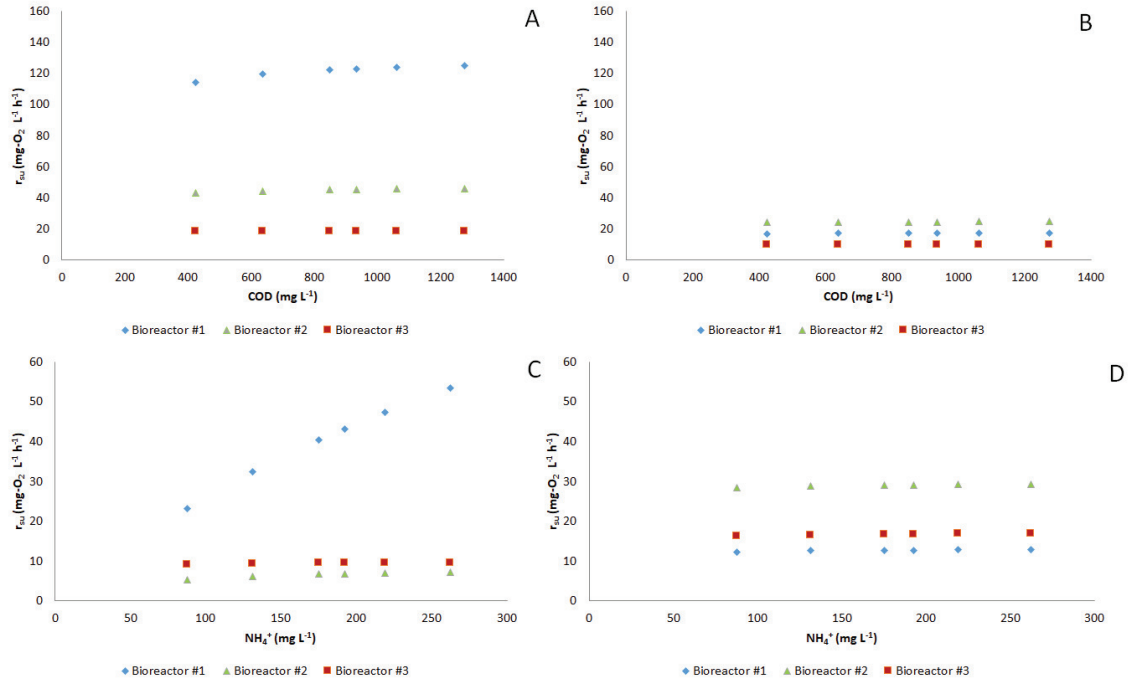

Figure 2 – Graphical representation of the rates of substrate utilization of the heterotrophic and autotrophic biomass of the three bioreactors during Phases 3 and 4. (A) Heterotrophic biomass at phase 3. (B) Heterotrophic biomass at Phase 4. (C) Autotrophic biomass at phase 3. (D) Autotrophic biomass at phase 4.

3.3 Coverage analyses of the iTag sequencing subsamples

The coverage of the *iTag* sequencing subsamples was checked by complexity curves and redundancy abundance-weighted coverage analyses. The complexity curves (Figure 3) showed that the species richness of all subsamples tended to a plateau at reads saturation, which confirmed a good coverage in terms of species diversity. In addition, the coverage values showed by the redundancy abundance-weighted coverage analysis were higher than 91% in all cases, with a mean value of 94.04% and a standard deviation of 1.32% (Table 5). In this sense, it was demonstrated that the iTag sequencing process captured sufficiently the bacterial diversity of the biomass samples analyzed.

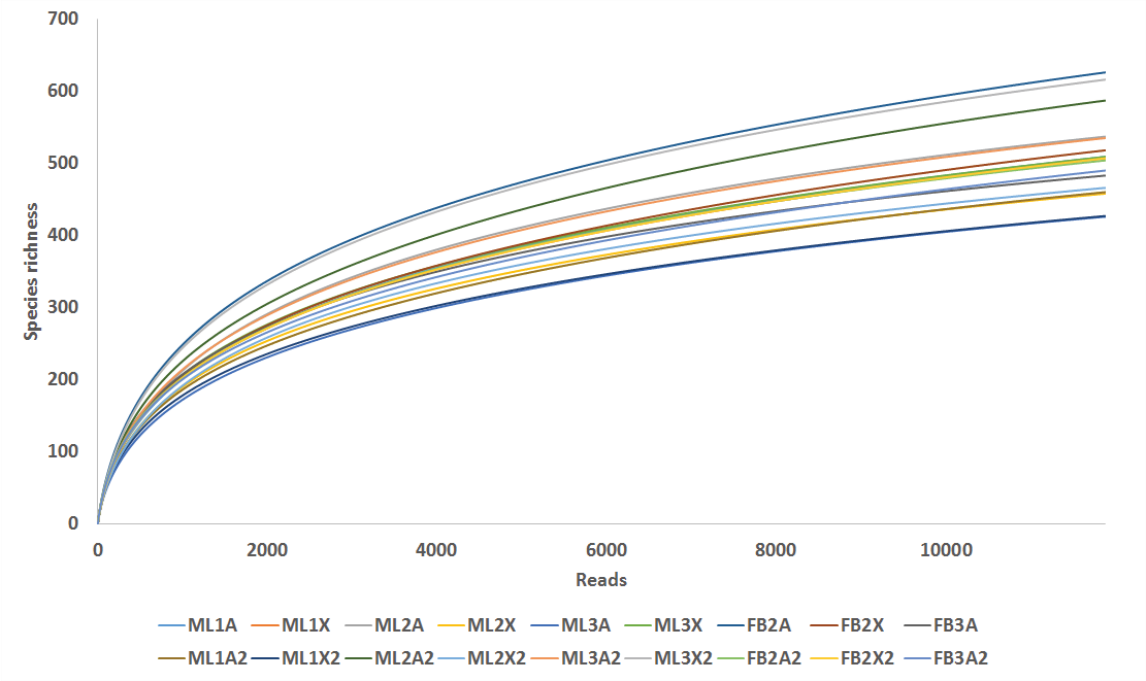

Figure 3 – Complexity curves of the iTag sequencing subsamples.

Table 5 – Redundancy abundance-weighted coverage analysis of the *iTag* sequencing subsamples

Sample	Coverage (%)	Actual effort (Mbp)	Required effort (Mbp)
ML1A	93.06	8.046	2.536
ML1X	93.77	6.994	2.813
ML2A	95.11	16.93	1.875
ML2X	94.66	8.084	2.16
ML3A	97.29	11.24	1.1878
ML3X	94.63	8.245	2.457
FB2A	91.51	17.67	5.024
FB2X	95.06	8.968	2.411
FB3A	94.77	6.401	2.837
ML1A2	94.19	5.879	1.643
ML1X2	95.48	6.355	1.298
ML2A2	92.32	16.91	5.126
ML2X2	92.97	8.677	2.65
ML3A2	93.87	10.2	3.104
ML3X2	93.32	16.9	3.84
FB2A2	93.09	6.147	2.935
FB2X2	94.24	8.596	2.653
FB3A2	93.3	7.363	3.03
Mean	94.03556	9.97805556	2.754433333
SD	1.321404	4.15291166	1.068467816

3.4 α- and β-diversity analyses

The values of the Hill diversity indices of order 1 (Shannon–Wiener index) and of order 2 (Simpson index) showed that the bacterial community structure of all biological samples had high diversity and evenness (Table 6). The similarities among the two sampling dates in the aerobic and anoxic compartments were high in terms of Hill diversity indices values. It was observed that the fixed biofilm had slightly higher values and species richness, as confirmed by the complexity curves. In this sense, the α-diversity analysis showed that the bacterial communities that developed in the bioreactors during Phases 3 and 4 had high richness and evenness, showing the adaptation of myriads of phylotypes during the process of salinity wastewater treatment.

Table 6 – Values of the Hill diversity indices of order zero (species richness), order one (Shannon-Wiener index) and of order two (Simpson index)

Sample	Species Richness	Shannon-Wiener	Simpson
ML1A	509	4.601183	0.97562
ML1X	507	4.730326	0.9774196
ML2A	537	4.677031	0.9756317
ML2X	458	4.511465	0.9657887
ML3A	426	4.380932	0.9709316
ML3X	509	4.791733	0.9819779
FB2A	626	5.059849	0.9848428
FB2X	518	4.725718	0.9761587
FB3A	483	4.81579	0.9834128
ML1A2	460	4.554952	0.975414
ML1X2	427	4.460065	0.9733973
ML2A2	587	4.853788	0.9767825
ML2X2	466	4.493074	0.9676751
ML3A2	535	4.842706	0.9821293
ML3X2	616	5.04133	0.9852005
FB2A2	504	4.78626	0.9827476
FB2X2	507	4.754664	0.9785065
FB3A2	490	4.757814	0.9810416

The values of the *β*-diversity analyses for the pairs of subsamples of interest are shown in Figure 4. The Morisita–Horn values demonstrated that the dominant phylotypes at the first sampling date were substantially different between the bioreactors #1 and #2 with respect to the bioreactor #3 for the aerobic and anoxic mixed liquor biomass, and significantly different for the case of the aerobic fixed biofilm. The similarities between the communities in bioreactor #3 with respect to bioreactors #1 and #2 were higher at the second sampling date. This was caused by a deep change in the dominant phylotypes in the aerobic biomass of bioreactors #1 and #2 from the first to the second sampling date. In this way, it can be said that stable dominant bacterial communities in the aerobic zones of bioreactor #3 were developed at phase 3, while in bioreactors #1 and #2, they developed at phase 4. This could be linked to the differences in respirometric parameters, which showed faster kinetics for the bioreactor #3 than for the bioreactors #1 and #2 during Phase 3, and similar kinetics during Phase 4. Consequently, it was demonstrated that respirometric capabilities of the biomass were closely related to the bacterial community structure in the aerobic compartments of the bioreactors. Interestingly, the anaerobic communities in bioreactors #2 and #3 did not change from Phase 3 to Phase 4 in both mixed liquor and fixed biofilm, while a deep shift was encountered for the case of bioreactor #1. It is possible that the presence of carriers in the bioreactors #2 and #3 provided more stability in the development of anaerobic communities. The Morisita–Horn index values showed that the differences between aerobic and anoxic biomass, both fixed and suspended, were more consistent during the start-up than during the stabilization phase. Given that the biomass could move from one compartment to another and that it was constantly recycled, certain homogeneity of the biomass across compartments was expected. Nevertheless, the results showed that the bioreactors had a more specialized biomass during the start-up phase than during the stabilization phase. In this way, it is possible that the adaptation of the bacterial

communities of the bioreactors tended to the domination of more versatile bacterial species over operation time.

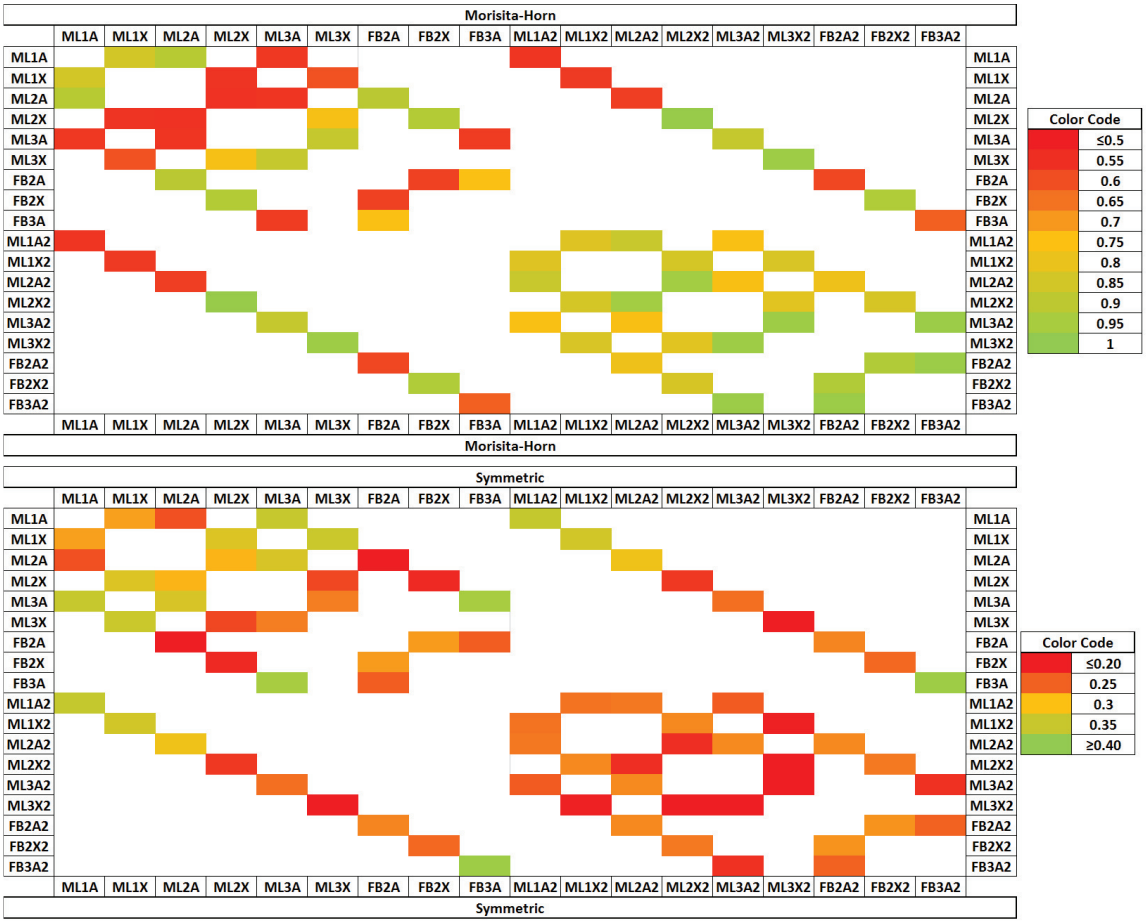

Figure 4 – Beta-diversity of the iTag sequencing subsamples.

On the other hand, the values of the symmetric index showed that the bacterial communities of the bioreactors had a high volatility in terms of rare phylotypes. It seemed that the aerobic zones had more stability in terms of rare species than anoxic zones. The possible cause of this behavior was the continuous entry of microbial communities with the influent, which would promote a competition between established and new rare species. Also, a comparison between the Morisita–Horn and the symmetric indices showed that deep changes in dominant phylotypes between Phases 3 and 4 were related to small changes in rare phylotypes diversity and vice versa. In this

sense, it is possible that the establishment of long-term dominant phylotypes in the bacterial community of the bioreactors would put pressure over the adaptation of rare phylotypes, which would change over time.

3.5 Bacterial community structure of the biomass

As observed by the α-diversity analyses and the complexity curves, the bacterial diversity in all subsamples was high. The bacterial community structure of all genera with >1% relative abundance in at least one of the subsamples is shown in Figure 5.

During Phase 3, the dominant phylotypes in the aerobic mixed liquor biomass of bioreactors #1 and #2 were *Flavobacterium*, *Chiayiivirga*, *Luteimonas*, *Arenimonas*, *Thauera*, and *Rhizobiales*-associated bacteria. This is the first time, to our notice, that genus *Chiayiivirga* has been identified as a major phylotype in a wastewater treatment system. On the other hand, the major represented genera in the aerobic mixed liquor biomass of bioreactor #3 were *Thermomonas*, *Nitrobacter*, *Rhodanobacter*, and *Mycobacterium*. For the anoxic mixed liquor samples, the dominant phylotypes were different for each bioreactor, with *Chiayiivirga*, *Luteimonas*, and *Thauera* in bioreactor #1; *Ottowia*, *Parvibaculum*, *Nitrobacter*, and *Caulobacter* in bioreactor #2; and *Thermomonas*, *Nitrobacter*, and *Comamonas* in bioreactor #3. In the fixed biofilm of bioreactor #2, the domination corresponded to phylotypes that also dominated the mixed liquor biomass. In the bioreactor #3, the dominant genera in the aerobic fixed biofilm were *Luteimonas*, *Chiayiivirga*, *Portibacter*, and *Mariniflexile*, which were substantially different than those in the mixed liquor biomass.

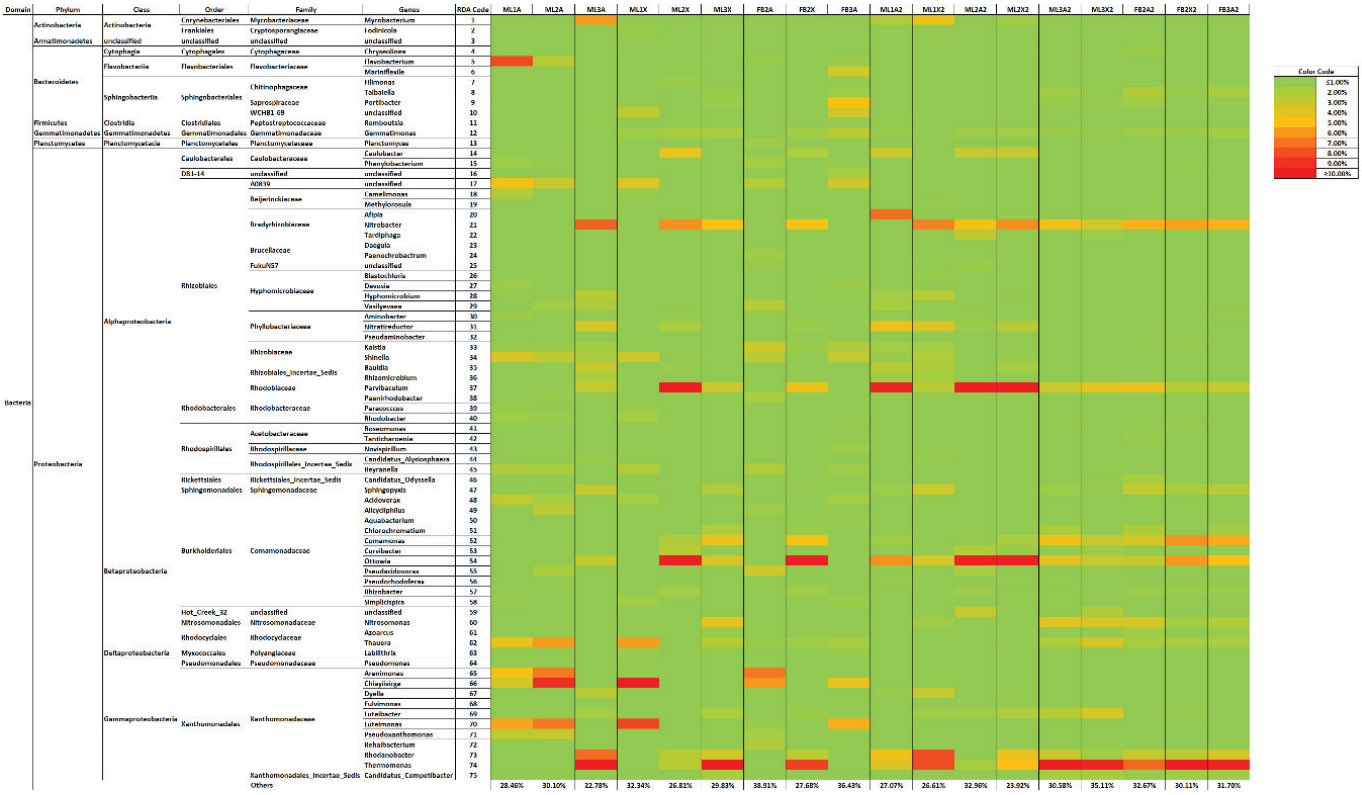

Figure 5 – Heat map of >1% relative abundance OTUs in the iTag sequencing subsamples.

During Phase 4, the bioreactors #1 and #2 suffered a deep change in their dominant aerobic communities, as suggested by the Morisita–Horn index analysis. In bioreactor #1, the dominant phylotypes changed to *Parvibaculum*, *Afipia*, *Ottowia*, and *Rhodanobacter*. In the aerobic biomass of bioreactor #2, the most represented genera were *Rhodanobacter*, *Thermomonas*, *Nitrobacter*, *Ottowia*, *Comamonas*, and *Mycobacterium*. In bioreactor #3, the dominant phylotypes in the aerobic biomass were *Thermomonas*, *Comamonas*, *Nitrobacter*, and *Rhodanobacter*. In the case of anoxic biomass, the dominant phylotypes were similar to those dominating the aerobic biomass. In the anoxic biomass, the major represented phylotypes in bioreactors #2 and #3 were the same than those most represented in the aerobic biomass, but for the bioreactor #1, the domination belonged to *Rhodanobacter*, *Thermomonas*, *Nitrobacter*, and *Mycobacterium*. During the stabilization phase, the dominant phylotypes for the fixed biofilm in the three bioreactors were *Thermomonas*, *Nitrobacter*, *Comamonas*, and *Ottowia*.

The group of genera found in all three bioreactors contained phylotypes related with some of the most important ecological roles of bacteria identified in activated sludge systems, such as organic matter degradation, nitrification, denitrification, floc formation, floc backbone, or scavenging/ predation of cells (Gonzalez-Martinez et al., 2016a).

Concerning suspended biomass formation, *Flavobacterium*, *Ottowia*, and *Mycobacterium* have been identified as filamentous, floc-forming bacteria (Cao et al., 2014; Guo et al., 2015; Gonzalez-Martinez et al., 2016a; Joshi et al., 2016). The degradation of organic matter could be developed by several genera, such as *Chiayiivirga*, *Luteimonas*, *Arenimonas*, *Thauera*, *Parvibaculum*, *Afipia*, *Comamonas*, and *Thermomonas*, which are aerobic, heterotrophic bacteria (Schleheck et al., 2004; Lai et al., 2011; Hsu et al., 2013; Fan et al., 2014; Wang et al., 2014a; Wang et al., 2014b; Xin et al., 2014; Zhu et al. 2015; Ma et al., 2015; Makk et al., 2016).

The oxidation of ammonium could be developed by different species of bacteria such as *Nitrosomonas* (Rodriguez-Sanchez et al., 2014) or *Comamonas* (Chen et al. ,2011; Ma et al., 2015), which have been found regularly in MBR and hybrid MBBR–MBR systems treating regular-salinity wastewater (Calderon et al., 2013). Also, *Thermomonas* can oxidize ammonium and outcompete autotrophic ammonium oxidizing bacteria in certain environments with high NO_2 or O_2 concentrations (Ali et al., 2016). The oxidation of nitrite could be carried by genera *Nitrobacter* (Leyva-Diaz et al., 2015a) or *Rhodanobacter* (Gonzalez-Martinez et al., 2016b). *Nitrosospira* and *Nitrospira* were found as the dominant ammonium and nitrite oxidizing bacteria in MBR and MBBR–MBR systems treating regular-salinity wastewater (Leyva-Diaz et al., 2015a). Therefore, these results suggested that ammonium- and nitrite-oxidizing bacteria species were different in bioreactors treating regular-salinity and amended-salinity wastewater.

Several species could be able to develop denitrification by reducing nitrite, nitrate, or both, such as *Rhodanobacter*, *Luteimonas*, *Thuera*, *Comamonas*, and *Caulobacter*, reported for these metabolisms (Prakash et al., 2012; Woo et al., 2012; Jin et al., 2014; Wang et al. 2014a; Xin et al., 2014). Finally, among all the major represented phylotypes, *Luteimonas* and *Thermomonas* can biodegrade *N*-acetylglucosamine (Fan et al., 2014; Wang et al., 2014b).

In this sense, the dynamics in the bacterial community structure showed a transition between bacteria from different genera but with the same ecological capabilities. Thus, the main heterotrophs in bioreactors #1 and #2 changed from *Chiayiivirga*, *Luteimonas*, and *Arenimonas* to *Thermomonas* and *Parvibaculum*. In terms of nitrifiers and denitrifiers, the appearance of *Nitrobacter* and *Rhodanobacter* as dominant phylotypes in bioreactors #1 and #2 was observed at Phase 4. These transitions were correlated with the physicochemical operation of the system, which showed more COD, BOD_5, and TN removal at Phase 4 than at Phase 3. Also, the changes in

the bacterial community structure were related to higher bacterial kinetics for autotrophic and heterotrophic substrates.

A comparison of the bacterial communities in the mixed liquor and carriers in the aerobic zones of the MBR and the two hybrid MBBR–MBR operating under regular and amended salinity conditions at their respective stabilization phases is shown in Figure 6. Several genera were clearly present in the bioreactors under salinity conditions and nearly absent under regular salinity conditions, such as *Parvibaculum*, *Ottowia*, *Thermomonas*, or *Nitrobacter*. These genera were present in all biomass samples at amended salinity conditions. On the other hand, clear differences in the microbial communities were observed between the three technologies studied under regular salinity condition.

However, those differences were not detected under amended salinity conditions, suggesting that the bacterial community structures of the three bioreactors were more similar when operating under amended salinity conditions. Thus, this fact may imply that salinity exerted more selective pressure than technology for the three bioreactors studied. In this way, influent salinity concentration would be of fundamental importance for the development of bacterial community structure MBR and hybrid MBBR–MBR technologies treating urban wastewater.

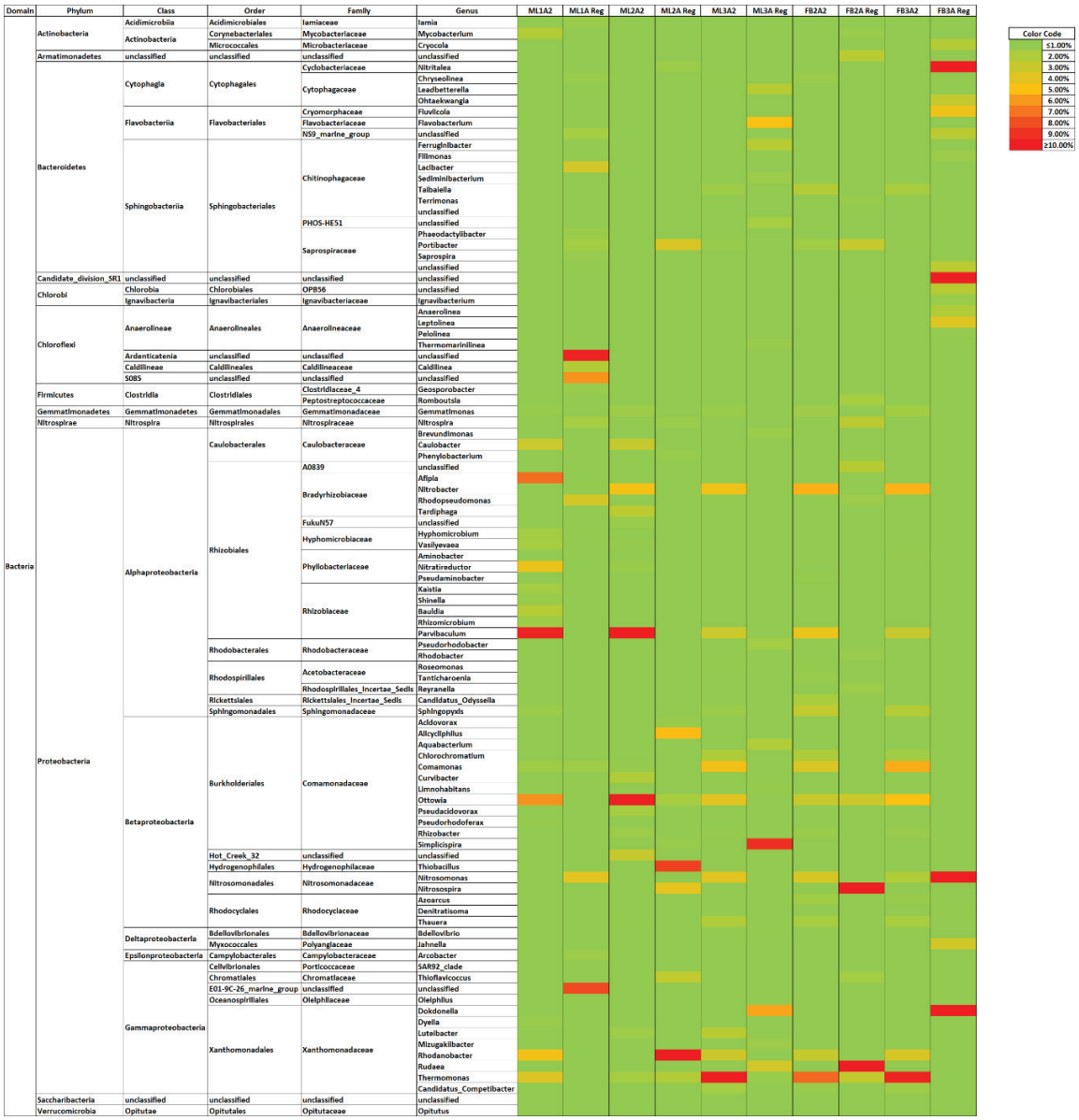

Figure 6 – Bacterial community structure of dominant phylotypes (>1% relative abundance) in the MBR and the two hybrid MBBR–MBR systems operated under regular- and amended-salinity conditions.

3.6 RDAs of the bioreactors

The RDA linking the operational parameters with the bacterial communities in the bioreactors is shown in Figure 7A. The ordination of the samples segregated them into 4 groups. Interestingly, the mixed liquor samples from bioreactors #1 and #3 were clustered together. On the other hand, the

aerobic mixed liquor samples from bioreactor #2 were separated from the anoxic samples coming from the same bioreactor. Also, the ordination separated the fixed biofilm from the mixed liquor biomass, and the fixed biofilm was differentiated in aerobic and anoxic. Among the operational parameters, those that were important in the ordination of the samples and genera were the pH, dissolved oxygen concentration, MLSS, and MLVSS. These were fairly independent with respect to each other. In this sense, the ecological ordination of the samples suggested that the presence of carriers in the anoxic zone is a differentiating factor in terms of bacterial community structure in the bioreactors treating salinity wastewater.

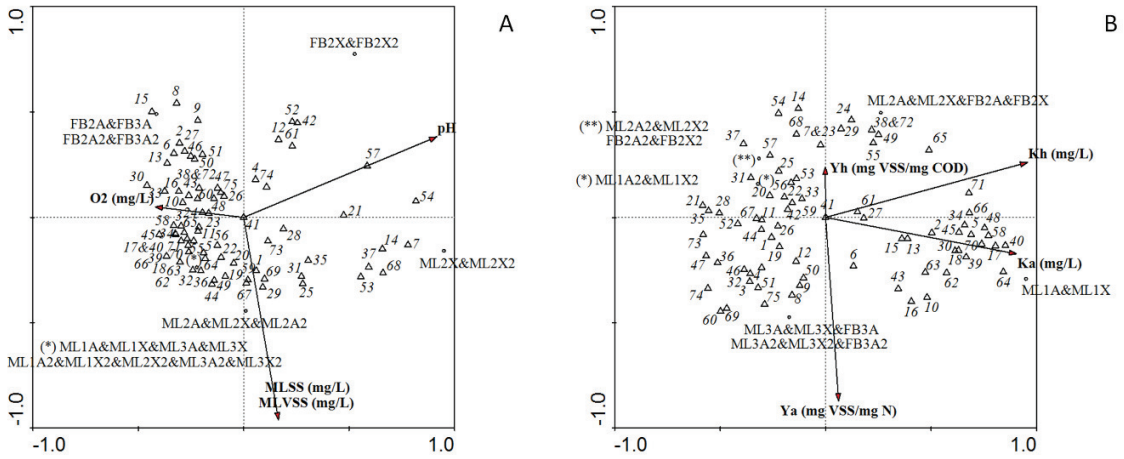

Figure 7 – Multivariate redundancy analysis linking bacterial genera in the iTag sequencing subsamples with (A) operational parameters of the bioreactors and (B) kinetic parameters of the biomass.

In addition, the RDA linking the respirometric parameters with the bacterial communities in the bioreactors is shown in Figure 7B. In this case, the ordination of samples generated

5 clusters and was controlled by the sampling date in the bioreactors #1 and #2, while all samples from bioreactor #3 were clustered within the same spot. The decay coefficient was not important for the ordination of samples and species and, interestingly, this also was true for the autotrophic and heterotrophic maximum growth rates. With respect to all other parameters, the half-saturation constants for the autotrophic and heterotrophic biomass were positively correlated and the

autotrophic and heterotrophic yield coefficients were negatively correlated. Half-saturation constants and yield coefficients were independent between them.

The dominant phylotypes consistently found in the bioreactors at Phase 4, such as *Thermomonas*, *Rhodanobacter*, *Nitrobacter*, *Ottowia*, or *Comamonas*, had a strong negative correlation with both autotrophic and heterotrophic half-saturation constants. On the other hand, the dominant phylotypes in the bioreactors #1 and #2 at Phase 3, such as *Chiayiivirga*, *Luteimonas*, or *Arenimonas*, had a strong correlation with both autotrophic and heterotrophic half-saturation constants. For the heterotrophic kinetics, the most important phylotypes were *Caulobacter* and *Ottowia*, but these were detrimental in terms of autotrophic kinetics. In a similar manner, it seemed that *Nitrosomonas* and *Thermomonas* were important for autotrophic kinetics, but on the other hand, were detrimental for heterotrophic kinetics. As both yield coefficients and half-saturation constants are detrimental for biomass kinetics, we proposed that the species with strong negative correlation with half-saturation constants and timid association with either of the yield coefficients were the most important players in terms of biomass kinetics. These were identified as *Nitrobacter*, *Comamonas*, and *Rhodanobacter*, among others. In this sense, in addition to phylotypes related to either faster heterotrophic or faster autotrophic kinetics, the presence of these phylotypes accelerated both the kinetics.

4. Conclusions

One pilot-scale MBR and two pilot-scale hybrid MBBR– MBR with different configurations were started-up and operated under 9.5 h HRT, 11.75 days SRT, and 2500 mg L^{-1} TSS during the stabilization phase for the treatment of 6.5 mS cm^{-1} electric conductivity salinity-amended urban wastewater. The study of the bacterial community structure of the MBR and the hybrid MBBR–MBR systems through *iTag* massive parallel sequencing showed different phylotypes dominating

the bioreactors during the start-up and stabilization phases. Several genera were found to be able to develop the relevant ecological roles for the functioning of the bioprocess, such as floc formation, nitrification, denitrification, and organic matter oxidation. During the start-up phase, the dominant phylotypes belonged to *Chiayiivirga* (3– 12% relative abundance), *Flavobacterium* (2.5–8%), *Luteimonas* (5–8%), *Arenimonas* (4–7%), and *Thauera* (1.5–5%). In contrast, during the stabilization phase, the dominance belonged to *Thermomonas* (3–14%), *Nitrobacter* (3–7%), *Comamonas* (2–6%), *Rhodanobacter* (1.5–8%), and *Ottowia* (3–11.5%). The differences in the bacterial community structure were also related to the differences in the microbial kinetics of autotrophic and heterotrophic biomass between the two phases. In this sense, stability in microbial community structure produced stable microbial kinetics for the autotrophic and heterotrophic biomass. Multivariate redundancy analysis showed the linkage of certain bacterial genera with microbial kinetics. In general, the dominant phylotypes in the stabilization phase were positively related to microbial kinetics. Thus, autotrophic kinetics were positively related to *Thermomonas* and *Nitrosomonas* and heterotrophic kinetics were related to *Caulobacter* and *Ottowia*. Overall, it was found that several genera such as *Nitrobacter*, *Comamonas*, and *Rhodanobacter* were positively correlated with both heterotrophic and autotrophic kinetics. The results obtained related the presence of certain bacterial species with favorable kinetics, and therefore offer valuable information for operators and designers of bioreactors treating salinity wastewater.

Acknowledgments

The authors would like to acknowledge the support given by the Department of Civil Engineering of the University of Granada and the Institute of Water Research of the University of Granada.

Specially, the authors want to acknowledge the help and guidance of Prof. Jesus Gonzalez-Lopez of the Institute of Water Research at the University of Granada.

Literature Cited

Ali M, Chai LY, Min XB, Tang CJ, Afrin S, Liao Q, Wang HY, Peng C, Song YX, Zheng P (2016) Performance and characteristics of a nitritation air-lift reactor under long-term HRT shortening. *Int Biodeterior Biodegrad* 111: 45–53.

APHA (2012) *Standard Methods for the Examination of Water and Wastewater*, 22nd ed. Washington DC, USA: American Public Health Association.

Barwell LJ, Isaac NJB, Kunin WE (2015) Measuring β-diversity with species abundance data. *J Anim Ecol* 84: 1112–1122.

Bassin JP, Kleerebezem R, Muyzer G, Rosado AS, Van Loosdrecht MCM, Dezotti M (2012) Effect of different salt adaptation strategies on the microbial diversity, activity, and settling of nitrifying sludge in sequencing batch reactors. *Appl Microbiol Biotechnol* 93: 1281–1294.

Calderón K, Reboleiro-Rivas P, Rodríguez FA, Poyatos JM, González-López J, Rodelas B (2013) Comparative analysis of the enzyme activities and the bacterial community structure based on the aeration source supplied to an MBR to treat urban wastewater. *J Environ Manage* 128: 471–479.

Cao J, Lai Q, Liu Y, Li G, Shao Z (2014) *Ottowia beijingensis* sp. nov., isolated from coking wastewater activated sludge, and emended description of the genus *Ottowia*. *Int J Syst Evol Microbiol* 64: 963–967.

Castillo-Carvajal LC. Sanz-Martin JL, Barragan-Huerta BE (2014) Biodegradation of organic pollutants in saline wastewater by halophilic microorganisms: a review. *Environ Sci Pollut Res* 21: 9578–9588.

Chen Q, Ni J (2011) Heterotrophic nitrification–aerobic denitrification by novel isolated bacteria. *J Ind Microbiol Biotechnol* 38: 1305–1310.

Cortes-Lorenzo C, Rodriguez-Diaz M, Lopez-Lopez C, Sanchez-Peinado M, Rodelas B, Gonzalez-Lopez J (2012) Effect of salinity on enzymatic activities in a submerged fixed bed biofilm reactor for municipal sewage treatment. *Bioresour Technol* 121: 312–319.

Di Trapani D, Di Bella G, Mannina G, Torregrossa M, Viviani G (2014) Comparison between moving bed-membrane bioreactor (MBMBR) and membrane bioreactor (MBR) systems: influence of wastewater salinity variation. *Bioresour Technol* 162: 60–69.

Edgar RC, Haas BJ, Clemente JC, Quince C, Knight R (2011) UCHIME improves sensitivity and speed of chimera detection. *Bioinformatics* 27: 2194–2200.

Fan X, Yu T, Li Z, Zhang XH (2014) *Luteimonas abyssi* sp. nov., isolated from deep-sea sediment. *Int J Syst Evol Microbiol* 64: 668–674.

Gonzalez-Martinez A, Rodriguez-Sanchez A, Lotti T, GarciaRuiz MJ, Osorio F, Gonzalez-Lopez J, van Loosdrecht MC (2016a) Comparison of bacterial communities of conventional and Astage activated sludge systems. *Sci Rep* 6: 18786.

Gonzalez-Martinez A, Rodriguez-Sanchez A, Garcia-Ruiz MJ, Muñoz-Palazon B, Cortes-Lorenzo C, Osorio F, Vahala R (2016b) Performance and bacterial community dynamics of a CANON bioreactor acclimated from high to low operational temperatures. *Chem Eng J* 287: 557–567.

Guo F, Wang Z-P, Yu K, Zhang T (2015) Detailed investigation of the microbial community in foaming activated sludge reveals novel foam formers. *Sci Rep* 5: 7637.

Haegeman B, Hamelin J, Moriarty J, Neal P, Dushoff J, Weitz JS (2013) Robust estimation of microbial diversity in theory and in practice. *ISME J* 7: 1092–1101.

Huse SM, Welch DM, Morrison HG, Sogin ML (2010) Ironing out the wrinkles in the rare biosphere through improved OTU cluster ing. *Environ Microbiol* 12: 1889–1898.

Hsu YH, Lai WA, Lin SY, Hameed A, Shahina M, Shen FT, Zhu ZL, Sen YL, Young CC (2013) *Chiayiivirga flava* gen. nov., sp. nov., a novel bacterium of the family Xanthomonadaceae isolated from an agricultural soil, and emended description of the genus *Dokdonella*. *Int J Syst Evol Microbiol* 63: 3293– 3300.

Jin L, La HJ, Lee HG, Lee JJ, Lee S, Ahn CY, Oh HM (2014) *Caulobacter profunda* sp. nov., isolated from deep freshwater sediment. *Int J Syst Evol Microbiol* 64: 762–767.

Joshi DR, Zhang Y, Tian Z, Gao Y, Yang M (2016) Performance and microbial community composition in a long-term sequential anaerobic-aerobic bioreactor operation treating coking wastewater. *Appl Microbiol Biotechnol* 100: 8191-8202 ; doi:10.1007/s00253-0167591-8.

Lai Q, Wang L, Liu Y, Yuan J, Sun F, Shao Z (2011) *Parvibaculum indicum* sp. nov., isolated from deep-sea water. *Int J Syst Evol Microbiol* 61: 271–274.

Le-Clech P, Chen V, Fane TAG (2006) Fouling in membrane bioreactors used in wastewater treatment. *J Memb Sci* 284: 17–53.

Leiknes T, Ødegaard H (2007) The development of a biofilm membrane bioreactor. *Desalination* 202: 135–143.

Leyva-Díaz JC, Martín-Pascual J, Muñío MM, González-López J, Hontoria E, Poyatos JM (2014) Comparative kinetics of hybrid and pure moving bed reactor-membrane bioreactors. *Ecol Eng* 70: 227–234.

Leyva-Diaz JC, Gonzalez-Martinez A, Gonzalez-Lopez J, Munio MM, Poyatos JM (2015a) Kinetic modeling and microbiological study of two-step nitrification in a membrane bioreactor and hybrid moving bed biofilm reactor-membrane bioreactor for wastewater treatment. *Chem Eng* 259: 692–702.

Leyva-Diaz JC, Lopez-Lopez C, Martin-Pascual J, Munio MM, Poyatos JM (2015b) Kinetic study of the combined processes of a membrane bioreactor and a hybrid moving bed biofilm reactormembrane

bioreactor with advanced oxidation processes as a post-treatment stage for wastewater treatment. *Chem Eng Process Process Intensif* 91: 57–66.

Luo W, Hai FI, Kang J, Price WE, Guo W, Ngo HH, Yamamoto K, Nghiem LD (2015) Effects of salinity build-up on biomass characteristics and trace organic chemical removal: implications on the development of high retention membrane bioreactors. *Bioresour Technol* 177: 274–281.

Ma Q, Qu Y, Shen W, Zhang Z, Wang J, Liu Z, Li D, Li H, Zhou J (2015) Bacterial community compositions of coking wastewater treatment plants in steel industry revealed by illumina highthroughput sequencing. *Bioresour Technol* 179: 436–443.

Makk J, Homonnay G, Ke Z, Nemes-Barnas K, Marialigeti K, Schumann P, Toth EM (2016) *Arenimonas subflava* sp. nov., isolated from a drinking water network, and emended description of the genus *Arenimonas*. *Int J Syst Evol Microbiol* 65: 1915–1921.

Norton-Brandão D, Scherrenberg SM, van Lier JB (2013) Reclamation of used urban waters for irrigation purposes A review of treatment technologies. *J Environ Manage* 122: 85–98.

Ødegaard H (2006) Innovations in wastewater treatment: the moving bed biofilm process. *Water Sci Technol* 53: 17–33.

Prakash O, Green SJ, Jasrotia P, Overholt WA, Canion A, Watson DB, Brooks SC, Kostka JE (2012) *Rhodanobacter denitrificans* sp. nov., isolated from nitrate-rich zones of a contaminated aquifer. *Int J Syst Evol Microbiol* 62: 2457–2462.

Rodriguez-R LM, Konstantinidis KT (2014a) Estimating coverage in metagenomic data sets and why it matters. *ISME J* 8: 2349–2351.

Rodriguez-R LM, Konstantinidis KT (2014b) Nonpareil: a redundancybased approach to assess the level of coverage in metagenomic datasets. *Bioinformatics* 30: 629–635.

Rodriguez-Sanchez A, Gonzalez-Martinez A, Martinez-Toledo MV, Garcia-Ruiz MJ, Osorio F, Gonzalez-Lopez J (2014) The effect of influent characteristics and operational conditions over the performance and microbial community structure of partial nitritation reactors. *Water (Switzerland)* 6: 1905–1924.

Rosenblum J, Nelson AW, Ruyle B, Schultz MK, Ryan JN, Linden KG (2017) Temporal characterization of flowback and produced water quality from a hydraulically fractured oil and gas well. *Sci Tot Environ* 596–597: 369–377.

Schleheck D, Tindall BJ, Rosselló-Mora R, Cook AM (2004) *Parvibaculum lavamentivorans* gen. nov., sp. nov., a novel heterotroph that initiates catabolism of linear alkylbenzenesulfonate. *Int J Syst Evol Microbiol* 54: 1489–1497.

Schloss PD, Westcott SL, Ryabin T, Hall JR, Hartmann M, Hollister EB, *et al.* (2009) Introducing mothur: open-source, platform-independent, community-supported software for describing and comparing microbial communities. *Appl Environ Microbiol* 75: 7537– 7541.

Unno T (2015) Bioinformatic suggestions on MiSeq-based microbial community analysis. *J Microbiol Biotechnol* 25: 765–770.

Visvanathan C, Aim RB, Parameshwaran K (2000) Membrane separation bioreactors for wastewater treatment. *Crit Rev Environ Sci Technol* 30: 1–48.

Wang Z, Zhang XX, Lu X, Liu B, Li Y, Long C, Li A (2014a) Abundance and diversity of bacterial nitrifiers and denitrifiers and their functional genes in tannery wastewater treatment plants revealed by high-throughput sequencing. *PLoS One* 9: 1–19.

Wang L, Zheng S, Wang D, Wang L, Wang G (2014b) *Thermomonas carbonis* sp. nov., isolated from the soil of a coal mine. *Int J Syst Evol Microbiol* 64: 3631–3635.

Woo SG, Srinivasan S, Kim MK, Lee M (2012) *Rhodanobacter caeni* sp. nov., isolated from sludge from a sewage disposal plant. *Int J Syst Evol Microbiol* 62: 2815–2821.

Xin Y, Cao X, Wu P, Xue S (2014) *Luteimonas dalianensis* sp. nov., an obligate marine bacterium isolated from seawater. *J Microbiol* 52: 729–733.

Yang J, Spanjers H, Jeison D, Van Lier JB (2013) Impact of Na1 on biological wastewater treatment and the potential of anaerobic membrane bioreactors: a review. *Crit Rev Environ Sci Technol* 43: 2722–2746.

Zhu S-M, Deng Y-L, Ruan Y-J, Guo X-S, Shi M-M, Shen J-Z (2015) Biological denitrification using poly(butylene succinate) as carbon source and biofilm carrier for recirculating aquaculture system effluent treatment. *Bioresour Technol* 192: 603–610

Chapter 3

Membrane bioreactor and hybrid moving bed biofilm reactor-membrane bioreactor for the treatment of variable salinity wastewater: Influence of biomass concentration and hydraulic retention time

This chapter has been published in its current form in Chemical Engineering Journal. The complete citation is the following:

Alejandro Rodriguez-Sanchez, Juan Carlos Leyva-Diaz, Jesus Gonzalez-Lopez, Jose Manuel Poyatos. 2018. Membrane bioreactor and hybrid moving bed biofilm reactor-membrane bioreactor for the treatment of variable salinity wastewater: Influence of biomass concentration and hydraulic retention time. Chemical Engineering Journal. 336, 102-111. doi: 10.1016/j.cej.2017.10.118

Abstract

A membrane bioreactor and two hybrid moving bed biofilm reactor-membrane bioreactor systems were operated for the treatment of wastewater with tidal salinity fluctuations under hydraulic retention times of 6, 9.5 and 12 h, and operational solids concentrations of around 2500 and 3500 mg L^{-1}. The three configurations were studied in terms of carbon and nitrogen removal, heterotrophic and autotrophic kinetics, and bacterial community structure. The performance of the systems was good in terms of organic matter removal – between 85–100% and 95–100% for COD and BOD_5, respectively, showing higher efficiencies at higher solids concentration and hydraulic retention times. Nitrogen removal obtained was in the range of 30–50%. The bacterial community structure of the suspended and attached biomass in the systems was more influenced by the operational solids (80% clustering cutoff) and hydraulic retention time (60% clustering cutoff) than by technological configuration (40% clustering cutoff), as determined by ordination analyses. Massive parallel sequencing showed the presence of *Nitrobacter* and *Rhodanobacter* at almost all operation scenarios, and thus were identified as major players in treatment of tidal salinity variation wastewater. Overall, this research proved that the MBR and hybrid MBBR-MBR systems could successfully treat urban wastewater subjected to tidal salinity variations. Nevertheless, more research is needed in order to enhance nitrogen removal performance under these conditions.

1. Introduction

Effluents discharged from human settlements and industrial processes could have high salinity concentrations. Regarding urban wastewater, high salinities can be caused by the use of seawater for toilet flushing in marine areas, the utilization of salt for outdoor snow-melting strategies, or by entrance of marine water in the sewage systems in coastal or island areas, which could raise sewage salinity permanently or during tidal cycles (Wang et al., 2009; Cortes-Lorenzo et al., 2016). In light of this, salinity has been shown to impact biological wastewater treatment processes. This is caused because presence of salt may reduce bioavailability of compounds used for bacterial metabolism, inhibition of degradation processes, production of harmful metabolites which could persist and accumulate in the bioreactor, and higher cell death rates due to higher differential osmotic pressure across cell membranes, among others (Bassin et al., 2012; Castillo-Carvajal et al., 2014). Therefore, biological wastewater treatment technologies should be analyzed for an efficient treatment of saline sewage.

The most common technology applied for the treatment of urban wastewater at global scale is the activated sludge process (Leyva-Diaz et al., 2013). Nevertheless, more novel technologies have been implemented in for this purpose. One of the most efficient among them is the membrane bioreactor (MBR) technology. In the MBR, following a conventional activated sludge system, wastewater is forced to pass through a membrane with a very small pore diameter, which exerts a very effective separation of solids from water. This allows the MBR to obtain several advantages over the activated sludge technologies (Leyva-Diaz et al., 2014). Mainly, the MBR system can operate at higher solids concentrations than the activated sludge, which improves bioremediation and makes possible the reduction of footprint required for bioreactor set-up. The very efficient separation process developed by the membrane allows for a complete retention of the biomass, increasing the sludge retention times in the MBR with respect to activated sludge systems, and yielding low excess of

sludge produced during the wastewater treatment (Leyva-Diaz et al., 2015a). On the other hand, the functioning of the membrane is subjected to the clogging of membrane pores by organic or inorganic materials, producing a phenomenon named as membrane fouling (Gonzalez-Martinez et al., 2014). Membrane fouling increases the costs of the MBR process and could finally lead to the disablement of the membrane (Leyva-Diaz et al., 2015b).

The activated sludge systems develop biomass that grows suspended on the mixed liquor. Nevertheless, other technologies exist that develop the growth of biomass attached to surfaces. Among these, the moving bed biofilm reactor (MBBR) is one of the most efficient. In the MBBR, a floating media is displaced within the activated sludge biological reactor so biomass grows attached to it while it moves continuously within the bioreactor volume. In this sense, the growth of attached biomass inside the bioprocess increases the solids concentration without increasing suspended solids, which leads to reduction in bioreactor footprint, easier biomass separation procedures and the development of more specialized biomass allowed by the growth in fixed biofilms (Leyva-Diaz et al., 2013; 2014). These advantages have been applied to the MBR technology, yielding the moving bed biofilm reactor-membrane bioreactor (MBBR-MBR) systems. These are denominated as hybrid when a recycling flow is imposed from the membrane compartment to the MBBR, or pure when no such recycling exists.

The advantages offered by the MBR and MBBR-MBR technologies, and specially the operation at high solids concentrations, could be appropriate for the treatment of saline sewage. Therefore, an experiment using a MBR and two hybrid MBBR-MBR was developed in order to analyze the performance of these technologies for the treatment of saline wastewater. In this case, the technologies were tested for the bioremediation of urban wastewater with tidal salinity variations at solids concentrations of 2500 and 3500 mg L^{-1} and hydraulic retention times of 6, 9.5 and 12 h. The tidal variation of salinity was mainly imposed in order to evaluate the performance of the

systems in hypothetical scenarios of seawater intrusions in wastewater treatment plants. The three systems were monitored for its organic matter and nitrogen performance, microbial community kinetics, and bacterial community structure in the systems. The results obtained will be of help for the treatment of saline sewage in coastal areas subjected to salinity variations.

2. Materials and methods

2.1 Configuration of the bioreactors

Three bioreactors were operated in parallel for this study (Fig. 1). They were pilot-scale systems and were equal in terms of physical configuration. They were composed by a reactor divided into four chambers of equal volume and a membrane tank from which the effluent was drawn through membrane filtration process. The influent was forced to pass through the four chambers before entering the membrane tank. A recycling flow was imposed from the membrane tank to the first chamber with a flow rate of 500% of the influent flow. The influent and effluent flows were obtained using Watson-Marlow peristaltic pumps (Watson-Marlow Pumps Group, USA). In each of the systems, the first, third and fourth chambers, as well as the membrane tank, were aerated, and the second chamber was given anoxic conditions and was continuously stirred by a mechanical agitator. The aeration was provided by a ACO-500 air compressor (Hailea, China) and introduced into the aerobic chambers and membrane tanks by AFD 2760 fine bubble diffusers and CAP 3 coarse bubble diffusers, respectively (ECOTEC SA, Spain). The aeration was measured and regulated by 2100 Model rotameter (TecFluid SA, Spain). The chambers were of 12 cm × 12 cm × 60 cm and were operated under an effective working volume of 6 L. The membrane tank was a cylinder of 10 cm dia meter × 60 cm height and was operated under a working volume of 4.32 L. In this way, the total operational volume of the system was of 28.32 L. The ultrafiltration membrane module was of 0.04 µm pore

diameter polyvinylidene hollow fibers with a total membrane area of 0.20 m^2 (Micronet Porous Fibers SL, Spain). The stirring in the anoxic chambers was provided by MultiMixer MM-100 stirrers (Biosan Laboratories Inc, USA). The membrane module was operated in a cycle consisting of 9 min of flowing and 1 min of backwashing, and was cleaned regularly to avoid membrane clogging and maintain the transmembrane pressure at 0.5 bar during the operation time.

The three systems were configured as different technologies. One was set up as a MBR system. The other two were set up as hybrid MBBRMBR systems. Among these two, one had 35% filling ratio of K1 carriers (AnoxKaldnes AS, Norway) in all four chambers and was named as hybrid MBBR-MBRanox. The other had 35% filing ratio of K1 carriers in the three aerobic chambers and no carriers in the anoxic chamber, and was named as hybrid MBBR-MBRn/anox. The K1 carriers had a 0.92–0.96 g cm^{-3} density and a specific surface area of 500 m^2 m^{-3} (Martin-Pascual et al., 2016).

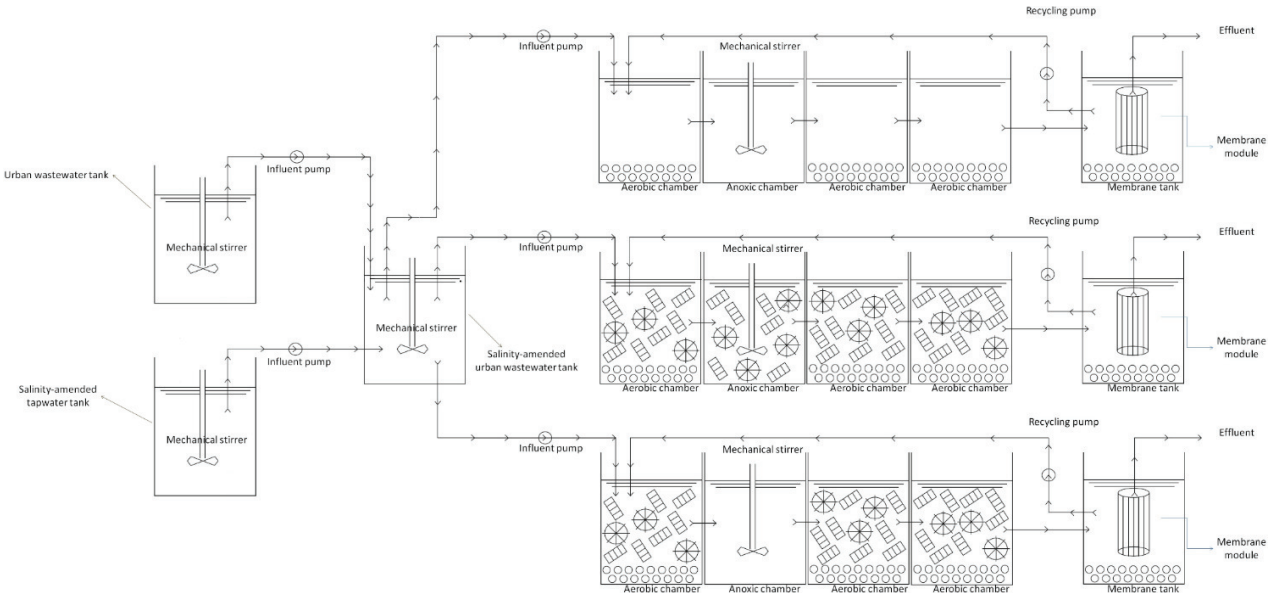

Figure 1 – Flow diagram of the three bioreactors operated in this study

2.2 Experimental procedure

The influent wastewater used in the study was a salinity-amended urban wastewater. To achieve this, urban wastewater was periodically collected from the Los Vados WWTP, Granada, Spain. This wastewater was stored in a tank. Another tank was filled with tap water amended with NaCl to achieve an electrical conductivity of 50 mS cm^{-1}. The urban wastewater and the salinity-amended tap water were mixed in a mixing tank, from which the three pilot-scale bioreactors took their feeds. The urban wastewater and the salinity-amended tap water were mixed by means of an electronic control to achieve the desired electric conductivity at each time of the day. The salinity conditions forced in the bioreactors' influent followed the cycle: 6 h of a mix with

6.5 mS cm^{-1}, then 6 h of urban wastewater. The conditions on the salinity-amended tap water provided that the mixture had a minimum of 90% urban wastewater, thus the influent did not significantly lose its content in organic matter and nutrients.

The three pilot-scale bioreactors were operated under six different operational conditions controlled by the hydraulic retention time (HRT) and the mixed liquor suspended solids (MLSS) concentration in the bioreactors. Three different hydraulic retention times (HRTs) of 6 h, 9.5 h and 12 h and two different MLSS concentrations of 2500 mg L^{-1} and 3500 mg L^{-1} were studied, therefore 6 different phases were observed. The bioreactors were operated under mean sludge retention time (SRT) of 21 days.

2.3 Physicochemical determinations

The determinations of influent and effluent biological oxygen demand on the fifth day (BOD_5), chemical oxygen demand (COD) and total suspended solids (TSS) were done following established

protocols (APHA, 2012). The determination of influent and effluent nitrogenous compounds NH_4^+, NO_2^- and NO_3^- was done by ionic chromatography.

Also, the determination of the attached biofilm to carriers in the hybrid MBBR-MBR systems was done following the method described earlier by Leyva-Diaz et al. (2015b) with the exception that the number of carriers taken for this purpose was of 10 instead of 4. The pH, temperature, electric conductivity and dissolved oxygen concentration were measured in each of the chambers of the three pilot-scale bioreactors using a multimeter. The pH and temperature in the influent was measured using a multimeter, and the electric conductivity was controlled electronically by mixing urban wastewater and salinity-amended tap water.

2.4. Respirometric tests for determination of microbial kinetics

The determination of microbial kinetics during each of the 6 phases of operation was done using respirometric tests. These were done over 1 L sample representing the configuration of the technology studied (mixed liquor without carriers for the MBR system and mixed liquor with 35% carriers for the MBBR-MBR systems). Prior to the respirometric tests, the samples were extracted from the bioreactors and continuously aerated during 18 h at 20 °C temperature. The respirometric tests were developed in a BM-Advance Multipurpose gas fluxstatic liquid respirometer to observe both the exogenous and endogenous biomass kinetics. For the exogenous kinetics, the dissolved oxygen concentration was measured during the respirometric tests and the oxygen utilization for the biodegradation of substrates added to the samples was related to the microbial kinetics of the biomass analyzed following Leyva-Diaz et al. (2013). The substrates added for the determination of heterotrophic and autotrophic kinetics of the biomass were 500 mg L^{-1} sodium acetate and 150 mg L^{-1} NH_4Cl, respectively. The substrates were added in three different dilutions of 50%, 80% and 100%.

For the endogenous kinetics, the samples were stripped of aeration and the consumption of oxygen was then related to the decay kinetics of the biomass. During the respirometric tests the temperature was controlled at 20 °C and the pH at 7.50 ± 0.25.

2.5 Multivariate redundancy analyses

The relationship between the microbial kinetics and the technologies and operational conditions used during the experimentation period was explored by multivariate redundancy analyses (RDA). For both the heterotrophic and autotrophic kinetics, the values of the rates of substrate utilization (r_{su}) at three different concentrations of substrate were matched against the three different technologies and the operational conditions of temperature, pH, dissolved oxygen concentrations, HRT and MLSS concentration. The RDA analyses were done through 499 unconstrained Monte-Carlo simulations under a full-permutation model using the CANOCO 4.5 for Windows software. Additionally, the dominant phylotypes found during the operation of the three bioreactors were also linked with the heterotrophic and autotrophic kinetics by the means of RDA analysis in the same way as described above.

2.6 Collection of biomass, DNA extraction procedure and massive parallel sequencing process

Sample of suspended and attached biomass were extracted from the bioreactors in order to evaluate their bacterial community structure composition by massive parallel sequencing techniques. In this sense, during operation, samples were taken from the first and second chambers in each of the bioreactors. Suspended biomass samples were taken by substraction of 200 mL of mixed liquor followed by a centrifugation at 3500 rpm at room temperature during 10 min. Attached biomass samples, if any, were taken by substraction of 200 mL of plastic carriers (around 198 carriers), which

were subsequently sonicated during 3 min for biomass detachment, vortexed and centrifuged during 10 min at room temperature and 3500 rpm for detached biomass collection. Collected biomass was then stored at −20 °C until further DNA extraction.

The extraction of DNA done using the FastDNA SPIN Kit for Soil (MP Biomedicals, Solon, OH, USA) and the FastPrep apparatus following the instructions given by the manufacturer. The extracted DNA was then kept at −20 °C and sent to Research & Testing Laboratory for subsequent massive parallel sequencing procedure. This was developed with the Illumina MiSeq equipment and Illumina MiSeq Reagents Kit v3. The primers 28F (5′-GAGTTTGATCNTGGCTCAG-3′)-519R (5′-GTNTTACNGCGGCKGCTG-3′) was used for the amplification of the bacterial 16S rRNA gene hypervariable regions V1-V2-V3. The PCR conditions for the amplification were: 3 min at 94 °C, then 32 cycles of: 30 s at 94 °C, 40 s at 60 °C, and 60 s at 72 °C; final elongation step of 5 min at 72 °C.

2.7 Bioinformatics pipeline

The raw data obtained through the massive parallel sequencing process was then treated using mothur v1.34.4 (Schloss et al., 2009) for the elucidation of its bacterial community structure. In this way, paired-end reads were first assembled into contigs. Then, all sequences with any ambiguous base or with more than 8 homopolymers were discarded for the analysis. The remaining sequences were aligned against the SiLVA SEED database release 128, and sequences that: i) did not align at the position of the 28F primer; or ii) sequences that terminated further than the 95% of all sequences; were removed from the analysis. Remanent sequences were then preclustered in a two-differences threshold (Huse et al., 2010), and then a chimera analysis was done using UCHIME v4.1 (Edgar et al., 2011). Sequences that passed the chimera slaying procedure were classified against the SiLVA SEED database release 128 for deletion of sequences not affiliated with the domain *Bacteria*.

At this point, all samples were rarified using a deconvolution algorithm and cut to the lowest number of high-quality samples, which was 10199, for a subsequent ecological analysis. For each of the rarified subsamples, a Phylip distance matrix was calculated among all of its sequences, then these were clustered into OTUs in a 97% similarity threshold, and a representative sequence of each of the OTUs was taxonomically affiliated using the SiLVA SEED database release 128. Finally, the OTUs were merged into a consensus taxonomy using a cutoff of 80% similarity.

2.8 Ordination and α-diversity analyses of massive parallel sequencing subsamples

The rarified subsamples from massive parallel sequencing process were ordinated in a cluster and principal coordinates analyses taking Bray-Curtis distances for calculation. This was done for their bacterial communities at genus level and using the vegan 2.0 package implemented in R statistical software. Also, the determination of Chao-1, Shannon-Wiener, Simpson, Pielou's evenness and Berger-Parker evenness, which were calculated with a 95% confidence range by 1000 bootstrap replications, was done for each of the rarified subsamples at genus level using PAST v3.06 software (Hammer & Harper, 2006).

3. Results and discussion

3.1 Organic matter, nitrogen and total suspended solids removal

The MBR and the two hybrid MBBR-MBR systems were operated in parallel under six different combinations of HRT and MLSS concentrations. The experiment was conducted from late February to early August. In this sense, the temperature of operation was an environmental variable that increased with the experimentation time from 14.4 ± 0.4 °C to 22.6 ± 0.3 °C for the first and last operation phases, respectively. The aeration in the chambers was controlled to avoid excessive

dissolved oxygen concentrations in the anoxic chambers, forcing a mean value of 0.2 ± 0.1 mg-O_2 L^{-1} during the whole experiment time. The control of aeration in the aerobic chambers was imposed around a dissolved oxygen concentration of 2.00 mg L^{-1}. Nevertheless, the aerobic chambers had different dissolved oxygen concentrations during the experiment time. Consistently, the dissolved oxygen concentrations found in the MBR systems were lower than those in the hybrid MBBR-MBR systems (mean values of 1.9–2.4 mg-O_2 L^{-1} and of 2.8–3.3 mg-O_2 L^{-1}, respectively). The differences in the dissolved oxygen concentration were explained due to the necessity of a higher aeration to mix the mass of carriers within the whole volume of the aerobic chambers in the hybrid MBBR-MBR systems. Inputs of dissolved oxygen in the aerobic chamber receiving membrane tank recycling flow could have increased the dissolved oxygen in this chambers in the three bioreactors. In spite of the aeration registered, it has been reported that dissolved oxygen concentrations above 2 mgO_2 L^{-1} did not impact the performance of the technologies analyzed in this study (Wang et al., 2006), and thus sufficient aeration was provided in the aerobic chambers to avoid the influence of oxygen among the different operational conditions tested. Interestingly, the biofilm density (BD) of the hybrid MBBR-MBR systems was low in comparison with that of the suspended biomass (values of around 20–40 mg L^{-1} compared with 2500–3500 mg L^{-1} of MLSS) during the whole experiment time. The operation of the systems under variable salinity conditions showed to impact the presence of biomass attached to the carriers. The difficulties of biomass formation under 6.5 mS cm^{-1} constant salinity conditions have been pointed out in various studies (Rodriguez-Sanchez et al., 2017). As well, the severe impact of the influent salinity wastewater in MBBR-MBR systems has been observed, with a loss of about 1000 mg L^{-1} with respect to the no-salinity scenario (Di Trapani et al., 2014). The use of a 0.04 µm pore diameter membrane process to treat the effluent lead to a very good removal of TSS in the three systems during the whole experimental period. All mean values for each phase were higher than 97%.

The influent concentrations of COD, BOD_5 and TN, and the removal performance of the three technologies in terms of these operational variables are given in Fig. 2. The three technologies could eliminate successfully the influent organic matter, measured as COD and BOD_5. With respect to COD, the MBR and the two hybrid MBBR-MBR systems achieved mean removal efficiencies higher than 85.3% during all experimentation phases. For the same operational HRT, the three technologies showed higher COD removal efficiencies at higher MLSS concentrations. Also, for the same MLSS of operation the three systems showed better COD removal at higher HRT. The MBR was the most efficient technology in terms of COD removal at the 2500 mg L^{-1} MLSS concentration (90–98%), but the hybrid MBBR-MBRanox was the best at 3500 mg L^{-1} MLSS (92–99.6%). The hybrid MBBR-MBRn/anox was the most inefficient of the systems at COD removal overall (92% mean value) and the MBR was the best (95% mean value). The removal of BOD_5 in the three systems during the whole operation time was also very good, with mean values for each phase higher than 97%. Overall, the BOD_5 followed the same trend than COD with different MLSS and HRT. The systems were very similar overall for the elimination of BOD_5, and therefore no one was preferred for the removal of biodegradable organic matter under variable salinity conditions. With respect to the COD and BOD_5 removal by the MBR and the hybrid MBBR-MBR systems operated, the values obtained for the treatment of variable salinity wastewater with maximum electric conductivity 6.5 mS cm^{-1} were similar to those found at constant salinity of 6.5 mS cm^{-1} (Rodriguez-Sanchez et al., 2017). For the same operational conditions, the three technologies had an overall higher BOD_5 removal under variable salinity conditions (97.41–98.47% versus 97.69–98.07%), while the COD removal was higher at constant salinity conditions (86.63–89.89% versus 88.55–91.67%). Under both salinity conditions the hybrid MBBR-MBRanox had the highest BOD_5 removal efficiency and the lowest COD removal efficiency. Also, the highest COD performance corresponded to the MBR in both salinity

scenarios. Thus, this is evidence that the cyclical salinity concentrations did not affect much the overall performance in organic matter by the MBR and the hybrid MBBR-MBR systems.

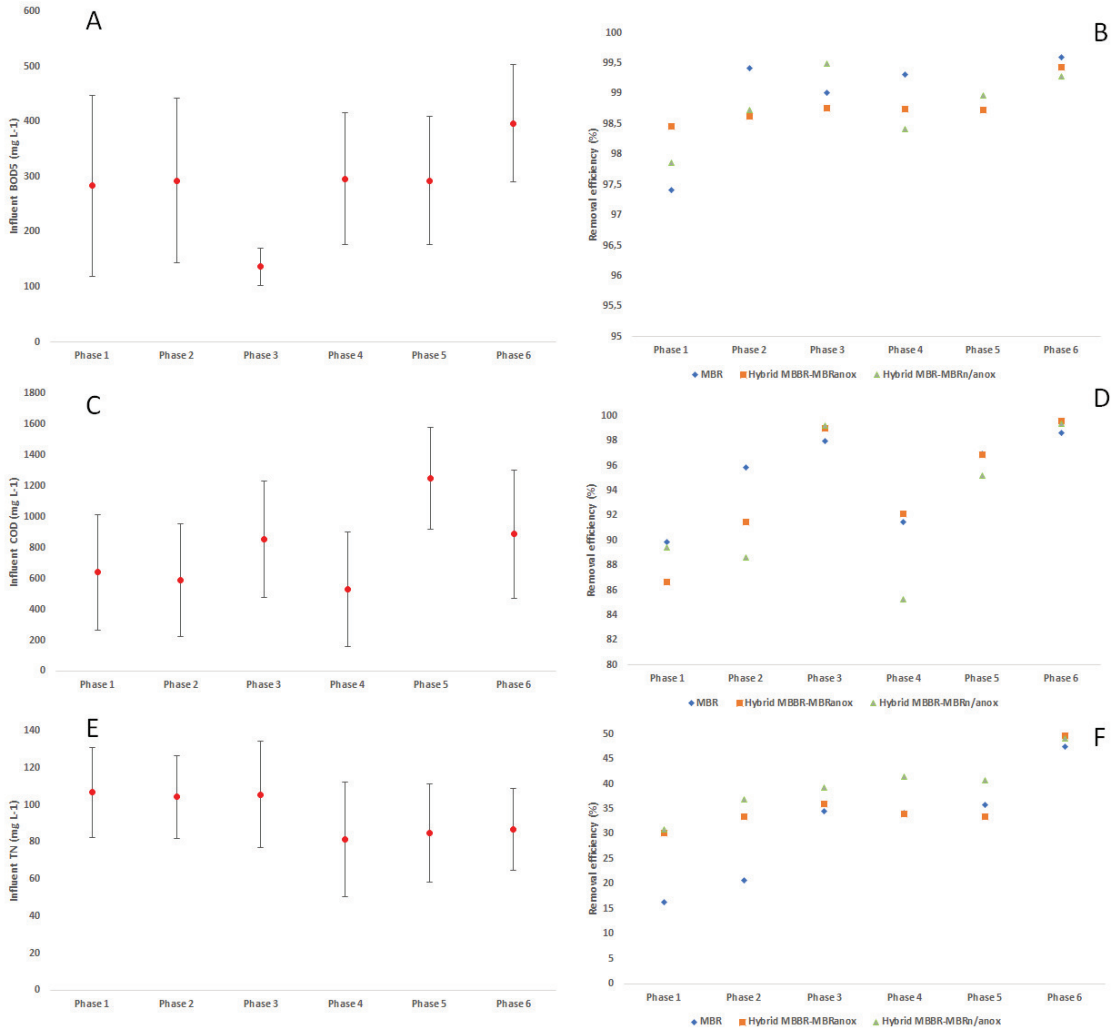

Figure 2 – Performance of the MBR and hybrid MBBR-MBR systems in terms of COD, BOD_5 and TN at the six operational scenarios tested. Subfigures A, C and E represent the influent values of BOD_5, COD and TN. The subfigures B, D and F represent the removal performance of BOD_5, COD and TN, respectively (see Table 1 for interpretation).

Table 1 – Mean values of the Monod model respirometric parameters for the three technologies operated under all of the operational conditions tested

Technology	Phase (Fig. 2, Figs S1-S3)	RDA Code (Figs. 3 & 5)	HRT (h)	Solids	$\mu_{m,H}$ (h^{-1})	$K_{M,H}$ (mg-O_2 L^{-1})	Y_H (mg-VSS mg-COD^{-1})	$\mu_{m,A}$ (h^{-1})	$K_{M,A}$ (mg-O_2 L^{-1})	Y_A (mg-VSS mg-N^{-1})	k_d (d^{-1})
MBR	1	1	6	2500	0.0095	708.2321	0.6203	0.012	240.8731	0.6069	0.0178
Hybrid MBBR-MBRanox		2	6	2500	0.0019	197.8068	0.6121	0.0072	2.3039	0.679	0.0097
Hybrid MBBR-MBRn/anox		3	6	2500	0.0084	989.0418	0.6062	0.0095	92.4332	0.6579	0.0114
MBR	2	4	9.5	2500	0.0035	71.8669	0.5848	0.0113	527.0066	0.5875	0.0268
Hybrid MBBR-MBRanox		5	9.5	2500	0.001	9.9981	0.5046	0.8035	31570.7858	0.5938	0.0219
Hybrid MBBR-MBRn/anox		6	9.5	2500	0.0031	167.6672	0.5783	0.0145	219.3647	0.6166	0.026
MBR	3	7	12	2500	0.0017	38.8388	0.5005	0.0051	619.4565	0.6223	0.0134
Hybrid MBBR-MBRanox		8	12	2500	0.0011	7.6355	0.6164	0.006	25.447	0.6637	0.0114
Hybrid MBBR-MBRn/anox		9	12	2500	0.0058	1227.9866	0.6162	0.0103	106.3457	0.6311	0.0154
MBR	4	10	6	3500	0.0043	345.2514	0.58	0.007	47.5525	0.5825	0.0118
Hybrid MBBR-MBRanox		11	6	3500	0.0048	759.9102	0.5709	0.0062	3.2659	0.6418	0.013
Hybrid MBBR-MBRn/anox13		12	6	3500	0.0084	989.0418	0.6062	0.0056	9.1895	0.5921	0.0183
MBR	5	13	9.5	3500	0.0035	221.5626	0.6086	0.0037	90.417	0.6271	0.0105
Hybrid MBBR-MBRanox		14	9.5	3500	0.0013	80.6953	0.6345	0.003	63.6735	0.5507	0.0084
Hybrid MBBR-MBRn/anox		15	9.5	3500	0.0057	848.4739	0.5775	0.009	264.3785	0.5368	0.0142
MBR	6	16	12	3500	0.0018	72.3594	0.4919	0.0166	1403.9297	0.577	0.0148
Hybrid MBBR-MBRanox		17	12	3500	0.0022	144.5881	0.562	0.0073	53.7352	0.5889	0.0225
Hybrid MBBR-MBRn/anox		18	12	3500	0.0051	854.445	0.4904	0.0101	106.8141	0.5958	0.0508

The elimination of nitrogen in the three technologies was not as efficient as organic matter removal. In terms of performance, the systems showed total nitrogen elimination efficiencies not higher than 50%. Data showed that the hybrid MBBR-MBRn/anox was the best technology for the elimination of nitrogen at all operational conditions tested in the study. With respect to regular salinity (around 1 mS cm^{-1}) conditions of wastewater, the MBR showed higher performance in nitrogen removal than the hybrid MBBR-MBR systems, showing slightly higher removal values – 56–69% – overall for the same operational solids concentrations (Leyva-Diaz et al., 2014; 2015b). On the other hand, the MBR technology was the least efficient for this purpose, remarkably at low operational MLSS and HRT. It seemed that nitrogen elimination was enhanced by the increase in MLSS concentration and the increase in the operational HRT for the MBR and the two hybrid MBBR-MBR systems. The values obtained for nitrogen elimination were substantially higher (about 30% higher) with respect to the same systems operated under constant 6.5 mS cm^{-1} salinity conditions (Rodriguez-Sanchez et al., 2017). In this sense, the results showed that nitrogen removal becomes limited by salinity and that cyclical variations in salinity offered better performances than constant salinity conditions.

3.2 Kinetic characterization of the MBR and hybrid MBBR-MBR systems

The biomass of the MBR and the two hybrid MBBR-MBR systems treating variable salinity wastewater under different operational conditions was analyzed for the heterotrophs, the autotrophs, and the endogenous global respiration (Table S1, Figs. 3–5).

Overall, the heterotrophic kinetics of the biomass in the three configurations had a low $r_{su,H}$, around 20-fold lower in comparison with systems at regular-salinity urban wastewater (Leyva-Diaz et al., 2015b). With respect to operation under constant salinity of 6.5 mS cm^{-1}, the heterotrophic kinetics had around 2-fold lower values (Rodriguez-Sanchez et al., 2017). For each of the HRTs studied at

cyclical salinity conditions, the heterotrophic kinetics was faster for higher MLSS concentrations. For the same MLSS concentration, higher HRTs lead to slower heterotrophic kinetics and to higher similarities among the three different configurations. For each of the six phases, the hybrid MBBR-MBRanox configuration showed the slowest heterotrophic kinetics. On the other hand, the MBR and the hybrid MBBR-MBRn/anox were similar in terms of kinetics for organic substrate degradation, with the MBR being faster at 2500 mg L^{-1} and the hybrid MBBR-MBRn/anox at 3500 mg L^{-1}. It is possible that the presence of carriers in the anoxic zone impacts the degradation of organic matter in these systems, as shown before (Leyva-Diaz et al., 2014).

Di Bella et al. (2015) also worked with MBR and hybrid MBBR-MBR systems at HRT values of 12–15 h, MLSS values of 6000 mg L^{-1} approximately, and biofilm concentration around 9000 mg L^{-1} and 30% filling fraction for the hybrid MBBR-MBR under salinity variation. These authors obtained values of $\mu_{m,H}$ around 100-fold higher than those corresponding to this research (2.51–3.65 day^{-1} for the MBR and 4.65–4.99 day^{-1} for the hybrid MBBR-MBR), as observed in Table 1 for the MBR and hybrid MBBR-MBR working at the most similar operation conditions (HRT = 12 h, MLSS = 3500 mg L^{-1}). Furthermore, the values of $K_{M,H}$ were around 10-fold lower (4.84–5.01 mgO_2 L^{-1}) than those obtained for the MBR, and around 100-fold lower (9.44–21.98 mgO_2 L^{-1}) than those obtained for the hybrid MBBRMBRn/anox, as observed in Table 1 (HRT = 12 h, MLSS = 3500 mg L^{-1}). Thus, the values of $r_{su,H}$ will probably be higher for the systems analyzed by Di Bella et al. (2015) due to the slightly longer HRT and higher biomass concentrations, implying a lower organic loading rate. Di Bella et al. (2015) carried out the start-up of the pilot-plants under a gradual increase of salinity that could improve the adaptation of heterotrophic biomass as the systems analyzed in this study were started up under variable salinity cycles.

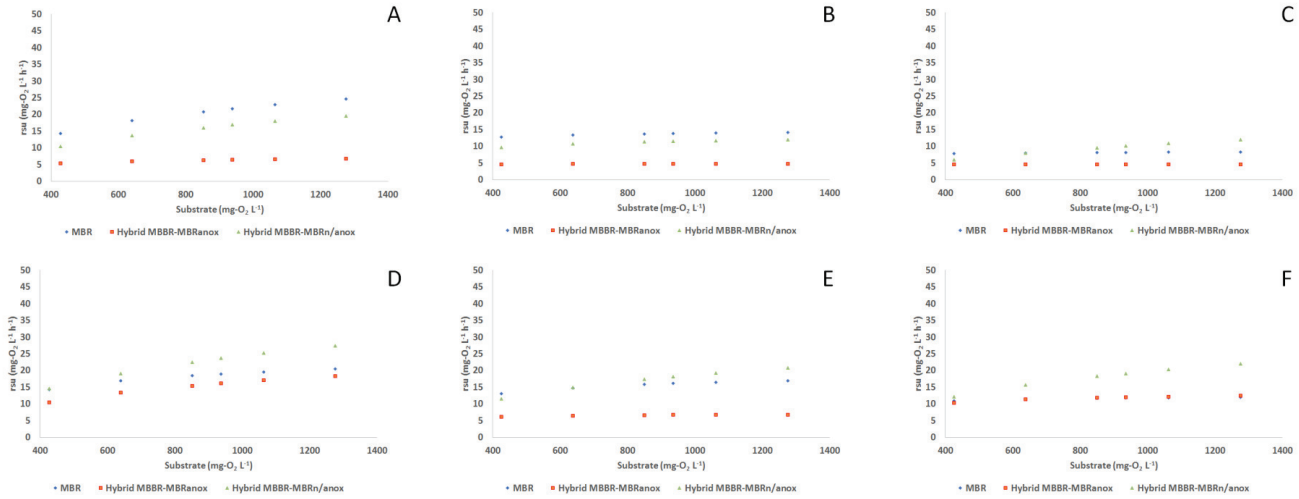

Figure 3 – Rates of substrate utilization of the heterotrophic biomass of the MBR and hybrid MBBR-MBR systems at the six operational scenarios (see Table 1 for interpretation)

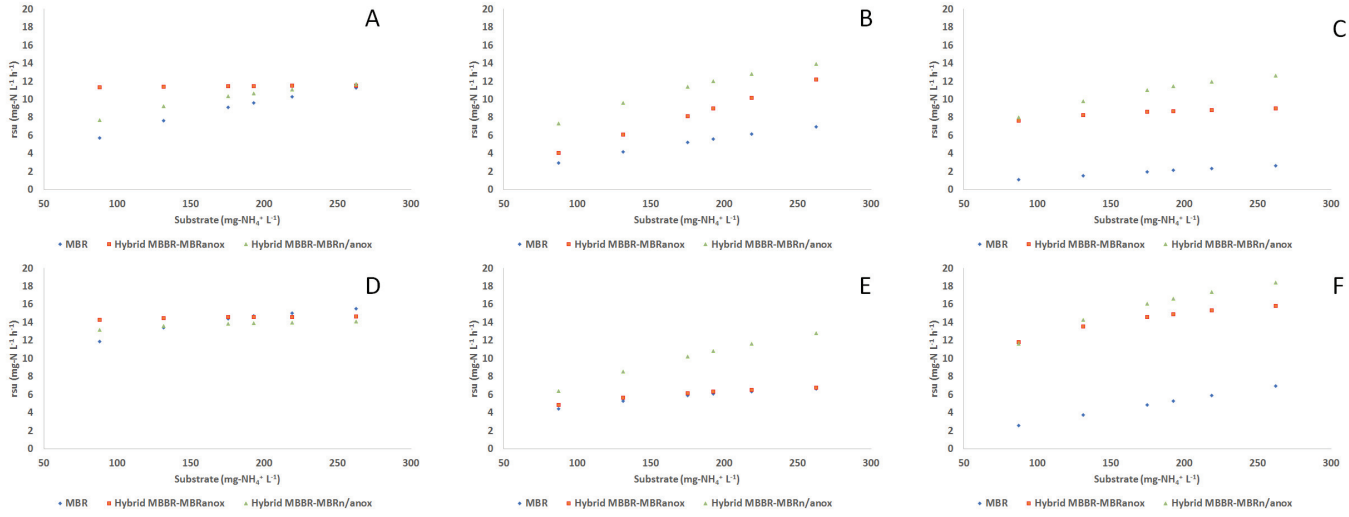

Figure 4 – Rates of substrate utilization of the autotrophic biomass of the MBR and hybrid MBBR-MBR systems at the six operational scenarios (see Table 1 for interpretation).

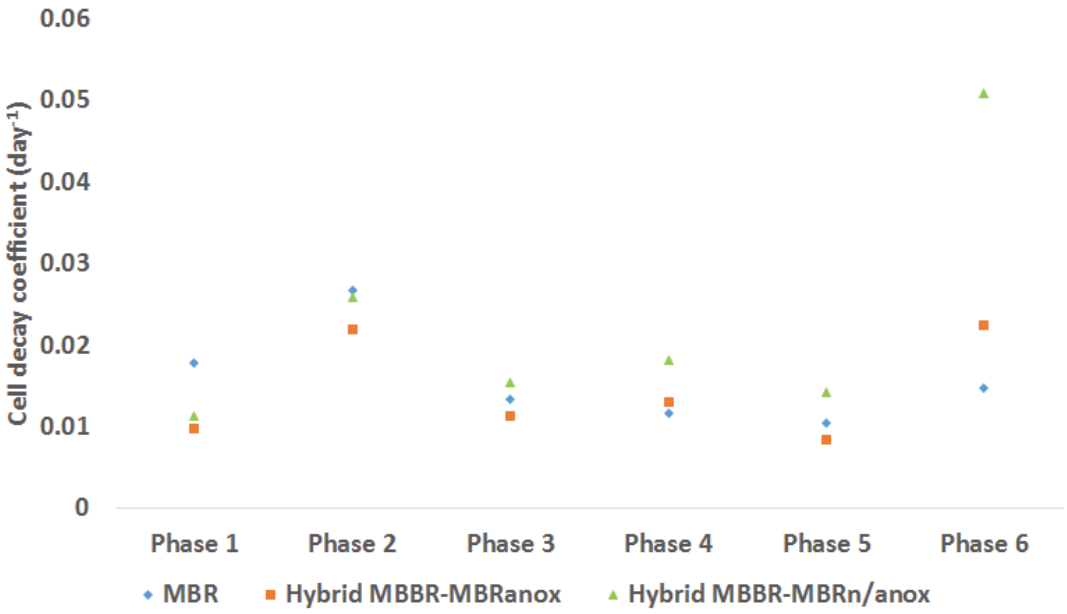

Figure 5 – Decay cell coefficient of the biomass of the MBR and hybrid MBBR-MBR systems at the six operational scenarios (see Table 1 for interpretation).

The kinetics for complete nitrification in the three configurations was slower in comparison to that of regular-salinity (around 1 mS cm^{-1}) wastewater, around 10-fold lower (Leyva-Diaz et al., 2015b), and slightly slower when compared to constant 6.5 mS cm^{-1} salinity (Rodriguez-Sanchez et al., 2017). The autotrophic kinetics was affected by the HRT. At 6 h of HRT, the three configurations had similar $r_{su,A}$ values with the hybrid MBBR-MBRanox having the fastest kinetics. On the other hand, at HRT of 9.5 and 12 h the hybrid MBBR-MBRn/anox had the fastest kinetics and the differences among the systems were more pronounced, with the MBR being the slowest for these four cases. For the HRTs of 6 and 12 h the autotrophic kinetics were faster for the 3500 mg L^{-1} than for the 2500 mg L^{-1}, but the values for the 9.5 h of HRT were similar. This behavior could be linked to the bacterial communities developing under the different HRTs. The kinetics of the MBR for the consumption of inorganic nitrogenous substrate became slower with the HRT, while the hybrid MBBR-MBR systems maintained the $r_{su,A}$ or increased it. Possibly, the presence of carriers enhanced the full nitrification of the hybrid MBBR-MBR systems with respect to the MBR, as was also observed in these

technologies working under regular salinity (around 1 mS cm^{-1}) urban wastewater (Leyva-Diaz et al., 2014).

In relation to the autotrophic kinetics behavior from Di Bella et al. (2015), which worked with MBR and hybrid MBBR-MBR systems under salinity variation as indicated previously, the values of $\mu_{m,A}$ were slightly lower than those obtained in this research for the MBR (0.21–0.29 day^{-1}), whereas they were slightly higher than those corresponding to this study for the hybrid MBBR-MBR (0.40–0.66 day^{-1}), as shown in Table 1 for the MBR and hybrid MBBR-MBR systems at 12 h of HRT and 3500 mg L^{-1} of MLSS. Nevertheless, the trend of $K_{M,A}$ values was radically different between both studies since Di Bella et al. (2015) had $K_{M,A}$ values around 1000-fold lower than those obtained in this research for the MBR (0.27–0.47 mg NH_4-N L^{-1}), and $K_{M,A}$ values around 100-fold lower concerning the hybrid MBBR-MBR systems (0.25–1.00 mg NH_4-N L^{-1}), according to Table 1 (HRT = 12 h, MLSS = 3500 mg L^{-1}). This great difference could imply a possible inability to oxidize the ammonium to nitrate by the systems of this study, which supports the low values of total nitrogen removal (< 50%). Thus, regarding autotrophic kinetics, the biological systems from Di Bella et al. (2015) also had higher $r_{su,A}$ than those corresponding to this study. The salinity adaptation developed by Di Bella et al. (2015) increased the salinity in steps forced after the adaptation of the biomass to current salinity conditions, thus selecting halophilic phylotypes slowly as salinity pressure was increased, which would select for ammonium and/or nitrite oxidizing biomass adapted to salinity conditions. Then, it is possible that the salinity-adapted autotrophic biomass obtained by Di Bella et al. (2015) could be more adapted as a consequence of this gradual increase of salinity with respect to the variable salinity cycles simulating tidal salinity variations imposed in the present study. In general, Di Trapani et al. (2014) obtained a similar trend to that shown by Di Bella et al. (2015) in relation to the heterotrophic and autotrophic kinetics analyzed in the present study. Di Trapani et al. (2014) worked with HRT values of 14–17 h, MLSS concentrations of 4100–7350 mg L^{-1} for the MBR and 1350–4350

mg L^{-1} for the hybrid MBBR-MBR, and biofilm concentration of 650–1350 mg L^{-1} and 50% filling fraction for the hybrid MBBR-MBR under salinity variation. This was also probably due to the operation under a gradual salinity increase with moderate salt shock steps.

There were no clear trends for the influence of the HRT and the MLSS in the cell decay coefficient of the three systems under variable salinity operation. Overall, the hybrid MBBR-MBRn/anox had the highest k_d values. The cell decay rate values were similar to those reported by other authors in MBR and hybrid MBBR-MBR systems working under regular-salinity urban wastewater (Leyva-Diaz et al., 2015b).

3.3 Linkage of microbial kinetics with operational and environmental conditions in the pilot-scale plants

The multivariate redundancy analyses triplots linking the operational parameters and environmental conditions with the heterotrophic and autotrophic kinetics are shown in Fig. 6A and B, respectively.

For the heterotrophic kinetics, the RDA showed that the $r_{su,H}$ at different substrate concentrations had a strong positive correlation with the MLSS and the influent BOD_5, a strong negative correlation with HRT and COD, a weak positive correlation with temperature and a weak negative correlation with dissolved oxygen. The $r_{su,H}$ at different substrates showed the same influence with respect to influent BOD, MLSS, HRT and COD. Therefore, these are the main factors that controlled the heterotrophic kinetics of the pilot-plants operated under variable salinity-amended urban wastewater. Differences in the heterotrophic kinetics at different substrate concentrations were controlled by dissolved oxygen concentration and temperature. In this way, heterotrophic kinetics

at low substrate concentrations were positively correlated with temperature and negatively with dissolved oxygen, while the opposite was found for high substrates.

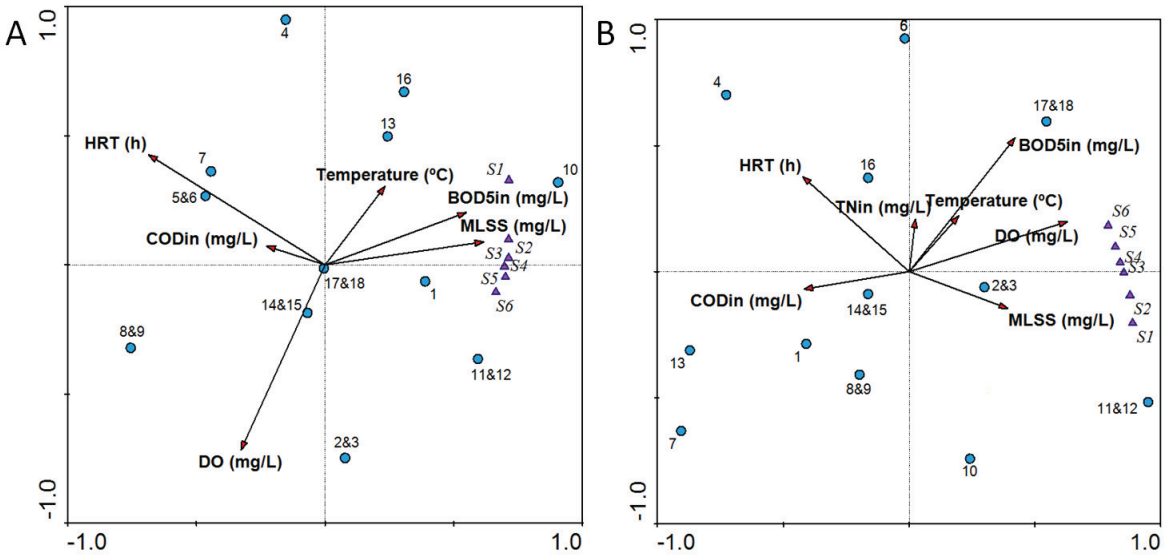

Figure 6 – Multivariate redundancy analyses of the heterotrophic (A) and autotrophic (B) kinetics for all the operational scenarios tested (see Table 1 and Table S2 for interpretation)

The r_{su} of autotrophs showed that complete nitrification had a strong negative correlation with COD and a strong positive correlation with dissolved oxygen concentration in the systems, which were the main parameters controlling the autotrophic kinetics. The nitrifying metabolism was outclassed during cycles with high influent COD concentrations. This could be caused by the outcompetition of autotrophic nitrifiers by heterotrophs and/or by preference of heterotrophic nitrifiers for organic substrate instead of nitrogen. This behavior was observed in partial nitritation systems subjected to inputs of organic matter in their influents (Gonzalez-Martinez et al., 2016). The same trend could be applied to oxygen concentration. The influent BOD_5 and temperature were positively correlated

with kinetics at high substrate concentrations, while the contrary occurred for the influent TN concentration.

3.4 Ordination and α-diversity analyses of the bacterial community structure in the bioreactors

The ordination of the massive parallel sequencing subsamples in the form of cluster and principal coordinates analyses are shown in Fig. 7. The clustering of samples showed a substantial differentiation between the two solids concentrations tested in the experiment, which occurred at 80% similarity threshold. In this way, the total solids at operation seemed to affect greatly the bacterial diversity at genus level within the bioreactors. For the systems operated around 2500 mg L^{-1} the clustering differentiated between the HRT of 6 h and the other two (9.5 and 12 h). On the other hand, at operation around 3500 mg L^{-1} the segregated HRT was that of 12 h. The differentiation in HRTs was found at 60% similarity threshold. The technological configurations of the three bioreactors trended for a clustering of the hybrid MBBR-MBR technologies while maintaining distance with the MBR technology at all total solids and HRTs analyzed. This difference was found at 40% similarity threshold, and was also confirmed by the principal coordinates analysis, where the subsamples from the MBR were separated from those coming from the hybrid MBBR-MBR technologies during the whole experiment time. In this regard, the clustering and principal coordinated analyses showed that total solids at operation, HRT and technology were, in that order, the most influential parameters in the bacterial community structure composition at genus level for the three bioreactors monitored in the experiment.

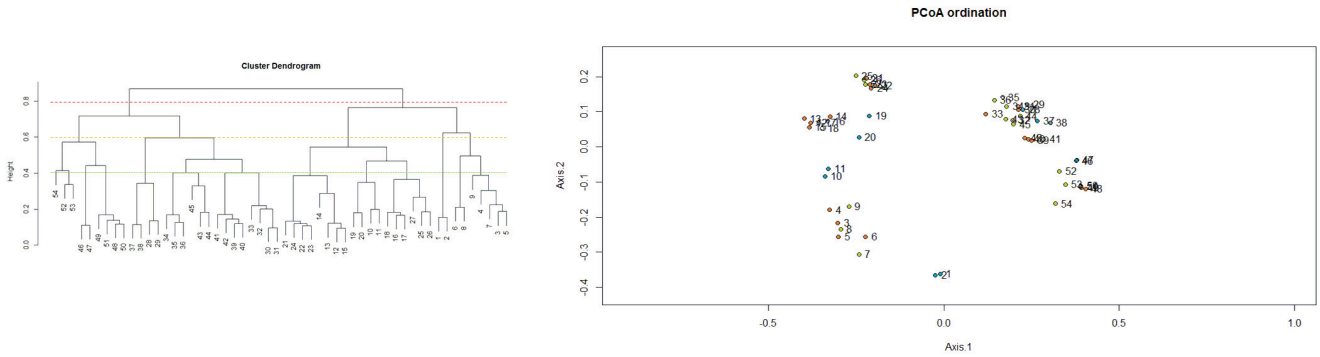

Figure 7 – Ordination of the bacterial community structure at genus level of the MBR and hybrid MBBR-MBR systems at the six operational scenarios tested.

This is related to the previous results obtained by the analysis of performance of the bioreactors. Accordingly, it was observed that the three technologies had a similar functioning in terms of total solids composition, as small concentrations of attached biomass were found for the hybrid MBBR-MBR systems. These became more similar to the MBR systems, and therefore the bacterial community structures at genus level were much more impacted by operational conditions than by the technological differences.

The values of the Chao-1, Shannon-Wiener, Simpson, Pielou's evenness and Berger-Parker evenness were affected by the operational conditions (Table S2). The evenness of the systems was found to decrease at the HRT of 9.5 h compared to the HRTs of 6 and 12 h, which was observed by the lower values in the Simpson and Pielou's evenness indices as well as the higher values for the Berger-Parker indices. Inthe same way, the Chao-1 and Shannon-Wiener indices were lower at HRT of 9.5 h. In this way, it seemed that operation at HRT of 9.5 h exerted more pressure over the bacterial communities in the MBR and hybrid MBBR-MBR systems, allowing for a less diverse bacterial community composition.

3.5 Bacterial community structure at genus level in the MBR and hybrid MBBR-MBR systems

The bacterial community at genus level for the MBR and hybrid MBBR-MBR systems showed differences for the three HRTs and two total solids concentrations tested in the study, although several genera accounted for a major present in almost all of the biological samples (Fig. S1). The most important among them were *Rhodanobacter* and *Nitrobacter*. *Rhodanobacter* was dominant in all bioreactors at around 2500 mg L^{-1} (4–36%) but lost relative abundance at around 3500 mg L^{-1} (0–10%), while the contrary occurred for *Nitrobacter* (0.5–7% and 0.2–6%, respectively). Thus, these two phylotypes could compete for the same substrate in the MBR and hybrid MBBR-MBR systems,

with solids concentration selecting them both. In this sense, both *Rhodanobacter* and *Nitrobacter* have been identified as main nitrite oxidizing bacteria in autotrophic nitrogen removal systems or in MBR and hybrid MBBR-MBR technologies, respectively (Leyva-Diaz et al., 2015b; Gonzalez-Martinez et al., 2016).

Several genera were more present at lower solids concentration, such as *Comamonas*, *Ottowia* *Dyella* and *Mizugakiibacter* (0.5–14%, 1.7–13%, 0.2–5% and 12–36% for 2500 mg L^{-1} solids concentrations, respectively), among others. *Comamonas* and *Ottowia* have been reported for heterotrophic ammonium oxidation and nitrate/nitrite reduction in biofilms, respectively (Liu et al., 2017). Also, *Dyella* genus has been identified as an important player of membrane biofouling in MBR systems (Lim et al., 2012). *Mizugakiibacter* was described as heterotrophic, nitrate-reducing capable bacterium (Hojima et al., 2017). Indeed, as well as *Comamonas* or *Rhodanobacter*, *Mizugakiibacter* can develop ferrous iron chemoautotrophic denitrification (Wang et al., 2017). Other genera were of importance only at HRT of 6 h, such as *Acinetobacter*, *Trichococcus* or *Ferruginibacter* (0.5–16%, 1–9%, 2–11%, respectively). *Acinetobacter* genera has been found of importance in coaggregation of bacterial cells for the formation of floc biomass (Malik et al., 2003). Moreover, *Ferruginibacter* has been associated with syntrophic denitrification metabolisms in environments with oxygen limitation (Chen et al., 2016; Zeng et al., 2016a), and it has been associated, in addition to *Ottowia*, with biofilm formation mechanisms in MBBR systems (Liu et al., 2017). *Acinetobacter*, *Trichococcus* and *Ferruginibacter* lost their relative abundance at the HRTs of 9.5 and 12 h, which confirms the clustering trend observed in the samples at around 2500 mg L^{-1} resulting in more similarities between 9.5 and 12 h HRT at this solids concentration. Genera *Mycetocola* was found to be of importance at HRTs of 9.5 and 12 h (1.5–5%), while *Thiothrix* was an important player in the bioreactors at HRT of 12 h only (2.5–4.8%).

When operating at around 3500 mg L^{-1} solids concentration an uncultured member of the *Gemmatimonadaceae* family appeared as a dominant phylotype (1–29%). Phylotypes belonging to this family have been reported as aerobic heterotrophic bacteria, with high resistance to extreme conditions of toxics and temperature, and with calcium carbonate precipitation in MBR systems (Wang et al., 2014; Zhang et al., 2017). Moreover, species of *Gemmatimonadaceae* family have the capability of phototrophic growth (Zeng et al., 2016b). Following the same trend in a timid manner, an uncultured *Cytophagaceae* family phylotype was found at this solids concentration (1.5–8%). *Cytophagaceae* members have been thought to outcompete other heterotrophs in MBR systems due to their capability for degradation of highand low-molecular weight organic compounds (Phan et al., 2016). *Paludibacterium*, *Thiothrix*, *Rudaea* and *Rhodanobacter* were found only at HRTs of 6 and 9.5 h (1.5–7.5%, 1.6–37%, 0–6% and 2–11%, respectively). *Paludibacterium* is a heterotrophic, nitrate-reducing bacterium (Kwon et al., 2017). *Rudaea* is a heterotrophic bacterium with preference for low dissolved oxygen levels in activated sludge systems (Ma et al., 2016; Weon et al., 2017). Their decline at 12 h HRT coincided with an increase in the relative abundance of the uncultured *Gemmatimonadaceae* and *Cytophagaceae* bacteria (7.5–25.5% and 1.5–8%), and *Phycisphaera* and *Azoarcus* genera (0–7% and 2–4%). *Phycisphaera* is a marine, facultative anaerobic heterotroph with capacity for nitrate reduction which has been linked with nitrogen removal in MBR systems (Fukunaga et al., 2009; Zhuang et al., 2016). This might indicate an outcompetition of *Paludibacterium* and *Rhodanobacter* by *Phycisphaera* for the substrate of nitrate, and also of *Thiothrix* and *Rudaea* by the *Gemmatimonadaceae*, *Cytophagaceae* and *Azoarcus* phylotypes. Also, this finding was in accordance with ordination analyses of the operation at around 3500 mg L^{-1} solids concentration, which segregated the sample

at 12 h HRT with respect to those at 6 and 9.5 h HRT.

3.6 Linkage between bacterial community and microbial kinetics

Multivariate redundancy analyses were developed in order to link the bacterial communities in the bioreactors with the autotrophic and heterotrophic kinetics of its biomass (Fig. 8). In both cases, the r_{su} at different substrates were close to each other. For the heterotrophic kinetics the multivariate redundancy analysis showed that *Thiothrix*, *Phycisphaera* and *Paludibacterium*, but mainly *Azoarcus* and *Trichococcus*, were positively correlated with heterotrophic r_{su}. On the other hand, *Azoarcus* and *Cytophagaceae* representative had the most positive correlation with autotrophic kinetics, but also *Phycisphaera*, *Thiothrix*, *Paludibacterium* and the uncultured *Gemmatimonadaceae* phylotype were positively correlated with autotrophic r_{su}. In this sense, it is possible that *Azoarcus* was the most efficient organic matter degradator in the bioreactors operating under tidal salinity wastewater conditions and, in addition, the most important phylotype linked to faster autotrophic kinetics, which could be explained by heterotrophic nitrification metabolism or co-metabolism that could help other phylotypes in the oxidation of nitrogenous compounds. Further investigation should be conducted in order to shed light on the nitrogen metabolism on bioreactors treating tidal salinity wastewater and on the contribution of *Azoarcus* genera in particular. On the other hand, dominant phylotypes *Rhodanobacter* and *Nitrobacter* were negatively correlated with autotrophic and heterotrophic kinetics, and therefore it is possible that their contribution was only related to denitrification metabolism in the biosystems.

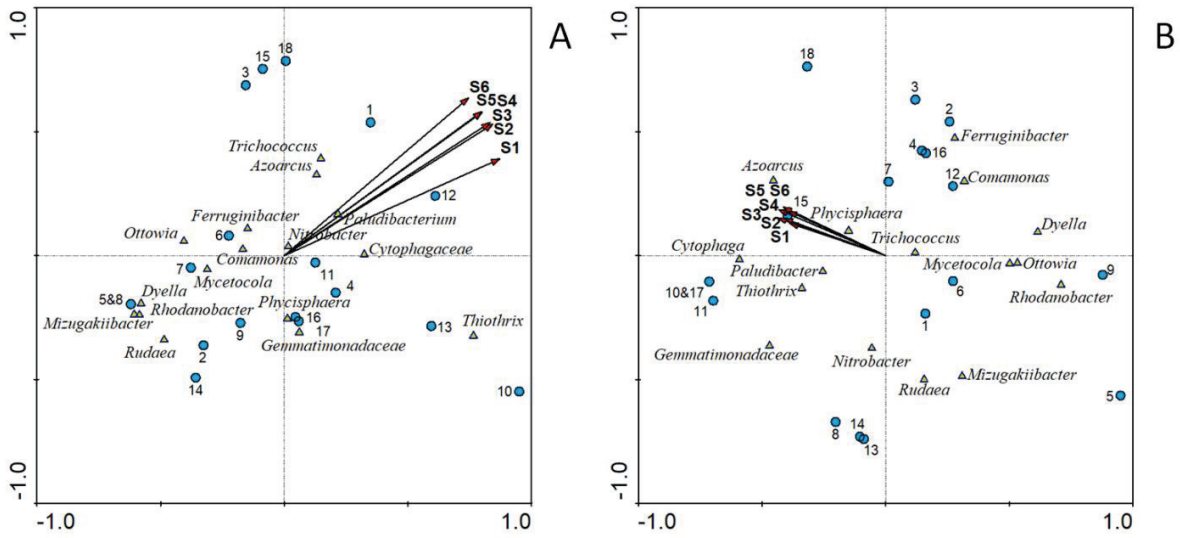

Figure 8 – Linkage of the bacterial community structure and the heterotrophic (A) and autotrophic (B) kinetics for all the operational scenarios tested (see Table 1 and Table S2 for interpretation)

4. Conclusions

A MBR and two hybrid MBBR-MBR systems were operated for the treatment of urban wastewater with tidal salinity variations. The performance of the systems, the kinetics of their microbial communities and their bacterial community structure were monitored for 2500 mg L^{-1} and 3500 mg L^{-1} of MLSS concentrations and 6 h, 9.5 h and 12 h of HRT. The performance in organic matter removal was better at higher solids and HRT, but were close for the six different scenarios (lowest of 89.63% COD and 98.47% BOD_5 up to 99.61% for COD and 99.45% for BOD_5 at maximum). The microbial kinetics for heterotrophic and autotrophic biomass were slow (ranging 4.57–24.60 mgO_2 L^{-1} h^{-1} for heterotrophic biomass and 1.12–18.39 mg-N L^{-1} h^{-1} for autotrophic biomass) and correlated positively with solids concentration. The bacterial community structure showed an ordination depending on operational solids concentration and hydraulic retention time, with technological configurations being of less importance. *Rhodanobacter* (4–36%) and *Nitrobacter* (0.2–7%) were present at almost all operational scenarios. *Comamonas*, *Ottowia Dyella* and *Mizugakiibacter* were

present at all conditions under 2500 mg L^{-1} solids operation (0.5–14%, 1.7–13%, 0.2–5% and 12–36%). *Acinetobacter*,

Trichococcus or *Ferruginibacter* (0.5–16%, 1–9%, 2–11%, respectively) were present only under 6 h HRT while *Mycetocola* (1.5–5%) and *Thiothrix* (2.5–4.8%) proliferated at 9.5 and 12 h HRT. Uncultured members of the *Gemmatimonadaceae* and *Cytophagaceae* families were found at all conditions for 3500 mg L^{-1} (1–29% and 1.5–8%), with *Paludibacterium*, *Thiothrix, Rudaea* and *Rhodanobacter* present only at HRTs of 6 and 9.5 h (1.5–7.5%, 1.6–37%, 0–6% and 2–11%, respectively) while *Phycisphaera* and *Azoarcus* genera thrived at 12 h HRT (0–7% and 2–4%). Overall, the results showed that, in practice, technological configurations between the MBR and the hybrid MBBR-MBR did not had an influence when treating urban wastewater subjected to tidal salinity variations.

Acknowledgements

The authors would like to acknowledge the support given by the Department of Civil Engineering of the University of Granada, as well as by the Institute of Water Research of the University of Granada.

Appendix A. Supplementary data

Supplementary data associated with this article can be found, in the online version, at http://dx.doi.org/10.1016/j.cej.2017.10.118.

References

APHA (2012) Standard Methods for the Examination of Water and Wastewater, 22nd ed., American Public Health Association, Washington DC.

Bassin JP, Kleerebezem R, Muyzer G, Soares Rosado A, van Loosdrecht MCM,

Dezzoti M (2012) Effect of different salt adaptation strategies on the microbial diversity, activity, and settling of nitrifying sludge in sequencing batch reactors. Appl Microbiol Biotechnol 93: 1281–1294.

Castillo-Carvajal LC, Sanz-Martin JL, Barragan-Huerta BE (2014) Biodegradation of organic pollutants in saline wastewater by halophilic microorganisms: a review. Environ Sci Pollut Res 21: 9578–9588.

Chen R, Luo Y, Chen J, Zhang Y, Wen L, Shi L, Tang Y (2016) Evolution of the microbial community of the biofilm in a methane-based membrane biofilm reactor reducing multiple electron acceptors. Environ Sci Pollut Res 23: 9540–9548, http://dx.doi.org/10.1007/s11356-016-6146-y.

Cortes-Lorenzo C, Gonzalez-Martinez A, Smidt H, Gonzalez-Lopez J, Rodelas B (2016) Influence of salinity on fungal communities in a submerged fixed bed bioreactor for wastewater treatment. Chem Eng J 285: 562–572.

Di Trapani D, Di Bella B, Mannina G, Torregrossa M, Viviani G (2014) Comparison between moving bed-membrane bioreactor (MB-MBR) and membrane bioreactor (MBR) systems: influent of wastewater salinity variation Bioresour Technol 162: 60–69.

Di Bella G, Di Prima N, Di Trapani D, Freni G, Giustra MG, Torregrossa M,

Viviane G (2015) Performance of membrane bioreactor (MBR) systems for the treatment of shipboard slops: assessment of hydrocarbon biodegradation and biomass activity under salinity variation. J Hazard Mater 300: 765–778.

Edgar RC, Haas BJ, Clemente JC, Quince C, Knight R (2011) UCHIME improves sensitivity and speed of chimera detection. Bioinformatics 27: 2194–2200.

Fukunaga Y, Kurahashi M, Sakiyama Y, Ohuchi M, Yokota A, Harayama S (2009) Phycisphaera mikurensis gen. nov., sp. nov., isolated from a marine alga, and pro- posal of Phycisphaeraceae fam. nov., Phycisphaerales ord. nov. and Phycisphaerae classis nov. in the phylum Planctomycetes. J Gen Appl Microbiol 55: 267–275.

Gonzalez-Martinez A, Leyva-Diaz JC, Rodriguez-Sanchez A, Muñoz-Palazon B,

Rivadeneyra A, Poyatos JM, Rivadeneyra MA, Martinez-Toledo MV (2014) Isolation and characterization of bacteria associated with calcium carbonate and struvite precipitation in a pure moving bed biofilm reactor membrane bioreactor. Biofouling 31: 333–348.

Gonzalez-Martinez A, Rodriguez-Sanchez A, Garcia-Ruiz MJ, Muñoz-Palazon B, Cortes-Lorenzo C, Osorio F, Vahala R (2015) Performance and bacterial community dynamics of a CANON bioreactor acclimated from high to low operational temperatures. Chem Eng J 287: 557–567, http://dx.doi.org/10.1016/j.cej. 2015.11.081..

Hammer Ø, Harper D (2006) Paleontological Data Analysis, Blackwell Publishing, Oxford.

Huse SM, Welch DM, Morrison HG, Sogin ML (2010) Ironing out the wrinkles in the rare biosphere through improved OUT clustering. Environ Microbiol 12: 1889–1898.

Kojima H, Tokizawa R, Fukui M (2017) Mizugakiibacter sediminis gen. nov., sp. nov., isolated from a freshwater lake. Int J Syst Evol Microbiol 64: 3983–3987, http://dx.doi.org/10.1099/ijs.0.064659-0.

Kwon S, Kim B, Kim W, Yoo K, Yoo S, Son J, Weon H (2017) Paludibacter yongneupense gen. nov. sp. nov., isolated from a wetland, Yongneup, in Korea. Int J Syst Evol Microbiol 58: 190–194, http://dx.doi.org/10.1099/ijs.0.64831-0.

Leyva-Diaz JC, Calderón K, Rodríguez FA, González-López J (2013) Comparative kinetic study between moving bed biofilm reactor-membrane bioreactor and membrane bioreactor systems and their influence on organic matter and nutrients removal. Biochem Eng J 77: 28–40, http://dx.doi.org/10.1016/j.bej.2013. 04.023.

Leyva-Diaz JC, Martin-Pascual J, Muñio MM, Gonzalez-Lopez J, Hontoria E, Poyatos JM (2014) Comparative kinetics of hybrid and pure moving bed reactor-membrane bioreactors, Ecol Eng 70: 227–234, http://dx.doi.org/10.1016/j. ecoleng.2014.05.017.

Leyva-Diaz JC, Lopez-Lopez C, Martin-Pascual J, Muñio MM, Poyatos JM (2015a) Kinetic study of the combined processes of a membrane bioreactor and a hybrid moving bed biofilm reactor-membrane bioreactor with advanced oxidation processes as a post-treatment stage for wastewater treatment. Chem Eng Process Process Intensif 91: 57–66, http://dx.doi.org/10.1016/j.cep.2015.03.017.

Leyva-Díaz JC, Gonzalez-Martinez A, Gonzalez-Lopez J, Muñio MM,

Poyatos JM (2015b) Kinetic modeling and microbiological study of two-step nitrification in a membrane bioreactor and hybrid moving bed biofilm reactor–membrane bioreactor for wastewater treatment. Chem Eng J 259: 692–702, http://dx. doi.org/10.1016/j.cej.2014.07.136.

Lim S, Kim S, Yeon K, Sang B, Chun J, Lee C (2012) Correlation between microbial community structure and biofouling in a laboratory scale membrane bioreactor with synthetic wastewater. Desalination 287: 209–215, http://dx.doi.org/ 10.1016/j.desal.2011.09.030.

Liu T, Mao Y, Shi Y, Quan X (2017) Start-up and bacterial community compositions of partial nitrification in moving bed biofilm reactor. Appl Microbiol Biotechnol 101: 2563–2574, http://dx.doi.org/10.1007/s00253-016-8003-9.

Ma S, Ding L, Huang H, Geng J, Xu K, Zhang Y, Ren H (2016) Effects of DO levels on surface force, cell membrane properties and microbial community dynamics of activated sludge. Bioresour Technol 214: 645–652, http://dx.doi.org/10. 1016/j.biortech.2016.04.132.

Malik A, Sakamoto M, Hanazaki S, Osawa M, Suzuki T, Tochigi M, Kakii K (2003) Coaggregation among nonflocculating bacteria isolated from activated sludge. Appl Environ Microbiol 69: 6056–6063, http://dx.doi.org/10.1128/AEM. 69.10.6056.

Martín-Pascual J, Reboleiro-Rivas P, Muñio MM, González-López J,

Poyatos JM (2016) Membrane fouling of a hybrid moving bed membrane bioreactor plant to treat real urban wastewater. Chem Eng Process 104: 112–119.

Nakamura K (2017) Gemmatimonas aurantiaca gen. nov., sp. nov., a Gram-negative, aerobic, polyphosphate accumulating micro-organism, the first cultured representative of the new bacterial phylum Gemmatimonadetes phyl. Nov. Int J Syst Evol Microbiol 53: 1155–1163, http://dx.doi.org/10.1099/ijs.0.02520-0.

Phan HV, Hai FI, Zhang R, Kang J, Price WE, Nghiem LD (2016) Bacterial community dynamics in an anoxic-aerobic membrane bioreactor: impact on nutrient and trace organic contaminant removal. Int Biodeterior Biodegrad 109: 61–72, http://dx.doi.org/10.1016/j.ibiod.2016.01.002.

Rodriguez-Sanchez A, Leyva-Diaz JC, Gonzalez-Lopez J, Poyatos JM (2017) Performance and kinetics of membrane and hybrid moving bed biofilm-membrane bioreactors treating salinity wastewater. AIChE J 1–14 (2017), http://dx.doi.org/10.1002/aic.

Schloss PD, Westcott SL, Ryabin T, Hall JR, Hartmann M, Hollister EB, et al. (2009) Introducing mothur: open-source, platform-independent, community-supported software for describing and comparing microbial communities. Appl Environ Microbiol 75: 7537–7541.

Wang XJ, Xia SQ, Chen L, Zhao JF, Renault NJ, Chovelon JM (2006) Nutrients removal from municipal wastewater by chemical precipitation in a moving bed biofilm reactor. Process Biochem 41: 824–828.

Wang J, Lu H, Chen G, Lau GN, Tsang WL, Van Loosdrecht MCM (2009) A novel sulfate reduction, autotrophic denitrification, nitrification integrated (SANI) process for saline wastewater treatment. Water Res 43: 2363–2372, http://dx. doi.org/10.1016/j.watres.2009.02.037.

Wang Z, Huang F, Mei X, Wang Q, Song H, Zhu C, Wu Z (2014) Long-term operation of an MBR in the presence of zinc oxide nanoparticles reveals no significant adverse effects on its performance. J Membr Sci 471: 258–264, http://dx.doi.org/ 10.1016/j.memsci.2014.08.024.

Wang R, Yang C, Zhang M, Xu S, Dai C, Liang L, Zhao H, Zheng P (2017) Chemoautotrophic denitrification based on ferrous iron oxidation: reactor performance and sludge characteristics. Chem Eng J 313: 693–701, http://dx. doi.org/10.1016/j.cej.2016.12.052.

Weon H, Yoo S, Kim Y, Lee C, Kim B, Jeon Y, Hong S, Anandham R, Kwon S (2017) Rudaea cellulosylitica gen. nov. sp. nov., isolated from soil. Int J Syst Evol Microbiol 59: 2308–2312, http://dx.doi.org/10.1099/ijs.0.005165-0.

Zeng T, Li D, Jiang X, Qiu W, Chen Q, Zhang J (2016a) Microbial characteristics of an ANAMMOX biofilter for sewage treatment. J Water Process Eng 12: 105–110, http://dx.doi.org/10.1016/j.jwpe.2016.07.002.

Zeng Y, Baumbach J, Guilherme E, Barbosa V, Azevedo V, Zhang C, Koblížek M (2016b) Metagenomic evidence for the presence of phototrophic Gemmatimonadetes bacteria in diverse environments. Environ Microbiol Rep 8: 139–149, http:// dx.doi.org/10.1111/1758-2229.12363.

Zhang H, Sekiguchi Y, Hanada S, Hugenholtz P, Kim H, Kamagata Y,

Zhuang H, Hong X, Han H, Shan S (2016) Effect of pure oxygen fine bubbles on the organic matter removal and bacterial community evolution treating coal gasification wastewater by membrane bioreactor. Bioresour Technol 221: 262–269, http://dx.doi.org/10.1016/j.biortech.2016.09.029.

Chapter 4

Effect of variable salinity wastewater on performance and kinetics of membrane-based bioreactors

This chapter has been sent for its publication to AIChE Journal in its current form. The authors of the manuscript and its title are the following:

Alejandro Rodríguez-Sanchez, Juan Carlos Leyva-Diaz, Barbara Muñoz Palazon, Jesus Gonzalez-Lopez, Jose Manuel Poyatos. Effect of variable salinity wastewater on performance and kinetics of membrane-based bioreactors.

Abstract

A MBR and two hybrid MBBR-MBR systems were operated in parallel for the treatment of variable-salinity wastewater. Influent salinity was changed according to tidal-like cycles: 6 h of maximum salinity (4.5 or 8.5 mS cm^{-1}) followed by 6 h of regular wastewater salinity (around 1 mS cm^{-1}). For the two salinity scenarios, the bioprocesses operated under different conditions of mixed liquor total suspended solids (2500 and 3500 mg L^{-1}), and hydraulic retention time (6, 9.5 and 12 h). The results showed that the bioprocesses had better performance under 4.5 mS cm^{-1} than under 8.5 mS cm^{-1} in terms of removal of BOD_5 (+6.07%), NH_4^+ (+41.29%) and total nitrogen (+37.64%), the heterotrophic and autotrophic yield coefficients (+0.02777 mg-VSS mg-COD^{-1} and +0.13990 mg-VSS mg-N^{-1}), and the autotrophic rate of substrate utilization (+3.39559 mg-N L^{-1} h^{-1}). The results obtained would become of help for the modeling of membrane-based systems treating variable saline wastewater.

1. Introduction

Saline wastewater could be generated from several industries such as food processing, fish canning, petroleum refining, textile manufacturing, and leather production companies (Lefebvre & Moletta, 2006; Aslan & Simsek, 2012). In addition, municipal wastewater could be affected by saline industrial wastewater, the use of seawater for toilet flushing in many coastal cities or the utilization of salt in the cities for thawing the streets (Ludzack & Noran, 1965; Sudarno et al., 2011; Alan & Simsek, 2012), as well as possible intrusions of seawater into the sewage system in wastewater treatment plants (WWTPs) from coastal areas.

Salt constitutes a stress factor that could destabilize the microbial communities, reduce their metabolic activities and modify their biomass kinetics within the biological processes of removal of carbonaceous and nitrogenous compounds in WWTPs (Vyrides & Stuckey, 2009; Bassin et al., 2012; Rodriguez-Sanchez et al., 2017). Especially, nitrification process is particularly sensitive to inhibition by salt (Moussa et al., 2006; Zhao et al., 2014). Although substantial research of the effect of influent salinity over bioreactors has been done, these researches have always been constrained to influents with constant salinity conditions. However, some phenomenon, such as seawater intrusion in coastal WWTPs, impose variable influent salinity conditions over bioreactors, which effect over their performance, kinetics and biomass is mostly unknown (Rodriguez-Sanchez et al., 2018a).

Lefebvre and Moletta (2006) stated that biological treatment of carbonaceous and nitrogenous pollution was viable at high salt concentrations although its efficiency is subject to the adaptation level of the biomass. In this regard, membrane bioreactor (MBR) has been effectively applied for saline wastewater treatment (Di Bella et al., 2013; Jang et al., 2013; Johir et al., 2013). In particular, MBR has several advantages in relation to the conventional activated sludge process, i.e. small space requirements, high-quality effluent, higher volumetric loadings and lower sludge production (Openheimer et al., 2001). Recently, the hybrid moving bed biofilm reactor-membrane bioreactor

(hybrid MBBR-MBR), which combines MBR technology with a biofilm system, has been used to improve the performance of the whole system. In this way, the biomass can grow both as suspended flocs and biofilm (Di Trapani et al., 2013). This system also provides several advantages over the activated sludge system, i.e. higher total biomass concentration inside the bioreactor, upgrading of overloaded activated sludge plants without the construction of new reactors, and increase of the sludge retention time in the system that could favor the development of adapted and specialized microbial communities (Huang et al., 2008; Mannina et al., 2009; Liu et al., 2010; Leyva-Diaz et al., 2013a). Nevertheless, the operation of these systems is limited to operational parameters such as concentrations of salt, salt adaption and acclimation strategy, biomass concentration inside the bioreactor, existence of pure or mixed culture in the bioreactor, and hydraulic retention time, among others.

In this context, it has not been completely elucidated the effect that variable salinity conditions can exert on heterotrophic and autotrophic biomass respiratory activities and system performance within MBR and hybrid MBBR-MBR systems for municipal wastewater treatment. In this regard, a respirometric method has been used to carry out the kinetic modeling for MBR and hybrid MBBR-MBR because of its high reproducibility and accuracy (Leyva-Diaz et al., 2013b).

Thus, the aim of this work was to evaluate the effect of the hydraulic retention time, the mixed liquor total suspended solids and the variable influent salinity on three biological systems working in parallel treating salinity-amended real wastewater, i.e. an MBR and two hybrid MBBR-MBR configurations, in terms of process performance and microbial kinetics with the peculiarity of carrying out the start-up of them at variable-salinity conditions without a previous acclimation. For this, the lab-scale plants worked at 4.5 and 8.5 mS cm^{-1} maximum influent salinity under different operation conditions concerning mixed liquor total suspended solids (MLTSS) (2500 and 3500 mg L^{-1}) and hydraulic retention time (HRT) (6, 9.5 and 12 h). The systems operated at room temperature

which oscillated between 16 and 21 °C. The different technologies were characterized concerning the removal performance of organic matter and nitrogen, as well as the heterotrophic and autotrophic kinetics, and a comparison of them was carried out by using PERMANOVA and multivariate redundancy analyses in order to observe the influence of maximum salinity.

2. Materials and methods

2.1 Description of the bioreactors, influent wastewater conditions and operation of the bioreactors

This experiment was developed using three similarly configured bioreactors (Figure 1). The bioreactors were composed of separated four-chambers bioreactor and membrane tank. The four chambers had dimensions of 12 cm × 12 cm × 60 cm and were operated under an effective working volume of 6 L each. The membrane tank had dimensions of 10 cm Ø × 60 cm height and operated under an effective volume of 4.32 L. The whole operational volume of the bioreactor was then of 28.32 L. The first, third and fourth chambers of the bioreactor were aerated by the means of AFD 2760 fine bubble diffusers (ECOTEC SA, Spain) located at the bottom of the chambers, while the membrane tank was aerated by a CAP 3 coarse bubble diffuser (ECOTEC SA, Spain) located at the bottom of the tank. The aeration was provided by an ACO-500 air compressor (Hailea, China) and controlled by a 2100 Model rotameter (TecFluid SA, Spain). The anaerobic second chamber of each bioreactor was not aerated and agitated by mechanical stirring provided by Multi Mixer MM-1000 stirrers (Biosan Laboratories Inc, USA). Each membrane tank contained a membrane module of polyvinylidene hollow fibers with a reinforcement in the core made of polyester (Micronet Porous Fibers SL, Spain). The fibers had an external diameter of 2.45 mm and an internal diameter of 1.10 mm, with 0.04 µm pore diameter, providing a total membrane area of 0.20 m^2.

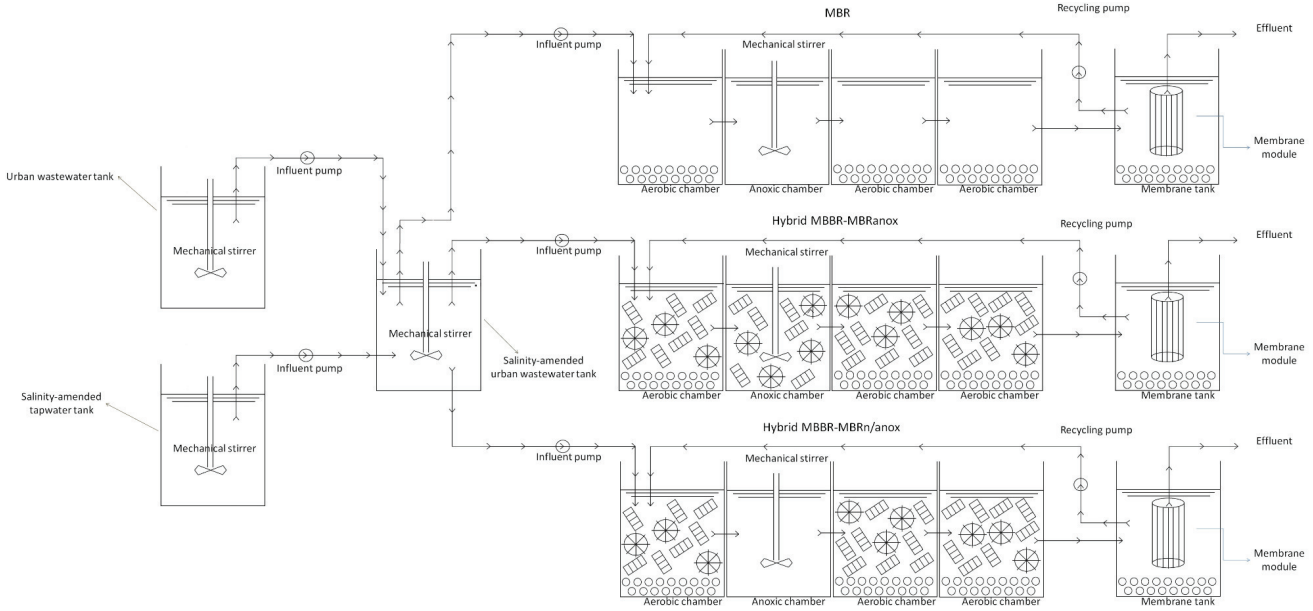

Figure 1 – Schematic of the three technologies working in parallel

During all experiments, influent wastewater was fed to the bioreactor using a 323S Watson Marlow peristaltic pump (Watson-Marlow Pumps Group) into the first chamber. Then, the wastewater was forced to pass through the second, third and fourth chambers before being discharged into the membrane tank. A recycling flow was imposed from the membrane tank to the first chamber with a flow rate equal to 500% of influent flow rate at any given operational conditions using a 323S Watson Marlow peristaltic pump. From the membrane tank, the effluent was withdrawn to the permeate tank with a 323S Watson Marlow peristaltic pump operating in cycles of: 9 min withdraw, 1 min backwash. The effluent was forced to pass through the membrane module before entering the permeate tank. The membrane was cleaned regularly to avoid clogging of membrane pores and to maintain an operational transmembrane pressure below 0.5 bar.

The three bioreactors were operated in parallel and under three different technological configurations: membrane bioreactor (MBR), hybrid moving bed biofilm reactor-membrane bioreactor with carriers in the anoxic zone (hybrid MBBR-MBRanox) and hybrid moving bed bioreactor-membrane bioreactor without carriers in the anoxic zone (hybrid MBBR-MBRn/anox). The difference of the configurations resided in the presence/absence of plastic carrier media in the bioreactor's chambers. One configuration was a membrane bioreactor (MBR), with no carriers in the bioreactor. The other two configurations used K1 carriers (Anox-Kaldnes AS, Norway) with a density of 0.92–0.96 g cm^{-3}. For the hybrid MBBR-MBRanox, all chambers were filled at 35% volume with carriers detailed above, giving a specific surface area within the bioreactor of 148.9 m^2 m^{-3}. The hybrid MBBR-MBRn/anox was filled at 35% volume with K1 carriers in all chambers except for the second, giving a specific surface area within the bioreactor of 111.7 m^2 m^{-3}.

The influent wastewater used in this experiment was subjected to a salinity-amendment process in order to operate under given NaCl, measured as electric conductivity, changing over time. For this purpose, two water storage tanks were used: one for real wastewater collected from the Los Vados

Wastewater Treatment Plant (Granada, Spain) and the other for salinity amended tap water with 50 mS cm^{-1} electric conductivity. The contents from the two water storage tanks were mixed in the mixing tank. The mixing was controlled electronically by a TOPAX LF1 conductivity module (Lutz-Jesco GmbH, Germany), connected to a conductivity sensor that measured the conductivity of the mixing tank wastewater and its temperature continuously, providing their values to the module. The module was also connected to two Watson Marlow peristaltic pumps, which pumped water from the two storage tanks. The conductivity control module controlled the pumping of both pumps through the reading of electric conductivity and its comparison to the electric conductivity desired at any given time, depending on the desired scenario of operation. The change in influent wastewater conductivity in the mixing tank was achieved by: addition of 50 mS cm^{-1} electric conductivity salinity-amended tap water to increase the conductivity or addition of regular-salinity urban wastewater to decrease the conductivity. Prior to the experimentation process, the automatic conductivity control was tested and modified properly in order to provide accurate electric conductivities and in order to optimize the time necessary to change water conductivity during cyclical conditions. Two scenarios of influent wastewater were analyzed: a) tidal-like variable with maximum salinity value of 4.5 mS cm^{-1} during 6 hours and regular wastewater salinity during 6 hours; b) tidal-like variable with maximum salinity value of 8.5 mS cm^{-1} during 6 hours and regular wastewater salinity during 6 hours.

The bioreactors were operated attending to the hydraulic retention time (HRT) and mixed liquor total suspended solids concentration (MLTSS). In this regard, the three technologies were operated at HRTs of 6, 9.5 and 12 h and MLTSS of 2500 and 3500 mg L^{-1} for each of the two influent wastewater scenarios. The mean cell residence time (MCRT) was imposed by the operation at constant solids concentrations.

2.2 Physicochemical determinations

The performance of the bioreactors was analyzed when the systems operated under steady-state conditions for any given combinations of influent salinity conditions, HRT and MLTSS. The performance in terms of organic matter removal was monitored by measuring the influent and effluent chemical oxygen demand (COD) and biological oxygen demand at day 5 (BOD_5), according to established protocols (Rice et al., 2012). Moreover, the performance in nitrogen removal was handled by measurement of influent and effluent concentrations of nitrogenous ions, i.e. ammonium, nitrite and nitrate. This was done following an established protocol (Rodriguez-Sanchez et al., 2017). Briefly, the water samples were filtered with a 0.45 µm pore diameter filter right after collection from the bioreactors, then immediately measured using a Metrohm ion chromatograph. The cations were measured by using a Metrosep C2–150 cation column, and a Metrosep A supp-4-250 anion column was used for the anions. Nitric acid/dipicolinic acid was used as eluent for the cation column, while carbonate-bicarbonate was used as eluent for the anion columns. Calibration curves were developed for ammonium, nitrite and nitrate in order to achieve accurate measures through ion chromatography. In addition, the MLTSS were measured using established protocols (Rice et al., 2012). For the measurement of biomass attached to carriers when appropriate, the determination method was described in Rodriguez-Sanchez et al. (2018a).

2.3 Kinetic characterization of biomass

The kinetic characterization of biomass in the bioreactors was done by the means of respirometric tests. The respirometric tests were conducted using a BM Advance Multipurpose gas flux-static liquid respirometer (SURCIS SL, Spain), equipped with a Peltier thermostat for temperature control (Dinko Instruments, Spain). During the process of respirometry, the dissolved oxygen in the

respirometric bioreactor was continuously measured by an oximeter (Hamilton Company, USA), observing its change when known substrate concentrations were added. Prior to the respirometric test, a sample of 1 L volume was extracted from the bioreactor, with 35% of carriers if appropriate. The extracted sample was aerated at 20 °C in the darkness for 18-24 h in order to deplete the sample of any possible biooxidizable matter. After aeration, the sample was introduced in the Peltier thermostat and its temperature was controlled at 20.0±0.1 °C during all tests. The sample was perfectly mixed by the means of mechanical stirring (Dinko Instruments) and continuous recycling from the bottom to the top of the respirometer that was imposed by means of a Watson Marlow (Watson Marlow Pumps Group) peristaltic pump. Air was constantly introduced in the sample using an air pump with an air flow rate of 0.906±0.001 L min^{-1}. The pH was controlled in the range of 7.75±0.25. The control of aeration, pH, temperature, recycling pumping and mechanical stirring was done by BM-Advance software (SURCIS SL, Spain).

The kinetic characterization of the heterotrophic biomass was achieved by addition of a concentration of 500 mg L^{-1} NaAc at 50%, 80% and 100% successive dilutions. Similarly, the total nitrification capacity of the biomass was characterized by addition of 150 mg L^{-1} NH_4Cl in successive dilutions at 50%, 80% and 100%. Finally, for the characterization of endogenous respiration of biomass the sample was not aerated and the oxygen consumption was monitored until the sample was depleted of oxygen.

Data of oxygen concentrations during the respirometric tests were treated using BM-Advance software (SURCIS SL) for the purpose of kinetic characterization of the biomass. The estimation of respirometric parameters followed the model provided by Leyva-Diaz et al. (2013b):

The yield coefficient was determined using the equation:

$$Y = \frac{S - OC}{S} \quad [1]$$

Where S is the added substrate concentration and OC is the oxygen consumption of the biomass caused by the addition of the substrate S.

On the other hand, it is known that the rate of substrate utilization (r_{su}), or the velocity with which the biomass consumes any given substrate, is:

$$r_{su} = \frac{\partial S}{\partial t} = \frac{1}{1-Y}\frac{\partial (OC)}{\partial t} = \frac{1}{1-Y} R_S \quad [2]$$

Where R_S is the dynamic oxygen uptake rate, measured by the respirometer. If we further take into account the following equation:

$$OC = \int_0^t R_S \, dt \quad [3]$$

Then the yield coefficient Y can be calculated, as well as the rate of substrate utilization r_{su}, from respirometric data.

Since the yield coefficient can be calculated, the following relation can give an estimation of the growth rate for the biomass:

$$r_X = \mu X = -Y r_{su} \quad [4]$$

Where X is the concentration of active biomass in the sample. Thus, solving:

$$\mu = -\frac{Y r_{su}}{X} \quad [5]$$

Following the Monod growth model, the growth rate is related to a maximum growth rate μ_{max} and a saturation constant K_S:

$$\mu = -\frac{Y r_{su}}{X} = \mu_{max} \frac{S}{K_S + S} \quad [5]$$

If we were to linearize the equation [5]:

$$\frac{1}{\mu} = \frac{K_S}{\mu_{max}} \frac{1}{S} + \frac{1}{\mu_{max}} \quad [6]$$

Since μ can be calculated with the data provided by the respirometric test, the Monod growth model parameters can be estimated.

In the case of heterotrophic and autotrophic biomass, two assumptions would be made. First, there is only a fraction of X that actively develops consumption of oxygen when organic matter is added, and similarly only a fraction of X actively develops consumption of oxygen when inorganic nitrogen is added. This was estimated as 90% of biomass for the heterotrophs and 10% of biomass for the autotrophs (Metcalf & Eddy, 2012). Therefore, the value of X will be replaced with X_H and X_A, calculated as:

$$X_H = 0.9\,X;\; X_A = 0.1\,X \quad [7]$$

Second, the yield coefficient Y calculated was adimensional. To convert into units of mgCOD $mgVSS^{-1}$ for the heterotrophic biomass and into units of mgO_2 $mg\text{-}VSS^{-1}$ for the autotrophic biomass, the values of Y will be replaced for Y_H and Y_A calculated as Leyva-Diaz et al. (2013b):

$$Y_H = \frac{Y}{1.48};\; Y_A = \frac{Y}{1.42} \quad [8]$$

On the other hand, the cell death coefficient k_d can be calculated as Leyva-Diaz et al. (2013b):

$$k_d = \frac{OUR_{end}}{1.42\,X} \quad [9]$$

Where OUR_{end} corresponds to the oxygen uptake rate at depletion of oxygen when no aeration was introduced in the sample.

Finally, taking into account all these equations, the r_{su} for any given operational state for the heterotrophic and autotrophic biomass was calculated using equation [5]:

$$r_{su} = X \frac{S\,\mu_{max}}{Y\,(S + K_S)} \quad [10]$$

In this sense, the Monod growth model parameters evaluated were the following:

$$\mu_h\ [h^{-1}]: maximum\ growth\ rate\ of\ the\ heterotrophic\ biomass$$

$$K_{sh}\ [mg - O_2\ L^{-1}]: half\ saturation\ constant\ of\ the\ heterotrophic\ biomass$$

$$Y_h\ [mg - VSS\ mg - COD^{-1}]: Yield\ coefficient\ of\ the\ heterotrophic\ biomass$$

$$\mu_a\ [h^{-1}]: maximum\ growth\ rate\ of\ the\ autotrophic\ biomass$$

$$K_{sa}\ [mg - O_2\ L^{-1}]: half\ saturation\ constant\ of\ the\ autotrophic\ biomass$$

$$Y_a\ [mg - VSS\ mg - COD^{-1}]: Yield\ coefficient\ of\ the\ autotrophic\ biomass$$

$$K_d\ [d^{-1}]: cell\ decay\ constant\ of\ the\ biomass$$

2.4 Statistical analyses

For the purpose of ordination of the different operational conditions and technologies tested, the performance data was subjected to a singular value decomposition analysis. This was done using R statistical software.

The identification of statistically significant effect of the operational conditions and technological configurations over the performance of the systems and the Monod growth model kinetic parameters of their biomass was done by the means of one-way and two-way permutational analysis of variance (PERMANOVA) analyses. For the PERMANOVA analyses, operational conditions (maximum salinity, MLTSS and HRT) and technological configuration were taken for comparison with the data regarding removal performances of BOD_5, COD, NH_4^+ and total nitrogen (TN), the SRT, and the kinetic parameters μ_h, K_{sh}, Y_h, μ_a, K_{sa}, Y_a and OUR_{end}. The one-way PERMANOVA regarded

only one of the operational variables or technological configuration, while the two-way PERMANOVA regarded two of these variables at the same time. All the PERMANOVA analyses were computed using PASTv3 (Hammer et al., 2001) with Euclidean distance and under 9999 permutations.

The combinations of operational parameter/performance parameter and operational parameter/Monod parameter were considered of interest if PERMANOVA analyses suggested that the operational parameter/Monod parameter were statistically significantly affected by the operational parameter. For these cases, paired *t*-test with null hypothesis of mean differences > 0 or mean differences < 0 were calculated using R statistical software.

The linkage of the operational conditions and technology with the performance and kinetic parameters of the bioreactors studied was carried out by calculation of 499 unconstrained Monte-Carlo simulations under a full permutation model using CANOCO 4.5 for Windows software. The technological configuration was computed as a trichotomic variable. All other parameters were transformed to the LOG(X+1) when they were expressed in different units.

3. Results and discussion

3.1 Performance of the bioreactors for the treatment of variable-salinity wastewater

The performance of the bioreactors in terms of removal of BOD_5, COD, TN and NH_4^+ are shown in Table 1. In general, the removal of organic matter was good, reaching very high values up to 99.63% for BOD_5 and 97.58% for COD. In all cases the removal of BOD_5 was higher than 80%, with a minimum value of 82.87% for the MBR technology at 8.5 mS cm^{-1} maximum salinity and HRT of 9.5 h. The removal of COD was higher than 70% in all cases, with a minimum of 71.03 % for the MBR system at 4.5 mS cm^{-1} maximum salinity and 12 h HRT. On the other hand, the removal of NH_4^+ and TN was

overall deficient for the systems in comparison with similar technologies operating for the treatment of regular salinity urban wastewater, achieving 100% NH_4^+ oxidation and more than 50% mean TN removal (Leyva-Diaz et al., 2015). NH_4^+ oxidation efficiency showed a maximum of 85.18% (hybrid MBBR-MBRanox, 4.5 mS cm^{-1}, 12 h, 3500 mg L^{-1}) and a minimum of 25.64% (MBR, 8.5 mS cm^{-1}, 6 h, 2500 mg L^{-1}). The total nitrogen removal seemed to be linked to the NH_4^+ removal efficiency, showing similar mean values in almost all operational scenarios. The lowest value obtained for TN was 24.46% (hybrid MBBR-MBRn/anox, 8.5 mS cm^{-1}, 9.5 h, 2500 mg L^{-1}) and the highest was 85.24% (MBR, 4.5 mS cm^{-1}, 12 h, 3500 mg L^{-1}). Apparently, the removal performances for NH_4^+ and TN were higher overall for the operation under 4.5 mS cm^{-1} than under 8.5 mS cm^{-1}.

It has been observed that biomass in MBR and hybrid MBBR-MBR could adapt to high salinity conditions, yielding high performances in terms of organic matter and ammonium removal (Di Trapani et al., 2014). However, the biomass in these experiments was gradually adapted to increasing salinity from steady-state systems treating regular urban wastewater. For the case of variable salinity influents, the performance in terms of ammonium oxidation was poor in the scenario of 8.5 mS cm^{-1}. This result highlights that biomass in the MBR and hybrid MBBR-MBR systems are more sensitive and less adaptable to variable salinity conditions than to constant salinity conditions. More research should be done on the adaptation capacity of biomass in bioreactor to variable salinity conditions in order to increase the performance in ammonium oxidation of bioprocesses subjected to such influents.

Table 1 – Mean removal performance of organic matter and nitrogenous compounds and mean cell residence time for the bioreactors during the experimentation time

Maximum Salinity [mS cm^{-1}]	Total Solids [mg L^{-1}]	HRT [h]	Technology	BOD_5 [%]	COD [%]	NH4+ [%]	TN [%]	MCRT [d]
4.5	2500	6	MBR	97.73	78.81	53.24	51.72	36.70
			Hybrid MBBR-MBRanox	99.30	82.59	58.05	27.07	36.70
			Hybrid MBBR-MBRn/anox	98.40	92.60	56.10	54.28	36.70
		9.5	MBR	99.63	86.69	85.97	84.92	39.25
			Hybrid MBBR-MBRanox	99.30	93.29	84.98	83.84	39.25
			Hybrid MBBR-MBRn/anox	97.14	95.91	85.18	81.24	39.25
		12	MBR	99.40	71.03	81.63	81.63	40.25
			Hybrid MBBR-MBRanox	99.50	82.16	80.74	80.74	40.25
			Hybrid MBBR-MBRn/anox	99.67	91.00	80.09	80.09	40.25
	3500	6	MBR	97.59	89.49	55.43	49.77	38.65
			Hybrid MBBR-MBRanox	99.57	94.15	63.99	60.98	38.65
			Hybrid MBBR-MBRn/anox	99.52	97.58	73.81	70.97	38.65
		9.5	MBR	99.37	80.44	84.72	82.64	40.63
			Hybrid MBBR-MBRanox	99.59	86.67	75.03	71.14	40.63
			Hybrid MBBR-MBRn/anox	99.43	92.04	82.27	71.73	40.63
		12	MBR	99.63	85.69	75.50	75.15	41.39
			Hybrid MBBR-MBRanox	99.21	91.87	85.59	85.24	41.39
			Hybrid MBBR-MBRn/anox	99.27	99.37	77.34	76.32	41.39
8.5	2500	6	MBR	86.56	74.29	25.64	25.46	42.16
			Hybrid MBBR-MBRanox	96.78	78.05	29.63	29.51	42.16
			Hybrid MBBR-MBRn/anox	97.52	93.13	27.11	26.77	42.16
		9.5	MBR	82.87	77.26	35.69	35.04	45.56
			Hybrid MBBR-MBRanox	89.89	93.61	37.35	36.08	45.56
			Hybrid MBBR-MBRn/anox	96.88	94.20	25.70	24.46	45.56
		12	MBR	89.01	76.02	32.90	32.60	46.91
			Hybrid MBBR-MBRanox	99.44	87.96	33.44	33.51	46.91
			Hybrid MBBR-MBRn/anox	98.55	94.23	36.92	37.09	46.91
	3500	6	MBR	89.53	81.18	36.42	36.42	44.75
			Hybrid MBBR-MBRanox	87.92	93.93	35.96	35.96	44.75
			Hybrid MBBR-MBRn/anox	98.42	93.88	32.74	32.74	44.75
		9.5	MBR	90.44	76.05	34.93	34.93	47.43
			Hybrid MBBR-MBRanox	99.33	87.72	38.49	38.49	47.43
			Hybrid MBBR-MBRn/anox	99.06	90.66	38.55	38.55	47.43
		12	MBR	86.12	79.22	34.97	34.97	48.47
			Hybrid MBBR-MBRanox	87.22	96.74	28.06	28.06	48.47
			Hybrid MBBR-MBRn/anox	98.50	94.20	32.02	31.35	48.47

The treatment of variable-salinity urban wastewater of MBR and hybrid MBBR-MBR systems has been analyzed in previous research and the results showed that the treatment at 6.5 mS cm^{-1} maximum influent salinity had good performances in terms of COD (greater than 85% for all scenarios of operation tested) and BOD_5 (higher than 97% in all scenarios tested), while the removal of TN was poor (never higher than 50%) (Rodriguez-Sanchez et al., 2018a). In this way, the operation at lower influent maximum salinity leads to higher removal performances in terms of TN and similar for BOD_5 and COD. However, when operating at higher maximum influent salinities, the results obtained were similar in terms of TN and COD but lower in terms of BOD_5.

An important feature of the operation of the hybrid MBBR-MBR systems was found in the fact that the attached biofilm to carriers was very low (< 50 mg L^{-1}) at all operational conditions. In this way, the contribution of the attached biofilm in the hybrid MBBR-MBR systems was low (about 98%-99% of total biomass was mixed liquor in the hybrid MBBR-MBRs), since there was not a significant contribution of the attached biofilm over the suspended biomass (2500-3500 mg L^{-1}). Even though it has been observed that attached biofilms in MBBR-MBR systems can adapt to salinity, the introduction of saline influent on a steady-state system operating for the treatment of regular-salinity urban wastewater showed a decrease of attached biofilm in concentrations of 1000 mg L^{-1} (Di Trapani et al., 2014). Accordingly, the inability of the microbial communities in the salinity-amended urban wastewater led to difficulties for the formation of attached biofilm to hybrid MBBR-MBR systems started-up using constant salinity or variable-salinity urban wastewater has been reported previously (Rodriguez-Sanchez et al., 2017; 2018a).

For the 6.5 mS cm^{-1} scenario, the best removal efficiencies for COD and BOD_5 were obtained for the MBR while the best removal efficiencies for TN were obtained for the hybrid MBBR-MBRn/anox, but overall not much difference was appreciated between the systems (less than 4% in all cases)

(Rodriguez-Sanchez et al., 2018a). For the 4.5 mS cm^{-1} salinity scenario, the best technologies for the removal of BOD_5, COD and TN were the hybrid MBBR-MBRn/anox, the hybrid MBBR-MBRanox, and the hybrid MBBR-MBRn/anox, respectively, even though not big differences in performance were observed (less than 5% in all cases). On the other hand, for the 8.5 mS cm^{-1} scenario, the best technologies were, respectively, the hybrid MBBR-MBRanox, the hybrid MBBR-MBRanox and the hybrid MBBR-MBRn/anox for BOD_5, COD and TN, respectively, again with very small differences (less than 3%). The very close similarity in removal performances between the MBR and the two different hybrid MBBR-MBR systems could be caused by the small contribution of attached biofilm in the hybrid MBBR-MBR systems to the MLTSS.

The MCRT was a variable imposed by the operation under constant MLTSS, mainly controlled by the purge flows needed under any given set of operational conditions. Therefore, its value could show the effect of the operational variables over the biomass growth in both systems. In this sense, the values obtained for the operation of the bioreactors was in the range of 36.70-48.47 d (Table 1).

3.2 Clustering of operational states by performance parameters and PERMANOVA analyses of bioreactor performance based on differential operational conditions

The ordination plot of the performance parameters for the three technologies operated under both maximum salinity conditions, both MLTSS and all HRT, is shown in Figure 2. The singular value decomposition (SVD) analysis showed that the samples separated perfectly by maximum salinity conditions in terms of NH_4^+ and TN removal performances (Figure 2A2). In this sense, influent maximum salinity had a clear effect on the ammonium oxidation and denitrification capacities of the bioprocesses. This trend was not that clear for organic matter removal (Figure 2A1), in which different influent maximum salinities clustered together in most of samples. The same timid

clusterization appeared for organic matter removal with respect to technological configuration (Figure 2D1). Thus, the clustering of operational states showed that organic matter could be influenced by maximum salinity and technology while nitrogen removal seemed to be affected only by maximum salinity. On the other hand, SVD analyses did not show that the HRT or the MLTSS had a significant influence over the organic matter removal (Figure 2B1 & 2B2) or over the ammonium oxidation and nitrogen removal (Figure 2B2 & 2C2).

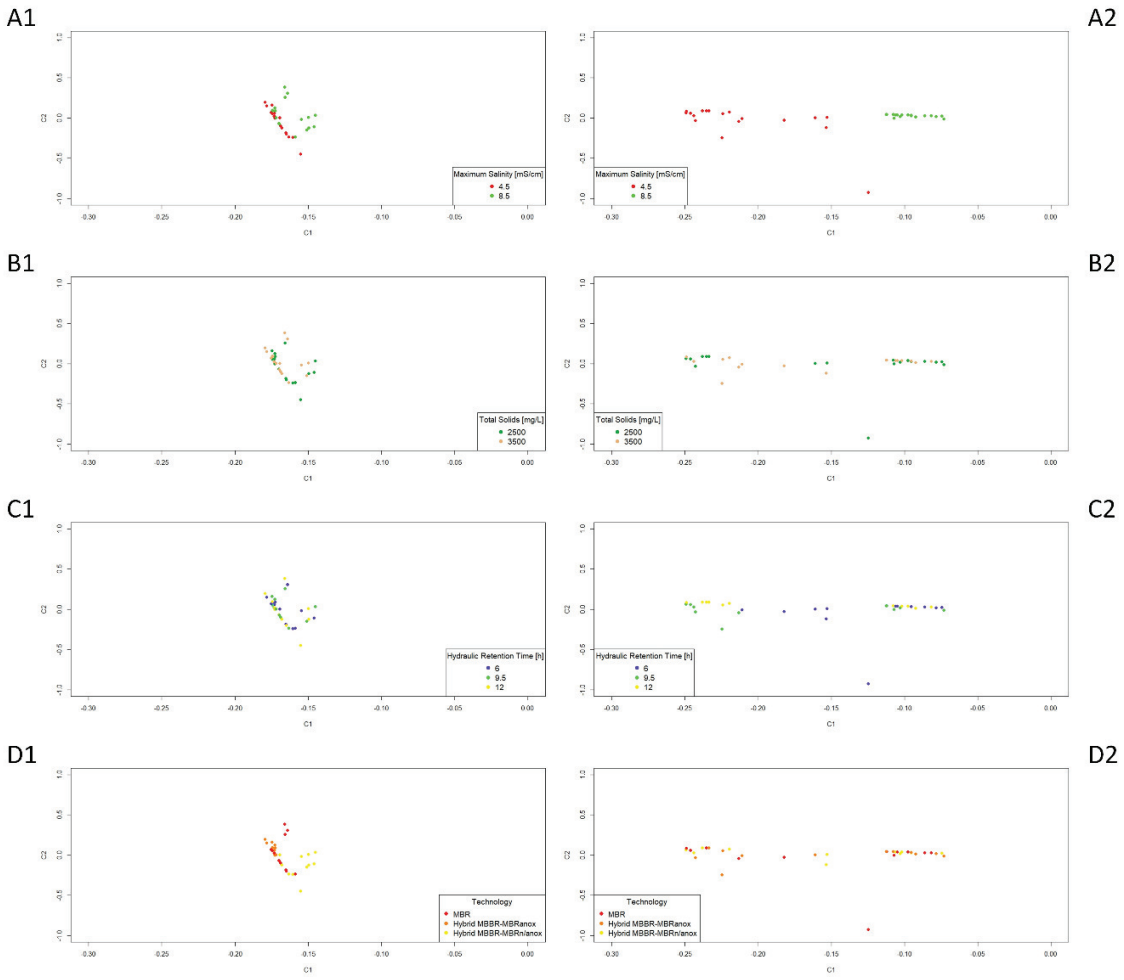

Figure 2 – Singular value decomposition of the performance parameters for the three technologies operated under both maximum salinity conditions, both MLTSS and all HRT (1: organic matter removal; 2: NH_4^+ and TN removal)

The two-way PERMANOVA analyses suggested that maximum salinity had an effect over the BOD_5, NH_4^+ and TN removal, and over the MCRT ($p < 0.05$) (in the supplementary material). Technology also affected removal of BOD_5 and COD, coupled to maximum salinity ($p < 0.05$). On the other hand, the removal of NH_4^+ and TN was also affected by the HRT, which also affected the MCRT ($p < 0.05$). Contrast one-way PERMANOVA analyses also suggested the influence of maximum salinity on BOD_5, NH_4^+ and TN removal and MCRT ($p < 0.05$), the effect of HRT over the MCRT ($p < 0.05$), and the effect of technological configuration over BOD_5 and COD removal ($p < 0.05$) (in the supplementary material). The joined results of both analyses suggested that maximum influent salinity affected the performance of the bioprocesses in terms of BOD_5, NH_4^+ and TN, while the technology of operation impacted the BOD_5 and COD. These results were also in accordance with those obtained by the SVD analyses. Moreover, the maximum influent salinity and the HRT showed a statistically significant effect over the MCRT, which suggested an influence of these variables over the biomass growth in the bioreactors. In contrast, there was no statistical significance between the MLVSS/MLTSS ratio and the MCRT ($p = 0.1115$), the maximum salinity ($p = 0.2082$), and the technological configuration ($p = 0.4199$).

The paired *t*-tests showed significant differences between the maximum salinity, HRT and technological configuration for the BOD_5, COD, NH_4^+ and TN removal performances, and for MCRT (in the supplementary material). For the maximum salinity, all mean differences were statistically significant ($p < 0.05$ or $p > 0.95$) and had a higher value for the 4.5 mS cm^{-1} salinity conditions in comparison with the 8.5 mS cm^{-1} scenario (+6.07% for BOD_5, +41.29% for NH_4^+ and +37.64% for TN) except for the MCRT (-6.41 d). In this way, the influent maximum salinity had a timid effect over the removal of organic matter but a great effect over the removal of nitrogenous compounds in the bioreactors studied. Lower influent salinity conditions decreased the MCRT in the bioreactors, which was related to higher growths of biomass. On the other hand, the technological configurations

showed significant differences for the COD and BOD_5 removal. For the COD, it was clear that the hybrid MBBR-MBRn/anox had higher removal percentage than the other two technologies (+5.00% over the hybrid MBBR-MBRanox and +9.38% over the MBR). For the case of BOD_5 removal, the hybrid MBBR-MBRn/anox and hybrid MBBR-MBRanox did not show significant differences in their mean values ($p > 0.05$) despite the mean difference of +2.11% of the former with respect to the last. Nevertheless, both had significantly higher mean values over the MBR technology (+5.37% for the hybrid MBBR-MBRn/anox, +3.26% for the hybrid MBBR-MBRanox). Thus, the paired *t*-tests showed that the hybrid MBBR-MBRn/anox was the most efficient technology in terms of organic matter removal at all influent maximum salinity, HRT and MLTSS conditions. The different HRT resulted in different MCRT values, which were higher for the longer HRT (+1.04 d for 12 h over 9.5 h and +3.69 d for 12 h over 6 h).

Table 2 – Summary of the mean values for the Monod growth model kinetic parameters of the bioreactors analyzed in the study

Maximum Salinity [mS cm^{-1}]	Total Solids [mg L^{-1}]	HRT [h]	Technology	µh [h^{-1}]	Ksh [mg-O_2 L^{-1}]	Yh [mg-VSS mg-COD^{-1}]	µa [h^{-1}]	Ksa [mg-N L^{-1}]	Ya [mg-VSS mg-N^{-1}]	OURend [mg-O_2 L^{-1} h^{-1}]
4.5	2500	6	MBR	0.0638	4977.6558	0.6344	0.020	43.0141	0.6764	0.023256
			Hybrid MBBR-MBRanox	0.2062	16293.0270	0.6321	0.031	194.4683	0.6434	0.017037
			Hybrid MBBR-MBRn/anox	0.0055	167.5825	0.6405	0.026	140.7913	0.6686	0.029003
		9	MBR	0.0484	5647.4864	0.6297	1.320	16228.6886	0.6796	0.00933
			Hybrid MBBR-MBRanox	0.0084	1418.8270	0.6294	3.941	48214.4265	0.6707	0.017375
			Hybrid MBBR-MBRn/anox	0.0121	1952.8321	0.6015	2.631	32221.5575	0.6752	0.018659
		12	MBR	0.0205	4631.5617	0.6343	0.007	319.2552	0.6773	0.013521
			Hybrid MBBR-MBRanox	0.0120	2587.1629	0.6294	0.007	319.2552	0.6773	0.014197
			Hybrid MBBR-MBRn/anox	0.0035	542.7641	0.6246	0.007	319.2552	0.6773	0.014873
	3500	6	MBR	0.0063	1801.3527	0.6006	0.002	104.6310	0.6729	0.006205
			Hybrid MBBR-MBRanox	0.0094	3004.6847	0.5954	0.004	135.3827	0.6898	0.002173
			Hybrid MBBR-MBRn/anox	0.0032	598.0208	0.6058	0.003	139.2255	0.6776	0.010237
		9	MBR	0.0047	1171.4144	0.6247	0.099	3000.8406	0.6517	0.008101
			Hybrid MBBR-MBRanox	0.0027	114.2044	0.6416	0.195	5991.9891	0.6632	0.008451
			Hybrid MBBR-MBRn/anox	0.0023	348.1877	0.6244	0.003	9.6922	0.6403	0.007726
		12	MBR	0.0031	541.4761	0.6489	0.001	108.4442	0.6196	0.009996
			Hybrid MBBR-MBRanox	0.0141	5991.9867	0.5856	0.001	104.4542	0.6363	0.009416
			Hybrid MBBR-MBRn/anox	0.0015	98.3546	0.6430	0.001	112.4342	0.6030	0.005215
8.5	2500	6	MBR	0.0655	16956.5303	0.5645	0.151	2132.1562	0.6513	0.019538
			Hybrid MBBR-MBRanox	0.0258	2974.4928	0.6250	0.007	61.1357	0.6097	0.01751
			Hybrid MBBR-MBRn/anox	0.0082	970.0034	0.6196	0.007	103.7614	0.5945	0.015482
		9	MBR	0.0077	1002.2810	0.5985	0.084	2807.9310	0.6377	0.012845
			Hybrid MBBR-MBRanox	0.0087	937.7259	0.6408	0.005	141.2397	0.6640	0.018118
			Hybrid MBBR-MBRn/anox	0.0026	150.0257	0.5741	0.163	5474.6224	0.6115	0.017172
		12	MBR	0.0042	402.0075	0.6059	0.002	83.9009	0.5620	0.007572
			Hybrid MBBR-MBRanox	0.0106	1299.2061	0.6210	0.006	103.2202	0.6780	0.013521
			Hybrid MBBR-MBRn/anox	0.0032	965.3499	0.5626	0.004	93.5606	0.6200	0.006625
	3500	6	MBR	0.0016	114.4659	0.6047	0.002	214.8566	0.6016	0.004588
			Hybrid MBBR-MBRanox	0.0020	317.6442	0.6055	0.003	79.3194	0.5993	0.005095
			Hybrid MBBR-MBRn/anox	0.0024	520.8226	0.6062	0.003	252.2481	0.6303	0.005602
		9	MBR	0.0020	70.4488	0.5770	0.002	345.8122	0.6413	0.01299
			Hybrid MBBR-MBRanox	0.0020	467.0236	0.5517	0.002	476.0589	0.6401	0.004346
			Hybrid MBBR-MBRn/anox	0.0022	680.2592	0.5775	0.002	410.9356	0.6407	0.00763
		12	MBR	0.0013	101.1664	0.5614	n.d.	n.d.	n.d.	0.005795
			Hybrid MBBR-MBRanox	0.0021	287.2176	0.6254	n.d.	n.d.	n.d.	0.005553
			Hybrid MBBR-MBRn/anox	0.0020	117.7532	0.6046	n.d.	n.d.	n.d.	0.006761

3.3 Monod growth model parameters of the bioprocesses and their rate of substrate utilizations and PERMANOVA analyses of bioreactor kinetics based on differential operational conditions

The Monod growth model parameters for all operational conditions tested are shown in Table 2. In general, values for the μ_h were low (only one scenario > 0.1 h^{-1}) and the K_{sh} values were high (in the range of 10^2-10^4 mg-O_2 L^{-1}). Similar trends were found for the μ_a (only 5 scenarios > 0.1 h^{-1}) and K_{sa} (also in the range of 10^2-10^4 mg-O_2 L^{-1}). The low values of μ_h and μ_a showed a slow growth rate of the microbial communities subjected to the variable salinity influent wastewater, in comparison with values obtained for similar systems treating regular urban wastewater (Leyva-Diaz et al., 2013b). The high values of the K_{sh} and K_{sa}, in comparison with regular salinity conditions (Leyva-Diaz et al., 2013b), denoted that influent substrate concentrations almost never were limiting factors for growth, which seemed to be restricted by the ability of the microbial communities to adapt to variable saline environments. For the 3500 mg L^{-1} MLTSS and 12 h HRT under 8.5 mS cm^{-1} no nitrifying activity was detected, showing the affection of maximum influent salinity to the removal of NH_4^+ discussed above.

The two-way PERMANOVA analyses on the effect of the operational conditions over the Monod growth model parameters showed that maximum influent salinity was important for both yield coefficients Y_h and Y_a ($p < 0.05$) (in the supplementary material). The HRT had a statistically significant effect over the autotrophic parameters μ_a, K_{sa} and Y_a ($p < 0.05$). Moreover, the MLTSS controlled the variability of heterotrophic parameters μ_h and K_{sh}, μ_a and Y_a, and the OUR_{end} parameter ($p < 0.05$). The interaction of these three variables was important for the control of μ_h (HRT and MLTSS); and μ_a, K_{sa} and Y_a (maximum salinity and HRT, HRT and MLTSS); and OUR_{end} (HRT and MLTSS) ($p < 0.05$). Contrast analysis of one-way PERMANOVA determined that maximum influent salinity had a statistically significant effect over the Y_h and Y_a, that MLTSS had an effect over μ_h, K_{sh}, μ_a and the OUR_{end}, and that HRT had an effect over the autotrophic parameters μ_a, K_{sa} and Y_a

($p < 0.05$) (in the supplementary material). On the other hand, it was observed that the technological configuration did not have a statistically significant influence over the kinetics of the bioreactors.

The r_{su} of the heterotrophic biomass for all operational conditions tested also suggested the influence of such operational conditions over the kinetics of the bioreactors (Figure 3). It was observed that r_{su} was higher for the 2500 mg L^{-1} MLTSS than for the 3500 mg L^{-1} at equal HRT, as suggested by paired *t*-tests (in the supplementary material) of the mean differences of the Monod growth model parameters affected by these parameters. There also were differences in the r_{su} between the two salinity scenarios, with 4.5 mS cm^{-1} being overall higher than the 8.5 mS cm^{-1} scenario. However, this difference was reduced when operating at longer HRT and higher MLTSS. In all cases, the higher r_{su} were found at lower HRTs. As observed by PERMANOVA analyses, these results also showed the influent maximum salinity, the HRT and the MLTSS are the operational variables that affect the kinetics of the heterotrophic biomass.

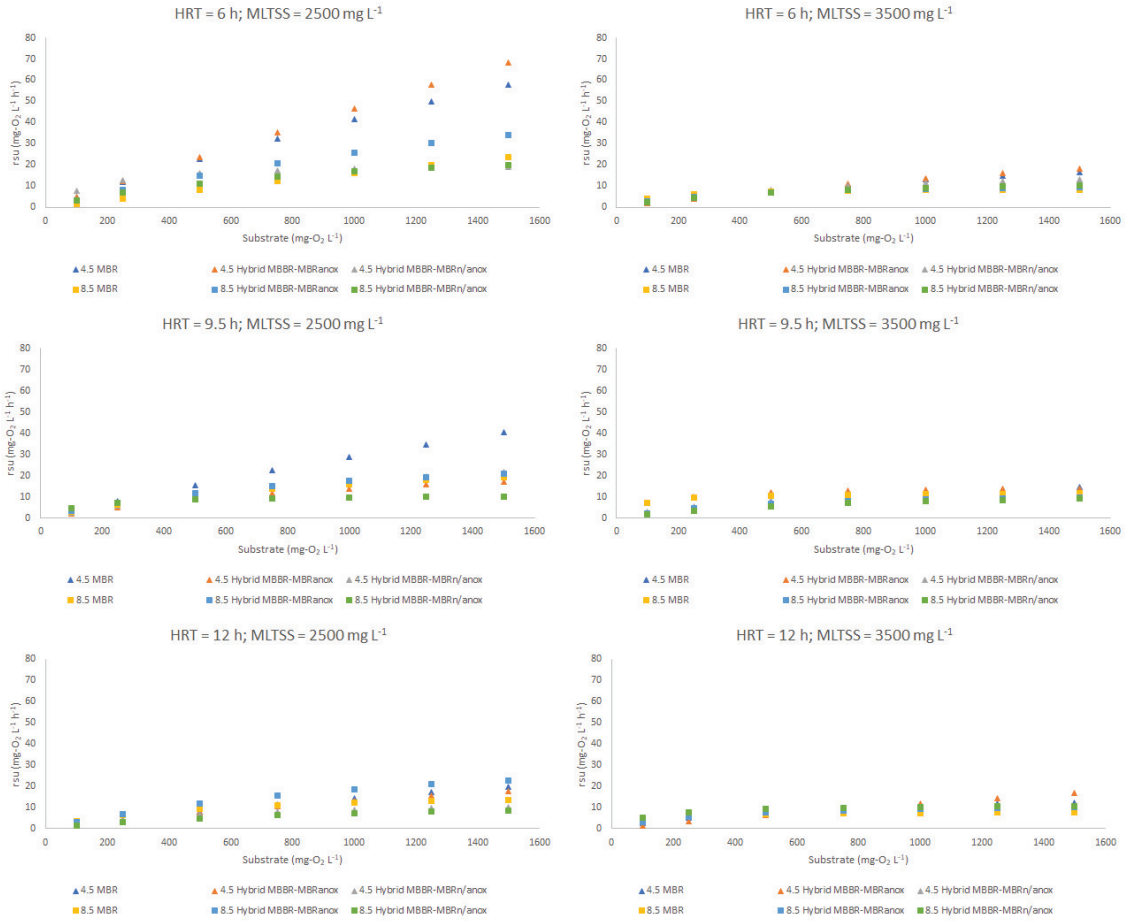

Figure 3 – Rates of substrate utilization for the heterotrophic biomass under all operational conditions tested

The r_{su} of the autotrophic biomass for all operational conditions tested is shown in Figure 4. It was clear that there were more marked differences between operational conditions for the autotrophic r_{su} than for the heterotrophic r_{su}. The patterns with respect to MLTSS and maximum influent salinity were similar than for the case of the heterotrophic biomass. Nevertheless, the autotrophic r_{su} for the 4.5 mS cm^{-1} maximum influent salinity was higher at HRT 9.5 than for HRT 6 and 12 at 3500 mg L^{-1}. This might have been related to influent ammonium concentrations, since there was a pattern observed relating this variable to the autotrophic r_{su} in such a way that higher r_{su} were encountered for influent NH_4^+ concentrations lower than 50 mg L^{-1} (Table 3). It is possible that the low availability

of ammonium enhances the specialization of autotrophic biomass under variable salinity conditions thus promoting microorganisms with higher affinity for ammonium and thus leading to faster autotrophic kinetics.

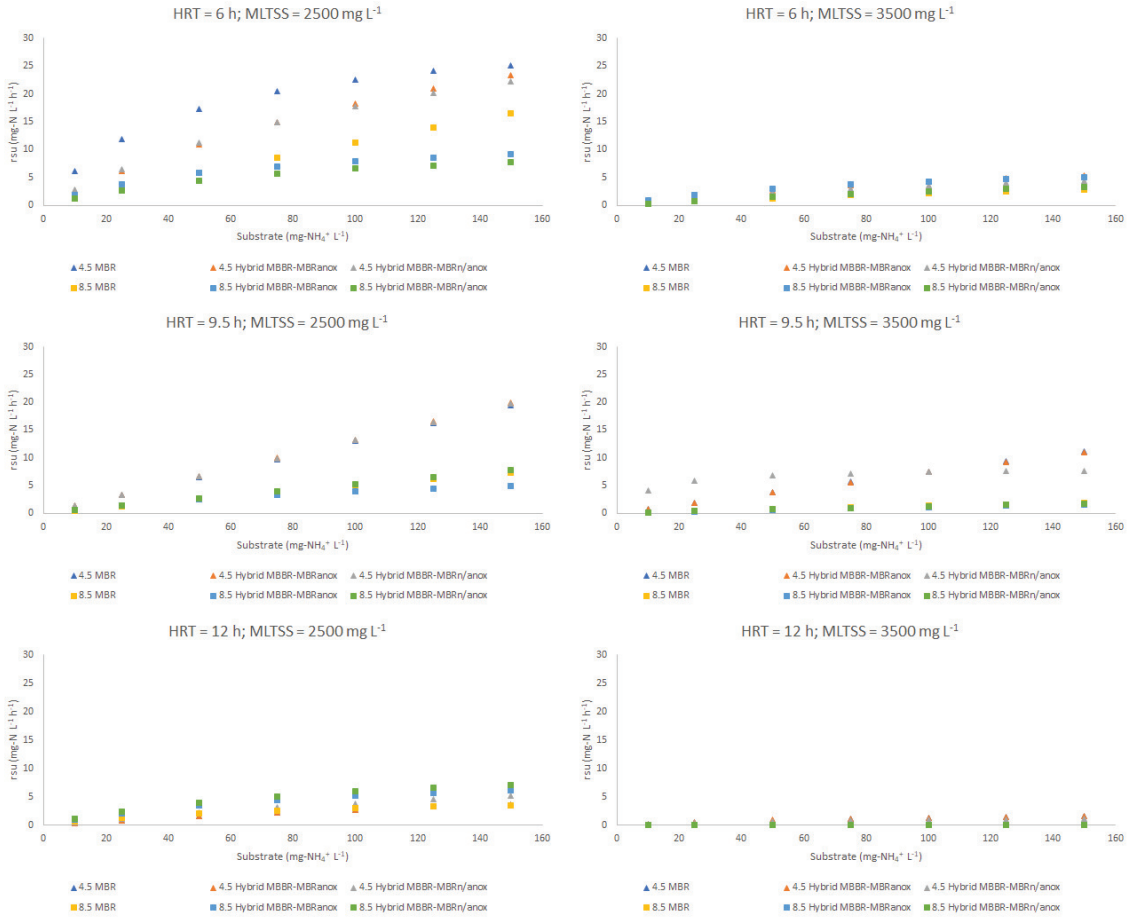

Figure 4 - Rates of substrate utilization for the autotrophic biomass under all operational conditions tested

Table 3 – Mean values for the influent concentrations of BOD_5, COD, NH_4^+ and TN for the bioreactors under all operational conditions tested

Salinity [mS cm^{-1}]	Solids [mg L^{-1}]	HRT [h]	BOD_5 [mg-O_2 L^{-1}]	COD [mg-O_2 L^{-1}]	TN [mg-N L^{-1}]	NH_4^+ [mg-N L^{-1}]
4.5	2500	6	380.00	782.33	43.75	43.70
		9.5	413.33	1178.33	34.56	34.56
		12	336.67	814.67	99.04	99.04
	3500	6	46.67	186.67	70.05	69.09
		9.5	446.67	1204.67	43.59	42.73
		12	233.33	779.00	78.74	78.30
8.5	2500	6	253.33	345.00	52.94	52.71
		9.5	106.67	225.67	12.82	12.62
		12	236.67	978.00	85.55	85.31
	3500	6	216.67	731.67	129.86	129.86
		9.5	80.00	1025.67	57.37	57.37
		12	315.00	727.00	45.29	45.29

For a scenario of influent variable salinity with 6.5 mS cm^{-1} as maximum, the heterotrophic r_{su} (4.57-24.60 mg-O_2 L^{-1} h^{-1}) was lower than that of 4.5 mS cm^{-1} (9.03-47.17 mg-O_2 L^{-1} h^{-1}) but similar to that of 8.5 mS cm^{-1} (7.23-26.01 mg-O_2 L^{-1} h^{-1}), while the autotrophic r_{su} (0.59-14.26 mg-N L^{-1} h^{-1}) was higher for the 4.5 mS cm^{-1} case (2.87-52.1 mg-N L^{-1} h^{-1}) and similar between the 6.5 and 8.5 mS cm^{-1} (2.88-18.49 mg-N L^{-1} h^{-1}) scenarios (Rodriguez-Sanchez et al., 2018). These results suggested that maximum influent salinity actively affects the r_{su} of both heterotrophic and autotrophic biomass, which become inhibited when maximum salinity reaches a certain threshold. In this sense, the findings suggested that variable salinity at > 4.5 mS cm^{-1} slowed down the nitrification and organic matter oxidation kinetics.

Paired *t*-tests showed that the differences in the mean values of the Monod growth parameters, under operational conditions of maximum influent salinity, MLTSS and HRT, were statistically significant in most cases ($p < 0.05$ or $p > 0.95$) (Table S6). Y_h and Y_a were statistically significantly higher ($p > 0.95$) for the 4.5 mS cm^{-1} maximum salinity than for the 8.5 mS cm^{-1} scenario (+0.02777 mg-VSS mg-COD^{-1} and + 0.13990 mg-VSS mg-N^{-1}, respectively). In this way, the influent salinity

scenario influenced the amount of biomass generated per unit of substrate consumed being higher for the 4.5 mS cm^{-1} scenario. All Monod growth model parameters affected by the MLTSS were significantly higher ($p > 0.95$) at 2500 mg L^{-1} than at 3500 mg L^{-1} (+0.02512 h^{-1} for μ_h, +2640.55800 mgO_2 L^{-1} for K_{sh}, +0.44983 h^{-1} for μ_a and +0.89903 mg-O_2 L^{-1} h^{-1} for OUR_{end}). For the HRT, the results varied depending on the kinetic parameter. For the μ_a and K_{sa}, the HRT of 9.5 h had statistically significant higher values ($p < 0.05$ or $p > 0.95$) than for HRT 6 h (+0.68240 h^{-1} and +9310.23400 mg-N L^{-1}, respectively) and for HRT 12 h (+0.70125 h^{-1} and +9480.00100 mg-N L^{-1}, respectively). On the other hand, for these two parameters the differences between the 6 and 12 h HRTs were not statistically significant ($0.05 < p < 0.95$). On the other hand, for the Y_a, the HRT of 12 h showed a statistically significant higher value ($p > 0.95$) than 6 h HRT (+0.96880 mg-VSS mg-N^{-1}) and 9.5 h HRT (+0.17212 mg-VSS mg-N^{-1}), while there was no significant difference between these last two values ($0.05 < p < 0.95$).

Two-way PERMANOVA analyses suggested that the MLTSS played an important role over the heterotrophic and autotrophic r_{su} in all operational scenarios (in the supplementary material). Moreover, the HRT and the influent maximum salinity were of importance for the autotrophic r_{su} as well. The contrast one-way PERMANOVA analyses showed the same results (in the supplementary material). Therefore, it was observed that the heterotrophic biomass kinetics was affected only by the MLTSS at operation, while the autotrophic biomass kinetics was less adaptable and was also affected by the HRT and the influent maximum salinity as well as the MLTSS. In this regard, the major concern in operation of MBR and hybrid MBBR-MBR systems under variable salinity conditions would be the effect over the nitrifying communities.

Paired *t*-tests over the values of heterotrophic r_{su} based on MLTSS showed statistically significant ($p > 0.95$) higher values for the operational scenario at 2500 mg L^{-1}, suggesting that lower MLTSS causes faster r_{su} for the heterotrophic biomass (+6.40432 mg-O_2 L^{-1} h^{-1}) (in the supplementary material).

For the case of autotrophic r_{su}, all comparisons among different conditions of maximum salinity, the MLTSS and HRT yielded statistically significant ($p > 0.95$) mean differences, suggesting higher mean values for 4.5 mS cm^{-1} over 8.5 mS cm^{-1} (+3.39559 mg-N L^{-1} h^{-1}), 2500 mg L^{-1} over 3500 mg L^{-1} and 6 h over 9.5 h and 12 h, and 9.5 h over 12 h. In this context, the autotrophic biomass presented faster kinetics when operating at low influent maximum salinity, low MLTSS and short HRT.

3.4 Multivariate redundancy analyses linking the performance, Monod growth model kinetics and rates of substrate utilization with operational conditions

Several multivariate redundancy analyses (RDAs) plot showing the relationship between the operational conditions and the performance with the Monod growth model parameters and r_{su} in the bioreactors is offered in Figure 5.

It was of importance that a strong positive correlation existed between the Y_h parameter and the BOD_5, NH_4^+ and TN removal (Figure 5A). This correlation supported that higher Y_h values would increase the performance of the systems regarding these parameters. As shown by PERMANOVA and *t*-tests analyses, the parameter Y_h was dependent on the maximum influent salinity, achieving higher values for the 4.5 mS cm^{-1}. In this sense, the higher performance in BOD_5, NH_4^+ and TN removal at 4.5 mS cm^{-1} compared to the 8.5 mS cm^{-1} scenario is also reflected by the RDA. On the other hand, the removal of NH_4^+ and TN were strongly and positively correlated with the K_{sa} parameter (Figure 5B). Therefore, at higher K_{sa} values or higher specificity for nitrifiable compound, the removal performance of NH_4^+ and TN was higher. The negative relationships of maximum salinity, HRT and MLTSS with the heterotrophic and autotrophic Monod growth model parameters observed using RDAs were also in accordance with the results obtained through PERMANOVA analyses.

The OUR_{end} parameter had a positive relationship with BOD_5, TN and NH_4^+ removal (Figure 5C).

The RDAs linking the r_{su} with the performance parameters showed two different correlations for the heterotrophic and autotrophic biomass. For the heterotrophic biomass, r_{su} at low and high substrate concentrations were uncorrelated (Figure 5D). Thus, the bioprocesses functioned differently in terms of heterotrophic kinetics depending on the substrate added. On the other hand, the autotrophic r_{su} was correlated for all substrate concentrations found during operation (Figure 5E), showing that the autotrophic kinetics was not differentiated by substrate availability. Both r_{su} were positively correlated with the removal of BOD_5 and TN, while only the autotrophic r_{su} was correlated with NH_4^+ removal performance. As observed from the PERMANOVA and *t*-test analyses, the MLTSS was negatively correlated with the heterotrophic r_{su} and the MLTSS, maximum influent salinity and HRT with the autotrophic r_{su}.

There was a negative correlation of maximum growth rate, half-saturation constant and yield coefficients kinetic parameters for both autotrophic and heterotrophic biomass with the MCRT (Figure 5). This result suggested that higher residence of the biomass in the bioreactor decreased its autotrophic and heterotrophic kinetics. This was also found true for the cell decay coefficient and the autotrophic and heterotrophic r_{su}. The explanation of this could reside in the capacity of the MCRT to select for different microbial species within the biomass. According to the results, higher MCRTs favored the presence of microorganisms with slower substrate consumption and growth. Moreover, the MCRT was negatively correlated with the removal performances of BOD_5, COD, NH_4^+ and TN, suggesting that the systems operated better at lower MCRTs. As shown by the PERMANOVA analyses, the MCRT was positively correlated with maximum salinity, in relation with the lower growth rates of the biomass. Therefore, the operation of the bioreactors at higher salinities affected the growth of the biomass, which increased the MCRT, which in turn selected for microorganisms with slower autotrophic and heterotrophic kinetics.

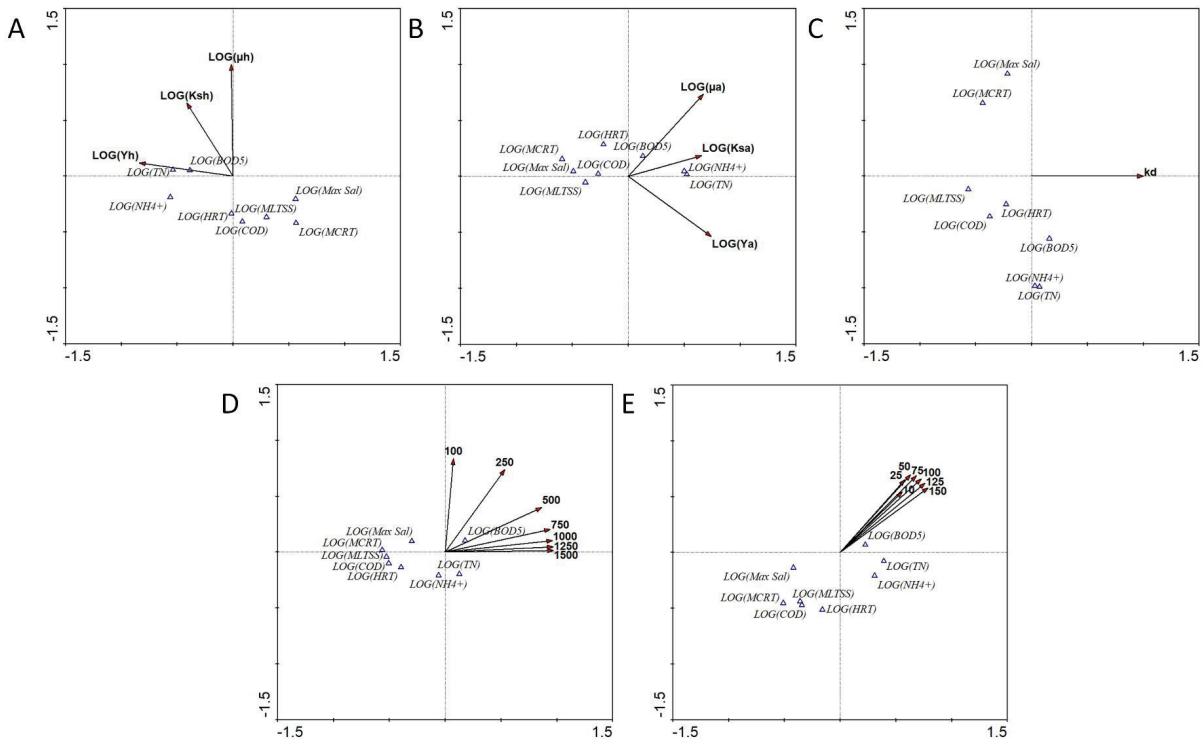

Figure 5 – Multivariate redundancy analyses linking the heterotrophic kinetic parameters (A), autotrophic kinetic parameters (B), cell death coefficient (C), heterotrophic rates of substrate utilization (D) and autotrophic rates of substrate utilization (E) with the operational conditions and removal performance

4. Conclusions

Three technologies -MBR, hybrid MBBR-MBRanox and hybrid MBBR-MBRn/anox- were operated for the treatment of variable-salinity urban wastewater under all combinations of the following operational conditions of: 2500 and 3500 mg L^{-1} MLTSS; 6, 9.5 and 12 h of HRT; and 4.5 and 8.5 mS cm^{-1} maximum influent salinity. It was observed a good removal performance of BOD_5 and COD (82.87%-99.63%, 71.03 %-97.58%, respectively), while the removal of NH_4^+ and TN were poor under the salinity conditions of 8.5 mS cm^{-1} (24.46%-38.55%) in comparison with 4.5 mS cm^{-1} (27.7%-85.24%). PERMANOVA and *t*-tests analyses showed that removal of BOD_5, NH_4^+ and TN was higher at lower maximum influent salinity, and that COD and BOD_5 removal was higher for the hybrid MBBR-MBR systems than for the MBR. The kinetic characterization of the bioprocesses under all operational conditions showed that the heterotrophic r_{su} (9.03-47.17 mg-O_2 L^{-1} h^{-1} for 4.5 mS cm^{-1}; 7.23-26.01 mg-O_2 L^{-1} h^{-1} for 8.5 mS cm^{-1}) was affected mainly by MLTSS with an inverse correlation and that the autotrophic r_{su} (2.87-52.1 mg-N L^{-1} h^{-1} for 4.5 mS cm^{-1}; 2.88-18.49 mg-N L^{-1} h^{-1} for 8.5 mS cm^{-1}) was affected by maximum influent salinity, HRT and MLTSS also with an inverse correlation pattern. Resulting MCRT was higher for the 8.5 mS cm^{-1} salinity conditions, also being linked to slower autotrophic and heterotrophic kinetic parameters. The research conducted could successfully characterize the behavior of MBR and hybrid MBBR-MBR systems treating variable-salinity urban wastewater and was able to determine accurately the main driving factors of the performance and the biomass kinetics of such systems. The results obtained could be useful in the modeling and design of variable-salinity wastewater treatment systems.

Acknowledgements

The authors would like to acknowledge the financial support given by the Ministry of Economy of the Government of Spain, which funded this research under the project CTM2013-48154-P and grant BES-2014-067852. The authors would also like to acknowledge the support given by the Department of Civil Engineering and the Institute of Water Research of the University of Granada.

References

Aslan S, Simsek E (2012) Influence of salinity on partial nitrification in a submerged biofilter. Bioresour Technol 118: 24–29.

Bassin JP, Dezotti M, Sant'Anna Jr GL (2011) Nitrification of industrial and domestic saline wastewaters in moving bed biofilm reactor and sequencing batch reactor. J Hazard Mater 185: 242–248.

Di Bella G, Di Trapani D, Torregrossa M, Viviani G (2013) Performance of a MBR pilot plant treating high strength wastewater subject to salinity increase:analysis of biomass activity and fouling behaviour. Bioresour Technol 147: 614–618.

Di Trapani D, Christensson M, Torregrossa M, Viviani G, Ødegaard H (2013) Performance of a hybrid activated sludge/biofilm process for wastewater treatment in a cold climate region: influence of operating conditions. Biochem Eng J 77: 214–219.

Di Trapani D, Di Bella G, Mannina G, Torregrossa M, Viviani G (2014) Comparison between moving bed-membrane bioreactor (MB-MBR) and membrane bioreactor (MBR) systems: influent of wastewater salinity variation. Bioresour Technol 162: 60–69.

Hammer Ø, Harper DAT, Ryan PD (2001) PAST: Paleontological Statistics Software Package for Education and Data Analysis. Palaeontology Electronic 4, 9 pp.

Huang X, Wei CH, Yu KC (2008) Mechanism of membrane fouling control by suspended carriers in a submerged membrane bioreactor. J Membr Sci 309: 7–16.

Jang D, Hwang Y, Shin H, Lee W (2013) Effects of salinity on the characteristics ofbiomass and membrane fouling in membrane bioreactors. Bioresour Technol 141: 50–56.

Johir MA, Vigneswaran S, Kandasamy J, BenAim R, Grasmick A (2013) Effect of salt concentration on membrane bioreactor (MBR) performances: detailed organic characterization. Desalination 322: 13–20.

Lefebvre O, Moletta R (2006) Treatment of organic pollution in industrial saline wastewater: a literature review. Water Res 40: 3671–3682.

Leyva-Díaz JC, Calderón K, Rodríguez FA, González-López J, Hontoria E, Poyatos JM (2013a) Comparative kinetic study between moving bed biofilm reactor-membrane bioreactor and membrane bioreactor systems and their influence on organic matter and nutrients removal. Biochem Eng J 77: 28–40.

Leyva-Diaz JC, Calderon K, Rodriguez FA, Gonzalez-Lopez J, Hontoria E, Poyatos JM (2013b) Comparative kinetic study between moving bed biofilm reactor-membrane bioreactor and membrane bioreactor systems and their influence on organic matter and nutrients removal. Ecol Eng 77: 28-40.

Leyva-Diaz JC, Gonzalez-Martinez A, Gonzalez-Lopez J, Muñio MM, Poyatos JM (2015) Kinetic modeling and microbiological study of two-step nitrification in a membrane bioreactor and hybrid moving bed biofilm reactor–membrane bioreactor for wastewater treatment. Chem Eng J 259: 692-702.

Liu Q, Wang XC, Liu Y, Yuan H, Du Y (201) Performance of a hybrid membrane bioreactor in municipal wastewater treatment. Desalination 258: 143–147.

Ludzack FJ, Noran DK (1965) Tolerance of high salinities by conventional wastewaters treatment processes. J Water Pollut Control Fed 37: 1404–1416.

Mannina G, Viviani G (2009) Hybrid moving bed biofilm reactors: an effective solution for upgrading a large wastewater treatment plant. Water Sci Technol 60: 1103–1116.

Metcalf & Eddy, Tchobanoglous G, Burton FL, Stensel HD (2012) Wastewater engineering: treatment and reuse. 4th edition. McGraw-Hill, New York, United States of America.

Moussa MS, Sumanasekera DU, Irahim SH, Lubberding HJ, Hooijmans CM, Gijzen HJ, van Loosdrecht MCM (2006) Long term effects of salt on activity, population structure and floc characteristics in enriched bacterial cultures of nitrifiers. Water Res 40: 1377–1388.

Oppenheimer J, Trussell R, Boulos L, Adham S, Gagliardo P (2001) Feasibility of the membrane bioreactor process for water reclamation. Water Sci Technol 43: 203–209.

Rice EW, Baird RB, Eaton AD, Clesceri LS (2012) Standard methods for the examination of water and wastewater. 22nd edition. American Public Health Association, American Water Works Association, Water Environment Federation.

Rodríguez-Sánchez A, Leyva-Díaz JC, Poyatos JM, González-López J (2017) Performance and Kinetics of Membrane and Hybrid Moving Bed Biofilm-Membrane Bioreactors Treating Salinity Wastewater. AIChE J 63: 3329-3342.

Rodriguez-Sanchez A, Leyva-Diaz JC, Gonzalez-Lopez J, Poyatos JM (2018a) Membrane bioreactor and hybrid moving bed biofilm reactor-membrane bioreactor for the treatment of variable salinity wastewater: Influence of biomass concentration and hydraulic retention time. Chem Eng J 336: 102-111.

Rodriguez-Sanchez A, Margareto A, Robledo-Mahon T, Aranda E, Diaz-Cruz S, Gonzalez-Lopez J, Barcelo D, Vahala R, Gonzalez-Martinez A (2018b). Performance and bacterial community structure

of a granular autotrophic nitrogen removal bioreactor amended with high antibiotic concentrations. Chem Eng J 325: 257-269.

Sudarno U, Winter J, Gallert C (2011) Effect of varying salinity, temperature, ammonia and nitrous acid concentrations on nitrification of saline wastewater in fixed-bed reactors. Bioresour Technol 102: 5665–5673.

Vyrides I, Stuckey DC (2009) Adaptation of anaerobic biomass to saline conditions: Role of compatible solutes and extracellular polysaccharides. Enzyme Microb Technol 44: 46–51.

Zhao W, Wang Y, Lin X, Zhou D, Pan M, Yang J (2014) Identification of the salinity effect on N2O production pathway during nitrification: using stepwise inhibition and 15N isotope labeling methods. Chem Eng J 253: 418–426.

Chapter 5

Influence of salinity cycles in bioreactor performance and microbial community structure of membrane-based tidal-like variable salinity wastewater treatment systems

This chapter has been published in its current form in Environmental Science & Pollution Research. The complete citation is the following:

Alejandro Rodriguez-Sanchez, Juan Carlos Leyva-Diaz, Barbara Muñoz-Palazon, Jose Manuel Poyatos, Jesus Gonzalez-Lopez. 2018. Influence of salinity cycles in bioreactor performance and microbial community structure of membrane-based tidal-like variable salinity wastewater treatment systems. Environmental Science & Pollution Research. (), 1-14. doi: 10.1007/s11356-018-3608-4

Abstract

A membrane bioreactor and two hybrid moving bed bioreactor-membrane bioreactors were operated for the treatment of variable salinity wastewater, changing in cycles of 6-h wastewater base salinity and 6-h maximum salinity (4.5 and 8.5 mS cm^{-1} electric conductivity, which relate to 2.4 and 4.8 g L^{-1} NaCl, respectively), under different hydraulic retention times (6, 9.5, and 12 h) and total solids concentrations (2500 and 3500 mg L^{-1}). The evaluation of the performance of the systems showed that COD removal performance was unaffected by salinity conditions, while BOD_5 and TN removals were significantly higher in the low-salinity scenario. The microbial community structure showed differences with respect to salinity conditions for *Eukarya*, suggesting their higher sensitivity for salinity with respect to *Prokarya*, which were similar at both salinity scenarios. Nevertheless, the intra-OTU distribution of consistently represented OTUs of *Eukarya* and *Prokarya* was affected by the different salinity maximums. Multivariate redundancy analyses showed that several genera such as *Amphiplicatus* (0.01–5.90%), *Parvibaculum* (0.27– 1.19%), *Thiothrix* (0.30–1.19%), *Rhodanobacter* (2.81–5.85%), *Blastocatella* (0.21–2.01%), and *Nitrobacter* (0.80–0.99%) were positively correlated with BOD_5 and TN removal, and the ecological roles of these were proposed. All these genera were substantially more represented under low-salinity conditions (10–500% higher relative abundance), demonstrating that they might be of importance for the treatment of variable salinity wastewater. Evaluation of *Eukarya* OTUs showed that many of them lack a consistent taxonomic classification, which highlights the lack of knowledge of the diversity and ecological role of *Eukaryotes* in saline wastewater treatment processes. The results obtained will be of interest for future design and operation of salinity wastewater treatment systems particularly because little is known on the effect of variable salinity conditions in wastewater treatment.

1. Introduction

Wastewater is one of the main environmental issues in the modern era and much effort has been put on mitigating its impact on the environment through wastewater treatment. The activated sludge system has been the traditional technology of choice for wastewater treatment (Gonzalez-Martinez et al., 2016a). More novel technologies have been successfully implemented for the treatment of wastewater, among which the membrane-based technologies are significant (Rodriguez-Sanchez et al., 2017, 2018a, b). Its first implementation was the membrane bioreactor (MBR), in which a membrane separation system is added to an activated sludge process. The MBR proved to have advantages over the activated sludge process: it offers the possibility of operation at higher solids concentration, yields effluents with higher quality, removes most of the pathogens, requires less footprint for the bioreactor facilities, and avoids the necessity of a secondary clarification (Leyva-Díaz et al., 2013; 2014).

A major problem of the membrane-based technologies is the fouling of the membrane. Membrane fouling is a process of membrane pore clogging by solid materials which leads to smaller permeate flux and thus to system inefficiency over time (Leyva-Díaz et al., 2014). The moving bed bioreactor-membrane bioreactor (MBBR-MBR) was developed to improve the sensitivity of the MBR to fouling. In the MBBRMBR, floating media, named as carriers, are introduced in the bioreactor (Leyva-Diaz et al., 2015a). The carriers allow the growth of attached biomass on their surface, with beneficial advantages with respect to the MBR: increase of solids concentration without increasing the suspended biomass and higher specialization of attached biomass than suspended biomass improves the removal of pollutants such as nitrogen (Leyva-Diaz et al., 2015b). The MBBR-MBR is called pure or hybrid depending on the presence of a recycling flux.

Wastewater has many characteristics that can harm the microbial communities in wastewater treatment bioreactors, among which salinity is of importance. High salinity in wastewater can cause

inhibition of microbial processes, increase cell transmembrane pressure leading to higher cell death rate, and trigger the accumulation of harmful intermediate metabolites in the bioreactor (Bassin et al., 2012; Castillo-Carvajal et al., 2014). In industrial wastewater, salinity is usually a byproduct of the manufacturing processes for seafood, dairy, fertilizers, petroleum, or olive oil (Cortés-Lorenzo et al., 2016). Urban wastewater can be subjected to high salinities due to snow melting operations, use of seawater as toilet flushing, or by seeping of seawater in coastal wastewater treatment plants (Cortes-Lorenzo et al., 2012; Wu et al., 2013; Hao et al., 2014; Welles et al., 2015).

The vast majority of studies have worked under constant salinity; thus, little is known about the effect of variable salinity in wastewater treatment systems (Rodriguez-Sanchez et al., 2018a; 2018b). Variable salinity conditions could exert different pressures on the microbial communities than constant salinity conditions, thus leading to very different microbial communities. More research is needed to unravel the effect of variable salinity on the microbial communities in wastewater treatment systems.

In this research, three configurations of bioreactors were used for the treatment of variable salinity wastewater with different maximum salinities, simulating tidal-like seawater intrusion, to test its influence over their performance and microbiome. The bioreactors were operated under three different hydraulic retention times (6, 9.5, and 12 h) and two different total solids concentrations (2500 and 3500 mg L^{-1}), measuring the performance of the system in terms of organic matter (BOD_5 and COD) and nitrogen removal (TN). The microbial communities in the bioreactors were analyzed by the means of next-generation sequencing. The results obtained demonstrated the effect of salinity over the performance and microbial communities and will be valuable for the future design, operation, and implementation of saline wastewater treatment systems.

2. Materials and methods

2.1 Description of the bioreactors used in the experiment

The three configurations consisted of a four-chamber (each was 12 cm in length, 12 cm in width, 60 cm in height, working volume of 6 L) reactor followed by a separated membrane tank (10 cm in diameter, 65 cm in height, working volume of 4.32 L) with submerged configuration. Thus, the whole volume of the bioreactor was of 28.32 L. The membrane module consisted of polyvinylidene fluoride with a core reinforcement of polyester ultrafiltration hollow fibers (0.04 µm pore diameter, 2.45 mm external diameter, 1.10 mm internal diameter, 0.2 m^2 total membrane area) displaced vertically (Micronet Porous Fibers SL, Spain).

Bottom-located fine bubble diffusers AFD 270 (ECOTEC SA, Spain) in the first, third, and fourth chambers and a bottom-located coarse bubble diffuser CAP 3 (ECOTEC SA, Spain) in the membrane tank, respectively, provided the aeration. An air compressor ACO-500 (Hailea, China) pumped the air flow to the diffusers, continuously measured by a rotameter 2100 Model (Tecfluid SA, Spain) and regulated using a valve. A mechanical stirrer Multi Mixer MM-1000 (Biosan Laboratories Inc., USA) provided the mixing in the second chamber.

Wastewater entered the first chamber using a peristaltic pump Watson-Marlow (Watson-Marlow Pumps Group, USA) and passed through the others before being discharged into the membrane tank. A Watson-Marlow peristaltic pump with suction-backwashing functioning withdrew the effluent from the membrane tank and through the membrane. The operation of the suction-backwash was cyclical and consisted of 9-min suction and 1-min backwash. Transmembrane pressure was controlled between 0.1 and 0.5 bar, cleaning the membrane with NaClO when needed. The systems operated with recycling as 500% of the influent flow, which was regulated by peristaltic pumps Watson-Marlow.

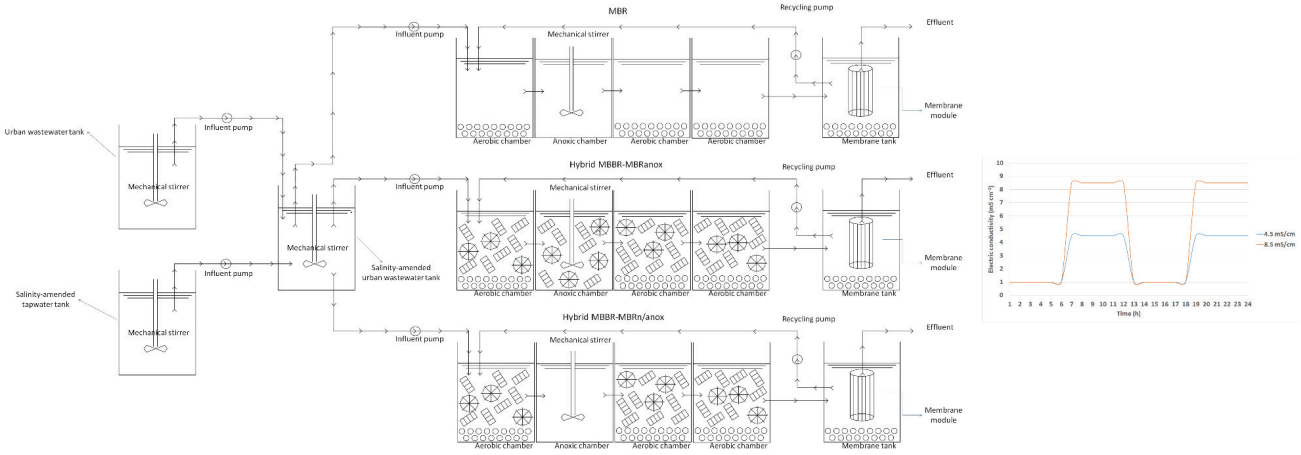

Figure 1 – Schematic of the bioreactors used in the study

The three systems were operated under three different configurations: MBR (no carriers), hybrid MBBR-MBRanox (carriers in all chambers), and hybrid MBBR-MBRn/anox (carriers in aerobic chambers only). The absence of carriers in the anoxic zone of hybrid MBBR-MBR systems has been reported to enhance the heterotrophic and autotrophic kinetics of this bioprocess (Leyva-Diaz et al., 2015a, 2016). In the hybrid MBBR-MBR systems, the carriers occupied the 35% chamber volume. The carrier used was the K1 (Anox-Kaldnes AS, Norway). A schematic of the bioreactors used in the experiment is shown in Fig. 1.

2.2 Operation of the bioreactors

The three configurations operated in parallel for the treatment of salinity-amended urban wastewater. An automatic control measured the salinity in the mix and it was added with urban wastewater and/or salinity tap water (50 mS cm^{-1}) to obtain the desired electric conductivity. The salinity of the wastewater followed tidal-like cycles, with 6 h of base salinity (1 mS cm^{-1}, 0.47 g L^{-1} NaCl) followed by 6 h of maximum (peak) salinity. The maximum salinities chosen for the experiment were 4.5 mS cm^{-1} (2.4 g L^{-1} NaCl) and 8.5 mS cm^{-1} (4.8 g L^{-1} NaCl). A graphical representation of the salinity cycles is shown in Fig. 1. Under each of the desired maximum salinities, the three technologies were operated under hydraulic retention times of 6, 9.5, and 12 h and total solids concentrations of 2500 and 3500 mg L^{-1}.

2.3 Determination of physicochemical parameters

The COD and BOD_5 were measured following established protocols (APHA 2012). The inorganic nitrogen compound (NH_4^+, NO_2^-, and NO_3^-) concentrations were measured by ionic

chromatography. Total solids were measured according to established protocols and following Rodriguez-Sanchez et al. (2018a; 2018b).

2.4 Collection of biomass samples, extraction of DNA, and next-generation sequencing

We collected the biological samples and treated them in the laboratory to extract their DNA, which was kept at − 20 °C and sent to RTLGenomics Laboratory (Lubbock, TX, USA) for further next-generation sequencing procedure. The primer pairs Bac357–Bac806 and EUK1391–EUKbr were selected to amplify regions of the 16S rRNA gene of prokaryotes and of the 18S rRNA gene of eukaryotes, respectively. A detailed list of the next-generation sequencing samples is shown in the Supplementary material.

2.5 Bioinformatics pipeline of next-generation sequencing data

We treated the raw sequencing data of 16S and 18S rRNA genes separately but under the same conditions using mothur v.1.39.5 (Schloss et al., 2009). We merged all paired-end reads into contigs, avoiding the generation of ambiguous bases in the overlap region due to nucleotide quality differences between the paired-end reads (Unno, 2015). Then, we screened the contigs to eliminate those with any ambiguous base or with more than eight homopolymers. We aligned the remaining contigs against the SiLVA SEED v128 database using Needleman conditions and eliminated those that failed to start and finish at the positions of forward and reverse primers, respectively. We then checked the remanent sequences for chimeras using VSEARCH (Rognes et al., 2016) through self-reference and removed chimeric sequences detected. We clustered the contigs that passed all previous screenings through VSEARCH and the abundance-based greedy clustering method (Westcott and Schloss, 2015; Schloss, 2016) using a cutoff for clustering of 3% for the 16S rRNA gene sequences

and of 5% for the 18S rRNA gene sequences. Finally, we deemed singleton OTUs as clustering errors and removed them.

We further treated the OTU tables generated through the bioinformatics pipeline for microbial ecology analysis. For similarity of microbial communities among the samples, we developed singular value decomposition analyses. We corrected the OTU tables to eliminate zero values using zCompositions package implemented in R software by a Bayesian multiplicative replacement method. Then, we transformed the zero-corrected OTU tables to a centered log ratio using robCompositions package implemented in R software. Then, we used the transformed OTU tables for the calculation of singular value decomposition, plotting them in a principal components analysis manner (Bian et al., 2017). To investigate differential abundance of OTUs, we developed an expected effect size analysis. We zero-corrected and transformed the OTU tables by generation of Dirichlet distributions under 128 Monte Carlo simulations using ALDEx2 package implemented in R software. We used this data to calculate the expected effect size of several different parameters.

We took the most abundant sequence within each of the OTUs as representative for taxonomic classification, which we classified against the SiLVA nr v128 and MiDAS 2.0 (McIlroy et al., 2017) through the k-nearest neighbor method and searching using k-mers of 8 bp size. We considered a consensus taxonomy from both classifications for each OTU.

2.6 Analysis of intra-OTU ecological variability for OTUs of interest

We declared as OTUs of interest those who had a relative abundance > 1% in all samples from all bioreactors when operating under the same conditions of salinity, hydraulic retention time, and total solids. We isolated all sequences belonging to each OTU of interest and investigated their intra-OTU ecological variability by the means of oligotyping (Eren et al., 2014). First, we did an entropy analysis

over the alignment of the OTU to calculate the Shannon entropy at each alignment position. Then, we investigated the oligotype distribution using the Shannon entropy data, starting with the nucleotide with the highest entropy value, and by iterative calculation and increasing the number of the highest entropy components in computation until a total purity score of 0.9 or higher was achieved (Okazaki et al., 2017). The quality parameters for the calculation of oligotype distribution were as follows: each oligotype had to be represented at least at 1% of total sequences in at least one sample and each oligotype had to account for a substantive abundance of at least 1000. We then BLASTed dominant oligotypes found for the OTUs of interest against the NCBI nt database to derive their more similar available sequence.

2.7 Multivariate redundancy analyses

We conducted multivariate redundancy analyses to link the prokaryal and eukaryal OTUs of interest with the performance of the systems and between them. We zero-corrected the prokaryal and eukaryal OTU tables using a Bayesian multiplicative replacement method developed with zCompositions package implemented in R software. We computed the multivariate redundancy analyses using the performance data and zero-corrected OTU tables utilizing CANOCO 4.5 for Windows through 499 Monte Carlo simulations under a full permutation model.

3. Results and discussion

3.1 Operational parameters of the bioreactors and influent and effluent concentrations of organic matter and nitrogen

BOD_5 effluent values were low for all technologies under the 4.5-mS-cm^{-1} salinity conditions (never higher than 9 mg L^{-1}), while these seemed higher for the 8.5-mS-cm^{-1} scenario (up to 38 mg L^{-1}) (Table

1). Differences among the two salinity scenarios were more marked for TN removal, with maximum effluent concentrations of 32 and 99 mg L^{-1} for low- and high-salinity maximums, respectively. The three technologies yielded good performance in terms of organic matter removal, but poor removal in terms of nitrogen was found for the 8.5mS-cm^{-1} scenario. The values obtained in this experiment could be related to those reported in variable salinity wastewater treatment with maximums of 6.5 mS cm^{-1} (Rodriguez-Sanchez et al., 2018a; 2018b). Organic matter removal was similar in both experiments regardless of salinity conditions. However, only the 4.5-mS-cm^{-1} scenario achieved a good removal of nitrogen. Thus, data collected indicated that maximum salinity of variable salinity wastewater is fundamental for nitrogen removal.

Table 1 – Mean values of the influent and effluent BOD_5, COD, TN and NH_4^+ concentrations for all experimental phases in the experimentation period

Maximum Salinity (mS cm^{-1})	TS (mg L^{-1})	HRT (h)	Technology	BOD_5inf (mg L^{-1})	CODin (mg L^{-1})	TNin (mg-N L^{-1})	NH_4^+in (mg-N L^{-1})	BOD_5eff (mg L^{-1})	CODeff (mg L^{-1})	TNeff (mg-N L^{-1})	NH_4^+eff (mg-N L^{-1})
4.5	2500	6.0	MBR	380.00	782.33	43.75	43.70	8.33	212.00	21.12	20.44
4.5	2500	6.0	Hybrid MBBR-MBRanox	380.00	782.33	43.75	43.70	2.33	220.00	31.91	18.33
4.5	2500	6.0	Hybrid MBBR-MBRn/anox	380.00	782.33	43.75	43.70	2.33	143.00	20.00	19.19
4.5	2500	9.5	MBR	413.33	1178.33	34.56	34.56	4.50	291.50	5.21	4.85
4.5	2500	9.5	Hybrid MBBR-MBRanox	413.33	1178.33	34.56	34.56	2.00	211.00	5.58	5.19
4.5	2500	9.5	Hybrid MBBR-MBRn/anox	413.33	1178.33	34.56	34.56	1.67	149.67	6.48	5.12
4.5	2500	12.0	MBR	336.67	814.67	99.04	99.04	6.33	51.67	18.20	18.20
4.5	2500	12.0	Hybrid MBBR-MBRanox	336.67	814.67	99.04	99.04	0.67	52.67	19.07	19.07
4.5	2500	12.0	Hybrid MBBR-MBRn/anox	336.67	814.67	99.04	99.04	2.33	51.33	19.72	19.72
4.5	3500	6.0	MBR	46.67	186.67	70.05	69.09	0.33	46.00	35.18	30.79
4.5	3500	6.0	Hybrid MBBR-MBRanox	46.67	186.67	70.05	69.09	1.00	20.67	27.33	24.88
4.5	3500	6.0	Hybrid MBBR-MBRn/anox	46.67	186.67	70.05	69.09	0.33	25.00	20.34	18.09
4.5	3500	9.5	MBR	446.67	1204.67	43.59	42.73	3.33	83.33	7.57	6.53
4.5	3500	9.5	Hybrid MBBR-MBRanox	446.67	1204.67	43.59	42.73	2.50	97.50	12.58	10.67
4.5	3500	9.5	Hybrid MBBR-MBRn/anox	446.67	1204.67	43.59	42.73	3.00	91.00	12.32	7.58
4.5	3500	12.0	MBR	233.33	779.00	78.74	78.30	5.33	54.00	19.57	19.18
4.5	3500	12.0	Hybrid MBBR-MBRanox	233.33	779.00	78.74	78.30	1.33	17.67	11.62	11.28
4.5	3500	12.0	Hybrid MBBR-MBRn/anox	233.33	779.00	78.74	78.30	1.33	21.00	18.65	17.74
8.5	2500	6.0	MBR	253.33	345.00	52.94	52.71	38.00	68.00	39.46	39.19
8.5	2500	6.0	Hybrid MBBR-MBRanox	253.33	345.00	52.94	52.71	18.33	72.67	37.32	37.09
8.5	2500	6.0	Hybrid MBBR-MBRn/anox	253.33	345.00	52.94	52.71	21.67	135.50	38.77	38.42
8.5	2500	9.5	MBR	106.67	225.67	12.82	12.62	3.33	55.00	8.33	8.11
8.5	2500	9.5	Hybrid MBBR-MBRanox	106.67	225.67	12.82	12.62	1.00	46.50	8.19	7.91
8.5	2500	9.5	Hybrid MBBR-MBRn/anox	106.67	225.67	12.82	12.62	0.67	24.67	9.68	9.38
8.5	2500	12.0	MBR	236.67	978.00	85.55	85.31	4.67	112.00	57.66	57.24
8.5	2500	12.0	Hybrid MBBR-MBRanox	236.67	978.00	85.55	85.31	4.33	94.50	56.88	56.79
8.5	2500	12.0	Hybrid MBBR-MBRn/anox	236.67	978.00	85.55	85.31	3.00	152.50	53.82	53.82
8.5	3500	6.0	MBR	216.67	731.67	129.86	129.86	3.67	46.33	82.56	82.56
8.5	3500	6.0	Hybrid MBBR-MBRanox	216.67	731.67	129.86	129.86	2.67	31.00	83.16	83.16
8.5	3500	6.0	Hybrid MBBR-MBRn/anox	216.67	731.67	129.86	129.86	3.00	38.67	87.34	87.34
8.5	3500	9.5	MBR	80.00	1025.67	57.37	57.37	4.00	75.67	37.33	37.33
8.5	3500	9.5	Hybrid MBBR-MBRanox	80.00	1025.67	57.37	57.37	7.33	71.67	35.29	35.29
8.5	3500	9.5	Hybrid MBBR-MBRn/anox	80.00	1025.67	57.37	57.37	4.33	60.00	35.26	35.26
8.5	3500	12.0	MBR	315.00	727.00	45.29	45.29	9.00	31.50	29.45	29.45
8.5	3500	12.0	Hybrid MBBR-MBRanox	315.00	727.00	45.29	45.29	5.00	35.00	32.58	32.58
8.5	3500	12.0	Hybrid MBBR-MBRn/anox	315.00	727.00	45.29	45.29	4.50	31.50	31.09	30.79

Student's paired *t* tests and Wilcoxon's signed rank tests demonstrated that there were no statistically significant differences for influent BOD_5, COD, and TN for the two maximum salinities ($p > 0.05$) (Table 2). However, there were statistically significant differences for BOD_5 and TN removal in the effluent ($p < 0.05$), but not for effluent COD ($p > 0.05$). It is possible that differences in maximum salinities affected the microbial metabolism in the bioreactors, thus leading to different removal performances of biological-driven parameters such as BOD_5 and TN.

Table 2 – Results of the Student's paired *t*-test and Wilcoxon's signed rank test showing statistical significance of differences in influent and effluent parameters BOD_5, COD and TN in the bioreactors comparing the 4.5 and 8.5 mS cm^{-1} scenarios.

		Student's paired t-test			Wilcoxon's signed rank test	
		t value	degrees of freedom	p-value	V	p-value
Influent	BOD_5	1.2617	5	0.2627	16	0.3125
	COD	0.7255	5	0.5006	14	0.5625
	TN	0.71581	5	0.5061	14	0.5625
Effluent	BOD_5	-2.5446	17	0.02094*	19	0.004036*
	COD	1.7315	17	0.1015	112	0.2645
	TN	-5.2532	17	0.00006474*	0	0.000007629*

The technological configuration did not have any statistically significant effect over the effluent concentrations of COD, BOD_5, TN, or NH_4^+ as derived from one-way PERMANOVA analyses ($p > 0.01$) (Table 3), which strongly suggested no significant differences in terms of performance when treating variable salinity wastewater. Thus, for the treatment of variable salinity effluents, the MBR and the hybrid MBBR-MBR systems worked similarly. The values of the influent variables did not have any significant effect when interacting with other statistically significant variables, as suggested by two-way PERMANOVA analyses. The effluent COD was significantly affected by TS at operation. The BOD_5, TN, and the NH_4^+ effluent concentrations were affected by the maximum influent salinity, while the TN and NH_4^+ were also affected by the hydraulic retention time. These results suggest that the main biological removal performances were affected by the maximum influent salinity,

highlighting the effect of this variable over the structure and/or metabolism of microbial populations in the bioreactors.

It has been found that microbial communities in membrane-based systems can adapt to high salinity when NaCl concentration is increased slowly over time, achieving good removal performances for organic matter and nitrogen (Di Trapani et al., 2014; Di Bella et al., 2015). However, the results obtained suggested that membrane-based systems started up under high-salinity conditions (about > 4.8 g L^{-1} in this study) showed inefficiency to adapt to salinity. This operational difficulty should be explored in the future to obtain more efficient saline wastewater treatment technologies.

Previous research in MBR and hybrid MBBR-MBR systems showed nitrogen removal performances in the range of 54.84–72.39% and removal of 84.55–88.73% for COD and 92.87–98.81% for BOD_5 (Leyva-Díaz et al., 2014; 2015a; 2015b). The results obtained in this experiment were similar for the removal of BOD_5, COD, and TN at 4.5 mS cm^{-1} scenario (98.58–99.42, 88.32–89.35, and 64.37–69.96%, respectively) but were significantly lower at the 8.5-mS-cm^{-1} scenario (91.75–93.81, 85.09–87.87, and 31.92–33.52%, respectively). The MBR and hybrid MBBR-MBR systems showed a decrease in BOD_5 and nitrogen removal performances when the salinity increased past the 2.4-g-L^{-1} NaCl. The process of start-up and operation of MBR and hybrid MBBR-MBR systems at greater salinities should be analyzed in order to achieve successful operation procedures for this purpose.

Table 3 – PERMANOVA analyses over the influence of the operational variables of maximum salinity, total solids, hydraulic retention time, technological configuration, and influent concentrations of COD, BOD_5, TN and NH_4^+ over the effluent concentrations of COD, BOD_5, TN and NH_4^+

		CODeff		BOD_5eff		TNeff		NH_4^+eff	
	Variable	F	p	F	p	F	p	F	p
One-Way PERMANOVA	Maximum Salinity	2.889	0.0946	4.822	0.0107	17.37	0.0001	20.5	0.0002
	Total Solids	14	0.0001	2.267	0.1513	1.543	0.219	1.499	0.2345
	HRT	1.539	0.2248	2.064	0.1062	6.713	0.0036	5.745	0.0065
	Technology	0.206	0.8246	0.9783	0.4336	0.0035	0.9959	0.0070	0.9929
	CODin	14.21	0.0001						
	BOD_5in			10.69	0.0001				
	TNin					125.8	0.0001		
	NH_4^+in							233.5	0.0001

		CODeff		BODeff		Tneff		NH4+eff	
Two-Way PERMANOVA	Total Solids	8.765	0.0001						
	CODin	2.367	0.0001						
	Interaction	-	1						
	Maximum Salinity			2.9317	0.0002				
	BOD_5in			1.7819	0.0003				
	Interaction			-	0.9999				
	Maximum Salinity					35.66	0.0001	35.66	0.0001
	HRT					12.243	0.0002	12.243	0.0002
	Interaction					2.3297	0.1133	2.3297	0.1133
	Maximum Salinity					162.54	0.0001		
	TNin					38.92	0.0001		
	Interaction					-15.503	1		
	HRT					-	-		
	TNin					-	-		
	Interaction					-	-		
	Maximum Salinity							162.54	0.0001
	NH_4^+in							38.92	0.0001
	Interaction							-15.503	1
	HRT							-	-
	NH_4^+in							-	-
	Interaction							-	-

3.3 Environmental parameters influence the structure of microbial communities in the bioreactors

We developed singular value decomposition (SVD) analyses to discern the influence of environmental parameters over the microbial community structure of the bioreactors under the different salinity scenarios.

SVD of *Eukarya* domain showed a clear pattern influenced by salinity (Fig. 2). On the contrary, it was found that neither HRT, total solids, technological configuration of bioreactor, aeration, and biomass configuration were important for the clustering of *Eukarya* community samples. For *Prokarya*, clustering of samples was not clear for any of the variables analyzed in the process (Fig. 3).

The similar patterns found for *Eukarya* and *Prokarya* for the aeration parameters suggested that the biomass in the system was well mixed, and thus, no differentiation was observed between the aerobic and anaerobic chambers. Interestingly, the microbial community structure of the attached biomass was very similar than that of the suspended biomass, suggesting that biomass configuration neither differentiated or promoted the growth of different phylotypes, negating the specialization of biomass that has been defended as a strength of MBBR systems. The low concentration of attached biomass in the hybrid MBBR-MBR systems at both salinity scenarios (< 50 mg L^{-1}) explains this fact, converting these into practically MBR systems.

The results indicated that HRT was not a main driver of the microbial community structure. This also occurred for total solids concentration. The influence of salinity conditions was different for *Eukarya* and *Prokarya*. It was found that prokaryal communities were not driven by the differences in salinity conditions, suggesting that similar phylotypes could thrive under both scenarios. In contrast, eukaryal communities could be clearly differentiated with respect to salinity conditions. This fact could indicate that there is a higher specialization in *Eukarya* domain with respect to salinity, while members of *Archaea* and *Bacteria* could adapt to a wider range of salinity concentration (in the range of 2.4 to 4.8

g L^{-1} NaCl, at least). According to this, observed differences in bioreactor performance between the two salinity scenarios in BOD_5, NH_4^+, and TN removal could then be explained either by an inhibitory effect of high salinity over *Prokarya* members. Another explanation could be a high influence of *Eukarya* domain over the process.

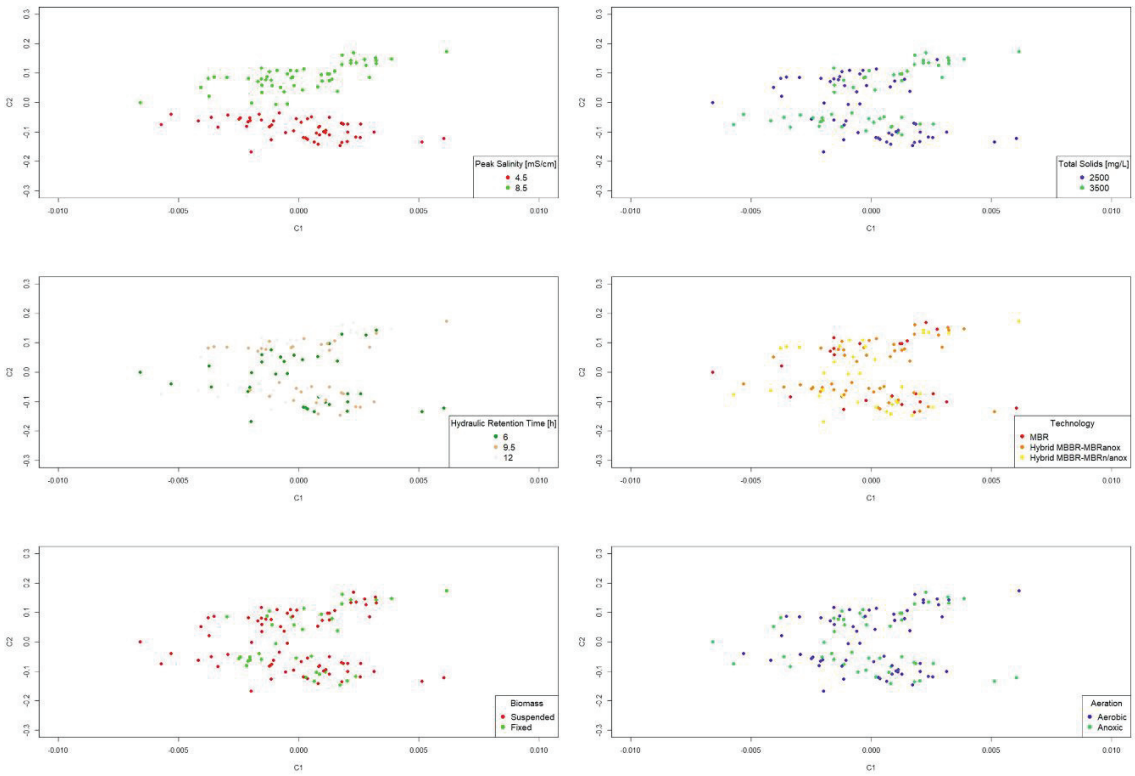

Figure 2 – Singular value decomposition plot showing the ordination of samples with respect to *Eukarya* communities and the effect of salinity conditions, total solids, hydraulic retention time, bioreactor technology, biomass configuration and aeration conditions

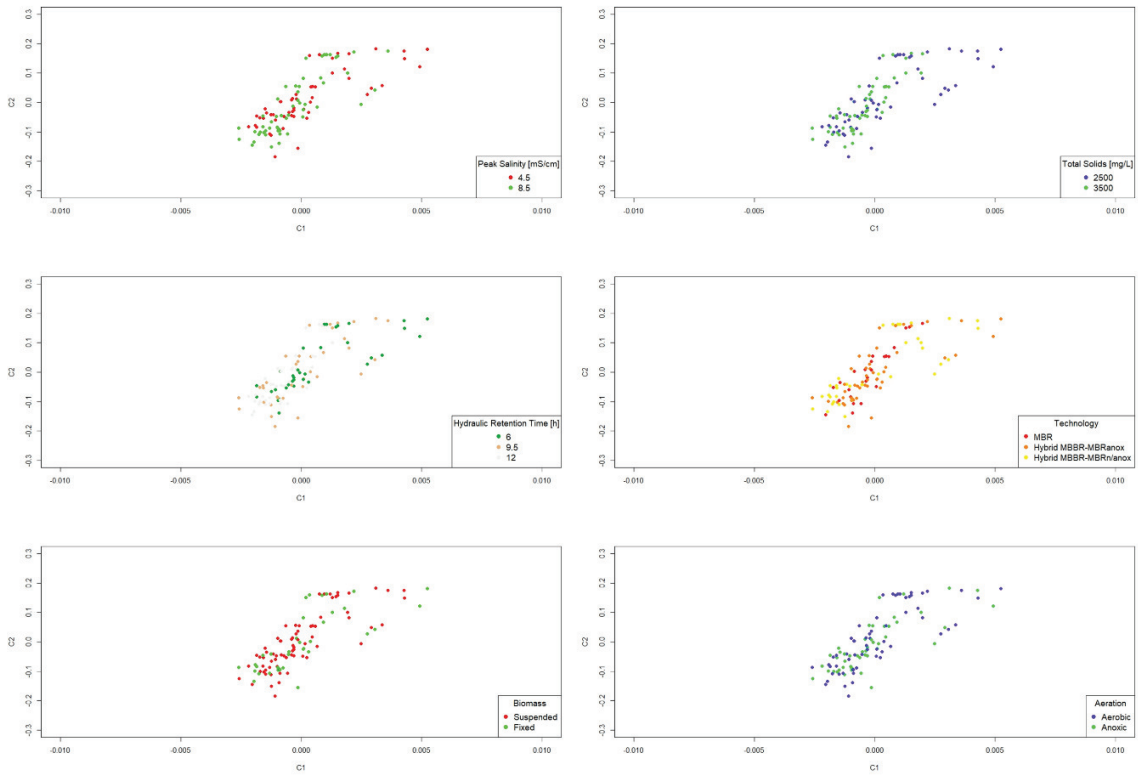

Figure 3 – Singular value decomposition plot showing the ordination of samples with respect to *Prokarya* communities and the effect of salinity conditions, total solids, hydraulic retention time, bioreactor technology, biomass configuration and aeration conditions

3.4 Differential abundance of OTUs with respect to environmental parameters

We assessed the influence of environmental parameters over the variability of *Eukarya* and *Prokarya* OTUs by the means of expected effect size analyses.

For the domain *Eukarya*, 17 OTUs were found to have significant variability with respect to salinity conditions (Fig. 4). On the other hand, 20 *Prokarya*-related OTUs had significant variability with respect to salinity, 6 were significantly encountered only in the MBR technology, and 1 OTU was found significant for the hybrid MBBR-MBRanox configuration and 1 for total solids concentration (Fig. 5). All OTUs that were found to have significant variability with respect to salinity condition could be potential players in the differences of removal performance between the two scenarios. For *Prokarya*, these were

affiliated to the genera *Cellulomonas* (mean relative abundance at 4.5 mS cm^{-1} of 0.00% vs mean relative abundance at 8.5 mS cm^{-1} of 0.12%), *Tetrasphaera* (0.17 vs 0.01%), *Flavobacterium* (0.88 vs 0.00%), *Clostridium* (0.06 vs 1.91%), *Amphiplicatus* (5.90 vs 0.01%), *Defluviimonas* (0.08 vs 0.00%), *Aquicella* (0.00 vs 0.07%), *Alkanindiges* (0.32 vs 0.00%), or *Thermomonas* (0.02 vs 0.19%). Among *Eukarya*, members of *Tremellales*, *Sacharomycetales*, and *Embryophita* were found, but many other OTUs could not be classified past kingdom level using SiLVA nr v128 or MiDAS 2.0. These were BLASTed against the nr/nt nucleotide collection of the NCBI, reporting the best BLAST hit with taxonomic affiliation past domain level (Table S1). The best BLAST hit results showed poor taxonomic classifications, highlighting the necessity of exploration of *Eukarya* domain in salinity wastewater treatment. This fact becomes even more pressing since the results reported in this experiment suggested that *Eukarya* community structure could be strongly related to the performance of membrane-based wastewater treatment technologies operating under variable salinity conditions. More effort should be spent on this in order to provide knowledge for future applications of variable salinity wastewater treatment.

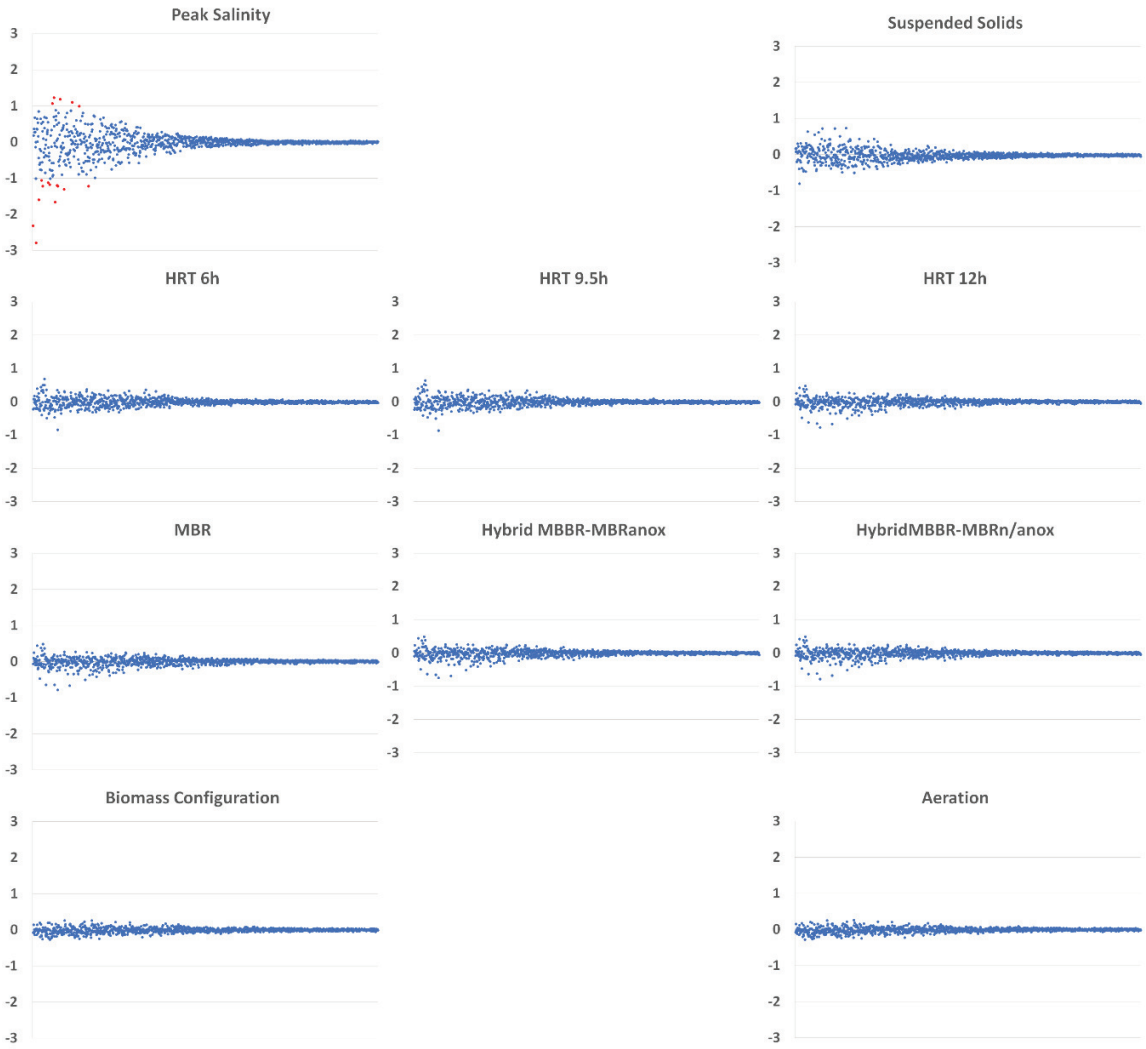

Figure 4 – Expected effect size plot of *Eukarya* OTUs with respect to operational parameters in the study: salinity conditions, total solids, hydraulic retention time, bioreactor technology, biomass configuration and aeration conditions. Red dots correspond to OTUs with significant variability with respect to individual environmental parameters. Blue dots correspond to OTUs without significant variability with respect to individual environmental parameters.

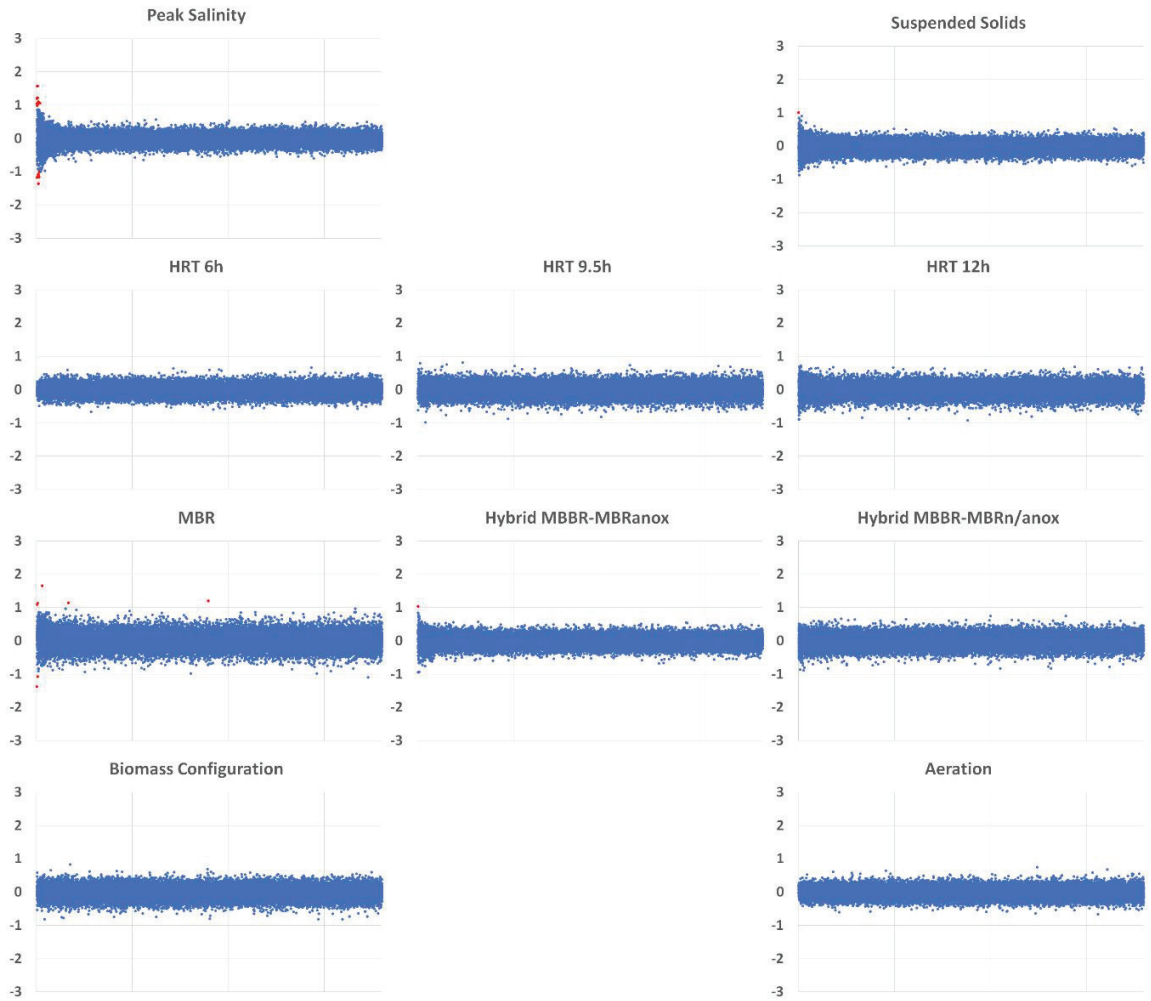

Figure 5 – Expected effect size plot of *Prokarya* OTUs with respect to operational parameters in the study: salinity conditions, total solids, hydraulic retention time, bioreactor technology, biomass configuration and aeration conditions. Red dots correspond to OTUs with significant variability with respect to individual environmental parameters. Blue dots correspond to OTUs without significant variability with respect to individual environmental parameters.

3.5 Microbial ecology of the bioreactors under different salinity conditions

3.5.1 Domain *Eukarya*

Within the *Eukarya*, 16 OTUs of interest were found (Fig. S1). Among them, following databases SiLVA nr v128 and MiDAS 2.0, two were affiliated with *Saccharomycetales*, one with *Tremellales*, one with *Crysophyceae*, one with *Ochrophyta*, one with *Embryophyta*, one with *Intramacronucleata*, one with *Rotifera*, one with *Oligohymenophora*, and seven with

unclassified *Eukayota*. The representative sequences of OTUs defined as unclassified *Eukaryota* by SiLVA nr v128 and MiDAS 2.0 were BLASTed against the nr/nt NCBI nucleotide collection, and the best BLAST hit results for taxonomy past domain level are given in Table S2. As what occurred for sensitive *Eukarya* OTUs, the necessity of a deeper exploration of *Eukarya* in saline wastewater treatment systems and salt water environments in general was highlighted.

3.5.2 Domain *Prokarya*

Fourteen OTUs of interest belonging to *Prokarya* were found among all biological samples (Fig. S1). One was affiliated with *Microbacteriaceae*, two with *Chitinophagaceae*, one with *Clostridium*, one with *Gemmatimonadaceae*, one with *Sphingopyxis*, one with *Comamonadaceae*, one with *Thiobacillus*, two with *Mizugakiibacter*, one with *Xanthomonadaceae*, two with *Rhodanobacter*, and one with *Saccharibacteria*. These phylotypes have different metabolic capabilities that allow them to proliferate in wastewater treatment systems. *Candidatus Saccharibacteria* phylum has been reported for aerobic and anaerobic organic matter degradation, nitrate reduction and ammonium removal, and *N*acetylglucosamine utilization (Kindaichi et al., 2016; Ouyang et al., 2017). *Rhodanobacter* and *Mizugakiibacter* have been reported for nitrite oxidation and heterotrophic, nitrate-reducing metabolisms in membrane-based systems treating saline wastewater (Rodriguez-Sanchez et al., 2017; 2018a; 2018b). *Sphingopyxis* strain isolated from activated sludge showed oxidative, chemoheterotrophic metabolism with no possibility of nitrogen metabolism (Kämpfer et al., 2005). *Thiobacillus* has autotrophic and anaerobic metabolism with capability for coupled denitrification-sulfur oxidation (Zhang et al., 2017). On the other hand, *Clostridium* is an obligate anaerobic microorganism found in human gut, sewage, and anaerobic digestion (Gonzalez-Martinez et al., 2016b; Niu et al., 2018).

Rhodanobacter and *Mizugakiibacter* genera have been reported as important members of the bacterial community of MBR and hybrid MBBR-MBR systems operating under tidal-like variable

salinity conditions at solids concentrations of 2500 mg L^{-1}. *Gemmantimonadaceae* representatives have been identified as important in these systems when operating at solids concentrations of 3500 mg L^{-1} (Rodriguez-Sanchez et al., 2018a). Compared to the operation at 4.5 and 8.5 mS cm^{-1}, *Rhodanobacter* and *Mizugakiibacter* were present in almost all samples at > 1% relative abundance. This highlights the relevant role of *Rhodanobacter* and *Mizugakiibacter* in the treatment of wastewater under variable salinity conditions. Additionally, *Gemmatimonadaceae* was present at > 1% at several operational conditions but seemed favored at 4.5 mS cm^{-1} than at 8.5 mS cm^{-1} and also more favored at 3500 mg L^{-1} solids than at 2500 mg L^{-1} solids.

The genera found in the bioreactors under the tidal-like variable salinity conditions were not found in the same technologies when treating urban wastewater with regular salinity. Instead, for the regular salinity conditions, different genera proliferated, such as *Nitrosomonas*, *Nitrospira*, *Thiobacillus*, *Alicycliphilus*, *Simplicispira*, *Dokdonella*, and *Rudaea*. The only genera found at regular conditions shared with the tidal variable salinity scenarios were *Ottowia* and *Rhodanobacter*. On the other hand, operation under regular salinity conditions showed a higher disparity in bacterial community structure between the MBR and the hybrid MBBR-MBR systems than under variable salinity conditions (Rodriguez-Sanchez et al., 2017).

3.6 Distribution of oligotypes in OTUs of interest

The intra-OTU diversity in *Eukarya* OTUs of interest was low, and the senso stricto subtype was not dominant in any (Figs. S2 through S16). These results demonstrated that *Eukarya* OTUs were more sensitive to salinity, allowing for less oligotypes to thrive in the bioreactors during operation. Moreover, there was a dominant oligotype in both salinity scenarios except for OTUs E_Otu0003, E_Otu0013, E_Otu0017, E_Otu0021, and E_Otu0026, where a domination turnover occurred

between salinity scenarios. In this sense, there were several *Eukarya* OTUs in the bioreactors that found different adaptations with respect to salinity conditions.

For *Prokarya* domains, the intra-OTU distribution in each OTU of interest showed great diversity of oligotypes except for OTU P_Otu0000016 (Fig. S17 through Fig. S27). For all OTUs except P_Otu0000001, P_Otu0000003, and P_Otu0000004, the senso stricto (not an oligotype) subtype had the greatest relative abundance across all samples. Only in OTU P_Otu0000016 a dominant oligotype could be found. The great diversity of oligotypes for *Prokarya* showed that many species adapted to variable salinity conditions.

For both domains, SVD analyses of the oligotype distribution of OTUs of interest suggested a differentiation between low and high maximum salinities (Fig. S28 through Fig. S53). In this sense, different salinity conditions affected the intra-OTU structure of the consistently repeated OTUs. This fact highlights that adaptation of microbes occurred when the biomass was exposed to different salinity conditions and demonstrates that intra-OTU variability could play an important role in biological wastewater treatment processes. Further implications of this finding for wastewater treatment systems should be studied in the future.

3.7 Linkage of core OTUs with effluent concentrations of BOD_5, COD, and TN in the bioreactors

For both *Eukarya* and *Prokarya* domains, there was independence between the effluent COD and the effluents BOD_5, TN, and NH_4^+ (Fig. 6). The linkage of *Eukarya* and *Prokarya* OTUs with BOD_5, TN, and NH^+ effluent concentrations became of significant importance to identify the main ecological players in saline wastewater treatment by the three technologies used in this study.

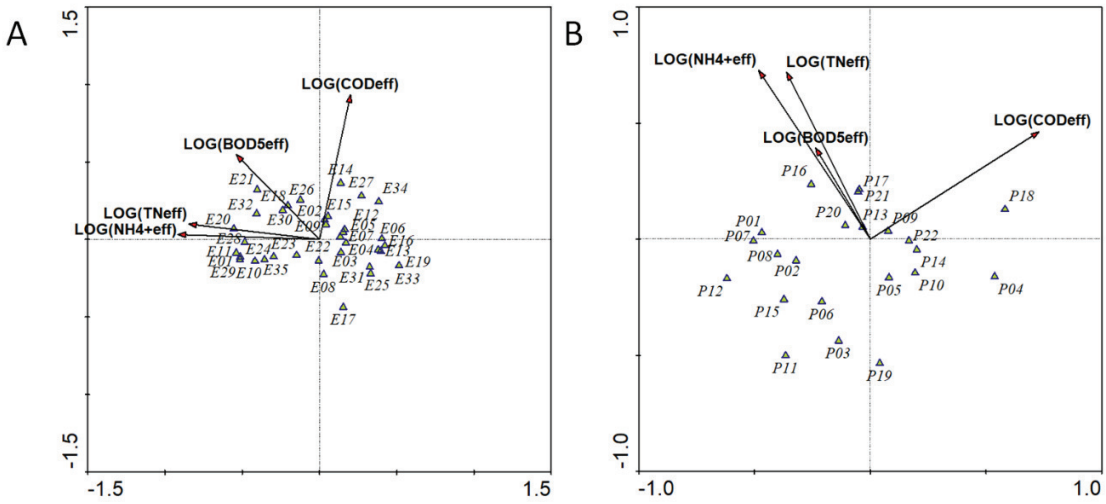

Figure 6 – Multivariate redundancy analyses biplot showing the linkage of core *Eukarya* (A) and *Prokarya* (B) OTUs with effluent concentrations of BOD_5, COD and TN

3.7.1 Members of *Eukarya* that influence the performance of the bioreactors

Many *Eukarya* OTUs of interest were correlated with BOD_5, TN, and NH_4^+ removal, with E_Otu0016, E_Otu0025, E_Otu0019, E_Otu0017, E_Otu0006, E_Otu0033, and E_Otu0013 being among the most important (Fig. 6a). These OTUs were phylogenetically related to a *Cercozoa* member, *Haptoria*, a *Chlorophyceae* member, an *Ochrophyta* member, and an unclassified *Eukaryota*, respectively. All these eukaryotes have been reported in marine habitats or wastewater treatment systems (Esmaeli et al., 2013; Schoenle et al., 2017; Tao et al., 2017; Lee et al., 2018; Yabuki and Ishida 2018). The mean relative abundance of these OTUs at 8.5 mS cm^{-1} was very low (in the range of 0.00 to 0.29%), while it was high for the 4.5-mS-cm^{-1} scenario (2.36–5.09%). On the other hand, several OTUs of interest were negatively correlated with these parameters, such as E_Otu0011, E_Otu0020, E_Otu0032, E_Otu0021, E_Otu0030, and E_Otu0029, classified as two *Saccharomycetales* members and an unclassified *Fungi*, *Rotifera*, *Archaeplastida* member, and *Embryophyta* member, respectively. Their mean relative abundance was

higher for the high-salinity maximum (1.04–4.78%) than for the low-salinity maximum (0.00–0.79%).

3.7.2 Members of *Prokarya* that influence the performance of the bioreactors

Several *Prokarya* OTUs of interest were positively correlated with TN, NH^+, and BOD removal, with the most important being P_Otu000004, P_Otu000019, P_Otu000018, P_Otu000006, P_Otu000005, P_Otu000010, and P_Otu000014, classified as *Amphiplicatus*, *Parvibaculum*, *Thiothrix*, *Microbacteriaceae* member, *Rhodanobacter*, *Blastocatella*, and *Nitrobacter*, respectively (Fig. 6b). Among them, *Amphiplicatus*, *Parvibaculum*, and *Thiothrix* have been reported for denitrification (Teske and Salman 2014; Zhen-Li et al., 2018; Li and Lu 2017); *Rhodanobacter* and *Nitrobacter* for nitrite oxidation (Rodriguez-Sanchez et al., 2018a); and *Blastocatella* for ammonium removal (Ouyang et al., 2017). All of them but *Nitrobacter* can develop heterotrophic metabolism. As what occurred with the OTUs of interest, the operation under different maximum salinities was selected for microorganisms with flexible metabolic capabilities.

Linkage of bacterial OTUs with kinetic parameters in MBR and hybrid MBBR-MBR systems operating at 6.5 mS cm^{-1} variable salinity demonstrated a positive correlation of *Phycisphaera*, *Thiothrix*, *Paludibacterium*, and a *Gemmatimonadaceae* representative with the autotrophic rate of substrate utilization, suggesting that they had an important role in nitrogen oxidation at those operational conditions. Also, *Thiothrix*, *Phycisphaera*, and *Paludibacterium* were correlated with heterotrophic rate of substrate utilization, suggesting that they could be involved in organic matter degradation (Rodriguez-Sanchez et al., 2018a). The relation of *Thiotrix* with BOD_5, TN, and NH^+ removal in the experiments performed at 4.5 and 8.5 mS cm^{-1} aimed that this genus could be involved in nitrification and organic matter oxidation in membrane systems treating variable salinity

wastewater. In this case, more effort should be put on investigating the metabolic potential of *Thiotrix* in variable salinity wastewater treatment systems.

Differences in nitrogen removal were significant between the high- and low-salinity maximums. This was also reflected in the lower relative abundance of microbial phylotypes related to nitrogen metabolism between the two scenarios. The mean relative abundance of *Blastocatella* for salinity of 4.5 mS cm^{-1} was of 2.01%, while it was of 0.21% for the 8.5-mS-cm^{-1} scenario. The lower presence of the possible efficient ammonium oxidizer *Blastocatella* would have impacted the ammonium oxidation efficiency, thus leading to poor nitrogen removal rates. In addition, the relative abundances of possible high-efficiency nitrite-oxidizing phylotypes *Rhodanobacter* and *Nitrobacter* were higher for the low-salinity scenario (5.85 and 0.99% vs 2.81 and 0.80%, respectively), which would also negatively impact nitrogen removal in the high-salinity scenario. Moreover, the possible efficient denitrifiers found in the systems *Amphiplicatus*, *Parvibaculum*, and *Thiothrix* had a much higher relative abundance for the low-salinity scenario (5.90, 1.19, and 1.19% vs 0.01, 0.27, and 0.30%). In this way, the microbial community studies suggested that poor nitrogen removal at high-salinity maximum compared to low-salinity maximum could be directly related with the lower presence of high-efficiency nitrifiers and denitrifiers. Moreover, distribution of oligotypes for these OTUs showed a variability driven by salinity in most cases. In this sense, oligotype distribution can affect the differences in bioreactor performance in addition to relative abundance differences.

Contrarily, a number of OTUs were negatively correlated with BOD_5, TN, and NH^+ removal, among which the most important were P_Otu000016, P_Otu000001, P_Otu000012, P_Otu000017, and P_Otu000021, related to *Clostridium*, *Rhodanobacter*, *Thiobacillus*, a *Comamonadaceae* member, and *Candidatus Microthrix*, respectively. The relative abundance of these poor-efficiency OTUs was higher for the 8.5-mS-cm^{-1} salinity scenario.

4. Conclusions

A MBR and two hybrid MBBR-MBR systems were operated for the treatment of salinity-amended urban wastewater with variable salinity in tidal cycles with maximum of 4.5 and 8.5 mS cm^{-1}, respectively, under 6, 9.5, and 12 h of hydraulic retention time and 2500 and 3500 mg L^{-1} total solids. The performance of the bioreactors showed that effluents of BOD_5, TN, and NH_4^+ concentrations were significantly lower at the 8.5-mS-cm^{-1} scenario ($p < 0.05$), which demonstrated that salinity conditions greatly affect the microbiological-driven performance of the systems. SVD analyses over the microbial community structure of the systems under all operational conditions showed that *Prokarya* was not differentiated by any, while *Eukarya* was differentiated by salinity conditions. This fact demonstrated the adaptation of *Prokarya* to the conditions of salinity, hydraulic retention time, and solids concentration and showed the sensitivity of *Eukarya* to salinity conditions. A small number of OTUs were found to have significant differences among salinity scenarios in *Eukarya* and *Prokarya*. It was found that the oligotype distribution in OTUs consistently present in the systems was affected by salinity, suggesting that intra-OTU variability could be related to the performance of the systems. Several *Prokarya* OTUs were positively correlated with BOD_5, TN, and NH_4^+ removal, such as *Amphiplicatus* (0.01–5.90%), *Parvibaculum* (0.27–1.19%), *Thiothrix* (0.30–1.19%), *Rhodanobacter* (2.81–5.85%), *Blastocatella* (0.21–2.01%), and *Nitrobacter* (0.80–0.99%), which could develop different metabolic roles of ammonium oxidation, nitrite oxidation, and denitrification. The differences in relative abundance of these OTUs at the two salinity scenarios (10–500%) could explain the significant differences in bioreactor performance under the different salinity conditions. The results obtained expanded the research field of saline wastewater treatment by investigation of variable salinity wastewater, which has been to date mostly disregarded, demonstrating its effect over the microbial communities of bioreactor treating these types of influents.

Funding information

The authors would like to acknowledge the support given by the Institute of Water Research and the Department of Civil Engineering in the University of Granada. Also, they would like to acknowledge the economic support given by the Ministry of Economy and Competitivity of the Government of Spain, which funded this project by the funding CTM2013-48154-P and grant BES-2014-067852.

References

APHA (2012) Standard Methods for the Examination of Water and Wastewater, 22nd ed., American Public Health Association, Washington DC.

Bassin JP, Kleerebezem R, Muyzer G, Rosado AS, Van Loosdrecht MCM, Dezotti M (2012) Effect of different salt adaptation strategies on the microbial diversity, activity, and settling of nitrifying sludge in sequencing batch reactors. Appl Microbiol Biotechnol 93: 1281– 1294. https://doi.org/10.1007/s00253-011-3428-7

Bian G, Gloor GB, Gong A, Jia C, Zhang W, Hu J, Zhang H, Zhang Y, Zhou Z, Zhang J, Burton JP, Reid G, Xiao Y, Zeng Q, Yang K, Li J (2017) The gut microbiota of healthy aged Chinese is similar to that of the healthy young. mSphere 2: e00327–e00317. https://doi.org/ 10.1128/mSphere.00327-17

Castillo-Carvajal LC, Sanz-Martin JL, Barragan-Huerta BE (2014) Biodegradation of organic pollutants in saline wastewater by halophilic microorganisms: a review. Environ Sci Pollut Res 21: 9578– 9588. https://doi.org/10.1007/s11356-014-3036-z

Cortes-Lorenzo C, Rodriguez-Diaz M, Lopez-Lopez C, Sanchez-Peinado M, Rodelas B, Gonzalez-Lopez J (2012) Effect of salinity on enzymatic activities in a submerged fixed bed biofilm reactor for municipal sewage treatment. Bioresour Technol 121: 312–319. https://doi. org/10.1016/j.biortech.2012.06.083

Cortés-Lorenzo C, González-Martínez A, Smidt H, González-López J, Rodelas B (2016) Influence of salinity on fungal communities in a submerged fixed bed bioreactor for wastewater treatment. Chem Eng J 285: 562–572. https://doi.org/10.1016/j.cej.2015.10.009

Di Trapani D, Di Bella G, Mannina G, Torregrossa M, Viviani G (2014) Comparison between moving bed-membrane bioreactor (MBMBR) and membrane bioreactor (MBR) systems: influence of wastewater salinity variation. Bioresour Technol 162: 60–69. https://doi.org/10.1016/j.biortech.2014.03.126

Di Bella G, Di Prima N, Di Trapani D, Freni G, Giustra MG, Torregrossa M, Viviane G (2015) Performance of membrane bioreactor (MBR) systems for the treatment of shipboard slops: assessment of hydrocarbon biodegradation and biomass activity under salinity variation, J Hazard Mater 300: 765–778.

Eren AM, Borisy GG, Huse SM, Mark Welch JL (2014) PNAS plus: from the cover: oligotyping analysis of the human oral microbiome. Proc Natl Acad Sci 111: E2875–E2884. https://doi.org/10.1073/pnas.1409644111

Esmaeli A, Jokar M, Kousha M, Daneshvar E, Zilouei H (2013) Acidic dye wastewater treatment onto a marine macroalga, Nizamuddina zanardini (phylum: Ochrophyta). Chem Eng J 217: 329–336. https://doi.org/10.1016/j.cej.2012.11.038

Gonzalez-Martinez A, Rodriguez-Sanchez A, Lotti T, Garcia-Ruiz MJ, Osorio F, Gonzalez-Lopez J, van Loosdrecht MC (2016a) Comparison of bacterial communities of conventional and A-stage activated sludge systems. Sci Rep 6: 18786. https://doi.org/10.1038/ srep18786

Gonzalez-Martinez A, Garcia-Ruiz MJ, Rodriguez-Sanchez A, Osorio F, Gonzalez-Lopez J (2016b) Archaeal and bacterial community dynamics and bioprocess performance of a bench-scale two-stage anaerobic digester. Appl Microbiol Biotechnol 100: 6013–6033. https://doi.org/10.1007/s00253-016-7393-z

Hao TW, Xiang P-Y, Mackey HR, Chi K, Lu H, Chui H-K, van Loosdrecht MCM, Chen G-H (2014) A review of biological sulfate conversions in wastewater treatment. Water Res 65: 1–21. https://doi.org/10.1016/j.watres.2014.06.043

Kämpfer P, Schulze R, Jäckel U, Malik KA, Amann R, Spring S (2005) Hydrogenophaga defluvii sp. nov. and Hydrogenophaga atypica sp. nov., isolated from activated sludge. Int J Syst Evol Microbiol 55: 341–344. https://doi.org/10.1099/ijs.0.03041-0

Kindaichi T, Yamaoka S, Uehara R, Ozaki N, Ohashi A, Albertsen M, Nielsen PH, Nielsen JL (2016) Phylogenetic diversity and ecophysiology of candidate phylum Saccharibacteria in activated sludge. FEMS Microbiol Ecol 1–11. https://doi.org/10.1093/femsec/fiw078

Lee S, Song EH, Lee T (2018) Eukaryotic plankton species diversity in the Western Channel of the Korea Strait using 18S rDNA sequences and its implications for water masses. Ocean Science Journal 153: 119–132

Leyva-Díaz JC, Calderón K, Rodríguez FA, González-lópez J (2013) Comparative kinetic study between moving bed biofilm reactor-membrane bioreactor and membrane bioreactor systems and their influence on organic matter and nutrients removal. Biochem Eng J 77: 28–40. https://doi.org/10.1016/j.bej.2013.04.023

Leyva-Díaz JC, Martín-Pascual J, Muñío MM, González-López J, Hontoria E, Poyatos JM (2014) Comparative kinetics of hybrid and pure moving bed reactor-membrane bioreactors. Ecol Eng 70 : 227–234. https://doi.org/10.1016/j.ecoleng.2014.05.017

Leyva-Diaz JC, Gonzalez-Martinez A, Gonzalez-Lopez J, Muñio MM, Poyatos JM (2015a) Kinetic modeling and microbiological study of two-step nitrification in a membrane bioreactor and hybrid moving bed biofilm reactor–membrane bioreactor for wastewater treatment. Chem Eng J 259: 692–702. https://doi.org/10.1016/j.cej.2014.07. 136

Leyva-Diaz JC, Lopez-Lopez C, Martin-Pascual J, Muñio MM, Poyatos JM (2015b) Kinetic study of the combined processes of a membrane bioreactor and a hybrid moving bed biofilm reactor-membrane bioreactor with advanced oxidation processes as a post-treatment stage for wastewater treatment. Chem Eng Process Process Intensif 91: 57–66. https://doi.org/10.1016/j.cep.2015.03.017

Leyva-Diaz JC, Gonzalez-Martinez A, Calderon K, Gonzalez-Lopez J, Muñio MM, Poyatos JM (2016) Microbial kinetics and enzymatic activities in hybrid moving-bed biofilm reactor-membrane bioreactor systems. Chem Eng Technol 39: 1067–1076. https://doi.org/10. 1002/ceat.201400750

Li E, Lu S (2017) Denitrification processes and microbial communities in a sequencing batch reactor treating nanofiltration (NF) concentrate from coking wastewater. Water Sci Technol 76: 11-12. https://doi. org/10.2166/wst.2017.493

McIlroy SJ, Kirkegaard RH, Mcilroy B, Nierychlo M, Kristensen JM, Karst SM (2017) MiDAS 2.0: an ecosystem-specific taxonomy and online database for the organisms of wastewater treatment systems expanded for anaerobic digester groups. Database (Oxford) 1–9. https://doi.org/10.1093/database/bax016

Niu W, Guo J, Lian J, Hao H, Li H, Song Y, Li H, Yin P (2018) Effect of fluctuating hydraulic retention time (HRT) on denitrification in the UASB reactors. Biochem Eng J 132: 29–37. https://doi.org/10.1016/ j.bej.2017.12.017

Okazaki Y, Fujinaga S, Tanaka A, Kohzu A, Oyagi H (2017) Ubiquity and quantitative significance of bacterioplankton lineages inhabiting the oxygenated hypolimnion of deep freshwater lakes. ISMEJ 11: 2279–2293. https://doi.org/10.1038/ismej.2017.89

Ouyang E, Liu Y, Ouyang J, Wang X (2017) Effects of different wastewater characteristics and treatment techniques on the bacterial community structure in three pharmaceutical wastewater treatment systems. Environ Technol 1: 1–13. https://doi.org/10.1080/09593330. 2017.1393010

Rodriguez-Sanchez A, Leyva-Diaz JC, Gonzalez-Martinez A, Poyatos JM (2017) Linkage of microbial kinetics and bacterial community structure of MBR and hybrid MBBR-MBR systems to treat salinity-amended urban wastewater. Biotechnol Prog 33: 1–13. https://doi. org/10.1002/btpr.2513

Rodriguez-Sanchez A, Leyva-Diaz JC, Gonzalez-Lopez J, Poyatos JM (2018a) Membrane bioreactor and hybrid moving bed biofilm reactor-membrane bioreactor for the treatment of variable salinity wastewater: influence of biomass concentration and hydraulic retention time. Chem Eng J 336: 102–111. https://doi.org/10.1016/j.cej. 2017.10.118

Rodriguez-Sanchez A, Leyva-Diaz JC, Poyatos JM, Gonzalez-Lopez J (2018b) Influent salinity conditions affect the bacterial communities of biofouling in hybrid MBBR-MBR systems. J Water Proc Engineer https://doi.org/10.1016/j.jwpe.2018.07.001

Rognes T, Flouri T, Nichols B, Quince C, Mahé F (2016) VSEARCH: a versatile open source tool for metagenomics. PeerJ 4: e2584. https:// doi.org/10.7717/peerj.2584

Schloss PD (2016) Application of a database-independent approach to assess the quality of. mSystems 1: 2–5. https://doi.org/10.1128/ mSystems.00027-16.Copyright

Schloss PD, Westcott SL, Ryabin T, Hall JR, Hartmann M, Hollister EB, Lesniewski RA, Oakley BB, Parks DH, Robinson CJ, Sahl JW, Stres B, Thallinger GG, Van Horn DJ, Weber CF (2009) Introducing mothur: open-source, platform-independent, community-supported software for describing and comparing microbial communities. Appl Environ Microbiol 75: 7537–7541. https://doi.org/10.1128/ AEM.01541-09

Schoenle A, Nitsche F, Werner J, Arndt H (2017) Deep-sea ciliates: recorded diversity and experimental studies on pressure tolerance. Deep Sea Res I 128: 55–66. https://doi.org/10.1016/j.dsr.2017.08. 015

Tao R, Kinnunen V, Praveenkumar R, Lakaniemi A (2017). Comparison of Scenedesmus acuminatus and Chlorella vulgaris cultivation in liquid digestates from anaerobic digestion of pulp and paper industry and municipal wastewater treatment sludge. 2845–2856. https://doi. org/10.1007/s10811-017-1175-6

Teske A, Salman V (2014) The family Leucotrichaceae. The Prokaryotes. Springer-Verlag Berlin Heidelberg.

Unno T (2015) Bioinformatic suggestions on MiSeq-based microbial community analysis. J Microbiol Biotechnol 25: 765–770

Welles L, Lopez-Vazquez CM, Hooijmans CM, van Loosdrecht MCM, Brdjanovic D (2015) Impact of salinity on the aerobic metabolism of phosphate-accumulating organisms. Appl Microbiol Biotechnol 99: 3659–3672. https://doi.org/10.1007/s00253-014-6287-1

Westcott SL, Schloss PD (2015) De novo clustering methods outperform reference-based methods for assigning 16S rRNA gene sequences to operational taxonomic units. PeerJ 3: e1487. https://doi.org/10.7717/ peerj.1487

Wu Y-J, Whang L-M, Fukushima T, Chang S-H (2013) Responses of ammonia-oxidizing archaeal and betaproteobacterial populations to wastewater salinity in a full-scale municipal wastewater treatment plant. J Biosci Bioeng 115: 424–432. https://doi.org/10.1016/j. jbiosc.2012.11.005

Yabuki A, Ishida K (2018) An orphan protist Quadricilia rotundata finally finds its phylogenetic home in Cercozoa. J Eukaryot Microbiol 65: 729–732. https://doi.org/10.1111/jeu.12502

Zhang B, Xu X, Zhu L (2017) Structure and function of the microbial consortia of activated sludge in typical municipal wastewater treatment plants in winter. Sci Rep 7: 1–11. https://doi.org/10.1038/ s41598-017-17743-x

Zhen-Li Z, Xin-Qi Z, Nan W, Wen-Wu Z, Xu-Fen Z, Yi C, Min W (2018) Amphiplicatus metriothermophilus gen. nov., sp. nov., a thermotolerant alphaproteobacterium isolated from a hot spring. Int J Syst Evol Microbiol 64: 2805–2811. https://doi.org/10.1099/ ijs.0.062471-0

Chapter 6

Biofouling formation and bacterial community structure in hybrid moving bed biofilm reactor-membrane bioreactors: influence of salinity concentration

This chapter has been published in its current form in Water. The complete citation is the following:

Alejandro Rodriguez-Sanchez, Juan Carlos Leyva-Diaz, Barbara Muñoz-Palazon, Maria Angustias Rivadeneyra, Miguel Hurtado-Martinez, Daniel Martin-Ramos, Alejandro Gonzalez-Martinez, Jose Manuel Poyatos, Jesus Gonzalez-Lopez. 2018. Biofouling formation and bacterial community structure in hybrid moving bed biofilm reactor-membrane bioreactors: influence of salinity concentration. Water. 10(9), 1133. doi: 10.3390/w10091133

Abstract

Two pilot-scale hybrid moving bed biofilm reactor-membrane bioreactors were operated in parallel for the treatment of salinity-amended urban wastewater under 6 hours of hydraulic retention time and 2500 mg L^{-1} total solids concentration. Two salinity conditions were tested: the constant salinity of 6.5 mS cm^{-1} electric conductivity (3.6 g L^{-1} NaCl) and the tidal-like variable salinity with maximum 6.5 mS cm^{-1} electric conductivity. An investigation was developed on the biofouling produced on the ultrafiltration membrane surface evaluating its bacterial community structure and its potential function in the fouling processes. The results showed that biofouling was clearly affected by salinity scenarios in terms of α-diversity and β-diversity and bacterial community structure, which confirms lower bacterial diversity under variable salinity conditions with *Rhodanobacter* and *Dyella* as dominant phylotypes. Microorganisms identified as bio-mineral formers belonged to genera *Bacillus*, *Citrobacter*, and *Brevibacterium*. These findings will be of help for the prevention and control of biofouling in saline wastewater treatment systems.

1. Introduction

Wastewater discharges to the environment are one of the main environmental problems in our world today. Several technologies have been developed for the treatment of wastewater such as the activated sludge process, which is the most commonly applied technology for urban wastewater treatment worldwide (Gonzalez-Martinez et al., 2016a). Nevertheless, more novel technologies than the activated sludge process such as the moving bed biofilm reactor-membrane bioreactor (MBBR-MBR) have been used for the treatment of urban and industrial wastewater (Leyva-Diaz et al., 2013; 2015a; 2015b).

Wastewater treatment bioreactors could be subjected to constant or variable salinity concentrations due to human activities such as the use of seawater as toilet flushing and the use of salt for snow-melting operations to industrial activities such as the seafood processing industry and due to natural events such as intrusion of seawater in coastal wastewater treatment plants (Cortes-Lorenzo et al., 2016). Salinity has been reported to affect microbial activity due to their impact in the bacterial cell mortality increase, in the increase in transmembrane osmotic pressure, and in the inhibition of different metabolic pathways (Rodriguez-Sanchez et al., 2017a). The effect of salinity over the membrane bioreactor (MBR) and MBBR-MBR systems has been evaluated and is still being investigated in order to fully understand its role in the functioning of these systems and to develop tools to mitigate its impact and increase the performance of salinity wastewater treatment systems (Rodriguez-Sanchez et al., 2017b).

The MBBR-MBR system is a combination of the moving bed biofilm reactor (MBBR), which was followed by a membrane bioreactor (MBR) process (Gonzalez-Martinez et al., 2015; Leyva-Diaz et al., 2014). Compared to the activated sludge process, the MBBR-MBR offers the development of fixed biofilm over the media placed within the bioreactor, which increases the sludge retention time of the biomass, promotes the development of more specialized microbial communities, and

increases the total solids' concentration in the system without increasing the mixed liquor suspended solids. This leads to more economic treatment of wastewater (Di Trapani et al, 2014; Leyva-Diaz et al., 2015c). Additionally, the placement of a downstream MBR after the MBBR process offers a very high-quality effluence due to membrane filtration, which also removes the majority of pathogens. Nevertheless, the main problem of MBBR-MBR systems is the membrane fouling, which is a process of clogging the membrane pore that leads to lower treatment efficiencies, lower wastewater flow treated per time unit, an increase of transmembrane pressure, and a destruction of the membrane.

The precipitation of minerals due to the activity of bacteria is known as biomineralization. It has been defined as a naturally occurring process comprising the formation of minerals with the mediation of metabolic activity of organisms (Dhami et al., 2013; Rao & Cölfen, 2016). Many different minerals can be formed by microorganisms in wastewater treatment systems, but close attention has been paid to calcium carbonate precipitates such as calcite, phosphate precipitates, and struvite (Rivadeneyra-Torres et al., 2013; Rivadeneyra et al., 2014; Gonzalez-Martinez et al., 2015; 2016a). Minerals precipitated can cause biofouling and permanent damage to membranes in wastewater treatment processes. Precipitated minerals have been identified along with biofilm as the most important components causing membrane fouling (Radu et al., 2015). It has been observed that bacterial strains isolated from moderate and high salinity environments mediate the formation of a variety of carbonate and phosphate minerals (Silva-Castro et al., 2015). Moreover, it has been suggested that bio-mineral formation under such environments could be of crucial relevance for the survival of the bacteria with capacity to mediate mineral formation (Silva-Castro et al., 2013). In this sense, biofouling during the operation of membrane technologies for the treatment of saline wastewater could be endangered by the potential formation of minerals derived from saline-adapted microbial communities thriving within the system. To date, no research has been spent to shed light over this phenomenon.

The potential risk of biofouling in MBBR-MBR systems due to precipitation of biominerals including calcium carbonate and magnesium phosphate has been reported (Gonzalez-Martinez et al., 2015). This potential risk could also be present in MBBR-MBR systems treating saline wastewater. For this reason, the aim of this research was to evaluate the effect of the influent salinity conditions over the potential risk of biofouling of an MBBR-MBR system due to bio-mineral formation. To unravel this, this technology was operated for treating saline wastewater under constant and variable saline concentrations in the influent, analyzing the bacterial community structure of the fixed biofilm (biofouling) by molecular techniques (Illumina MiSeq), and cultivating the fixed biofilm in mineral-precipitating media in order to evaluate the main bacterial strains involved in the formation of calcium and phosphate biominerals. In light of this, the potential risk of membrane biofouling of an MBBR-MBR system treating saline effluents could be established in a function of its bacterial microbiome.

2. Materials and Methods

2.1 Bioreactor Configuration and Operational Conditions

The bioreactor used in the study was configured as a four-chamber system followed by a membrane tank (Figure S1) with the potential capacity to properly remove C and N. The operational volume of each chamber was of 6 L and of 4.32 L for the membrane tank. The first, third, and fourth chambers were aerated and filled with K1 carriers in the 35% of their volume. K1 carriers (Anox-Kaldnes AS, Lund, Sweden) had a density of 0.92–0.96 g cm^{-3}, a specific surface area of 690 m^2 m^{-3}, and had a hollow cylindrical shape of 7 mm ×Ø10 mm with a cross inside the cylinder with fins on the outside of the cylinder. The second chamber was not aerated (anoxic) and not filled with carriers and mixed completely by using a mechanical stirrer. The influent was introduced through the first chamber and

forced to pass all the others before entering the membrane tank from where the effluent was withdrawn using an ultrafiltration membrane separation process. Additionally, a recycling flow was imposed from the membrane tank to the first chamber. This configuration has been called a hybrid MBBR-MBRn/anox (Rodriguez-Sanchez et al., 2017a; 2017b; 2018a).

The membrane tank contained an ultrafiltration membrane module continuously submerged and displaced vertically. The membrane module was made of hollow fibers of polyvinylidene fluoride with a core reinforcement of polyester that had 2.45 mm of external diameter and 1.10 mm of internal diameter with a 0.04 µm pore size. The total surface of the membrane was 0.2 m^2. The membrane was operated in a cycle of 9 min drawing and 1 min backwash in order to avoid membrane clogging. The flow rate was forced to be constant during the operation time by increasing the transmembrane pressure in the event of continuous fouling of the membrane. When the membrane pressure exceeded the value of 0.5 bar, the membrane was cleaned manually. In this sense, the flow rate was 4.72 L h^{-1} and the flux rate of the membrane was 23.6 L h^{-1} m^{-2}.

The bioreactor was operated for the treatment of salinity-amended urban wastewater with two different salinity inputs: i) constant salinity of 6.5 mS cm^{-1} electric conductivity (3.6 g L^{-1} NaCl),

ii) tidal variation salinity with an upper limit of 6.5 mS cm^{-1} electric conductivity (3.6 g L^{-1} NaCl), lower limit of regular urban wastewater salinity (around 1 mS cm^{-1} electric conductivity, 0.5 g L^{-1} NaCl), and in cycles of 6 h of upper limit/6 h lower limit. The achievement of the salinity amended wastewater was accomplished differently for the two salinity conditions.

For the constant salinity conditions, NaCl was manually diluted in batches of real urban wastewater collected at the Los Vados wastewater treatment plant (Granada, Spain) until the electric conductivity of the batch reached 3.6 g L^{-1} NaCl.

For the variable salinity conditions, it was obtained by the mixing of real urban wastewater (collected at the Los Vados full-scale wastewater treatment plant, located near Granada, Spain) with salinity amended tap water (50 mS cm^{-1} in order to avoid excessive dilution of real urban wastewater) in a mixing tank. The mixing was controlled electronically by a conductivity module TOPAX LF1 (Lutz-Jesco GmbH, Wedemark, Germany) connected to a conductivity sensor that measured the conductivity of the mixing tank wastewater and its temperature continuously, which also activated two Watson Marlow peristaltic pumps that provided real urban wastewater or salinity-amended tap water to the mixing tank depending on the desired salinity with respect to the cycle time.

A representation of the salinity conditions is given in Figure S1. The systems were operated in similar conditions except for the influent composition. The hydraulic retention time was 6 h and the total solids concentrations in the bioreactors were controlled to provide a total concentration of around 2500 mg L^{-1}.

Furthermore, different physico-chemical parameters were measured in the influent wastewater and the effluent of the MBBR-MBR system such as the five-day biochemical oxygen demand (BOD_5) and chemical oxygen demand (COD), according to the standard protocols and inorganic nitrogenous ions ammonium, nitrite, and nitrate through ionic chromatography analysis (Rodriguez-Sanchez et al., 2017a; 2017b).

2.2 Biomass Collection

Samples of the mixed liquor from the membrane tank and membrane-attached biomass (biofouling) were extracted from the systems operating once every two weeks during steady-state operational conditions (one-month period). The sampling protocols followed those described in Gonzalez-Martinez et al. (2015). Thus, 100 mL of mixed liquor were collected for this purpose. Additionally, a

given part of the membrane was sonicated in order to detach its fixed biomass and then detached biomass was placed in 0.9% NaCl saline solution. Collected biomass samples of mixed liquor from the membrane tank and membrane-attached biomass were used for the isolation of cultivable bacterial cells and DNA extraction.

2.3 Culture, Isolation, and Identification of the Bacterial Strains with Biomineralization Capacity

Biomass from biofouling samples was used for the isolation of bacterial strains capable of calcium carbonate and phosphate crystals precipitation, according to the protocols given by Gonzalez-Martinez et al. (2015). Thus, two different media were used for crystal formation of calcium carbonate (MC) and struvite precipitation (ME). Both media consisted on 18 g L^{-1} agar, 10 g L^{-1} yeast extract, 5 g L^{-1} protease peptone, and 1 g L^{-1} glucose. The MC medium was added of 4 g L^{-1} calcium acetate while ME medium was added with 8 g L^{-1} magnesium acetate. The components of the media were autoclaved at 112 °C for 20 min by avoiding the autoclaving of calcium acetate with the rest of the MC medium, which added it to the other components after the autoclave process. The pH of the media was 7.2 and was adjusted using 0.1 M KOH solution.

Biofouling samples (1 mL) were serially diluted and spread on struvite and calcium carbonate culture media. For each dilution and each media, five replicates were aerobically incubated at 25 °C for 12 days and checked every 24 h for the presence of minerals in the media. Colonies associated with minerals formation were then isolated in their respective medium of growth for their taxonomic identification. Bacterial strains isolated from the biofouling samples with a struvite or calcium carbonate bio-precipitation capacity were surface-inoculated onto MC and ME solid media, aerobically incubated at 25 °C, and examined every 24 h (during 12 days) with an optical microscope for the presence of biomineralization processes. The experiments were carried out in triplicate and

were repeated twice. Moreover, culture media inoculated with autoclaved cells and un-inoculated culture media were included in all experiments as a control.

2.4 Environmental DNA Extraction and Massive Parallel Sequencing Procedure

Samples were collected from the systems and processed for extraction of environmental DNA. Samples were centrifuged at 3500 rpm during 10 min at room temperature and the pelleted biomass was kept at −20 °C for further DNA extraction using a FastDNA SPIN Kit for Soil (MP Biomedicals, Solon, OH, USA) and the FastPrep 24 (MP Biomedicals, Inc., Leicestershire, UK) apparatus by following the instructions given by the manufacturers of the DNA extraction kit. The environmental DNA was kept at −20 °C while being sent to the Research & Testing Laboratory (Lubbock, TX, USA) for the massive parallel sequencing procedure.

The environmental DNA samples underwent a massive parallel sequencing for the identification of their bacterial community structure using the Illumina MiSeq equipment and the Illumina MiSeq Reagents Kit v3 (Illumina, Inc., San Diego, CA, USA). The sequencing procedure targeted the V1-V2-V3 hypervariable regions of the domain *Bacteria* using the primer pair 28F (5'-GAGTTTGATCNTGGCTCAG-3')-519R (5'-GTNTTACNGCGGCKGCTG-3') (Rodriguez-Sanchez et al., 2017a; 2017b; 2018a). The PCR conditions used for the Illumina MiSeq massive parallel sequencing were preheating at 94 °C during 120 s. Then the regions underwent 32 cycles of 94 °C for 30 s, 40 °C for 40 s, and 72 °C for 60 s as well as a final elongation at 72 °C for 300 s.

The raw data from the massive parallel sequencing has been uploaded to the SRA of the NCBI under the accession SRP145468.

2.5 Bioinformatics Pipeline

The raw data obtained from the massive parallel sequencing process was further treated to yield the bacterial community ecology of the biomass sampled using mothur (Schloss et al., 2009) and UCHIME (Edgar et al., 2011) software. First, paired-end reads were merged into contigs by avoiding the generation of ambiguous bases in the overlap region (Unno, 2015). Then the sequences underwent a quality-trimming process consisting of the following steps: (i) removal of sequences with more than eight ambiguous bases or more than eight homopolymers, (ii) removal of sequences that failed to start at the position of the primer 28F after alignment with the SiLVA SEED release 128 database, or those that terminated further than the 95% of total aligned sequences. After this, sequences were pre-clustered in a two-difference threshold (Huse et al., 2010) and checked for chimeras using UCHIME and removing them. The non-chimeric sequences were then taxonomically affiliated using the SiLVA SEED release 128 database and those that were found to not belong to the domain *Bacteria* were eliminated. The remaining sequences were then used for the determination of the bacterial community structure of the biomass sampled. This was done by the construction of a Phylip distance matrix for the sequences in each sample, which was then used for the clustering of the sequences in each sample to operational taxonomic units (OTUs) in a 97% similarity threshold. A representative sequence was then selected for each of the OTUs and these representative sequences were classified using the SiLVA SEED release 128 database. The classified OTUs were then merged into a consensus taxonomy using an 80% consensus taxonomy threshold.

2.6 Ecological Analyses of the Massive Parallel Sequencing Samples: Analysis of Bacterial Ecological Coverage, Analyses of α-Diversity and β-Diversity of Bacterial Community Structure, Similarity Analysis of the Mixed Liquor and Biofouling Bacterial Community Structure, and SIMPER Analyses Comparing Mixed Liquor and Biofouling Communities

The ecological coverage of the domain *Bacteria* in the massive parallel sequencing was evaluated using a redundancy abundance-weighted coverage approach following Rodriguez-R & Konstantinidis (2014a). For this purpose, NonPareil software was used for calculating the redundancy abundance-weighted coverage using query sets of 1000 sequences and considering the redundancy for sequences with at least 50% overlap and at least 95% similarity since these are the default parameters offered by the developers of the software (Rodriguez-R & Konstantinidis, 2014b).

The α-diversity analysis of the bacterial community structure of the massive parallel sequencing samples was conducted with PAST v3.0 (Hammer & Harper, 2007), which was used for the calculating the species richness, Chao-1, Shannon-Wiener, Simpson, Pielou's evenness, and Berger-Parker indices through 9999 bootstrap replications. The β-diversity analysis of samples of interest was done by the calculation of the Morisita-Horn and symmetric indices through the packages vegan 2.0 and vegetarian implemented in R software (Gonzalez-Martinez et al., 2016b).

The ecological data of the bacterial community structure of mixed liquor and biofouling samples was used for a similarity analysis to show differences among samples. The similarity analysis was done by the generation of a cluster dendrogram and a principal component analysis plot, which were calculated by Bray-Curtis distances using the vegan 2.0 package implemented in Rsoftware.

The SIMPER analyses were calculated using the Bray-Curtis distance and under 9999 bootstrap replications through the software PAST v3.0.

2.7 Characterization of Biominerals through X-Ray Diffractometry, Optic Microscopy, and Scanning Electron Microscopy

The minerals formed in the solid MC medium were extracted, according to Gonzalez-Martinez et al. (2015) from such medium by cutting out pieces of the medium and placed boiling water to dissolve the agar. The

precipitates were then washed using distilled water to remove impurities. Struvite crystals were obtained from the ME medium by using a small spatula and washed with distilled water to remove impurities. Both crystals types were air-dried at 37 °C for further analysis.

The characterization of the minerals was done using X-Ray diffractometry and scanning electron microscopy (SEM). The minerals were observed by using powder X-Ray diffractometry using a Philips PW 1710/00 diffractometer with a graphite monochromator automatic slit and CuKaα radiation. Data were collected for a 0.4 s integration time in 0.02 °C steps at 40 kV and 40 mA in a 2θ interval between 3 °C and 80 °C. Data was processed using the XPowder program for a qualitative and quantitative determination of the mineral composition. For quantitative analysis, full diffraction profiles of the experimental diffractograms were adjusted to weighed mixtures of the individual pattern phases. The crystalline mosaic size on hkl reciprocal vectors was obtained from full width at half of the maximum intensity after instrumental broadening and Kα2 corrections. The SEM of the minerals was made by carbon-coating samples and by using a high-resolution field emission scanning electron microscope Carl Zeiss, Supra 40 V (Carl Zeiss, Oberlocken, Germany). Selected samples were also analyzed for their chemical composition using energy dispersive X-ray (EDX) microanalysis (Aztec 350, Oxford Instruments, Abingdon, UK) and using the AMSCD mineral database.

3. Results

3.1 Physical-Chemical Parameters and Nutrient Removal

The removal of organic matter in the hybrid MBBR-MBR system subjected to variable salinity conditions was very good during the whole steady-state operation period with 99.51% removal of BOD_5 and 88.64% removal of COD for mean influent values of 293.33 ± 149.78 mg-BOD_5 L^{-1} and

588.36 ± 366.39 mg-COD L^{-1}. Total nitrogen elimination reached 36.83% removal for the influent mean value of 104.34 ± 22.25 mg-N L^{-1} (Rodriguez-Sanchez et al., 2018a). For the constant salinity scenario, the removal rates of BOD_5 and COD were 98.09% and 88.55% for influent concentrations of 408.33 ± 46.18 mg-BOD_5 L^{-1} and 654.07 ± 154.57 mg-COD L^{-1}, respectively. In the case of total nitrogen removal, the influent mean value of 181.14 ± 28.59 mg-N L^{-1} yielded a 22.97% removal rate (Rodriguez-Sanchez et al., 2017a; 2017b). For both salinity conditions, the attached biofilm over the carrier media had small concentrations (< 20 mg L^{-1} and < 40 mg L^{-1} for the constant and variable salinity scenarios, respectively) with respect to the biomass concentrations in the MLSS (around 2500 mg L^{-1}).

The different salinity conditions showed an influence over the performance of the bioreactors in terms of total nitrogen removed. In this case, constant salinity conditions led to about 10% lower total nitrogen removal performance. On the other hand, the removal of organic matter was similar between the different salinity conditions. Therefore, the results suggested that maximum influent salinity was related to the removal of organic material and that influent salinity conditions (constant vs. variable) influenced the total nitrogen removal in the bioreactors. It is possible that constant salinity conditions exerted more pressure over the nitrifying and/or denitrifying microbial communities in the hybrid MBBR-MBR than the variable salinity conditions.

3.2 Ecological Coverage, α-Diversity and β-Diversity Analyses of the Bacterial Community Structure in the Mixed Liquor and Biofouling Samples

The data of the ecological coverage of the massive parallel sequencing samples is shown in Table S1. The mean coverage value was 94.19% and the lowest value was 89.69%. The values obtained showed

that the massive parallel sequencing successfully covered the bacterial ecology diversity of the biomass analyzed.

The α-diversity analysis of the mixed liquor and biofilm samples analyzed is shown in Table S2. The chosen indices to observe α-diversity where the species richness, Chao-1, Shannon-Wiener, Simpson, Pielou's evenness, and Berger-Parker index. The species richness computes the number of species found in the biological sample. The Chao-1 index calculates the expected species richness of the sample. The Shannon-Wiener (H) and Simpson (1-D) indices are the Hill diversity indices of order 1 and order 2, respectively, and takes into account the diversity and evenness of the environment.

The Pielou's evenness shows the evenness of the samples. Lastly, the Berger-Parker index expresses the weighted true diversity and evenness of a sample.

Overall, the evenness of the variable salinity samples was lower than that of the constant salinity samples, which is shown by lower values of the Simpson and Pielou's evenness indices and higher values of the Berger-Parker index for the variable salinity scenario. In addition, the species richness along with the Shannon-Wiener and Chao-1 indices followed the same trend for constant and variable salinity scenarios than evenness indices.

Overall, the values of the Morisita-Horn indices were higher among variable salinity samples than among constant salinity samples (Figure 1). This was also found true for the symmetric index values. Morisita-Horn and symmetric indices have been reported as the best β-diversity estimators of dominant and rare phylotypes, respectively (Barwell et al., 2015). The variable salinity scenario showed higher similarity between biofouling and mixed liquor communities than the constant salinity scenario for dominant phylotypes. Biofouling had higher dissimilarity in dominant phylotypes than mixed liquor samples between the two salinity scenarios.

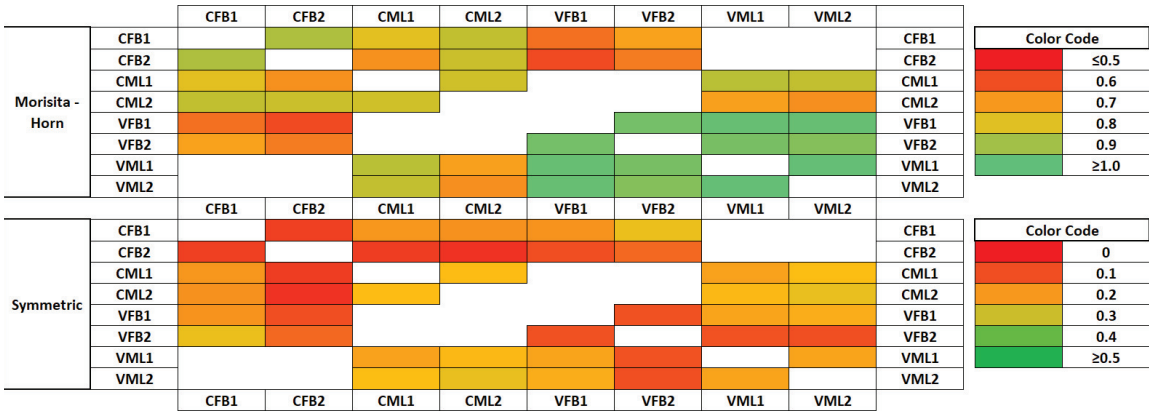

Figure 1 – Heat map of β-diversity indices of pair of biological samples of interest (CFB: Constant salinity Fixed Biofilm; CML: Constant salinity Mixed Liquor; VFB: Variable salinity Fixed Biofilm; VML: Variable salinity Mixed Liquor)

3.3 Similarity Analysis of the Bacterial Community Structure of the Mixed Liquor and Biofouling Samples

The principal coordinates analysis plot and the cluster dendrogram ordinating the samples analyzed are shown in Figure 2. Both ordination methods showed two different groups separating the constant salinity and the variable salinity communities. The cluster dendrogram separated the communities of the two salinity scenarios at around 20% similarity, which showed that salinity conditions had a higher selection capacity over the bacterial community structure in the membrane fixed biomass and the membrane tank mixed liquor. As shown by *β*-diversity analysis, the constant salinity samples were different among them and clustered in a 30% to 60% similarity when compared to variable salinity conditions in which samples were clustered in the 60% to 80% similarity threshold.

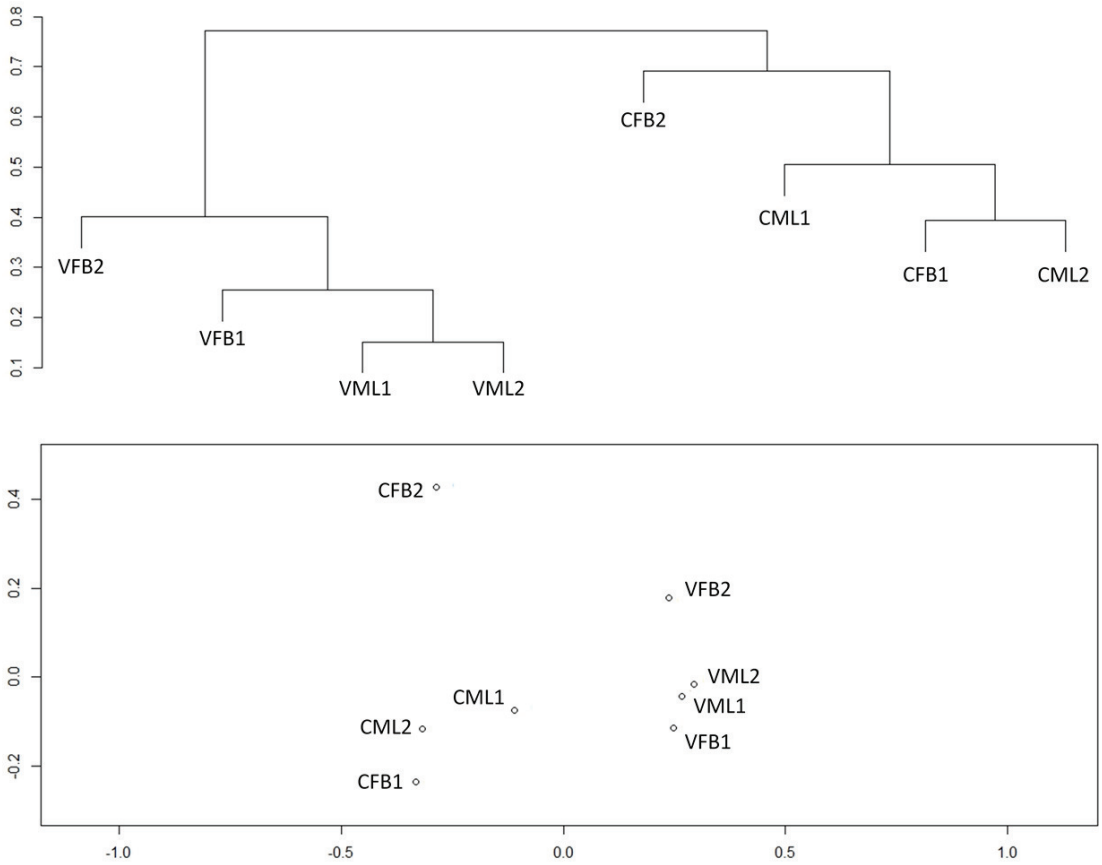

Figure 2 – Bray-Curtis similarity studies of the biological samples (top: cluster analysis; bottom: principal coordinates analysis)

3.4 Bacterial Community Structure of the Mixed Liquor and Biofouling Samples under Constant and Variable Salinity Conditions

The bacterial community structure of the mixed liquor and biofouling samples is shown in Figure 3. It was clear that certain bacterial genera were consistently found in mixed liquor and biofouling samples under both salinity conditions. Thus, *Rhodanobacter* (1.62% to 36.74%), *Ottowia* (2.23% to 8.32%), and *Dyella* (2.28% to 4.96%) were found in all samples studied while *Mycobacterium* (2.74% to 6.82%) and *Nitrobacter* (2.05% to 4.91%) were found in seven of the eight samples analyzed. Therefore, it could be suggested that these phylotypes are a major fraction of the microbiota

involved in the MBBR-MBR system for the treatment of saline urban wastewater regardless of the influent salinity conditions.

As confirmed by α-diversity analysis, the variable salinity samples had a lower microbial diversity when compared to the constant salinity samples, which was caused by a strong dominance of *Rhodanobacter* (21.59% to 36.74%), *Mizugakiibacter* (3.77% to 4.39%), *Ottowia* (5.47% to 6.37%), and *Mycobacterium* (2.74% to 6.82%). Among these, *Gemmatimonas* (0.60% to 2.53%), *Thermomonas* (0.56% to 4.14%), and an uncultured *Comamonadaceae* clone (1.04% to 7.80%) were found only at constant salinity conditions. In addition, it should be highlighted that *Mizugakiibacter* (3.77% to 4.39%), *Comamonas* (3.3% to 4.56%), *Ferruginibacter* (2.59% to 7.71%), *Mycetocola* (2.20% to 3.24%), and *Cryocola* (2.78% to 4.51%) were detected only under the variable salinity scenario. On the contrary, a higher microbial diversity and evenness in the constant salinity samples was clearly defined by the ecological analysis, which shows a wide variety of different genera (Table S2). Under conditions of variable salinity, the genus *Ferruginibacter* (6.94% to 7.71%) was clearly more present in the biofouling than in the mixed liquor. On the other hand, genus *Rhodanobacter* was of lower relative abundance in the fixed biofilm conditions under constant salinity (1.62% to 3.30%) than for the rest of the samples.

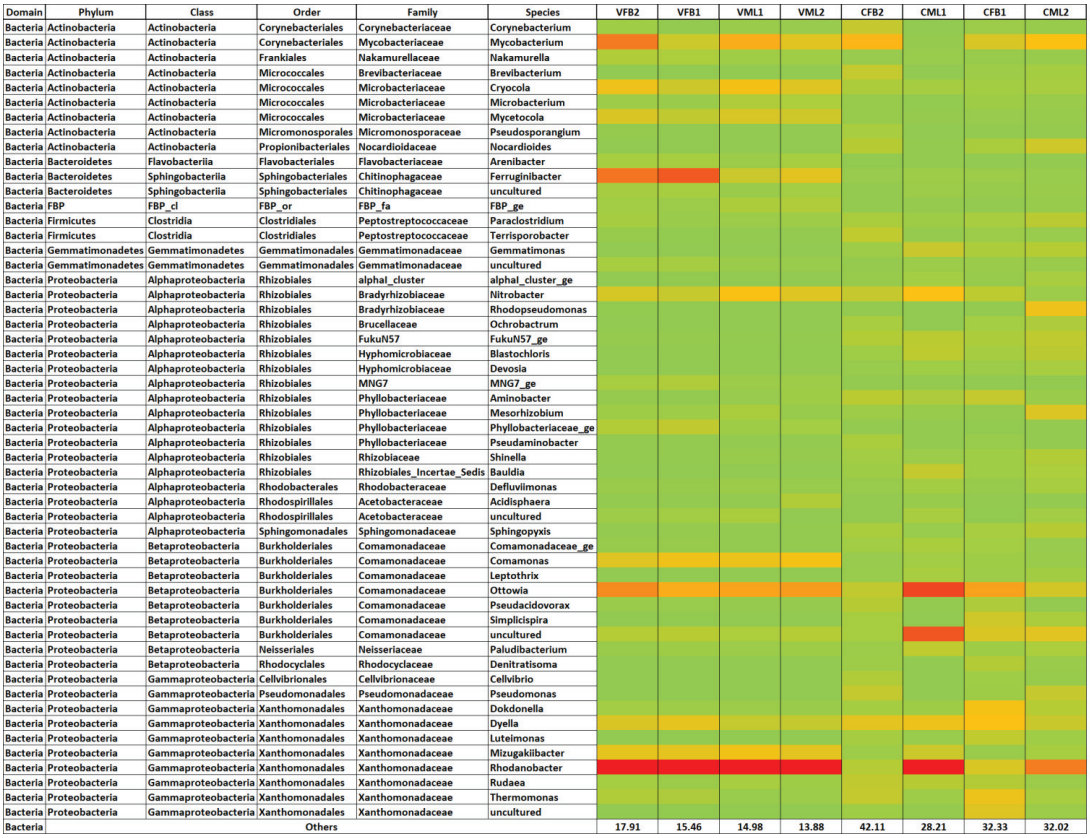

Domain	Phylum	Class	Order	Family	Species	VFB2	VFB1	VML1	VML2	CFB2	CML1	CFB1	CML2
Bacteria	Actinobacteria	Actinobacteria	Corynebacteriales	Corynebacteriaceae	Corynebacterium								
Bacteria	Actinobacteria	Actinobacteria	Corynebacteriales	Mycobacteriaceae	Mycobacterium								
Bacteria	Actinobacteria	Actinobacteria	Frankiales	Nakamurellaceae	Nakamurella								
Bacteria	Actinobacteria	Actinobacteria	Micrococcales	Brevibacteriaceae	Brevibacterium								
Bacteria	Actinobacteria	Actinobacteria	Micrococcales	Microbacteriaceae	Cryocola								
Bacteria	Actinobacteria	Actinobacteria	Micrococcales	Microbacteriaceae	Microbacterium								
Bacteria	Actinobacteria	Actinobacteria	Micrococcales	Microbacteriaceae	Mycetocola								
Bacteria	Actinobacteria	Actinobacteria	Micromonosporales	Micromonosporaceae	Pseudosporangium								
Bacteria	Actinobacteria	Actinobacteria	Propionibacteriales	Nocardioidaceae	Nocardioides								
Bacteria	Bacteroidetes	Flavobacteriia	Flavobacteriales	Flavobacteriaceae	Arenibacter								
Bacteria	Bacteroidetes	Sphingobacteriia	Sphingobacteriales	Chitinophagaceae	Ferruginibacter								
Bacteria	Bacteroidetes	Sphingobacteriia	Sphingobacteriales	Chitinophagaceae	uncultured								
Bacteria	FBP	FBP_cl	FBP_or	FBP_fa	FBP_ge								
Bacteria	Firmicutes	Clostridia	Clostridiales	Peptostreptococcaceae	Paraclostridium								
Bacteria	Firmicutes	Clostridia	Clostridiales	Peptostreptococcaceae	Terrisporobacter								
Bacteria	Gemmatimonadetes	Gemmatimonadetes	Gemmatimonadales	Gemmatimonadaceae	Gemmatimonas								
Bacteria	Gemmatimonadetes	Gemmatimonadetes	Gemmatimonadales	Gemmatimonadaceae	uncultured								
Bacteria	Proteobacteria	Alphaproteobacteria	Rhizobiales	alphal_cluster	alphal_cluster_ge								
Bacteria	Proteobacteria	Alphaproteobacteria	Rhizobiales	Bradyrhizobiaceae	Nitrobacter								
Bacteria	Proteobacteria	Alphaproteobacteria	Rhizobiales	Bradyrhizobiaceae	Rhodopseudomonas								
Bacteria	Proteobacteria	Alphaproteobacteria	Rhizobiales	Brucellaceae	Ochrobactrum								
Bacteria	Proteobacteria	Alphaproteobacteria	Rhizobiales	FukuN57	FukuN57_ge								
Bacteria	Proteobacteria	Alphaproteobacteria	Rhizobiales	Hyphomicrobiaceae	Blastochloris								
Bacteria	Proteobacteria	Alphaproteobacteria	Rhizobiales	Hyphomicrobiaceae	Devosia								
Bacteria	Proteobacteria	Alphaproteobacteria	Rhizobiales	MNG7	MNG7_ge								
Bacteria	Proteobacteria	Alphaproteobacteria	Rhizobiales	Phyllobacteriaceae	Aminobacter								
Bacteria	Proteobacteria	Alphaproteobacteria	Rhizobiales	Phyllobacteriaceae	Mesorhizobium								
Bacteria	Proteobacteria	Alphaproteobacteria	Rhizobiales	Phyllobacteriaceae	Phyllobacteriaceae_ge								
Bacteria	Proteobacteria	Alphaproteobacteria	Rhizobiales	Phyllobacteriaceae	Pseudaminobacter								
Bacteria	Proteobacteria	Alphaproteobacteria	Rhizobiales	Rhizobiaceae	Shinella								
Bacteria	Proteobacteria	Alphaproteobacteria	Rhizobiales	Rhizobiales_Incertae_Sedis	Bauldia								
Bacteria	Proteobacteria	Alphaproteobacteria	Rhodobacterales	Rhodobacteraceae	Defluviimonas								
Bacteria	Proteobacteria	Alphaproteobacteria	Rhodospirillales	Acetobacteraceae	Acidisphaera								
Bacteria	Proteobacteria	Alphaproteobacteria	Rhodospirillales	Acetobacteraceae	uncultured								
Bacteria	Proteobacteria	Alphaproteobacteria	Sphingomonadales	Sphingomonadaceae	Sphingopyxis								
Bacteria	Proteobacteria	Betaproteobacteria	Burkholderiales	Comamonadaceae	Comamonadaceae_ge								
Bacteria	Proteobacteria	Betaproteobacteria	Burkholderiales	Comamonadaceae	Comamonas								
Bacteria	Proteobacteria	Betaproteobacteria	Burkholderiales	Comamonadaceae	Leptothrix								
Bacteria	Proteobacteria	Betaproteobacteria	Burkholderiales	Comamonadaceae	Ottowia								
Bacteria	Proteobacteria	Betaproteobacteria	Burkholderiales	Comamonadaceae	Pseudacidovorax								
Bacteria	Proteobacteria	Betaproteobacteria	Burkholderiales	Comamonadaceae	Simplicispira								
Bacteria	Proteobacteria	Betaproteobacteria	Burkholderiales	Comamonadaceae	uncultured								
Bacteria	Proteobacteria	Betaproteobacteria	Neisseriales	Neisseriaceae	Paludibacterium								
Bacteria	Proteobacteria	Betaproteobacteria	Rhodocyclales	Rhodocyclaceae	Denitratisoma								
Bacteria	Proteobacteria	Gammaproteobacteria	Cellvibrionales	Cellvibrionaceae	Cellvibrio								
Bacteria	Proteobacteria	Gammaproteobacteria	Pseudomonadales	Pseudomonadaceae	Pseudomonas								
Bacteria	Proteobacteria	Gammaproteobacteria	Xanthomonadales	Xanthomonadaceae	Dokdonella								
Bacteria	Proteobacteria	Gammaproteobacteria	Xanthomonadales	Xanthomonadaceae	Dyella								
Bacteria	Proteobacteria	Gammaproteobacteria	Xanthomonadales	Xanthomonadaceae	Luteimonas								
Bacteria	Proteobacteria	Gammaproteobacteria	Xanthomonadales	Xanthomonadaceae	Mizugakiibacter								
Bacteria	Proteobacteria	Gammaproteobacteria	Xanthomonadales	Xanthomonadaceae	Rhodanobacter								
Bacteria	Proteobacteria	Gammaproteobacteria	Xanthomonadales	Xanthomonadaceae	Rudaea								
Bacteria	Proteobacteria	Gammaproteobacteria	Xanthomonadales	Xanthomonadaceae	Thermomonas								
Bacteria	Proteobacteria	Gammaproteobacteria	Xanthomonadales	Xanthomonadaceae	uncultured								
Bacteria	Others					17.91	15.46	14.98	13.88	42.11	28.21	32.33	32.02

Figure 3 – Heat map of bacterial community structure of genera with at least >1% relative abundance in at least one sample

Figure S2 showed that there were certain dominant phylotypes that caused the major dissimilarities between the mixed liquor and fixed biofilm samples for the constant and variable salinity scenarios. For the constant salinity conditions, the major contributors to dissimilarity were *Rhodanobacter* and *Mycobacterium*. For the variable salinity scenario, *Rhodanobacter* and *Mycobacterium* joined *Ferruginibacter* and *Ottowia*. Lower evenness at variable salinity conditions caused that contributions to dissimilarity were more marked for a few phylotypes than at constant salinity conditions. In general, *Rhodanobacter* had higher relative abundance in the mixed liquor (6.78% to 15.27%) than in the fixed biofilm (1.62% to 3.30%) under constant salinity (Figure 3). For the variable salinity conditions, this was also true. However, differences in relative abundance were less important (21.59% to 31.54% vs. 32.90% to 36.74%, respectively). *Mycobacterium* showed the opposite trend than that observed for *Rhodanobacter*. *Ottowia* showed higher relative abundance in the fixed biofilm under variable salinity conditions and higher relative abundance at the mixed liquor under constant salinity. *Ferruginibacter* had much higher (two-fold) relative abundance in the fixed biofilm than in the mixed liquor at variable salinity conditions.

3.5 Biomineral Precipitation by Bacteria Isolated from Fixed Biofilm under Constant and Variable Salinity Conditions

The formation of biofouling in the MBBR-MBR system was detected after 24 h under both experimental conditions (constant and variable salinity). Biofouling generation was easily detected by an optical microscope. Moreover, the formation of biominerals (calcium carbonate and struvite crystals) in artificial media (MC and ME solid media) by the bacterial strains isolated from the biofouling took place after three days of incubation time. However, no formation of crystals was detected in un-inoculated control media or in those culture media inoculated with a high concentration of dead cells, which lacked metabolic activity.

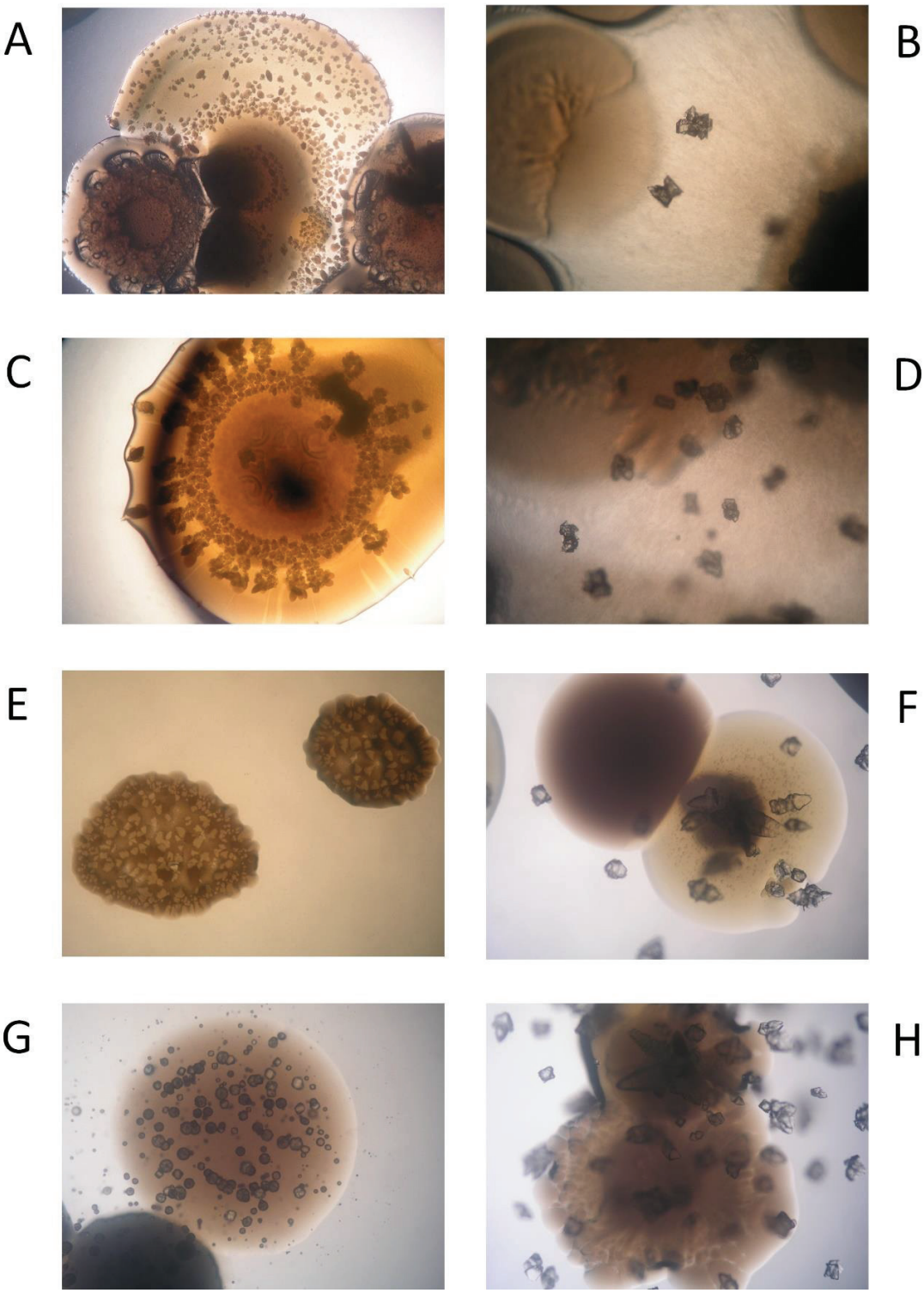

Figure 4 – Optical microscopy images of biomineralization in culture media (A and C: MC medium for constant salinity scenario; E and G: MC medium for variable salinity scenario; B and D: ME medium for constant salinity scenario; F and H: ME medium for variable salinity scenario)

Images of the biominerals formed in ME and MC media by the strains isolated from the biofouling generated in the membranes under constant and variable salinity conditions are shown in Figure 4. The images showed that the minerals formed in ME were very similar between the constant and variable salinity conditions while the minerals formed in the MC had some slight differences among them.

The results of the SEM X-ray microanalysis showed that the minerals were mainly formed by the same principal components, which were Ca^{2+} for the MC medium and Mg^{2+} for the ME medium. SEM images of the minerals obtained from MC medium showed isolated or aggregated carbonate objects with spherical shapes, hereafter called bioliths (Figure 5), independently of the salinity conditions (constant and variable). In many cases, mineralized bacteria were evident on spherulites surfaces and a bacterial mold entirely covered the surfaces of certain bioliths (Figure 5). It can be observed in the SEM images of the spherulite surfaces (Figure 5) that carbonate precipitates were nucleated on bacterial nanoglobules (Figure 5A,B,D,E) thought to be the first stage of precipitation processes that are mediated by microbes (Rivadeneyra et al., 2010). When crystal minerals produced in ME medium by the isolated strains from the membrane biofouling were examined under SEM, it was observed that phosphate minerals were not formed by the aggregation of mineralized cells (Figure 6) and, in such cases, bacterial cells contributed to the formation only by changing the environment as a consequence of their metabolic activity.

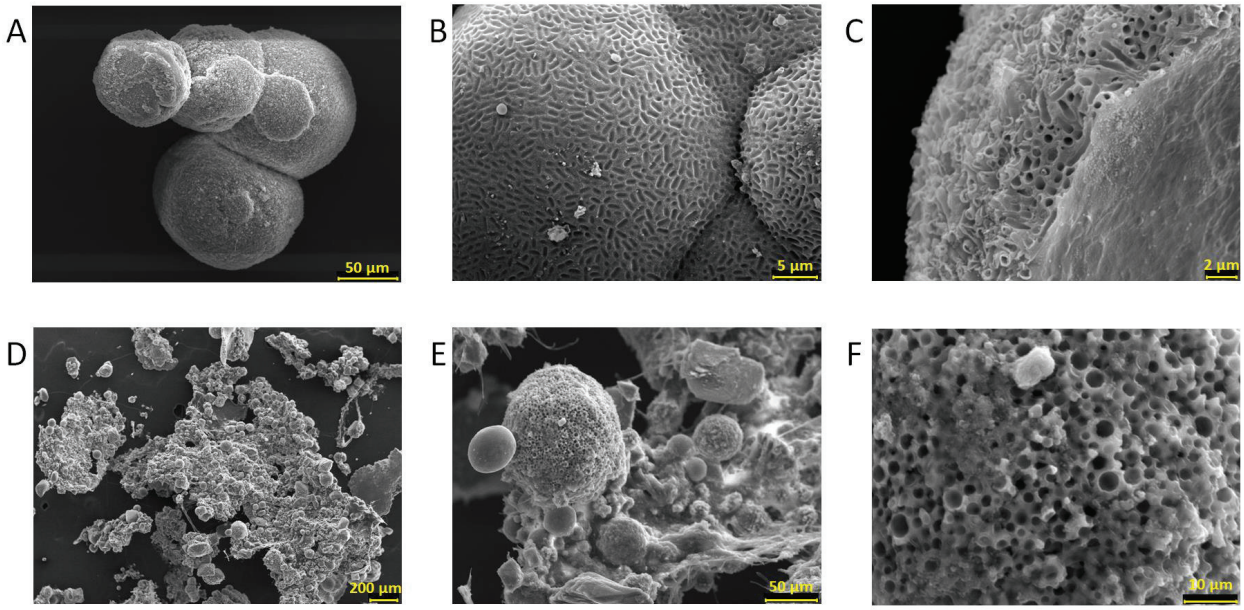

Figure 5 – Scanning electron microscopy images of biominerals precipitated in the MC medium under constant (A, B and C) and variable (D, E and F) salinity conditions

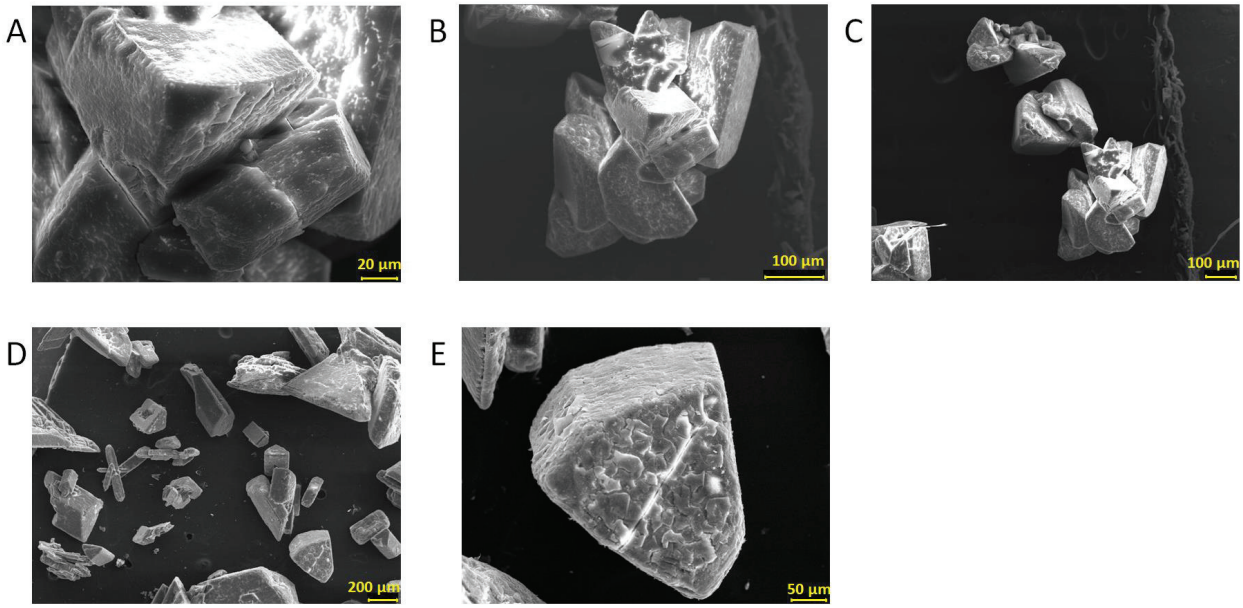

Figure 6 - Scanning electron microscopy images of biominerals precipitated in the ME medium under constant (A, B and C) and variable (D and E) salinity conditions

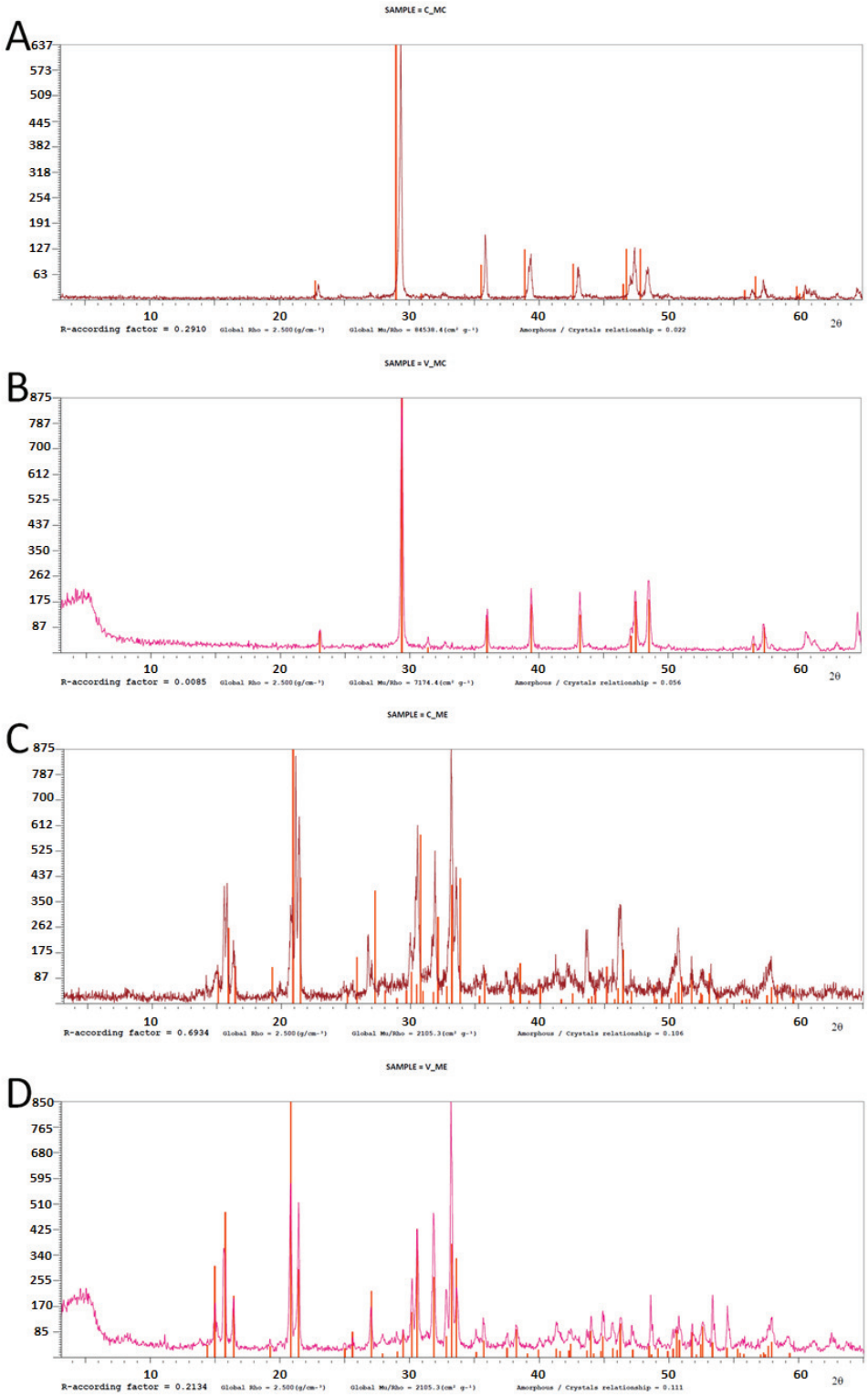

Figure 7 – X-Ray diffractometry analyses of biominerals precipitated in the culture media (A: MC medium for constant salinity conditions; B: ME medium for constant salinity conditions; C: MC medium for variable salinity conditions; D: MC medium for variable salinity conditions)

The X-ray diffractometry analysis results showed that the X-ray difractograms from precipitates in the MC medium by isolated strains from membrane biofouling under salinity conditions (constant and variable) were always calcite (Figure 7A,B). On the other hand, the minerals formed in ME medium by isolated strains from membrane biofouling at constant and variable salinity scenarios were closely related to K-struvite and struvite, respectively (Figure 7C,D).

3.6 Identification of Bacterial Species Associated with Mineral Precipitation from the Biofouling Formed under Constant-Salinity and Variable-Salinity Conditions

Only one bacterial species, classified as *Citrobacter freundii* and associated with calcite precipitation capacity, was detected in MC medium for the constant salinity condition while, in ME medium under these same conditions, three strains were identified with K-struvite precipitation activity: *Citrobacter freundii*, *Bacillus licheniformis*, and *Bacillus pumilus*. For the variable salinity conditions, only one strain was found in MC medium being classified as *Brevibacterium linens* while the sole strain found in the ME medium with struvite precipitation activity was *Bacillus licheniformis*. The similarity values with NCBI sequences are given in Table S3.

For the constant salinity condition, the identified phylotypes with >1% relative abundance reported for calcite precipitation were *Nocardioides* (1.163% to 1.694%) (Busquets et al., 2014), *Brevibacterium* (0.604% to 2.324%) (Zhu et al., 2017), and *Pseudomonas* (0.671% to 2.284%) (Bai et al., 2017). For the case of struvite precipitation, the identified phylotypes were *Corynebacterium* (0.492% to 2.374%) (Martin Navarro et al., 2015), *Brevibacterium* (0.604% to 2.324%) (Soares et al., 2014), and *Ochrobactrum* (0.671% to 2.284%) (Rivadeneyra et al., 2014). On the other hand, only one phylotype with >1% relative abundance in the variable salinity scenario was found

with potential capabilities to precipitate calcite or struvite such as *Comamonas* (3.525% to 4.325%) identified for struvite precipitation (Rogers et al., 2014).

4. Discussion

4.1 Physical-Chemical Parameters and Nutrient Removal

With respect to regular salinity operation, the bioreactors showed similar COD and BOD_5 removal while lower performance was observed in TN elimination (Leyva-Diaz et al., 2015a). The data suggested that amended-salinity wastewater could pressure nitrifying and/or denitrifying communities in the hybrid MBBR-MBR, which resulted in a TN removal efficiency loss. The absence of attached biofilm in the bioreactors showed that microbial communities in the bioprocesses could not form biofilms over the carrier surface in the presence of constant and variable 3.6 g L^{-1} NaCl maximum salinity. This result has been observed previously in hybrid MBBR-MBR systems (Rodriguez-Sanchez et al., 2017b) by proposing that salinity inhibits the ability of microorganisms in urban wastewater for the formation of attached biofilms. In practice, the hybrid MBBR-MBR systems operated under both scenarios of salinity operated as MBR systems.

4.2 Ecological Coverage, α-Diversity, and β-Diversity Analyses of the Bacterial Community Structure in the Mixed Liquor and Biofouling Samples

The α-diversity and β-diversity data suggested that, in the MBBR-MBR systems treating effluent with variable salinity conditions, the bacterial populations in the mixed liquor and in the biofouling had less diversity and evenness, which can be observed by the species richness, Chao-1, Shannon-Wiener, Simpson, Pielou's evenness, and Berger-Parker indices (Table S2) as well as higher similarity among dominant phylotypes, based on the Morisita-Horn index (Figure 1), than the bacterial populations

present in the constant salinity scenario. Thus, it seemed that variable salinity conditions allowed for a more stringent selection of membrane biomass phylotypes.

4.3 Similarity Analysis of the Bacterial Community Structure of the Mixed Liquor and Biofouling Samples

The results obtained by the similarity analysis suggested that the influent conditions with respect to salinity loading (constant vs. variable) had a high influence over the bacterial community structure in the MBBR-MBR systems analyzed in this study, which is shown by the α-diversity and β-diversity analyses. In this sense, samples trended to cluster for similar influent salinity variations, which was more important in the ordination of samples than the nature of the biomass (Figure 2).

4.4 Bacterial Community Structure of the Mixed Liquor and Biofouling Samples under Constant and Variable Salinity Conditions

Dominant phylotypes found under both salinity conditions, *Rhodanobacter* and *Nitrobacter* (Figure 3), have been reported as the main nitrite oxidizers in hybrid MBBR-MBR systems treating salinity-amended wastewater (Rodriguez-Sanchez et al., 2017a). In this context, *Rhodonobacter* is a microorganism that has the capacity to produce high amounts of EPS (Aqeel et al., 2016) and this fact could be of importance in the formation of membrane biofouling. Moreover, *Nitrobacter* has been identified as a microorganism involved in the formation of biofouling processes in MBR systems treating bathing wastewater (Guo et al., 2008). On the other hand, microorganisms of the genus *Ottowia* has been described as halophilic phylotype in saline wastewater treatment systems (Rodriguez-Sanchez et al., 2017b) where it develops an important role in the formation of the floc biomass. In addition, members of the *Ottowia* genus have been reported to be involved in important

metabolic activities such as heterotrophic ammonium oxidation and nitrite/nitrate reduction in biofilms (Liu et al., 2017). Lastly, the *Dyella* genus has been found in membrane biocake and thus has been related to late biofouling processes of membrane treating wastewater (Lim et al., 2012). With respect toimportant genus *Ferruginibacter*, Liu et al. (2017) reported its important function in the fixed biofilm formation in membrane bioreactors where it contributes directly to the membranes' colonization and later to the establishment of a mature biofilm.

In the case of operation under regular salinity (around 1 mS cm^{-1} electric conductivity), there were huge differences in the biofouling community structure dominated by *Simplicispira*, *Rhodobacter*, *Comamonas*, and *Clostridium* (Gonzalez-Martinez et al., 2015).

The results of bacterial community structure analysis could suggest that salinity conditions (variable or constant) determined changes in the microbial community structure in the mixed liquor and in the membrane biofouling of the MBBR-MBR system possibly as a consequence of the different osmolarity produced during the operational conditions in the system. Moreover, β-diversity and similarity analyses confirmed this suggestion (Figures 1 and 2).

It was found that different salinity conditions resulted in similar organic matter removal performance but that total nitrogen removal was slightly higher for the variable salinity conditions. This could be caused by a difference in the nitrifiers and/or denitrifiers in the bacterial communities of the bioreactors at both salinity conditions. Among the dominant phylotypes found in both systems, it has been claimed that *Rhodanobacter*, *Nitrobacter*, and *Ottowia*, among others, have an important role in autotrophic nitrification kinetics in MBR and MBBR-MBR systems treating saline wastewater (Rodriguez-Sanchez et al., 2017b). Additionally, *Rhodanobacter* has been associated with denitrification in MBR and MBBR-MBR systems (Rodriguez-Sanchez et al., 2018a). The differential relative abundance of *Rhodanobacter* in the mixed liquor of the MBBR-MBR systems at different salinity

conditions (6.78% to 15.27% under constant salinity, 32.90% to 36.74% under variable salinity) may be related to the differential total nitrogen removal. In this way, *Rhodanobacter* would have a very important ecological role in the nitrification and/or denitrification processes in MBBR-MBR systems treating saline wastewater.

The SIMPER analyses showed dissimilar representations of dominant phylotypes *Rhodanobacter* and *Mycobacterium* at both salinity conditions with *Mycobacterium* having more importance in the mixed liquor and *Rhodanobacter* in the biofouling, which occurred with *Ferruginibacter*. On the other hand, genus *Ottowia* was more represented in the mixed liquor than in the biofouling for the constant salinity conditions than for the variable salinity conditions. Taking into consideration that *Rhodanobacter* and *Ottowia* have been related to autotrophic nitrification kinetics (Rodriguez-Sanchez et al., 2017b), it is possible that their competition in the mixed liquor inside the MBBR-MBR systems had an effect over the total nitrogen removal of the bioreactors. Nevertheless, the results showed that possible performance of the MBBR-MBR treating saline wastewater was more affected by the relative abundance of major players in the nitrification and/or denitrification than by their differential presence between mixed liquor and biofouling, which was also suggested by the similarity analyses.

It has been found that the bacterial communities developing in membrane systems treating salinity wastewater are sensitive to the maximum influent salinity and its regime (constant or variable) (Rodriguez-Sanchez et al., 2018b). Regarding this information, it can be stated that the results obtained in this paper could be escalated to systems at full-scale, which operate under similar influent salinity conditions. In the same manner, the high variability of the full-scale effluents limits the application of these results to existing operating systems due to high sensitivity of bacterial communities in MBBR-MBR systems treating saline wastewater.

4.5 Biomineral Precipitation by Bacteria Isolated from Fixed Biofilm under Constant and Variable Salinity Conditions

The results obtained from the biomineralization experiment confirmed that the generation of biominerals was determined by the biological activity of the bacterial strains and that this is consequently a biomineralization process. Similar results have been previously described by Gonzalez-Martinez et al. (2015). The formation of crystals of struvite (ammonium-magnesium hydrated phosphate) or K-struvite (magnesium-potassium hydrated phosphate) should be associated with the characteristics of the bacterial strains isolated in the biofouling obtained under the different salinity conditions tested. Previous analyses of minerals precipitated in MC and ME media by bacterial strains isolated from MBBR-MBR systems operating at low salt concentration (around 1 mS cm^{-1} electric conductivity) demonstrated their capacity for bio-precipitation of struvite in the ME medium and calcite and vaterite in the MC medium (Gonzalez-Martinez et al., 2015). This last mineral (vaterite) was never detected in our study.

4.6 Identification of Bacterial Species Associated with Mineral Precipitation from the Biofouling Formed under Constant-Salinity and Variable-Salinity Conditions

It is evident that the presence of high saline concentrations in wastewater originated in an important reduction in the biodiversity of cultivable strains with the capacity to precipitate minerals in culture media in the biofouling obtained from the MBBR-MBR system especially when compared with previous studies in MBBR-MBR systems with low saline concentration (Gonzalez-Martinez et al., 2015).

Citrobacter freundii strains have been isolated from a hypersaline marine environment (Jacob et al., 2012). *Citrobacter freundii* strains isolated from hypersaline coastal lagoons have been reported to

mediate on calcite precipitation (Guo et al., 2013). It is, therefore, important to point out that it is the first time that the formation of calcite crystals by *Citrobacter freundii* has been reported in engineering systems, which is important since its role in the formation of membrane biofouling in high salinity conditions is unknown. In addition, it is noteworthy that *C. freundii* was the only bacterial species isolated from membrane biofouling samples in carbonate precipitation media under conditions of constant salinity. The massive parallel sequencing procedure performed on the biofouling showed that the *Citrobacter* genus was present in the membrane biofouling samples at the constant salinity scenario in a range of relative abundance from 0.015% to 0.036%. These data suggested that, even though, from a quantitative point of view *C. freundii*, it did not represent a majority fraction of the microbiota present in biofouling, it did have a functionally important characteristic such as its ability to actively precipitate calcium carbonate crystals.

Genomic insights into the formation of calcite by *Brevibacterium linens* have shown that this species regulates three carbonic anhydrases in response to Ca^{2+} concentration in the precipitation medium (Zhu et al., 2017). The relative abundance of *Brevibacterium* in the biofouling of the variable salinity scenario ranged from 0.007% to 0.009%. Even though the *Brevibacterium* genus was found at higher values of 0.604% to 2.324% at the constant salinity scenario, none of its strains isolated from biofouling formed under these conditions was found to produce crystals. It could be suggested that salinity conditions (constant or variable) establish a process of microbial adaptation that determines the capacity of certain strains to precipitate with greater or lesser efficiency in different biominerals such as calcite. The ions' concentration in the environment plays an important role in these events, which is previously suggested by other authors (Rivadeneyra et al., 2017).

The precipitation of calcite by *Bacillus licheniformis* is widely known both in natural and engineering systems. In this context, it has been proposed that *Bacillus licheniformis* biomineralization activity can help to raise the strength of cast concrete (Krishnapriya et al., 2015). Nevertheless, the

precipitation of k-struvite and struvite by *Bacillus licheniformis* strains has never been reported. Particularly, in our study, *B. licheniformis* formed k-struvite and struvite under constant and variable salinity conditions, respectively. Furthermore, we must highlight that, in conditions of variable salinity, *B. licheniformis* was the only cultivable microorganism with the ability to form struvite minerals. The other *Bacillus* representative, *Bacillus pumilus*, has been reported for having a strong capacity for struvite crystallization from wastewater (Bai et al., 2017). The relative abundance of *Bacillus* genus in the constant salinity scenario was from 0.015% to 0.029% while, for the case of the variable salinity scenario, ranged from 0.009% to 0.014%.

Following the measurement established by Gonzalez-Martinez et al. (2015), the bacterial microbiota with biomineralization potential risk identified in the high constant salinity scenario was less than 10% of the total microbiota and less that 5% for the high variable salinity scenario in comparison with the microbiota with a biomineralization potential risk encountered at low salinity conditions for pure hybrid MBBR-MBR (around 20% of the total microbiota). In this sense, our studies seemed to suggest that the treatment of effluents with a high concentration of salts (especially with high variable concentrations) decreases the potential risk of formation of biominerals in biofouling processes in MBBR-MBR systems probably as a consequence of a decrease in microbial diversity in response to high environmental osmolarity.

It must be noted that the influent salinity conditions greatly affected the bacterial communities in membrane biofilm of MBBR-MBR systems (Rodriguez-Sanchez et al., 2018b). In this sense, operation at higher salinities would certainly select for other bacterial species in membrane biofilm and, therefore, the bacterial strains with the capability for biomineralization as well as the nature of the biominerals formed would be different. The evaluation of membrane biofouling in two hybrid MBBR-MBR systems subjected to different influent salinity conditions (constant at 3.6 g L^{-1} NaCl electric conductivity and tidal-like variational with a peak of 3.6 g L^{-1} NaCl) showed clear differences and

thus the effect of the salinity conditions was demonstrated. The biofouling bacterial community had lower evenness and diversity under the variable salinity conditions, which is shown by α-diversity analysis. The variable salinity conditions also caused a greater similarity between mixed liquor and biofouling biomass than for the constant salinity scenario, which is observed by β-diversity analysis. The higher pressure of selection exerted by variable salinity conditions over constant salinity conditions were also demonstrated by ordination analysis based on Bray-Curtis distances. The bacterial community structure showed that *Rhodanobacter*, *Ottowia*, *Dyella*, *Mycobacterium*, and *Nitrobacter* were consistently found at high relative abundance across both salinity scenarios. Cultivation of bacterial strains with a capacity for calcium carbonate formation revealed that calcite precipitated for biomass adapted to both constant and tidal-like variable conditions, but, in the medium designed for phosphate precipitation, differences were found with mineralization of K-struvite and struvite for the constant and variable salinity scenarios, respectively. Only a few bacterial strains were identified as mineral-forming microorganisms and were related to *Citrobacter freundii*, *Bacillus pumilus*, *Bacillus licheniformis*, and *Brevibacterium linens*. The results obtained demonstrated that differences in salinity conditions affected the bacterial assemblage and biomineralization characteristics of the membrane biofouling.

Supplementary Materials: The following are available online at http://www.mdpi.com/2073-4441/10/9/1133/ s1, Table S1: Ecological coverage of massive parallel sequencing analyses, Table S2: α-diversity of massive parallel sequencing samples, Table S3: Best hits against the NCBI database for the 16S rRNA genes of isolated strains with high biomineralization capacity, Figure S1: Schematic representation of the hybrid MBBR-MBR systems, Figure S2: Heat map showing the results of the SIMPER analyses differentiating the phylotypes that contributed to >1% dissimilarity between the fixed biofilm and mixed liquor samples for the constant and variable salinity scenarios.

Author Contributions: Conceptualization, J.G.L. and J.M.P. Methodology, J.G.L. and J.M.P. Software, A.R.S. Validation, J.G.L., J.M.P. and A.R.S. Formal Analysis, A.R.S., B.M.P., M.H.M. and D.M.R. Investigation, A.R.S., B.M.P., M.H.M. and D.M.R. Resources, A.R.S., B.M.P., M.H.M. and D.M.R. Data Curation, A.R.S., B.M.P., M.H.M. and D.M.R. Writing—Original Draft Preparation, A.R.S. Writing—Review & Editing, J.G.L., J.M.P. and A.G.M. Visualization, M.A.R. Supervision, J.G.L. and J.M.P. Project Administration, J.G.L. and J.M.P. Funding Acquisition, J.G.L. and J.M.P.

Funding: This study was funded by the project CTM2013-48154-P and grant BES-2014-067852 from the Ministry of Economy and Competitivity of Spain.

Acknowledgments: The authors would like to acknowledge the support given by the Institute of Water Research, the Department of Civil Engineering, the Department of Microbiology and the Department of Mineralogy and Petrology with all from the University of Granada. Additionally, they would like to acknowledge the economic support given by the Government of Spain and the Ministry of Economy and Competitivity under the funding project CTM2013-48154-P and grant BES-2014-067852.

Conflicts of Interest: The authors declare no conflict of interest.

References

Aqeel H, Basuvaraj M, Hall M, Neufeld JD, Liss SN (2016) Microbial dynamics and properties of aerobic granules developed in a laboratory-scale sequencing batch reactor with an intermediate filamentous bulking stage. Appl Microbiol Biotechnol 100: 447–460.

Bai Y, Guo X, Li Y, Huang T (2017) Experimental and visual research on the microbial induced carbonate precipitation by Pseudomonas aeruginosa. AMB Express

Barwell LJ, Isaac NJB, Kunin WE (2015) Measuring β-diversity with species abundance data. J. Anim Ecol 84: 1112–1122.4

Busquets A, Fornós JJ, Zafra F, Lalucat J, Merino A (2014) Microbial communities in a coastal cave: Cova des Pas de Vallgornera (Mallorca, Western Mediterranean). Int J Speleol 43: 205–216.

Cortés-Lorenzo C, González-Martínez A, Smidt H, González-López J, Rodelas B (2016) Influence of salinity on fungal communities in a submerged fixed bed bioreactor for wastewater treatment. Chem Eng J 285: 562–572.

Dhami NK, Reddy MS, Mukherjee A (2013) Biomineralization of calcium carbonates and their engineered applications: A review. Front Microbiol 4

Di Trapani D, Di Bella G, Mannina G, Torregrossa M, Viviani G (2014) Comparison between moving bed-membrane bioreactor (MB-MBR) and membrane bioreactor (MBR) systems: Influence of wastewater salinity variation. Bioresour Technol 162: 60–69.

Edgar RC, Haas BJ, Clemente JC, Quince C, Knight R (2011) UCHIME improves sensitivity and speed of chimera detection. Bioinformatics 27: 2194–2200.

Gonzalez-Martinez A, Leyva-Díaz JC, Rodriguez-Sanchez A, Muñoz-Palazon B, Rivadeneyra A, Poyatos JM, Rivadeneyra MA, Martinez-Toledo MV (2015) Isolation and metagenomic characterization of bacteria associated with calcium carbonate and struvite precipitation in a pure moving bed biofilm reactor-membrane bioreactor. Biofouling 31: 333–348.

Gonzalez-Martinez A, Rodriguez-Sanchez A, Lotti T, Garcia-Ruiz M-J, Osorio F, Gonzalez-Lopez J, van Loosdrecht MCM (2016a) Comparison of bacterial communities of conventional and A-stage activated sludge systems. Sci Rep 6: 18786.

Gonzalez-Martinez A, Garcia-Ruiz MJ, Rodriguez-Sanchez A, Osorio F, Gonzalez-Lopez J (2016b) Archaeal and bacterial community dynamics and bioprocess performance of a bench-scale two-stage anaerobic digester. Appl Microbiol Biotechnol 100: 6013–6033.

Gonzalez-Martinez A, Rodriguez-Sanchez A, Rivadeneyra MA, Rivadeneyra A, Martin-Ramos D, Vahala R, Gonzalez-Lopez J (2017) 16S rRNA gene-based characterization of bacteria potentially associated with phosphate and carbonate precipitation from a granular autotrophic nitrogen removal bioreactor. Appl Microbiol Biotechnol 101: 817–829.

Guo J, Xia S, Wang R, Zhao J (2008) Study on membrane fouling of submerged membrane bioreactor in treating bathing wastewater. J Environ Sci 20, 1158–1167.

Guo W, Ma H, Li F, Jin Z, Li J, Ma F, Wang C (2013) Citrobacter sp. strain GW-M mediates the coexistence of carbonate minerals with various morphologies. Geomicrobiol J 30: 749–757.

Hammer Ø, Harper DAT (2007) Palaeontological Data Analysis; Wiley: Hoboken, NJ, USA

Huse SM, Welch DM, Morrison HG, Sogin ML (2010) Ironing out the wrinkles in the rare biosphere through improved OTU clustering. Environ Microbiol 12: 1889–1898.

Jacob JH, Irshaid FI (2012) Biochemical and molecular taxonomy of a mild halophilic strain of citrobacter isolated from hypersaline environment. Res J Microbiol 7: 219–226.

Krishnapriya S, Venkatesh Babu DL, Arulra GP (2015) Isolation and identification of bacteria to improve the strength of concrete. Microbiol Res 174: 48–55.

Leyva-Diaz JC, Calderon K, Rodriguez FA, Gonzalez-Lopez J, Hontoria E, Poyatos JM (2013) Comparative kinetic study between moving bed biofilm reactor-membrane bioreactor and membrane bioreactor systems and their influence on organic matter and nutrients removal. Biochem Eng J 77: 28–40.

Leyva-Díaz JC, Martín-Pascual J, Muñío MM, González-López J, Hontoria E, Poyatos JM (2014) Comparative kinetics of hybrid and pure moving bed reactor-membrane bioreactors. Ecol Eng 70: 227–234.

Leyva-Diaz JC, Gonzalez-Martinez A, Gonzalez-Lopez J, Muñio MM, Poyatos JM (2015a) Kinetic modeling and microbiological study of two-step nitrification in a membrane bioreactor and hybrid moving bed biofilm reactor-membrane bioreactor for wastewater treatment. Chem Eng J 259, 692–702.

Leyva-Diaz JC, Lopez-Lopez C, Martin-Pascual J, Muñio MM, Poyatos JM (2015b) Kinetic study of the combined processes of a membrane bioreactor and a hybrid moving bed biofilm reactor-membrane bioreactor with advanced oxidation processes as a post-treatment stage for wastewater treatment. Chem Eng Process 91, 57–66.

Leyva-Diaz JC, Gonzalez-Martinez A, Muñio MM, Poyatos JM (2015c) Two-step nitrification in a pure moving bed biofilm reactor-membrane bioreactor for wastewater treatment: Nitrifying and denitrifying microbial populations and kinetic modeling. Appl Microbiol Biotechnol 99: 10333–10343.

Lim S, Kim S, Yeon K, Sang B, Chun J, Lee C (2012) Correlation between microbial community structure and biofouling in a laboratory scale membrane bioreactor with synthetic wastewater. Desalination 287: 209–215.

Liu T, Mao Y, Shi Y, Quan X (2017) Start-up and bacterial community compositions of partial nitrification in moving bed biofilm reactor. Appl Microbiol Biotechnol 101: 2563–2574.

Martín-Navarro JA, Petkov-Stoyanov V, Gutiérrez-Sánchez MJ, Gordo-Flores ME (2015) Struvite urolithiasis with Corynebacterium urealyticum infection: A case report. Nefrologia 35: 410–417.

Radu AI, Bergwerff L, van Loosdrecht MCM, Picioreanu C (2015) Combined biofouling and scaling in membrane feed channels: A new modeling approach. Biofouling 31: 83–100.

Rao A, Cölfen H (2016) Mineralization and non-ideality: On nature's foundry. Biophys Rev 8: 309–329.

Rivadeneyra MA, Martin-Algarra A, Sanchez-Roman M, Sanchez-Navas A, Martin-Ramos JD (2010) Amorphous Ca-phosphate precursors for Ca-carbonate biominerals mediated by Chromohalobacter marismortui. ISME J 4: 922–932.

Rivadeneyra Torres A, Martinez-Toledo MV, Gonzalez-Martinez A, Gonzalez-Lopez J, Martín-Ramos D, Rivadeneyra MA (2013) Precipitation of carbonates by bacteria isolated from wastewater samples collected in a conventional wastewater treatment plant. Int J Environ Sci Technol 10: 141–150.

Rivadeneyra A, Gonzalez-Martinez A, Gonzalez-Lopez J, Martin-Ramos D, Martinez-Toledo MV, Rivadeneyra MA (2014) Precipitation of phosphate minerals by microorganisms isolated from a fixed-biofilm reactor used for the treatment of domestic wastewater. Int J Environ Res Public Health 11: 3689–3704.

Rivadeneyra A, Gonzalez-Martinez A, Portela GR, Martin-Ramos D, Gonzalez-Lopez J, Rivadeneyra MA (2017) Biomineralisation of carbonate and sulphate by the halophilic bacterium Halomonas maura at different manganese concentrations. Extremophiles 21: 1049–1056.

Rodriguez-R LM, Konstantinidis KT (2014a) Nonpareil: A redundancy-based approach to assess the level of coverage in metagenomic datasets. Bioinformatics 30: 629–635.

Rodriguez-R LM, Konstantinidis KT (2014b) Estimating coverage in metagenomic data sets and why it matters. ISME J 8: 2349–2351.

Rodriguez-Sanchez A, Leyva-Diaz JC, Gonzalez-Lopez J, Poyatos JM (2017a) Performance and kinetics of membrane and hybrid moving bed biofilm-membrane bioreactors treating salinity wastewater. AIChE J 63: 3329–3342.

Rodriguez-Sanchez A, Leyva-Diaz JC, Gonzalez-Martinez A, Poyatos JM (2017b) Linkage of microbial kinetics and bacterial community structure of MBR and hybrid MBBR-MBR systems to treat salinity-amended urban wastewater. Biotechnol Prog 33: 1483–1495.

Rodriguez-Sanchez A, Leyva-Diaz JC, Gonzalez-Lopez J, Poyatos JM (2018a) Membrane bioreactor and hybrid moving bed biofilm reactor-membrane bioreactor for the treatment of variable salinity wastewater: Influence of biomass concentration and hydraulic retention time. Chem Eng J 336: 102–111.

Rodriguez-Sanchez A, Leyva-Diaz JC, Poyatos JM, Gonzalez-Lopez J (2018b) Influent salinity conditions affect the bacterial communities of biofouling in hybrid MBBR-MBR systems. J Water Process Eng In press

Rogers CJ, ten Broek CMA, Hodson B, Whitehead MP, Schmerer WM, Sutton R (2014) Identification of crystals forming on porcine articular cartilage: A new method for the estimation of the postmortem interval. J Forensic Sci 59: 1575–1582.

Schloss PD, Westcott SL, Ryabin T, Hall JR, Hartmann M, Hollister EB, Lesniewski RA, Oakley BB, Parks DH, Robinson CJ, et al. (2009) Introducing mothur: Open-source, platform-independent, community-supported software for describing and comparing microbial communities. Appl Environ Microbiol 75: 7537–7541.

Silva-Castro GA, Uad I, Gonzalez-Martinez A, Rivadeneyra A, Gonzalez-Lopez J, Rivadeneyra MA (2015) Bioprecipitation of calcium carbonate crystals by bacteria isolated from saline environments grown in culture media amended with seawater and real brine. BioMed Res. Int.

Silva-Castro GA, Uad I, Rivadeneyra A, Vilchez JA, Martin-Ramos D, Gonzalez-Lopez J, Rivadeneyra MA (2013) Carbonate precipitation of bacterial strains isolated from sediments and seawater: Formation mechanisms. Geomicrobiol J 30: 840–850.

Soares A, Veesam M, Simoes F, Wood E, Parsons SA, Stephenson T (2014) Bio-Struvite: A new route to recover phosphorus from wastewater. Clean Soil Air Water 42: 994–997.

Unno T (2015) Bioinformatic suggestions on MiSeq-based microbial community analysis. J Microbiol Biotechnol 25: 765–770.

Zhu Y, Ma N, Jin W, Wu S, Sun C (2017) Genomic and transcriptomic insights into calcium carbonate biomineralization by marine actinobacterium Brevibacterium linens BS258. Front. Microbiol. 8.

Chapter 7

Maximum influent salinity affects the diversity of mineral-precipitation-mediating bacterial communities in membrane biofilm of hybrid moving bed biofilm reactor-membrane bioreactor

This chapter has been published in its current form in Water, Air & Soil Pollution. The complete citation is the following:

Alejandro Rodríguez-Sanchez, Barbara Muñoz-Palazon, Miguel Hurtado-Martinez, Maria Angustias Rivadeneyra, Jose Manuel Poyatos, Jesus Gonzalez-Lopez. 2018. Maximum influent salinity affects the diversity of mineral-precipitation-mediating bacterial communities in membrane biofilm of hybrid moving bed biofilm reactor-membrane bioreactor. Water, Air & Soil Pollution. 229:342. doi: 10.1007/s11270-018-4020-x

Abstract

Two hybrid moving bed biofilm reactor-membrane bioreactors were used for the treatment of variable-salinity influent wastewater with maximums of 4.5 and 8.5 mS cm^{-1} electric conductivity. Operational conditions of the bioreactors were 6 h hydraulic retention time and 2500 mg L^{-1} total solids. The membrane operated in a cycle of 9 min draw-1 min backwash and at 23.6 L h^{-1} m^{-2} flux rate. Membrane biofilm was collected from both systems and cultured in growth media for precipitation of carbonate and phosphate minerals, yielding only *Bacillus stratosphericus* for the 4.5 mS cm^{-1} scenario and *Bacillus stratosphericus*, *Bacillus toyonensis*, *Microbacterium esteraromaticum*, *Comamonas testosteroni*, and *Janibacter meloni* for the 8.5 mS cm^{-1} scenario. Scanning electron microscopy and X-ray analysis showed similarities in morphology and composition for the carbonate crystals from both salinity conditions and differences for the phosphate minerals. Study of the bacterial community of membrane biofilm and mixed liquor showed close similarities between them for the same salinity conditions, with both dominated by genera *Rhodanobacter*, *Chujaibacter*, and *Thermomonas*.

1. Introduction

For the purpose of wastewater treatment, one of the best available technologies is the membrane bioreactor (MBR) (Rodriguez-Sanchez et al., 2017a). The MBR joins the biological treatment with a very efficient separation of solids and water that allows for high performances in the removal of solids and pathogens, operation at higher solids concentrations, low sludge production, complete retention of biomass and higher solids retention times in operation, with the drawback of higher energy costs in operation (Rodriguez-Sanchez et al., 2017b).

In spite of their numerous advantages, the MBR systems have to face a major operational problem caused by the clogging of membrane pores, nominated as fouling, which occurs more rapidly at higher suspended solids concentrations during operation. This fouling can be caused by materials of inorganic origin or organic origin (Rodriguez-Sanchez et al., 2018a). To alleviate the fouling problems of MBR systems, the combined system of the moving bed biofilm reactor-membrane bioreactor (MBBR-MBR) has been developed. In this context, the addition of carrier media to the bioreactor allows for the growth of attached biomass, which increases the total solids concentrations in the system without raising the suspended solids, allowing for operation with less risk of fouling. Nevertheless, MBBR-MBR systems still have to face fouling problems (Gonzalez-Martinez et al., 2015).

A major cause of fouling is the colonization of microbial communities of the membrane surface, leading to biofouling, which is mainly caused by the extracellular polymeric substances and the soluble microbial products they produce (Gao et al., 2014). Therefore, it has been proposed that the characterization of the microbial communities in the membrane biofilm is of vital importance in order to understand, predict, and control the process of biofouling (Rodriguez-Sanchez et al., 2018b). Moreover, the serious risk that minerals whose precipitation is caused by bacterial activity have been highlighted before (Gonzalez-Martinez et al., 2017).

It has been proven that bacteria play a role in the formation of some minerals in different natural and engineered environments, and that this is not restricted to a certain taxonomy but widely distributed across many members of the domain *Bacteria* with different phylogenies (Rivadeneyra et al., 2017). On the other hand, it has been proposed that biomineralization occurs due to changes in the immediate environment of the microorganism, such as changes in pH and ion concentrations, and therefore, it has been proposed that there is a specific association between microbial taxonomy, the environment where it grows, and the mineral formed (Gonzalez-Martinez et al., 2016). In wastewater treatment systems, the most common biominerals found are of carbonate and phosphate nature. Carbonate precipitation in wastewater has been regarded as an effective and economic feasible solution for the sequestration of CO_2 in stable forms, such as calcium carbonate, thus reducing the impact of CO_2 over the Earth's biosphere (Uad et al., 2014). On the other hand, phosphate mineral struvite has been associated with operational problems in wastewater treatment systems as far as to develop specific reactors for its precipitation and safeguard the process downstream (Rivadeneyra et al., 2014).

Wastewater can raise its salinity levels by several ways, such as addition of salt for snow-melting activities, addition of salt for cooking, use of seawater in toilets for flushing or by the intrusion of seawater in wastewater treatment plants of coastal areas (Cortes-Lorenzo et al., 2012). Salinity in wastewater can have a dramatic effect over the performance and the bacterial community structure of bioprocesses. It has been proposed that increasing salinity affects microbial metabolism, causes the accumulation of toxic metabolic intermediates, and that increases cell membrane osmotic pressure leading to higher cell death rates (Bassin et al., 2012; Castillo-Carvajal et al., 2014; Cortés-Lorenzo et al., 2016). Moreover, previous research has found these effects precisely in MBR and MBBR-MBR systems (Rodriguez-Sanchez et al., 2017a; 2017b; 2018a). Salinity conditions in MBR and

MBBR-MBR systems affect their microbial communities and can successively affect the biofouling of the membrane process within them, a phenomenon that has been unexplored to date.

The MBBR-MBR systems operated under a membrane flux rate of 23.6 L h^{-1} m^{-2} in a 9-min draw-1-min backwash cycle for the membrane, and with a hydraulic retention time of 6 h and 2500 mg L^{-1} total solids. The analysis of the biomineralization phenomenon in the membrane biofilms of systems operating under tidal salinity variations with maximum influent salinities of 4.5 and 8.5 mS cm^{-1} was done. Bacterial strains with capacity to mediate mineralization of carbonates and phosphates were identified by culture-dependent techniques. The nature of the minerals formed was evaluated by scanning electron microscopy and X-ray analysis. Moreover, the whole bacterial community in the bioreactors operating under such conditions was observed by culture-independent techniques such as next-generation sequencing, with emphasis on the quantification of strains with mineralization capacity.

2. Materials and Methods

2.1 Bioreactor Configuration and Operation

The bioreactor configuration used in the study was a hybrid MBBR-MBR system (Fig. 1). The bioreactor had four chambers of 6 L operational volume and a membrane tank of 4.32 L operational volume. The first, third, and fourth chambers were filled with carriers in 35% of their volumes. The carrier used was the K1 carrier (AnoxKaldnes AS, Norway) (density of 0.92–0.96 g cm^{-3}) accounting for a total of 111.7 m^2 m^{-3} in the whole bioreactor. Fine bubble diffusers AFD 270 (ECOTEC SA, Spain) and air compressors ACO-500 (Hailea, China) were used to aerate the first, third, and fourth chambers, with input air entering at the bottom of the chamber, assuring for a complete mix of the volume of the chamber. The aeration of the chambers was measured by rotameters 2100 Model

(Tecfluid SA, Spain) and regulated using a valve. The second chamber was anaerobic and completely mixed by the means of a mechanical stirrer Multi Mixer MM-1000 (Biosan Laboratories Inc., USA). Coarse bubble diffusers CAP 3 (ECOTEC SA, Spain) and air compressors ACO-500 (Hailea, China) were used to aerate and completely mix the membrane tank. The aeration of the membrane tank was measured by rotameters 2100 Model (Tecfluid SA, Spain) and regulated using a valve.

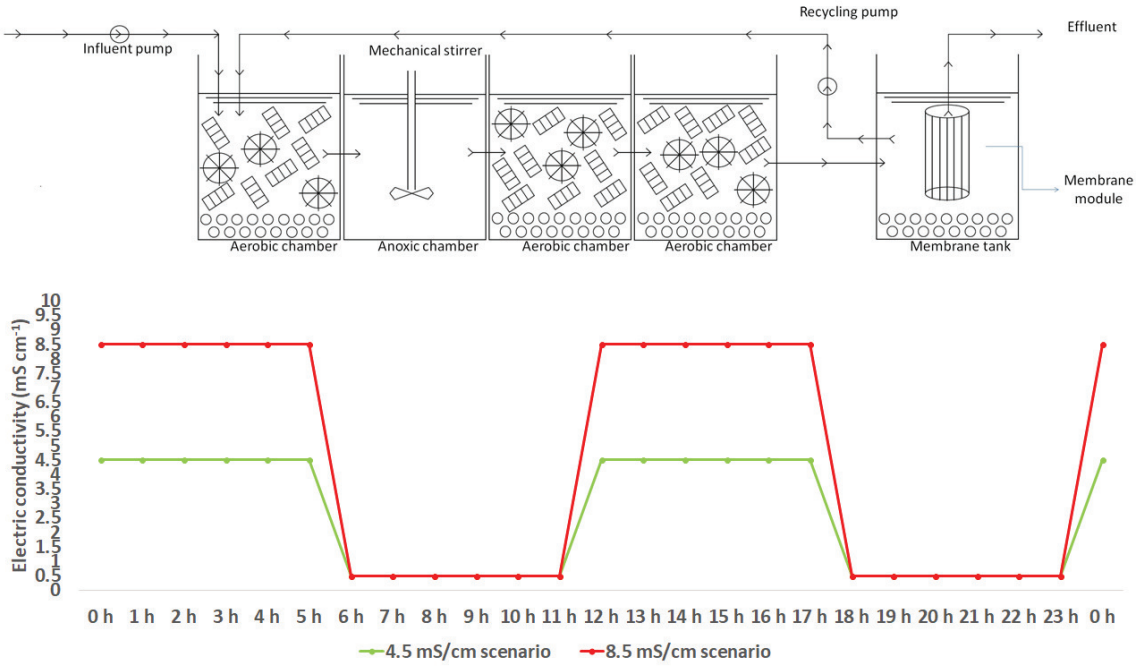

Figure 1 – Schematic of the MBBR-MBR system and plot of influent salinity cycles used in the study

Inside the membrane tanks, a module of 0.04 µm pore diameter hollow fibers of polyvinylidene fluoride with a core reinforcement of polyester was displaced vertically and continuously submerged. The total membrane surface area per bioreactor was of 0.2 m^2.

The influent flow was pumped, using a WatsonMarlow peristaltic pump (Watson-Marlow Pumps Group, USA), to the first chamber and forced to pass through the second, third, and fourth, then discharged into the membrane tank. From the membrane tank, a recycling flow of 500% the influent flow was imposed using a Watson-Marlow peristaltic pump. Also, the effluent was withdrawn by the

means of pumping, using a Watson-Marlow peristaltic pump through the membrane module. The pump withdrawing the effluent operated in a 10-min cycle consisting of 9 min effluent withdrawal followed by 1 min backwash.

The influent wastewater was a salinity-amended urban wastewater, pumped into the bioreactors from a mixing tank. The amendment was achieved by automatic addition of tap water with NaCl diluted resulting in 50 mS cm^{-1} electric conductivity, stored in the NaCl tap water tank, to the regular urban wastewater, stored in the urban wastewater tank. The automatic addition of NaCl tap water to the urban wastewater in the mixing tank was done by a TOPAX LF1 conductivity module (LutzJesco GmbH, Germany), which continuously monitored the electric conductivity of the influent wastewater by continuous measuring using a conductivimeter. Two Watson-Marlow peristaltic pumps connected to the conductivity module allowed to automatically increase the proportion of urban wastewater and NaCl tap water in the influent wastewater depending on the specified salinity conditions in the influent. Two different salinity scenarios for operation were chosen, both resembling tidal-like salinity variations: (a) cycle of 6 h maximum electric conductivity of 4.5 mS cm^{-1} (around 2.4 g L^{-}1NaCl) followed by 6 h of regular urban wastewater electric conductivity (around 0.5 g L^{-1} NaCl); (b) cycle of 6 h maximum electric conductivity of 8.5 mS cm^{-1} (around 4.8 g L^{-1}NaCl) followed by 6 h of regular urban wastewater electric conductivity (around 0.5 g L^{-1} NaCl). A schematic of the daily cycle of operation is given in Fig. 1.

The bioreactors were operated controlling the hydraulic retention time to 6 h and the total solids to 2500 mg L^{-1}. The biofouling on the membrane was controlled by periodical cleaning of the membrane to avoid transmembrane pressures higher than 0.5 bar. The total solids in the bioreactor were purged in order to maintain them at 2500 mg L^{-1} concentration. In this sense, the calculated solids retention time for the bioreactors was of 22.32 days.

2.2 Sampling of Biomass, DNA Extraction, and Next-Generation Sequencing

When the bioreactors were operating under steady-state conditions, biomass samples were collected from the membrane tank. Two sampling dates were considered for each bioreactor, separated in time by 2 weeks of operation under the same conditions. The collection of samples was done from the mixed liquor in the membrane tank and from the membrane biofilm following Gonzalez-Martinez et al. (2014). To collect the mixed liquor biomass, 100 mL was taken from the completely mixed membrane tank. For the membrane biofilm, a part of the membrane was sonicated at room temperature for 2 min at 40 kHz in a bath sonicator (Ultrasonic bath, Selecta, Barcelona, Spain), then placed in an orbital shaker at 155 rpm for 1 h. In parallel, suspensions of mixed liquor and membrane biofilm were centrifuged at 3500 rpm (821.73 g) during 10 min at room temperature, then discarding the supernatant and subjecting the biomass to DNA extraction process.

The DNA extraction was done using the FastDNA SPIN Kit for Soil (MP Biomedicals, Solon, OH, USA) and the FastPrep apparatus, following the instructions given by the manufacturer. DNA was extracted from each of the biomass samples in five replicates, then the five replicates were merged into the same DNA pool, as previously done (Gonzalez-Martinez et al., 2016). The extracted DNA pools were kept at – 20 °C and sent to RTLGenomics laboratory (Lubbock, TX, USA) in order to proceed with the next-generation sequencing procedure using the Illumina MiSeq equipment and the Illumina MiSeq Reagents Kit v3. The primer pair 28F (5'-GAGTTTGATCNTGGCTCAG-3')-519R (5'-GTNTTACNGCGGCKGCTG-3') (Rodriguez-Sanchez et al., 2018a; 2018b) was used for the amplification of the hypervariable regions V1-V2-V3 of the 16S rRNA gene of the domain *Bacteria*. The PCR conditions for the amplification of such region were preheating at 94 °C during 120 s; then 32 cycles of 94 °C for 30 s, 40 °C for 40 s, and 72 °C for 60 s; a final elongation at 72 °C for 300 s.

2.3 Ecological Data from the Biological Samples

The raw data provided by the Illumina MiSeq sequencing was treated to yield valuable ecological data of the biological samples. Mainly mothur v1.34.4 (Schloss et al., 2009) was used for the treatment of such data. In the first place, the paired-end reads generated by the Illumina MiSeq equipment were aligned against each other using Needleman conditions to create contigs, avoiding the generation of ambiguous bases in the overlap region due to differences in overlapping nucleotides Phred score values (Unno, 2015). Then, the contigs were screened to eliminate those with > 0 ambiguous bases and > 8 homopolymers. The remaining contigs were aligned against the SiLVA SEED v132 database using the k-nearest neighbor algorithm with k-mer search methodology using a k-mer size of 8 bp and under Needleman conditions. The contigs that failed to start and end at the positions of the primers of choice were discarded as mis-target errors. The remanent contigs were then preclustered to eliminate sequencing noise, following a preclustering threshold of 1 bp difference for each 100 bp in the sequence (Huse et al., 2010). The contigs were then checked for their chimeric nature using VSEARCH algorithm (Rognes et al., 2016) implemented in mothur software. Non-chimeric sequences were then classified against the SiLVA nr v132 database using the k-nearest neighbor algorithm with k-mer search methodology using a k-mer size of 8 bp under a taxonomic cutoff of 80% in order to remove sequences that could not affiliate to the domain *Bacteria*. After removal of cross-domain contamination, the highquality contigs remaining were used to construct OTUs.

Construction of OTUs was done using a cutoff of 97% similarity, using the abundance-based greedy algorithm implemented in VSEARCH (Westcott and Schloss, 2015; Schloss, 2016), taking into consideration the Matthew's correlation coefficient as metric of clusterization quality. A taxonomic consensus for all sequences within an OTU was calculated, thus assigning a taxonomy to each OTU based on SiLVA nr v132. The taxonomic consensus of each OTU was then used for the creation of the taxonomic

consensus of the biological sample. Taxonomic consensus of sequences within each OTU and of OTUs within a sample was calculated using a cutoff of 80%. The taxonomic consensus of OTUs within all samples was considered as relevant ecological data.

2.4 Analysis of Similarity of Bacterial Community Structures

The analysis of similarity of the bacterial community structures was done in three different ways: PERMANOVA analyses (Weiss et al., 2017), singular value decomposition of centered log-ratio-transformed OTU distribution (Bian et al., 2017), and Dirichlet Multinomial Mixture model analysis (Holmes et al., 2012). The PERMANOVA analyses were computed based on Bray-Curtis distance over the taxonomic consensus of OTU distribution and under 9999 bootstrap replications using PASTv3. The singular value decomposition analyses used a transformation of the taxonomic consensus of OTU distribution was done by zero-value correction through a Bayesian multiplicative replacement method using zCompositions package implemented in R software followed by a centered log-ratio calculation using robComposition package implemented in R software. The singular value decomposition computation was done over such transformed data. The calculation of Dirichlet multinomial mixture models was done by partitioning the taxonomic consensus of OTUs distribution into metacommunities with minimum partition of 2 and maximum partition of 8, assessing the most appropriate partitioning as the minimum value reported by Laplace approximation calculations for each partitioning model.

2.5 Diversity Indices and Detection of Sensitive OTUs and the Correlations Between Them

The α-diversity indices of Shannon-Wiener (H) and Simpson (1D) were calculated for each of the biological samples taking into account the consensus taxonomy OTU distribution. The sensitivity of

the OTUs among the different samples was observed by the means of expected effect size and SIMPER analysis. The expected effect size used the OTU distribution was done over the zero-corrected and centered log-ration transformed data obtained from the posterior distribution of 128 Monte Carlo simulations drawn from a Dirichlet distribution, computed through the ALDEx2 package implemented in R (Bian et al., 2017). The SIMPER analyses were done over the OTU distribution using PASTv3 software. The sensitivity of OTUs in both cases was assessed for the variables of maximum influent salinity (4.5 vs 8.5 mS cm^{-1}) and biomass type (membrane biofilm vs mixed liquor).

2.6 Culture and Isolation of Mineral-Formation-Mediating Bacteria

The biomass samples from the membrane biofilm were used as inoculum for the culture of bacterial strains with capacity to mediate the formation of carbonate minerals and phosphate minerals, following previous research in MBBR-MBR systems (Gonzalez-Martinez et al., 2017). This biomass was obtained by sonication of a part of the membrane at room temperature for 2 min at 40 kHz in a bath sonicator (Ultrasonic bath, Selecta, Barcelona, Spain).

The biomass was used as seed for growth in two different media specifically designed for the formation of carbonate minerals (MC) and phosphate minerals (ME). The composition of the two media was as follows: 18 g L^{-1} agar, 10 g L^{-1} yeast extract, 5 g L^{-1} protease peptone, and 1 g L^{-1} glucose, 4 g L^{-1} calcium acetate for the MC medium and 8 g L^{-1} magnesium acetate for ME medium. The media was autoclaved at 112 °C for 20 min avoiding the precipitation of carbonate minerals in the MC medium due to intense heating. The pH of the media was set to 7.0 by addition of 0.1 M KOH. Additional ME liquid medium was done using the following composition: 10 g L^{-1} yeast extract, 5 g L^{-1} protease peptone, and 1 g L^{-1} glucose, 4 g L^{-1} calcium acetate for the MC medium and 8 g L^{-1}

magnesium acetate. The difference between the ME solid and ME liquid media was the presence or absence of agar, respectively.

Samples of membrane biofilm were serially diluted up to 10^{-6}, then 1 mL of concentrations of 10^{-4}, 10^{-5}, and 10^{-6} were used for inoculation of the media by surface-spreading and streaking. Each dilution for each medium had five replicates in total. The liquid ME medium was inoculated with 10^{-4} dilution in a 1%*v*/*v*. These were incubated at 25 °C in the dark and examined every 24 h to check for the apparition of minerals using optical microscopy. Uninoculated media and media inoculated with autoclaved membrane biofilm were used as control.

Colonies detected for relevant biomineralization-mediation capacity were isolated into the respective medium MC or ME in order to obtain a pure culture for further taxonomic identification of their 16S rRNA gene by using Sanger sequencing and the primer pair fD1-rD1, conducted at the University of León, Spain.

2.6 Characterization of Isolated Strains

The 16S rRNA gene of the isolated strains with relevant capacity to mediate mineral formation were used for their taxonomic classification. The strains were classified by BLAST search of highly similar sequences (MegaBLAST) against the nt database of the NCBI. The taxonomic affiliation of the strains was assigned by the first BLAST match with high quality (max score > 2500, e-value ~0, query cover ≥ 98%, identity, ≥ 99%, curated RNA (NR) collection) of a sequence with known species level that was detected in the next-generation sequencing. Strains that did not pass these criteria were discarded as contamination. The remaining sequences were aligned against themselves using CLUSTALW algorithm (Larkin et al., 2007), and the alignment was used to construct a phylogenetic

tree under the neighbor-joining method using the Jukes-Cantor model with a bootstrap test of 1000 replications, developed in MEGA7 (Kumar et al., 2016).

2.8 Extraction of Minerals and Analysis Using Optical Microscopy, Scanning Electron Microscopy, and X-Ray Diffractometry

Optical microscopy was used for the evaluation of mineral formation in the solid media. After a period of 14 days of incubation, the minerals formed in the solid MC medium were extracted by cutting the medium to pieces, submerged in water and boiled to dissolve the agar. The minerals obtained were then washed with distilled water for impurity removal, then let to dry at 37 °C. Accordingly, the minerals from the liquid ME medium were obtained by sedimentation, then washed with distilled water to remove impurities and let to dry at 37 °C.

The obtained minerals were observed by the means of scanning electron microscopy. The samples were carbon-coated and seen by using a high-resolution field emission scanning electron microscope Carl Zeiss, Supra 40 V (Carl Zeiss, Oberlocken, Germany). Samples of interest were also analyzed for their chemical composition using energy-dispersive X-ray (EDX) microanalysis (Aztec 350, Oxford Instruments, Abingdon, UK) and using the AMSCD mineral database.

3. Results and Discussion

3.1 Operation of the MBBR-MBR Systems

Data for the performance of the MBBR-MBR systems is shown in Table 1. From there, it was inferred that the removal performances were substantially different between the bioreactors in terms of organic matter and nitrogen (99.47 vs 91.60% for BOD_5, 81.72 vs 60.72% for COD, 56.09 vs 27.11%

for NH_4^+, 54.29 vs 26.77% for TN for the 4.5 and the 8.5 mS cm^{-1} scenarios, respectively) (Rodriguez-Sanchez et al., 2018b). Based on these results, the MBBR-MBR system working under the 4.5 mS cm^{-1} loading performed better (about 10–30%) in terms of BOD_5 removal and COD removal. In this way, the higher salinity concentrations mildly affected the removal of organic matter in the bioreactors. Also, the 4.5 mS cm^{-1} scenario presented much higher NH_4^+ oxidation and TN removal values (around 200%) than the 8.5 mS cm^{-1} scenario.

Importantly, none of the systems could successfully form attached biomass to the carriers, as confirmed by low biofilm density values (< 50 mg L^{-1}), which demonstrated the low contribution in terms for the total solids as these were controlled at 2500 mg L^{-1}. Therefore, the contribution of the attached biofilm to the MBBR-MBR systems was less than 2% (Rodriguez-Sanchez et al., 2018b). It has been shown that introduction of saline influent in a steady-state MBR system treating regular urban wastewater exerts a high pressure over the attached biofilms of carriers, lowing important amounts in the process (Di Trapani et al., 2014). Moreover, difficulties for the formation of attached biofilm to carriers in MBBR-MBR systems treating constant salinity and variable salinity wastewater has been reported before, and the explanation of the inadequacy of the wastewater microbiota to develop biofilm in the presence of high salt concentrations was given as the reason for the absence of carrier biomass (Rodriguez-Sanchez et al., 2017a; 2017b; 2018a). For the purposes of MBBRMBR engineering, the low attached biofilm concentrations found under saline wastewater conditions had two valuable future implications. First, the MBBR-MBR systems under salinity conditions operated as MBR systems in practice. Second, the presence of carriers did not support higher total solids with reduced suspended solids, which in turn did not protect the membrane against operation at high solids concentrations, which has been claimed as one of the advantages of the MBBR-MBR systems over the MBR systems with respect to prevention of membrane fouling.

According to the results obtained, the implications of the treatment of saline wastewater using MBBR-MBR technologies are of concern from the biofouling point of view. More research should be conducted over the influence that the improvement of attached biofilm over carriers has on the biofouling of MBBR-MBR systems operating under saline effluents.

3.2 Analyses of Similarity of Biological Samples

The analyses of similarity of biological samples based on their consensus taxonomy of OTUs was done by quantitative and qualitative methodologies. For quantitative methodologies, the PERMANOVA analysis discriminating the samples in terms of maximum influent salinity (4.5 and 8.5 mS cm^{-1}) and biomass type (membrane biofilm and mixed liquor) showed statistically significant differences ($p < 0.05$) for the different salinity conditions (Table S1). On the other hand, the biomass type did not have any statistically significant difference ($p > 0.05$). The pairs of samples sharing maximum influent salinity conditions and biomass type did not show any statistically significant difference ($p > 0.05$) as well, suggesting that the whole taxonomic consensus of OTUs between both scenarios and biomass were not that different overall. The other quantitative analyses, the Dirichlet multinomial mixing modelization, suggested that the best partitioning model accounted for 2 partitions (minimum Laplace approximation value), and the model grouped the samples according to maximum influent salinity (Fig. 2), corroborating the results obtained by the PERMANOVA analyses. Moreover, the results of the qualitative analysis of similarity was in accordance with these of the quantitative analyses of similarity, suggesting that the taxonomic consensus of OTUs was more affected by the maximum influent salinity than by the biomass type (Fig. 3).

A

Partitions	Laplace approximation value
1	11723.02
2	11370.32
3	11820.78
4	12384.38
5	13077.41
6	13812.02
7	∞
8	∞

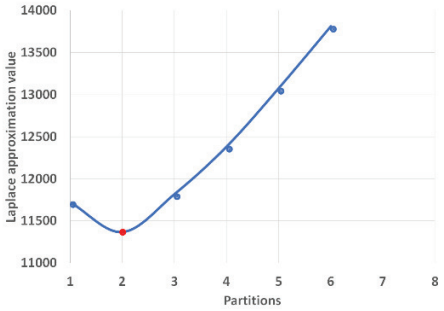

B

Partitions = 2		
Sample	Partition 1	Partition 2
HVFB1		
HVFB2		
HVML1		
HVML2		
LVFB1		
LVFB2		
LVML1		
LVML2		

Figure 2 – Results of the Dirichlet multinomial mixing (A: Laplace's approximation value for partition models; B: grouping of samples for the partitioning models)

The analyses of similarity showed that there was evidence of the strong effect of the influent maximum salinity over the consensus taxonomy of OTUs of both mixed liquor and membrane biofilm in the hybrid MBBR-MBR systems studied. In this sense, the attached biomass and the suspended biomass were similar in terms of consensus taxonomy of OTUs, suggesting that under variable influent salinity, the specialization of biomass did not appear in the attached biomass with respect to the mixed liquor, on the contrary, as reported for hybrid MBBR-MBR systems treating regular-salinity urban wastewater (Leyva-Diaz et al., 2015). Thus, the most important factor for the development of microbial communities in the hybrid MBBR-MBR subjected to influent variable salinities was found to be the maximum influent salinity concentration.

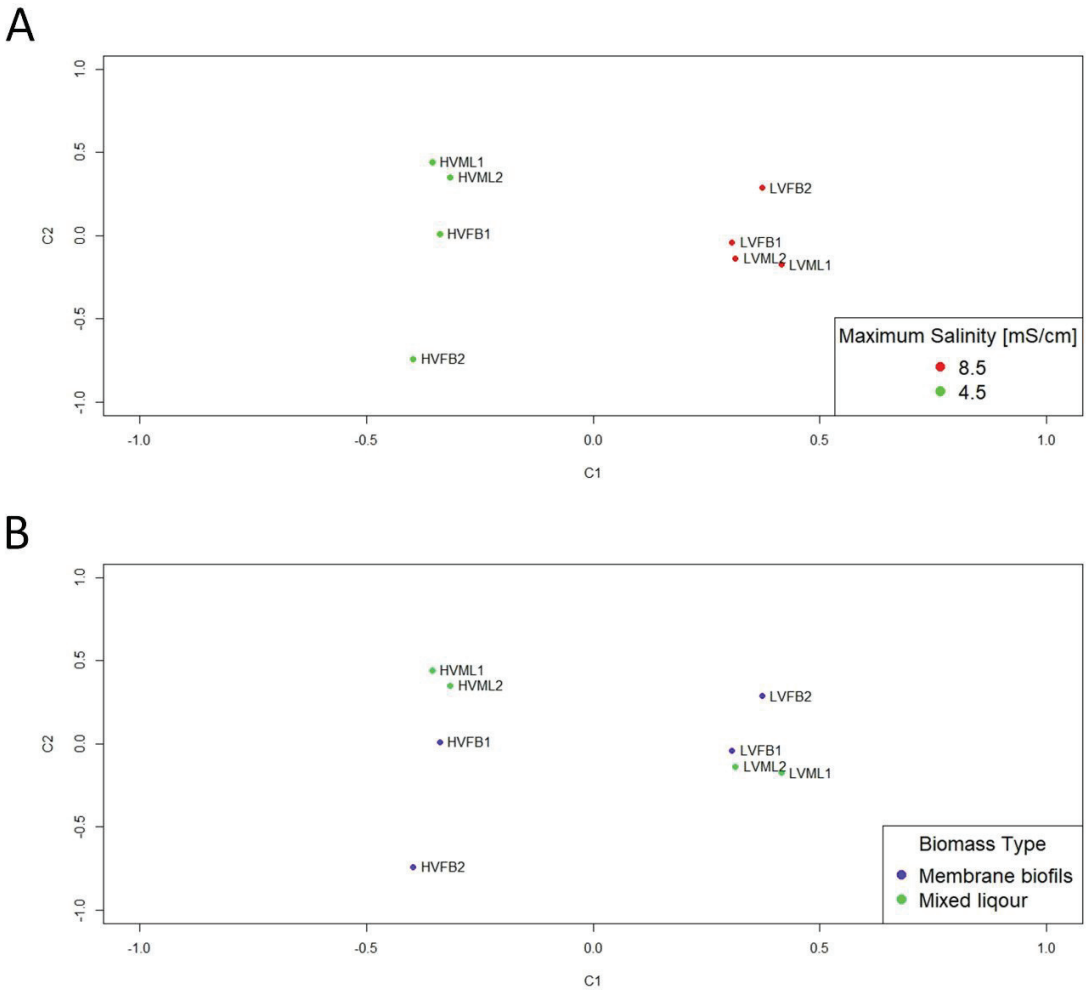

Figure 3 – Singular value decomposition of the bacterial community structure of the MBBR-MBR systems (A: maximum salinity; B: biomas type)

3.3 Ecology of the Biological Samples

The ecology of the 20 dominant consensus taxonomy OTUs in the biological samples studied is shown in Fig. 4. The relative abundance of these consensus taxonomy OTUs as well as their contribution to dissimilarity among groups of samples as determined per SIMPER analyses is presented.

Group	Domain	Phylum	Class	Order	Family	Genus	Relative abundance							Dissimilarity					
							HVFB1	HVFB2	HVML1	HVML2	LVFB1	LVFB2	LVML1	LVML2	Max Salinity	Biomass	HVMB vs HVML	LVMB vs LVML	HVMB vs LVMB	HVML vs LVML
Otu001	Bacteria	Proteobacteria	Gammaproteobacteria	Xanthomonadales	Rhodanobacteraceae	Rhodanobacter														
Otu002	Bacteria	Proteobacteria	Gammaproteobacteria	Xanthomonadales	Rhodanobacteraceae	Chujaibacter														
Otu003	Bacteria	Proteobacteria	Gammaproteobacteria	Xanthomonadales	Rhodanobacteraceae	Rhodanobacteraceae_unclassified														
Otu004	Bacteria	Proteobacteria	Gammaproteobacteria	Xanthomonadales	Xanthomonadaceae	Thermomonas														
Otu005	Bacteria	Proteobacteria	Gammaproteobacteria	Betaproteobacteriales	Burkholderiaceae	Burkholderiaceae_unclassified														
Otu006	Bacteria	Proteobacteria	Gammaproteobacteria	Xanthomonadales	Xanthomonadales_unclassified	Xanthomonadales_unclassified														
Otu007	Bacteria	Bacteroidetes	Bacteroidia	Chitinophagales	Chitinophagaceae	Ferruginibacter														
Otu008	Bacteria	Proteobacteria	Gammaproteobacteria	Betaproteobacteriales	Hydrogenophilaceae	Thiobacillus														
Otu009	Bacteria	Actinobacteria	Actinobacteria	Micrococcales	Microbacteriaceae	Microbacteriaceae_unclassified														
Otu010	Bacteria	Actinobacteria	Actinobacteria	Corynebacteriales	Mycobacteriaceae	Mycobacterium														
Otu011	Bacteria	Proteobacteria	Gammaproteobacteria	Gammaproteobacteria_unclassified	Gammaproteobacteria_unclassified	Gammaproteobacteria_unclassified														
Otu012	Bacteria	Proteobacteria	Alphaproteobacteria	Rhizobiales	Xanthobacteraceae	Xanthobacteraceae_unclassified														
Otu013	Bacteria	Firmicutes	Clostridia	Clostridiales	Clostridiaceae_1	Clostridium_sensu_stricto_1														
Otu014	Bacteria	Proteobacteria	Alphaproteobacteria	Parvibaculales	Parvibaculaceae	Parvibaculum														
Otu015	Bacteria	Gemmatimonadetes	Gemmatimonadetes	Gemmatimonadales	Gemmatimonadaceae	uncultured														
Otu016	Bacteria	Proteobacteria	Alphaproteobacteria	Acetobacterales	Acetobacteraceae	Acetobacteraceae_unclassified														
Otu017	Bacteria	Proteobacteria	Alphaproteobacteria	Alphaproteobacteria_unclassified	Alphaproteobacteria_unclassified	Alphaproteobacteria_unclassified														
Otu018	Bacteria	Proteobacteria	Alphaproteobacteria	Rhizobiales	Rhizobiaceae	Rhizobiaceae_unclassified														
Otu019	Bacteria	Firmicutes	Clostridia	Clostridiales	Peptostreptococcaceae	Peptostreptococcaceae_unclassified														
Otu020	Bacteria	Proteobacteria	Gammaproteobacteria	Xanthomonadales	Rhodanobacteraceae	Dokdonella														

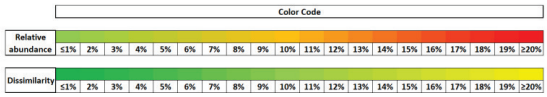

Figure 4 – Heat map representing the relative abundance and the contribution to dissimilarity of the top 20 represented phylotypes in the MBBR-MBR systems under both salinity conditions tested

Interestingly, the dominant genus found in all samples was related to *Rhodanobacter*. This genus had a mean relative abundance for the 4.5 mS cm^{-1} scenario than for the 8.5 mS cm^{-1} scenario, as calculated by Dirichlet multinomial mixing modelization—29.42% mean (26.26–32.96% as 95% confidence interval) for 8.5 mS cm^{-1}, 46.04% mean (41.58–50.97% as 95%

confidence interval) for 4.5 mS cm^{-1} (Table S2).

Rhodanobacter genus has been reported as a dominant phylotypes in MBR and hybrid MBBR-MBR systems treating saline wastewater under constant and variable conditions (Rodriguez-Sanchez et al., 2017b; 2018a). It has been reported that *Rhodanobacter* was positively correlated with heterotrophic and nitrification kinetics of these bioreactors, suggesting possible roles in organic matter removal, nitrification, and denitrification. Moreover, *Rhodanobacter* seemed to compete with autotrophic nitrifier *Nitrobacter*, which aims to consider its possible role as nitrite oxidizer in membrane technologies treating saline wastewater (Rodriguez-Sanchez et al., 2017b; 2018a).

Another *Rhodanobacteraceae* family member, affiliated to genus *Chujaibacter*, was found to be important for the 4.5 mS cm^{-1} scenario (9.19%, (8.17–10.33%)), but less important for the 8.5 mS cm^{-1} conditions (2.49%, (2.02–3.08%)). The only strain isolated belonging to the genus *Chujaibacter* showed strict aerobic metabolism and no growth in 1% NaCl concentration, no capacity for nitrate reduction but positive assimilation of *N*-acetylglucosamine (Kim et al., 2015). This is therefore the first report of *Chujaibacter* in wastewater treatment systems, and it could be inferred that this strain should be different from the previously described *Chujaibacter soli*. This strain could thrive in the hybrid MBBR-MBR by aerobic degradation of organic matter with special attention to *N*-acetylglucosamine, which is readily available in the bioreactor since variable salinity conditions exerts high pressure over the microbial communities and thus increase mortality of cells (Rodriguez-Sanchez et al., 2017b). More research should focus on the elucidation of the ecological role of

Chujaibacter in hybrid MBBR-MBR systems in particular and wastewater treatment bioprocesses in general.

On the other hand, *Thermomonas* genus accounted for a higher representation in the 8.5 mS cm^{-1} scenario (6.30%, (5.4–7.35%)) compared to the 4.5 mS cm^{-1} scenario (0.64% (0.55–0.83%)). It has been found that the *Thermomonas* genus thrives in MBR and hybrid MBBR-MBR systems treating saline wastewater, and their metabolic capability for oxidation of both organic matter, including *N*-acetylglucosamine, and ammonium has been reported (Wang et al., 2014; Ali et al., 2016). Indeed, kinetic analyses showed that *Thermomonas* relative abundance was linked to faster autotrophic kinetics but slower heterotrophic kinetics, and therefore, its ecological role in the MBR and hybrid MBBR-MBR systems treating saline wastewater has been suggested as heterotrophic nitrifier outcompeting autotrophic nitrifier for ammonium substrate due to lack of adaptation of ammonium oxidizing bacteria to saline wastewater environment (Rodriguez-Sanchez et al., 2017b).

Among all the dominant consensus taxonomy OTUs, the one that accounted for the highest dissimilarity contribution was the *Rhodanobacter* genus, followed by *Chujaibacter* genus (Fig. 4). The contributions to dissimilarity between biological samples for *Rhodanobacter* and *Chujaibacter* were very high (27.82–33.51% and 8.00–10.65%, respectively), except for the comparison between mixed liquor and fixed film biomass at the 8.5 mS cm^{-1} scenario, were their dissimilarity contributions were lower (15.24 and 1.15%, respectively). For the comparison between mixed liquor and fixed film biomass at the 8.5 mS cm^{-1} scenario, the top dissimilarity contributor was *Ferruginibacter* (10.76%). On the contrary, for the other groups of samples, *Rhodanobacter* and *Chujaibacter* together summed up to 44.16% of dissimilarity. In this sense, the SIMPER results showed that the proliferation of *Rhodanobacter* and *Chujaibacter* were major driving factors for the differences among the biological samples. This could be caused by the competitive nature of these genera in the hybrid MBBR-MBR systems treating variable influent salinity wastewater, thus reducing

the diversity in the systems due to out-competition of these groups with respect to other phylotypes. The diversity and evenness in the biological samples was confirmed by the Shannon-Wiener and Simpson indices, which have been claimed as the most robust indices to compare diversity of microbial communities (Haegeman et al., 2013). In this sense, the reduction of diversity and evenness in the biological samples could be linked to the relative abundance of dominant *Rhodanobacter* and *Chujaibacter*, since all samples at 4.5 mS cm^{-1} had lower evenness (as per lower values in Simpson index) and lower diversity (as per lower Shannon-Wiener index values) (Table S3). Thus, the importance of *Rhodanobacter* and *Chujaibacter*, and of *Rhodanobacteraceae* family in general, in variable salinity wastewater treatment processes should be further analyzed.

Quantitative differential analyses over the consensus taxonomy OTU distribution showed 4 consensus taxonomies with significant different relative abundance between mixed liquor and membrane biofilm (expected effect size < − 1 or expected effect size > 1) (Fig. S1). Only one of these phylotypes was among the dominant 20 but did not have major importance in terms of relative abundance for the bioreactors compared to other phylotypes (0.63%, (0.48–0.81%) for 4.5 mS cm^{-1}, 1.00%, (0.73–1.35%) for 8.5 mS cm^{-1}). On the other hand, 119 phylotypes showed significant relative abundance between the different maximum influent salinities. Among them, the dominant *Rhodanobacter*, *Chujaibacter*, and *Thermomonas* genera were present. As previously shown, maximum influent salinity levels selected for different dominance of *Rhodanobacter*, *Chujaibacter*, and *Thermomonas* in terms of relative abundance.

These dominant genera showed statistically significant correlation as shown by calculation of Erb's ρ correlation coefficient (Fig. S2). *Rhodanobacter* genera had statistically significant positive correlation (ρ > 0.65) with *Chujaibacter* and a dominant unclassified *Rhodanobacteraceae* family member. On the other hand, *Chujaibacter* had statistically significant negative correlation (ρ < − 0.65) with *Thermomonas* genus. In this sense, the competition among the dominant phylotypes in both

salinity scenarios showed a competition between *Thermomonas* and *Chujaibacter*. Since *Thermomonas* has been linked to autotrophic kinetics and had been suggested as an important nitrifier in hybrid MBBR-MBR systems treating saline wastewater (Rodriguez-Sanchez et al., 2017b), it is possible that *Chujaibacter* is able to develop this type of metabolism in the hybrid MBBR-MBR systems treating variable-salinity influent wastewater.

These results were also correlated with those from the SIMPER analysis developed over the 95% confidence interval relative abundance values of the Dirichlet multinomial mixing partitions showed that the most significant contributions to dissimilarity belonged to *Rhodanobacter* (15.81%), *Chujaibacter* (6.29%), and *Thermomonas* (5.20%) (Table S3). Moreover, the relative abundances of these OTUs were significantly different between the 8.5 and the 4.5 mS cm^{-1} salinity scenarios (26.9 vs 43.6%, 2.55 vs 9.25%, 6.37 vs 0.67%, respectively). In this way, significantly different higher presence of *Rhodanobacter* and *Chujaibacter* could be related to higher organic matter and ammonium oxidation potential in the MBBR-MBR systems. More research on the metabolic capabilities with respect to contributions to organic matter removal and ammonium oxidation of *Rhodanobacter* and *Chujaibacter* should be performed, as well as over the capacity of *Chujaibacter* to oxidize ammonium.

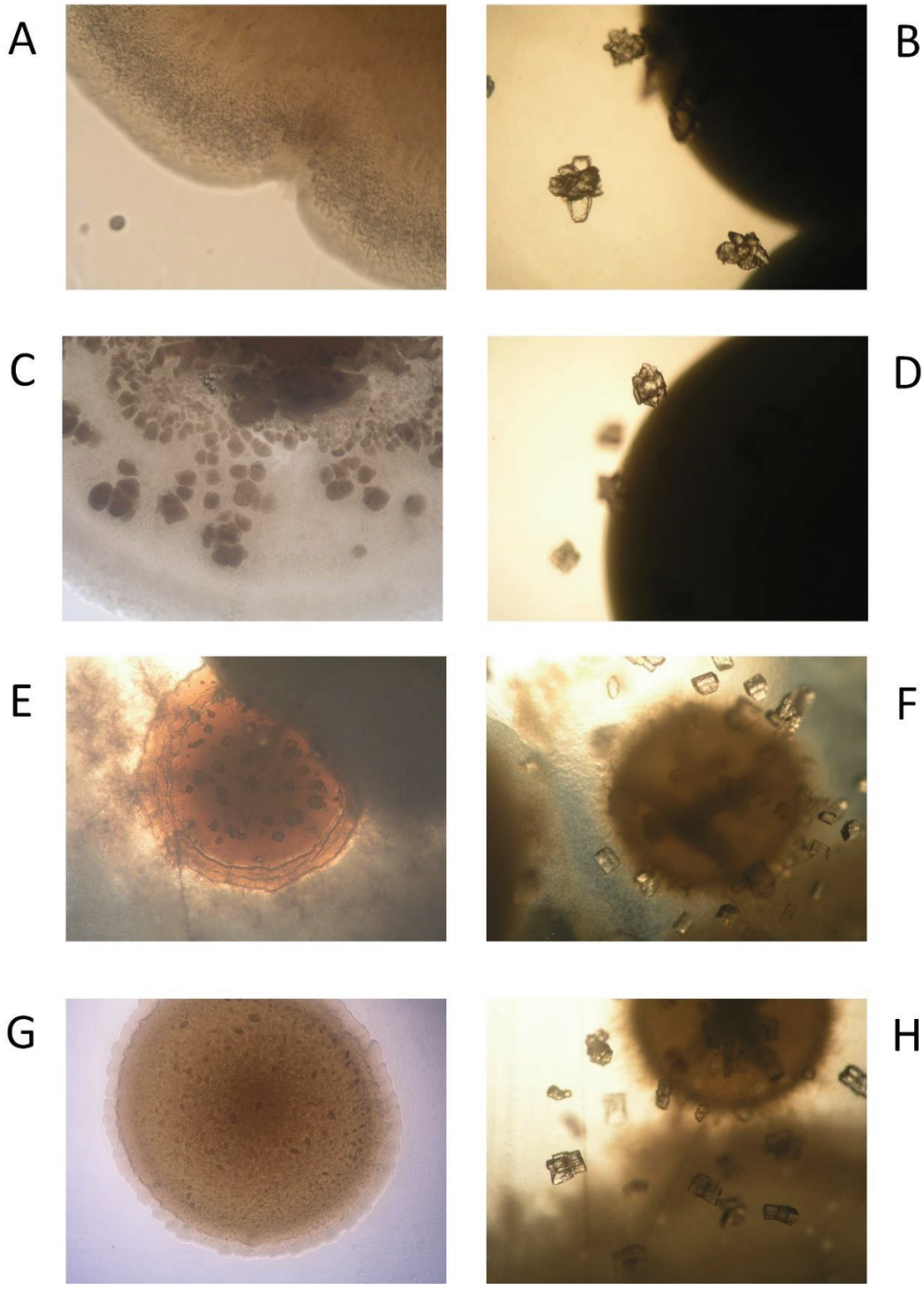

Figure 5 – Optical microscopy images of colonies from the culture media MC and ME inoculated with biofilm from both salinity conditions tested in the study (A & C: MC medium, 4.5 mS cm^{-1}; E & G: MC medium, 8.5 mS cm^{-1}; B & D: ME medium, 8.5 mS cm^{-1}; F & H: ME medium, 8.5 mS cm^{-1})

3.4 Formation of Minerals Mediated by Bacterial Activity from Membrane Biofilm

It was found that the growth of bacterial colonies in the MC and ME media was accompanied by the appearance of mineral-like structures (Fig. 5). The morphology of the minerals formed in the media were different for the two salinity scenarios. In the MC medium, the minerals formed by membrane biofilm collected under 4.5 mS cm^{-1} were of smaller size and sphere-like (Fig. 5a, c) in comparison to those obtained in MC medium inoculated with membrane biofilm collected under 8.5 mS cm^{-1} operation, which had a rhomboid-like shape (Fig. 5e, g). With respect to the ME medium, the minerals formed in plates inoculated with 4.5 mS cm^{-1} membrane biofilm presented a marked tetrahedral structure (Fig. 5b, d) when compared to those in the plates with 8.5 mS cm^{-1} membrane biofilm, which were smaller and more compact (Fig. 5f, h).

The plates seeded with autoclaved media did not show formation of any mineral, as occurred with the plates not inoculated. In this sense, the culture of membrane biofilm from both salinity scenarios showed that formation of minerals in the MC and ME media was mediated by microbial activity and that different minerals were formed for the biomass from different maximum influent salinity conditions.

The colonies that showed a significant number of biominerals around them were isolated in respective MC or ME media in order to determine the taxonomy of such mineral-formation-mediating strains. Construction of a phylogenetic tree and taxonomic affiliation of their almost-complete 16S rRNA gene showed that, among the 20 successfully cultured strains, 5 different species were found (Fig. 6). For the membrane biomass of salinity scenario 4.5 mS cm^{-1}, only the species *Bacillus stratosphericus* was identified three times from the MC medium and once from. On the other hand, the membrane biofilm for the 8.5 mS cm^{-1} scenario yielded five different strains with capability to mediate mineral formation. In the MC, medium 6 strains were identified and all were affiliated to *Bacillus toyonensis* species. Among those identified in the ME medium, 1 was affiliated to *Bacillus*

stratosphericus, 1 to *Microbacterium esteraromaticum*, 1 to *Janibacter melonis*, and 2 to *Comamonas testosteroni*.

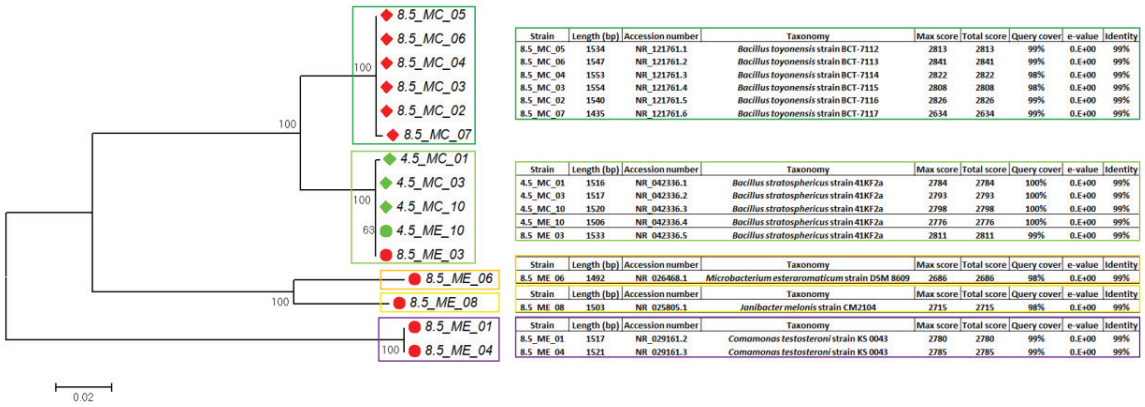

Strain	Length (bp)	Accession number	Taxonomy	Max score	Total score	Query cover	e-value	Identity
8.5_MC_05	1534	NR_121761.1	*Bacillus toyonensis* strain BCT-7112	2813	2813	99%	0.E+00	99%
8.5_MC_06	1547	NR_121761.2	*Bacillus toyonensis* strain BCT-7113	2841	2841	99%	0.E+00	99%
8.5_MC_04	1553	NR_121761.3	*Bacillus toyonensis* strain BCT-7114	2822	2822	98%	0.E+00	99%
8.5_MC_03	1554	NR_121761.4	*Bacillus toyonensis* strain BCT-7115	2808	2808	98%	0.E+00	99%
8.5_MC_02	1540	NR_121761.5	*Bacillus toyonensis* strain BCT-7116	2826	2826	99%	0.E+00	99%
8.5_MC_07	1435	NR_121761.6	*Bacillus toyonensis* strain BCT-7117	2634	2634	99%	0.E+00	99%

Strain	Length (bp)	Accession number	Taxonomy	Max score	Total score	Query cover	e-value	Identity
4.5_MC_01	1516	NR_042336.1	*Bacillus stratosphericus* strain 41KF2a	2784	2784	100%	0.E+00	99%
4.5_MC_03	1517	NR_042336.2	*Bacillus stratosphericus* strain 41KF2a	2793	2793	100%	0.E+00	99%
4.5_MC_10	1520	NR_042336.3	*Bacillus stratosphericus* strain 41KF2a	2798	2798	100%	0.E+00	99%
4.5_ME_10	1506	NR_042336.4	*Bacillus stratosphericus* strain 41KF2a	2776	2776	100%	0.E+00	99%
8.5_ME_03	1533	NR_042336.5	*Bacillus stratosphericus* strain 41KF2a	2811	2811	99%	0.E+00	99%

Strain	Length (bp)	Accession number	Taxonomy	Max score	Total score	Query cover	e-value	Identity
8.5_ME_06	1492	NR_026468.1	*Microbacterium esteraromaticum* strain DSM 8609	2686	2686	98%	0.E+00	99%

Strain	Length (bp)	Accession number	Taxonomy	Max score	Total score	Query cover	e-value	Identity
8.5_ME_08	1503	NR_025805.1	*Janibacter melonis* strain CM2104	2715	2715	98%	0.E+00	99%

Strain	Length (bp)	Accession number	Taxonomy	Max score	Total score	Query cover	e-value	Identity
8.5_ME_01	1517	NR_029161.2	*Comamonas testosteroni* strain KS 0043	2780	2780	99%	0.E+00	99%
8.5_ME_04	1521	NR_029161.3	*Comamonas testosteroni* strain KS 0043	2785	2785	99%	0.E+00	99%

Figure 6 – Phylogenetic tree and taxonomy of isolated strains with capacity to mediate the formation of minerals in the MC and ME media

Bacillus stratosphericus was firstly isolated from air samples collected at great altitude and was reported to have very high resistance to NaCl (up to 17.4%) (Shivaji et al., 2006). *Bacillus toyonensis* has been reported to have resistance to high salinities (up to 5% NaCl) (Jiménez et al., 2013a) and has been used widely in animal nutrition since 1975 as it is the basis of the probiotics food additive Toyocerin® (Jiménez et al., 2013b). Neither *Bacillus stratosphericus* nor *Bacillus toyonensis* have previously been reported to mediate mineral formation. Nevertheless, many *Bacillus* strains have been found to help calcite and phosphate mineral formation in wastewater systems and high-salinity environments, such as *Bacillus marisflavi*, *Bacillus pumilus*, *Bacillus megaterium*, *Bacillus subtilis*, *Bacillus thuringensis*, or *Bacillus flexum* (Gonzalez-Martinez et al., 2017; Uad et al., 2014; Silva-Castro et al., 2015).

Microbacterium esteraromaticum was firstly described in 1993 (Yokota et al., 1993) as *Aureobacterium esteraromaticum* and unified in 1998 to the genus *Microbacterium* (Takeuchi and Hatano 1998).The strain *Microbacterium esteraromaticum* DSM 8609 has been reported for

ammonium oxidation under low concentrations and low temperatures (Zhang et al., 2016), which could be explained as a heterotrophic nitrificationaerobic denitrification metabolism as observed in other strains of *Microbacterium esteraromaticum* (Vinothkumar et al., 2016). A strain of the *Microbacterium* genus has been reported for mediation of mineral formation of calcite nature (Xu et al., 2017). Nevertheless, no reports to this date have informed about mineralization of phosphate minerals mediated by *Microbacterium* genus.

Janibacter melonis was firstly isolated from an abnormally spoiled melon in Korea, showing strict aerobic growth (Yoon et al., 2004). Further than infecting melons, *Janibacter melonis* has been reported a cause of bacteremia in humans causing low fever, skin swelling, pain, and erythema (Elsayed and Zhang, 2005) and has been noticed that some strains of *Janibacter melonis* have higher virulence than *Janibacter terrae*, known to cause infections in humans (Chander et al., 2018). No *Janibacter* strains have been reported for mineral precipitation.

Comamonas testosteroni has been reported as NaCl tolerant (up to 3% concentration) and facultative anaerobic bacterium (Zhu et al., 2014). It has been found that *Comamonas testosteroni* could be of importance for the development of membrane biofilm since it has a strong capacity for biofilm formation (Li et al., 2009). *Comamonas* isolated from membrane biofilm of hybrid MBBR-MBR system treating urban wastewater have previously been reported to mediate the precipitation of carbonates (Gonzalez-Martinez et al., 2017).

The relative abundances of the consensus taxonomy OTUs affiliated to the same genus that the stains isolated from the mineralization cultures (except for *Janibacter*, which was not found but attributed to the only unclassified *Intrasporangiaceae* member present among the taxonomic consensus) showed that their presence in the bacterial community structure in the hybrid MBBRMBR systems treating variable-salinity influent wastewater was not dominant. In terms of biofouling risk, as assessed by Gonzalez-Martinez et al. (2015), the most dangerous phylotype at 4.5 mS cm^{-1} scenario

was *Janibacter melonis*, and for the 8.5 mS cm^{-1}, it was *Microbacterium*. Nevertheless, summed presence of the total consensus taxonomy OTUs related to isolated strains with mediation in mineral formation process was of 0.29–0.41% for the 4.5 mS cm^{-1} and 0.31– 0.76% for the 8.5 mS cm^{-1} scenarios (Fig. 7).

Group	Taxonomy	Phylum	Class	Order	Family	Genus	HVFB1	HVFB2	HVML1	HVML2	LVFB1	LVFB2	LVML1	LVML2
Otu043	Bacteria	Actinobacteria	Actinobacteria	Micrococcales	Microbacteriaceae	Microbacterium								
Otu060	Bacteria	Actinobacteria	Actinobacteria	Micrococcales	Intrasporangiaceae	Intrasporangiaceae_unclassified								
Otu113	Bacteria	Proteobacteria	Gammaproteobacteria	Betaproteobacteriales	Burkholderiaceae	Comamonas								
Otu169	Bacteria	Firmicutes	Bacilli	Bacillales	Bacillaceae	Bacillus								
Total (%)							0.39	0.31	0.51	0.76	0.30	0.33	0.41	0.29

Color Code	0.00%	0.05%	0.10%	0.15%	0.20%	0.25%	≥0.30%

Figure 7 – Heat map representing the relative abundance of isolated strains with capacity to mediate the formation of minerals in the MC and ME media

3.5 Nature of Minerals Extracted from the MC and ME Media Formed by Mediation of Bacterial Activity

Differences were observed between the minerals extracted from the MC and ME media for the two maximum salinity scenarios (Fig. 8). Moreover, the results of the X-ray microanalyses for regions of interest on the mineral surfaces are shown in Fig. 9. For the minerals extracted from the MC media, their external morphology was similar for the scenarios of 4.5 and 8.5 mS cm^{-1}, showing rhombohedral and sphere-like structures with either a smooth surface or rough surface with presence of bacterial footprints (Fig. 8a, b, e, g). Their X-ray microanalysis spectra demonstrated similar elemental formation with main Ca element composition regardless of the roughness of the surface, the presence of the bacterial footprints, or the morphology of the mineral tested (Fig. 9a, b). The similarity in morphology and composition for minerals in MC medium culturing membrane biofilm from 4.5 and 8.5 mS cm^{-1} scenarios could potentially be caused by the presence of only one strain with capacity for mediation of mineral formation in such medium, related to genus *Bacillus*. Therefore, it is possible that the mediation of *Bacillus stratosphericus* from the 4.5 mS cm^{-1} membrane biofilm and *Bacillus toyonensis* from the 8.5 mS cm^{-1} membrane biofilm resulted in the formation of similar minerals. In

this sense, it is possible that these two *Bacillus* strains have the same behavior in terms of mineral formation mediation.

On the other hand, the morphologies of the minerals extracted from the ME medium were different between the two salinity scenarios (Fig. 8c, d, f, h). For the 4.5 mS cm^{-1} scenario, the mineral observed had a tetrahedral morphology. On the other hand, the morphology of minerals for the 8.5 mS cm^{-1} scenario showed compact minerals with polished surfaces marked with bacterial footprints. The differences in morphology were also correlated to differences in composition as determined by X-ray microanalysis. For the 4.5 mS cm^{-1} membrane biofilm, the minerals generated in the ME medium has a composition made mainly of Mg and P elements. On the other hand, the elemental composition of the minerals extracted from the ME medium inoculated with membrane biofilm from the 8.5 mS cm^{-1} scenario consisted on Ca and P. Differences in the composition and morphology of the minerals formed could depend on the taxonomy of isolated strains with capacity to mediate mineral formation from ME media: *Bacillus stratosphericus* only for the 4.5 mS cm^{-1} membrane biofilm, and *Bacillus stratosphericus*, *Microbacterium esteraromaticum*, *Janibacter melonis*, and *Comamonas testosterone* for the 8.5 mS cm^{-1} membrane biofilm. In this sense, presence of the three non-*Bacillus* strains could lead to formation of a majority of minerals in the ME medium with different characteristics than those for the *Bacillus stratosphericus* strains.

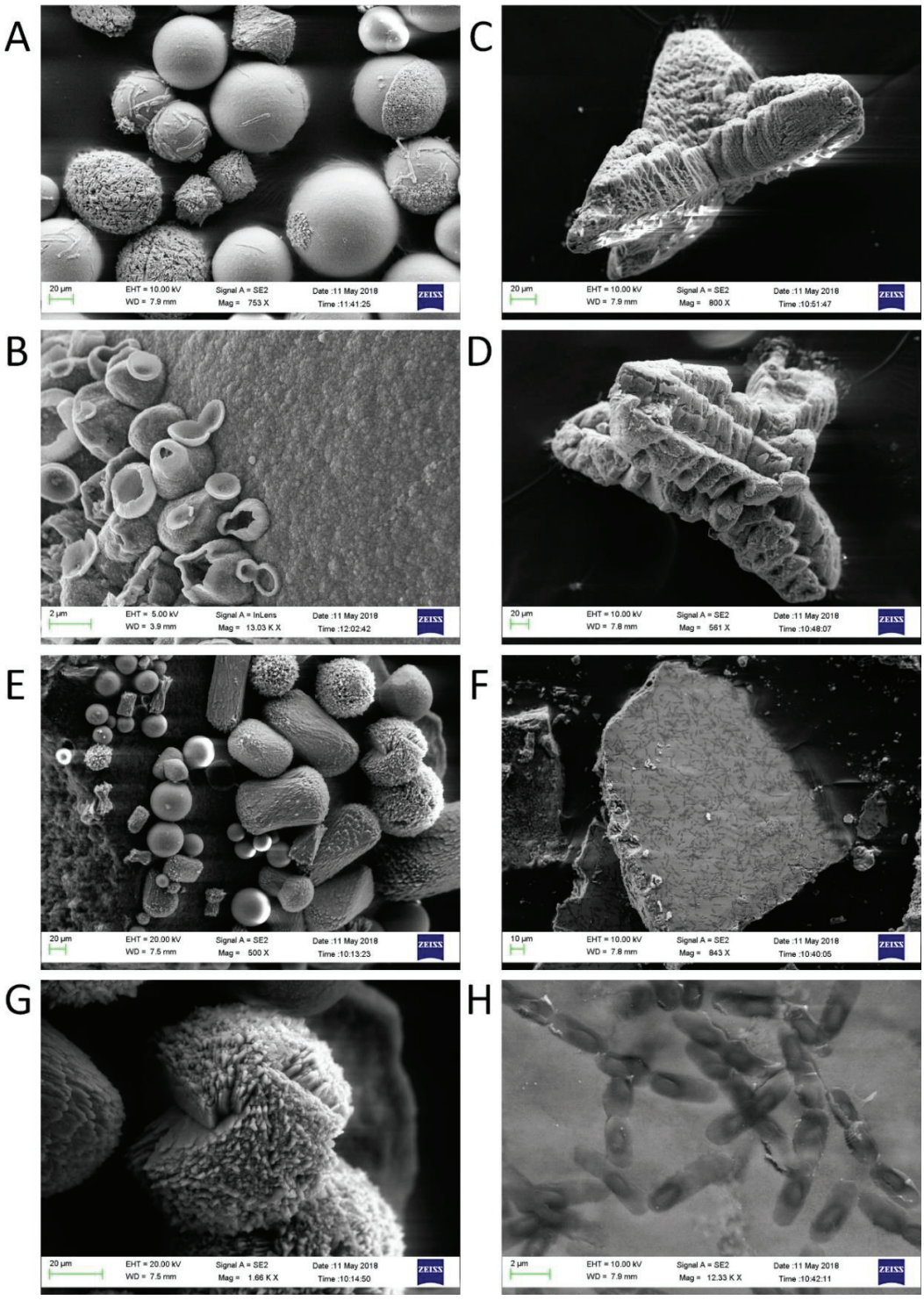

Figure 8 – Scanning electron microscopy images from minerals extracted from the MC and ME media (A & B: MC medium, 4.5 mS cm^{-1}; E & G: MC medium, 8.5 mS cm^{-1}; C & D: ME medium, 8.5 mS cm^{-1}; F & H: ME medium, 8.5 mS cm^{-1})

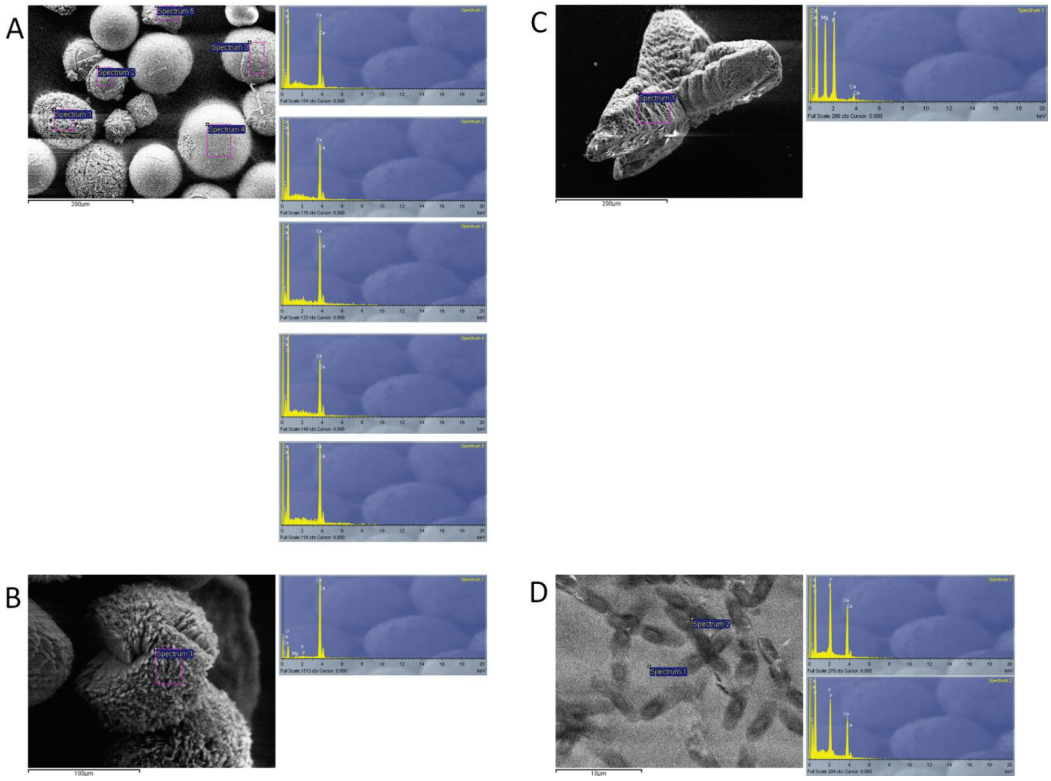

Figure 9 – X-Ray microanalysis of minerals extracted from the MC and ME media (A: MC medium, 4.5 mS cm^{-1}; B: MC medium, 8.5 mS cm^{-1}; C: ME medium, 8.5 mS cm^{-1}; D: ME medium, 8.5 mS cm^{-1})

4. Conclusions

Two hybrid MBBR-MBR systems were operated at 23.6 L h^{-1} m^{-2} flux rate under 6 h hydraulic retention time and 2500 mg L^{-1} total solids for the treatment of tidal-like variable-salinity influent with maximums of 4.5 and 8.5 mS cm^{-1}, respectively. Maximum influent salinity showed to affect organic matter removal and ammonium oxidation between the MBBR-MBR, favoring the lowest influent salinity conditions (99.47 vs 91.60% for BOD_5, 81.72 vs 60.72% for COD, 56.09 vs 27.11% for NH_4^+, 54.29 vs 26.77% for TN). The effect of the maximum influent salinity over the bacterial communities and their capability for mediating carbonate and phosphate mineral precipitation was analyzed. The culture of mineral-precipitation-mediating bacteria from membrane biomass under both conditions showed that *Bacillus stratosphericus* was the only mineralization-inducing strain under 4.5 mS cm^{-1}, with 8.5 mS cm^{-1} membrane biofilm showing a higher diversity with *Bacillus stratosphericus*, *Bacillus toyonensis*, *Comamonas testosteroni*, *Microbacterium esteroaromaticum*, and *Janibacter meloni* being found as important for biological-induced mineralization. Carbonate-based minerals were identical in morphology and composition among the two salinity scenarios, while the phosphate-based minerals did differ in structure and chemical composition. The whole bacterial community structure for membrane biofilm was very similar than that of the mixed liquor at each salinity scenario, with maximum influent salinity driving the diversity of the system by diminishing the relative abundance of dominant *Rhodanobacter* (26.26–32.96% vs 41.58–50.97%), *Chujaibacter* (8.17–10.33% vs 2.02–3.08%) and *Thermomonas* (5.4–7.35% vs 0.55–0.83%) genera with increasing salinity.

Acknowledgments

We would like to acknowledge the support given by the Institute of Water Research, the Department of Civil Engineering and the Faculty of Pharmacy of the University of Granada.

Funding information

Funding was given by the Ministerio de Economia, Industria y Competitividad of the Government of Spain by the project with reference CTM2013-48154-P and the grant with reference BES-2014-067852.

Compliance with Ethical Standards

Conflict of Interest The authors declare that there are no conflicts of interest.

References

Ali M, Chai LY, Min XB, Tang CJ, Afrin S, Liao Q, et al. (2016) Performance and characteristics of a nitritation air-lift reactor under long-term HRT shortening. Internat Biodeter Biodegr 111: 45–53. https://doi.org/10.1016/j.ibiod.2016.04.003.

Bassin JP, Kleerebezem R, Muyzer G, Rosado AS, Van Loosdrecht, MCM, Dezotti M (2012) Effect of different salt adaptation strategies on the microbial diversity, activity, and settling of nitrifying sludge in sequencing batch reactors. Appl Microbiol Biotechnol 93(3): 1281–1294. https://doi.org/10.1007/s00253-011-3428-7.

Bian G, Gloor GB, Gong A, Jia C, Zhang W, Hu J, et al. (2017) The gut microbiota of healthy aged Chinese is similar to that of the healthy young. mSphere 2(5): e00327–e00317. https://doi.org/10.1128/mSphere.00327-17.

Castillo-Carvajal LC, Sanz-Martin JL, Barragan-Huerta BE (2014) Biodegradation of organic pollutants in saline wastewater by halophilic microorganisms: a review. Environ Sci Poll Res, 21(16): 9578–9588. https://doi.org/10.1007/s11356-014-3036-z.

Chander AM, Kochhar R, Dhawan DK, Bhadada SK, Mayilraj S (2018) Genome sequence and comparative genomic analysis of a clinically important strain CD11-4 of Janibacter melonis isolated from celiac disease patient. Gut Pathogens 10(1): 1–8. https://doi.org/10.1186/s13099-018- 0229-x.

Cortes-Lorenzo C, Rodriguez-Diaz M, Lopez-Lopez C, Sanchez-Peinado M, Rodelas B, Gonzalez-Lopez J (2012) Effect of salinity on enzymatic activities in a submerged fixed bed biofilm reactor for municipal sewage treatment. Biores Technol 121: 312–319. https://doi. org/10.1016/j.biortech.2012.06.083.

Cortés-Lorenzo C, González-Martínez A, Smidt H, González-López J, Rodelas B (2016) Influence of salinity on fungal communities in a submerged fixed bed bioreactor for wastewater treatment. Chem Eng J 285: 562–572. https://doi.org/10.1016/j.cej.2015.10.009.

Di Trapani D, Di Bella G, Mannina G, Torregrossa M, Viviani G (2014) Comparison between moving bedmembrane bioreactor (MB-MBR) and membrane bioreactor (MBR) systems: influence of wastewater salinity variation. Biores Technol 162: 60–69. https://doi.org/10.1016

/j.biortech.2014.03.126.

Elsayed S, Zhang K (2005) Bacteremia caused by Janibacter melonis. J Clin Microbiol 43(7): 3537– 3539. https://doi.org/10.1128/JCM.43.7.3537-3539.2005.

Gao DW, Wen ZD, Li B, Liang H (2014) Microbial community structure characteristics associated membrane fouling in A/O-MBR system. Biores Technol 154: 87–93. https://doi.org/10.1016/j.biortech.2013.11.051.

Gonzalez-Martinez A, Leyva-Díaz JC, Rodriguez-Sanchez A, Muñoz-Palazon B, Rivadeneyra A, Poyatos JM, et al. (2015) Isolation and metagenomic characterization of bacteria associated with calcium carbonate and struvite precipitation in a pure moving bed biofilm reactor-membrane bioreactor. Biofouling 31(4), 333–348. https://doi. org/10.1080/08927014.2015.1040006.

Gonzalez-Martinez A, Rodriguez-Sanchez A, Lotti T, Garcia-Ruiz MJ, Osorio F, Gonzalez-Lopez J, van Loosdrecth MCM (2016) Comparison of bacterial communities of conventional and A-stage activated sludge systems. Sci Rep 6: 18786. https://doi.org/10.1038

/srep18786.

Gonzalez-Martinez A, Rodriguez-Sanchez A, Rivadeneyra MA, Rivadeneyra A, Martin-Ramos D, Vahala R, Gonzalez-Lopez J (2017) 16S rRNA gene-based characterization of bacteria potentially associated with phosphate and carbonate precipitation from a granular autotrophic nitrogen removal bioreactor. Appl Microbiol Biotechnol 101(2): 817–829. https://doi.org/10.1007

/s00253-016-7914-9.

Haegeman B, Hamelin J, Moriarty J, Neal P, Dushoff J, Weitz JS (2013) Robust estimation of microbial diversity in theory and in practice. ISME J 7(6): 1092–1101. https://doi.org/10.1038/ismej.2013.10.

Holmes I, Harris K, Quince C (2012) Dirichlet multinomial mixtures: generative models for microbial metagenomics. PLoS One 7(2) https://doi.org/10.1371/journal. pone.0030126.

Huse SM, Welch DM, Morrison HG, Sogin ML (2010) Ironing out the wrinkles in the rare biosphere through improved OTU clustering. Environ Microbiol 12: 1889 – 1898. https://doi.or g /10.1111 /j.14 622920.2010.02193.x.

Jiménez G, Blanch AR, Tamames J, Rosselló-mora R (2013a) Complete genome sequence of Bacillus toyonensis BCT-7112 T , the active ingredient of the feed additive preparation toyocerin. Genome Announ ASM, 1(6): e01080–e01013. https://doi.org/10.1128/genomeA.01080- 13.Copyright.

Jiménez G, Urdiain M, Cifuentes A, López-López A, Blanch AR, Tamames J, et al. (2013b) Description of Bacillus toyonensis sp. nov., a novel species of the Bacillus cereus group, and pairwise genome comparisons of the species of the group by means of ANI calculations. Syst Appl Microbiol, 36(6): 383–391. https://doi. org/10.1016/j.syapm.2013.04.008.

Kim S-J, Ahn J-H, Weon H-Y, Hong S-B, Seok S-J, Kim J-S, Kwon S-W (2015) Chujaibacter soli gen. nov., sp. nov., isolated from soil. J Microbiol 53(9): 592– 597. https://doi.org/10.1007/s12275-015-5136-y.

Kumar S, Stecher G, Tamura K (2016) MEGA7 : molecular evolutionary genetics analysis version 7 . 0 for bigger datasets. Mol Ecol Evol, 33(7): 1870– 1874. https://doi.org/10.1093/molbev/msw054.

Larkin MA, Blackshields G, Brown NP, Chenna R, Mcgettigan PA, McWilliam H, et al. (2007) Clustal W and Clustal X version 2.0. Bioinformatics 23(21), 2947–2948. https://doi.org/10.1093/bioinformatics/btm404.

Leyva-Diaz JC, González-Martinez A, Gonzalez-Lopez J, Muñio MM, Poyatos JM (2015) Kinetic modeling and microbiological study of two-step nitrification in a membrane bioreactor and hybrid moving bed biofilm reactor— membrane bioreactor for wastewater treatment. Chem Eng J 259: 692–702. https://doi.org/10.1016/j.cej.2014.07.136.

Li MY, Zhang J, Lu P, Xu JL, Li SP (2009) Evaluation of biological characteristics of bacteria contributing to biofilm formation. Pedosphere 19(5): 554–561. https://doi. org/10.1016/S1002-0160(09)60149-1.

Rivadeneyra A, Gonzalez-Martinez A, Gonzalez-Lopez J, Martin-Ramos D, Martinez-Toledo MV, Rivadeneyra MA (2014) Precipitation of phosphate minerals by microorganisms isolated from a fixed-biofilm reactor used for the treatment of domestic wastewater. Int J Environ Res Public Health 11(4): 3689– 3704. https://doi.org/10.3390/ijerph110403689.

Rivadeneyra A, Gonzalez-Martinez A, Portela GR, Martin-Ramos DJ, Gonzalez-Lopez J, Rivadeneyra MA (2017) Biomineralisation of carbonate and sulphate by the halophilic bacterium Halomonas maura at different manganese concentrations. Extremophiles 21(6): 1049–1056. https://doi.org/10.1007/s00792-017-0965-8.

Rodriguez-Sanchez A, Leyva-Diaz JC, Gonzalez-Martinez A, Poyatos JM (2017a) Performance and kinetics of membrane and hybrid moving bed biofilm-membrane bioreactors treating salinity wastewater. AIChE J 63(8): 3329–3342. https://doi.org/10.1002/aic.15694.

Rodriguez-Sanchez A, Leyva-Diaz JC, Gonzalez-Martinez A, Poyatos JM (2017b) Linkage of microbial kinetics and bacterial community structure of MBR and hybrid MBBR–MBR systems to treat salinity-amended urban wastewater. Biotechnol Progr 33(6) https://doi. org/10.1002/btpr.2513.

Rodriguez-Sanchez A, Leyva-Diaz JC, Gonzalez-Lopez J, Poyatos JM (2018a) Membrane bioreactor and hybrid moving bed biofilm reactor-membrane bioreactor for the treatment of variable salinity wastewater: influence of biomass concentration and hydraulic retention time. Chem Eng J 336. https://doi.org/10.1016/j. cej.2017.10.118.

Rodriguez-Sanchez A, Leyva-Diaz JC, Poyatos JM, Gonzalez-Lopez J (2018b) Influent salinity conditions affect the bacterial communities of biofouling in hybrid MBBR-MBR systems. J Water Process Eng. https://doi.org/10.1016/j.jwpe.2018.07.001.

Rognes T, Flouri T, Nichols B, Quince C, Mahé F (2016) VSEARCH: a versatile open source tool for metagenomics. PeerJ, 4: e2584. https://doi.org/10.7717/peerj.2584.

Schloss PD (2016) Application of a database-independent approach to assess the quality of. mSystems 1(2): 2–5. https://doi.org/10.1128/mSystems.00027-16.Copyright.

Schloss PD, Westcott SL, Ryabin T, Hall JR, Hartmann M, Hollister EB, et al. (2009) Introducing mothur: open-source, platform-independent, community-supported software for describing and comparing microbial communities. Appl Environ Microbiol 75(23): 7537–7541. https://doi.org/10.1128/AEM.01541-09.

Shivaji S, Chaturvedi P, Suresh K, Reddy GSN, Dutt CBS, Wainwright M, et al. (2006) Bacillus aerius sp. nov., Bacillus aerophilus sp. nov., Bacillus stratosphericus sp. nov. and Bacillus altitudinis sp. nov., isolated from cryogenic tubes used for collecting air samples from high altitudes. Int J System Evol Microbiol 56(7): 1465–1473. https://doi.org/10.1099

/ijs.0.64029-0.

Silva-Castro GA, Uad I, Gonzalez-Martinez A, Rivadeneyra A, Gonzalez-Lopez J, Rivadeneyra MA (2015) Bioprecipitation of calcium carbonate crystals by bacteria isolated from saline environments grown in culture media amended with seawater and real brine. BioMed Res Int 2015. https://doi.org/10.1155/2015/816102.

Takeuchi M, Hatano K (1998) Union of the genera Microbacterium OrlaJensen and Aureobacterium Collins et a/. in a redefined genus Microbacterium. Int J System Bacteriol 48: 739–747.

Uad I, Gonzalez-Lopez J, Silva-Castro AG, Vílchez JI, Gonzalez-Martinez A, Martin-Ramos D, et al. (2014) Precipitation of carbonates crystals by bacteria isolated from a submerged fixed-film bioreactor used for the treatment of urban wastewater. Int J Environ Res 8(2): 435–446.

Unno T (2015) Bioinformatic suggestions on MiSeq-based microbial community analysis. 25(6): 765–770.

Vinothkumar R, Bharti VS, Vennila A, Kumar HS, Pandey PK (2016) Isolation and characterization of heterotrophic nitrifying—denitrifying bacteria from shrimp farming ponds. Ecol Environ Conserv 22(1): 275–279.

Wang L, Zheng S, Wang D, Wang L, Wang G (2014) Thermomonas carbonis sp. nov., isolated from the soil of a coal mine. Int J System Evol Microbiol 64(Pt 11), 3631–3635. https://doi.org/10.1099/ijs.0.063800-0.

Weiss S, Xu ZZ, Peddada S, Amir A, Bittinger K, Gonzalez A, et al. (2017) Normalization and microbial differential abundance strategies depend upon data characteristics. Microbiome 5(1): 1–18. https://doi.org/10.1186/s40168-017-0237-y.

Westcott SL, Schloss PD (2015) De novo clustering methods outperform reference-based methods for assigning 16S rRNA gene sequences to operational taxonomic units. PeerJ 3: e1487. https://doi.org/10.7717/peerj.1487.

Xu G, Li D, Jiao B, Li D, Yin Y, Lun L, et al. (2017) Biomineralization of a calcifying ureolytic bacterium Microbacterium sp. GM-1. Electr J Biotechnol 25: 21–27. https://doi.org/10.1016/j.ejbt.2016.10.008.

Yokota a, Takeuchi M, Sakane T, Weiss N (1993) Proposal of six new species in the genus Aureobacterium and transfer of Flavobacterium esteraromaticum Omelianski to the genus Aureobacterium as Aureobacterium esteraromaticum comb. nov. Int J System Bacteriol 43(3): 555–564. https://doi.org/10.1099/00207713-43-3-555.

Yoon JH, Lee HB, Yeo SH, Choi JE (2004) Janibacter melonis sp. nov., isolated from abnormally spoiled oriental melon in Korea. Int J System Evol Microbiol 54(6): 1975–1980. https://doi.org/10.1099/ijs.0.63167-0.

Zhang D, Huang X, Li W, Qin W, Wang P (2016) Characteristics of heterotrophic nitrifying bacterium strain SFA13 isolated from the Songhua River. Annals of Microbiol 66(1): 271–278. https://doi.org/10.1007/s13213-015-1105-2.

Zhu D, Xie C, Huang Y, Sun J, Zhang W (2014) Description of Comamonas serinivorans sp. nov., isolated from wheat straw compost. Int J System Evol Microbiol 64(2014): 4141–4146. https://doi.org/10.1099/ijs.0.06668.

Chapter 8

Influent salinity conditions affect the bacterial communities of biofouling in hybrid MBBR-MBR systems

This chapter has been published in its current form in Journal of Water Process Engineering. The complete citation is the following:

Alejandro Rodriguez-Sanchez, Juan Carlos Leyva-Diaz, Jose Manuel Poyatos, Jesus Gonzalez-Lopez. 2018. Influent salinity conditions affect the bacterial communities of biofouling in hybrid MBBR-MBR systems. Journal of Water Process Engineering. In Press. doi: 10.1016/j.jwpe.2018.07.001

Abstract

The system performance, biomass kinetics and microbial community structure in biofouling and suspended biomass of a hybrid MBBR-MBR system operating at 6 h of hydraulic retention time subjected to four different scenarios of salinity wastewater -constant 6.5 mS cm^{-1}, and tidal-like variable at 4.5, 6.5 and 8.5 mS cm^{-1} was studied. The performance of the bioreactors in terms of organic matter removal was efficient, nevertheless only the scenario of variable 4.5 mS cm^{-1} showed good nitrogen removal (59.59%). The salinity conditions exerted an effect over the kinetics of the system, with rates of substrate utilization dependent on substrate for variable salinity conditions and non-dependent for constant salinity conditions. Also, higher peak salinities lead to lower rates of substrate utilization. Massive parallel sequencing showed that *Xanthomonadaceae* family (2.57–33.00%) and *Mycobacterium* genus (4.70%) dominated biofouling under variable and constant salinity conditions, respectively. Principal component analyses showed higher community similarity between biofouling and suspended biomass under variable salinity conditions than for constant salinity. However, differences in biofouling-related OTUs were observed between attached and suspended communities by the means of effect size quantification. The composition of oligotypes of OTUs important for biofouling showed no differences between biofouling and suspended biomass at all salinity scenarios. The results suggested that biofouling process could be mainly determined by increases in relative abundance of biofouling-related OTUs in the attached biomass with respect to suspended biomass (25.76–204.63% increase). The results obtained will be of importance for future design and implementation of strategies for operation and biofouling control of salinity wastewater treatment systems.

1. Introduction

Discharge of wastewater is one of the main environmental problems of our era. For the last century, the activated sludge system has been the most used technology for the treatment of urban wastewater (Gonzalez-Martinez et al., 2016a). However, other technologies have emerged, such as the membrane bioreactor (MBR) technology, that offers several important advantages over the activated sludge, such as reduced footprint, operation at higher solids concentrations, or very high removal efficiency of pathogens (Rodriguez-Sanchez et al., 2017a). Furthermore, MBR systems can be benefited by the implementation of an upstream moving bed biofilm reactor (MBBR), in which floating media are added to the bioreactor for the formation of attached biofilms in addition to suspended biofilms (Leyva-Diaz et al., 2017). The combined technology has been named as moving bed biofilm reactor-membrane bioreactor (MBBR-MBR), and its superior capacity to the MBR for the treatment of urban wastewater has been reported (Leyva-Diaz et al., 2013; 2014; 2015a; 2015b). In spite of this, MBBR-MBR systems, as well as other membrane-based technologies, have to deal with the serious operational problem caused by the biofilm-related clogging of membrane surface, named as biofouling. In this sense, the MBBR-MBR technology has been reported as less susceptible to biofouling than the MBR technology (Fu et al., 2017).

Biofilms are aggregates of microorganisms, which can grow in suspension or attached to surfaces, and that play a very important role in wastewater treatment systems (Barr et al., 2016). The effect of biofilms in wastewater treatment systems is mostly beneficial, because they are involved in the elimination of organic matter, nitrogen and phosphorous (Rodriguez-Sanchez et al., 2018). Nevertheless, biofilms can impact the performance of membrane systems, because the adhesion of microorganisms and extracellular polymeric substances (EPS) can clog membrane pores thus reducing the transmembrane pressure and decreasing efficiency of waste water treatment of the membrane system (Gonzalez-Martinez et al., 2015). In this context, the analysis of the agents that

cause membrane biofouling is a requirement in order to implement new practices for its control (Sanchez, 2018; Sepehri & Sarrafzadeh, 2018). Both urban and industrial wastewater could have high salinity concentrations. For industrial applications, many manufacturing industries can raise salinity in industrial effluents, such as seafood processing, milk processing, petroleum refining or textile manufacturing (Yang et al., 2013). In the case of urban wastewater, the increase in salinity concentration over regular values could be caused by snow-melting activities, seawater toilet flushing, or intrusion of seawater in coastal wastewater treatment plants (Cortes-Lorenzo et al., 2016). These increases in salinity exert pressure over the microbial communities in wastewater treatment systems, which become negatively affected due to increase in cell mortality rate and decrease in microbial metabolism, among others (Bassin et al., 2012; Remmen et al., 2017), thus leading to inefficiencies in wastewater treatment processes (Maharaja et al., 2017). The capability of the hybrid MBBR-MBR system for the treatment of salinity wastewater has been proven (Rodriguez-Sanchez et al., 2017a; 2018). Nevertheless, an in-depth study on the effect of different salinity conditions over the performance, microbial kinetics, microbial community structure and biofouling of this technology has not been attempted to date.

In this research, a hybrid MBBR-MBR system was operated at 6 h hydraulic retention time and under four different salinity conditions: constant at 6.5 mS cm^{-1} and tidal-like variable with maximums at 4.5, 6.5 and 8.5 mS cm^{-1}. Under these operational conditions, the performance of the system, its kinetics under the different salinity scenarios and microbial community structures of the membrane biofouling and suspended biomass present in the bioreactor were studied in order to evaluate the influence of the salinity conditions on this novel technology. The microbial community analyses were done based on massive parallel sequencing to explore the OTU ecology and oligotypes within important OTUs in the bioreactor.

2. Materials and methods

2.1 Bioreactor configuration and operation

The bioreactor used in this study was a hybrid MBBR-MBR system. A schematic of the bioreactor is shown in Fig. 1. The bioreactor showed a configuration of four chambers and a separated membrane tank. The four chambers were equal and had an operational volume of 6 L each. The membrane tank had an operational volume of 4.32 L. The first, third and fourth chambers contained K1 carriers (density of 0.92–0.96 g cm^{-3}) (Anox-Kaldnes AS, Norway), accounting for a volume of 35% of the total volume of the chamber and adding to a total specific biofilm surface area for the whole bioreactor of 111.7 m^2 m^{-3}. The aeration of the first, third and fourth chambers was accomplished by the means of bottom-displaced fine bubble diffusers AFD 270 (ECOTEC SA, Spain) and air compressors ACO-500 (Hailea, China), measured by rotameters 2100 Model (Tecfluid SA, Spain) and regulated using a valve. The second chamber was under anoxic conditions since no aeration was provided, and therefore its mixing was accomplished by continuous agitation by a mechanical stirrer Multi Mixer MM-1000 (Biosan Laboratories Inc, USA). The membrane tank was aerated by a coarse bubble diffuser CAP 3 (ECOTEC SA, Spain) and by an air compressor ACO-500 (Hailea, China), which flow was continuously measured by a rotameter 2100 Model (Tecfluid SA, Spain) and regulated using a valve. An ultrafiltration membrane module was displaced inside the membrane tank in submerged configuration, and was composed by 0.04 µm pore diameter hollow-fibers of polyvinylidene fluoride with a core reinforcement of polyester displaced vertically (Micronet Porous Fibers SL, Spain). The fibers measured 2.45 mm for external diameter and 1.10 mm for internal diameter, and the membrane accounted for a total membrane area of 0.2 m^2.

The influent flow was forced to enter through the first chamber by the means of a Watson-Marlow peristaltic pump (Watson-Marlow Pumps Group, USA) and to pass all of them, discharging from the fourth chamber into the membrane tank. From there, the effluent was withdrawn by membrane

separation using a Watson-Marlow peristaltic pump (Watson-Marlow Pumps Group, USA) with suction-backwashing functioning in cycles of: 9 min suction-1 min backwash. The A recycling flow of 500% of the influent flow was imposed from the membrane tank to the first chamber using another Watson-Marlow peristaltic pump (Watson-Marlow Pumps Group, USA).

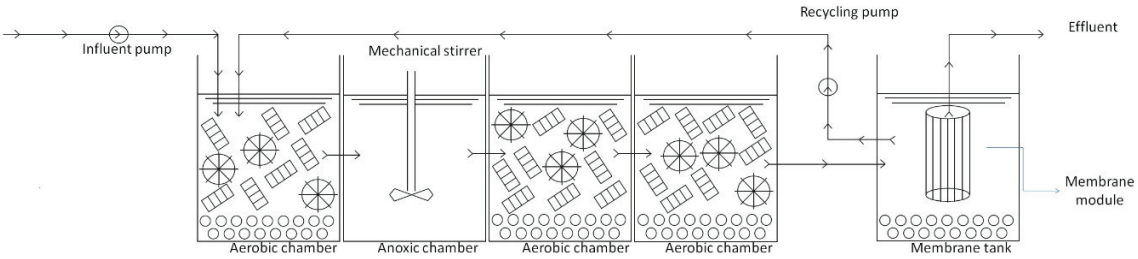

Figure 1 – Configuration of the hybrid MBBR-MBR

The bioreactor was fed with salinity-amended urban wastewater from the start-up. To create this influent, urban wastewater was collected from the Los Vados WWTP in Granada, Spain, and stored in a tank. This wastewater was mixed with tap water amended with NaCl to rise its electric conductivity of 50 mS cm^{-1}. NaCl has been traditionally used to increase salinity of wastewater for the purpose of saline urban wastewater treatment (Cortes-Lorenzo et al., 2016). However, the use of other different salts in order to simulate urban wastewater mixed with seawater is a promising future prospect for saline wastewater treatment. The mixing was controlled electronically by a TOPAX LF1 conductivity module (Lutz-Jesco GmbH, Germany), which was connected to two Watson Marlow peristaltic pumps: one pumping from the regular urban wastewater tank and another from the 50 mS cm^{-1} salinity-amended tap water tank. A conductivity sensor measured the conductivity of the salinity-amended influent wastewater and its temperature continuously in the mixing tank, providing their values to the module. Automatically, the conductivity control changed the electric conductivity of the influent wastewater depending on the desired scenario of operation. The change in influent wastewater conductivity in the mixing tank was achieved by: addition of 50 mS cm^{-1}

electric conductivity salinity-amended tap water to increase the conductivity; addition of regular-salinity urban wastewater to decrease the conductivity. Prior to the experimentation process, the automatic conductivity control was tested and modified properly in order to provide accurate electric conductivities and in order to optimize the time needed to change water conductivity during cyclical conditions. The four salinity scenarios were: i) constant salinity at 6.5 mS cm^{-1} (3.6 g L^{-1} NaCl) (MC) ; ii) tidal-variable salinity with maximum electric conductivity of 6.5 mS cm^{-1} (3.6 g L^{-1} NaCl) for 6 h and minimum of natural urban wastewater conductivity (0.5 g L^{-1} NaCl) for 6 h (MV); iii) tidal-variable salinity with maximum electric conductivity of 8.5 mS cm^{-1} (4.8 g L^{-1} NaCl) for 6 h and minimum of natural urban wastewater conductivity (0.5 g L^{-1} NaCl) for 6 h (HV); iv) tidal-variable salinity with maximum electric conductivity of 4.5 mS cm^{-1} (2.4 g L^{-1} NaCl) for 6 h and minimum of natural urban wastewater conductivity (0.5 g L^{-1} NaCl) for 6 h (LV). The hydraulic retention time was set to 6 h, and the total suspended solids concentration in the systems was controlled around 2500 mg L^{-1}. A summary of the conditions tested are shown in Table S1.

2.2 Characterization of performance of the bioreactors

The determination of influent and effluent biological oxygen demand at day 5 (BOD_5), chemical oxygen demand (COD) and total suspended solids (TSS) were done following established protocols (APHA, 2012).

The measurement of nitrogenous ions NH_4^+, NO_2^- and NO_3^- was done by the means of ionic chromatography, following Gonzalez-Martinez et al. (2014). For this purpose, the samples were collected and immediately filtered in a 0.45 µm pore diameter filter, then immediately assayed on the ion chromatograph. The ion chromatograph used a Metrosep C2–150 cation column and a Metrosep A supp-4-250 anion column for measurements. Nitric acid/dipicolinic acid was used as

eluent for the cation column, while carbonate-bicarbonate was used as eluent for the anion columns. Calibration curves were developed for ammonium, nitrite and nitrate in order to achieve accurate measures with the ion chromatograph. The results were used to determine the amount of nitrogen entering and leaving the hybrid MBBR-MBR systems.

2.3 Kinetic characterization of bioreactor biomass

The kinetic characterization of the biomass in the bioreactors was done by the means of respirometric tests (Rodriguez-Sanchez et al., 2017a; 2017b). For each test, 1 L of sample was collected from the bioreactor. The sample was aerated for 18 h at 20 °C temperature in the dark. After aeration period, the sample was tested in a gas flux-static liquid respirometer BM-Advance Multipurpose. The sample was subjected to determination of heterotrophic kinetics, autotrophic kinetics, and endogenous respiration. The determination of heterotrophic and autotrophic kinetics was measured as oxygen consumption of substrate over time, and used the addition in three different dilutions (50%, 80% and 100%) of 500 mg L^{-1} $NaCOOCH_3$ and of 150 mg L^{-1} NH_4Cl for heterotrophic and autotrophic kinetics, respectively. The determination of endogenous respiration was done by measuring oxygen consumption in the non-aerated sample. All tests were run at pH 7.5 ± 0.25 and 20 °C. Examples of the respirometric tests for the heterotrophic and autotrophic biomass for the variable salinity conditions of 4.5 and 8.5 mS cm^{-1} are shown in the supplementary material (Fig. S1).

2.4 Biomass sampling, DNA extraction and massive parallel sequencing procedure

Biomass samples were collected from the membrane biofouling and the mixed liquor in the bioreactor following Gonzalez-Martinez et al. (2015). Sampling time between samples was of two weeks. The samples were taken when the systems were operating under steady state conditions. Biofouling samples were submerged in sterile saline solution (0.9% NaCl) previous to centrifugation. Samples from biofouling and mixed liquor were centrifuged at room temperature during 10 min at 821.73 g for biomass-liquid separation. The biomass was kept at -20 °C for a period not exceeding 7 days before being subjected to DNA extraction using the FastDNA SPIN Kit for Soil (MP Biomedicals, Solon, OH, USA) and following the manufacturer's protocol. The DNA extracts were kept at -20 °C and sent to Research and Testing Laboratory (Lubbock, TX, USA) for massive parallel sequencing amplification procedure. This was done using the Illumina MiSeq apparatus and the Illumina MiSeq Reagents Kit v3. The amplification of DNA extracts targeted the V1-V3 hypervariable regions of the 16S rRNA gene of *Bacteria* domain through the utilization of primer pair 28F-519R and PCR conditions given in Rodriguez-Sanchez et al. (2018).

2.5. Bioinformatics pipeline for target gene massive parallel amplification

The processing of raw data from massive parallel sequencing procedure was done using mothur (Schloss et al., 2009). First, the paired-end sequences were merged into contigs avoiding the generation of ambiguous bases in the overlap region due to differences in same-position nucleotide Phred scores (Unno, 2014). The contigs were then screened to remove sequences with > 0 ambiguous bases and > 8 homopolymers. The remaining contigs were aligned against the MiDAS S123 2.1.3 release (McIlroy et al., 2017), which was previously aligned against the SiLVA nr v128 release; both alignments used a kmer searching method with 8 bp kmer size and Needleman alignment conditions. The aligned sequences were forced to start and end at the primers positions,

removing all sequences that failed to align properly. The remaining contigs were then checked for chimeras using VSEARCH (Rognes et al., 2015) implemented in mothur and considering a self-reference for chimera detection. All non-chimeric contigs were then taxonomically classified using the MiDAS S123 2.1.3 release as template and using the k nearest neighbor method searching by kmers of 8 bp size. All contigs that failed to classify as *Bacteria* domain were eliminated from the analysis. Then, contigs were clustered into OTUs in a 97% similarity threshold using VSEARCH implemented in mothur and through the abundance-based greedy clustering method (Westcott & Schloss, 2015; Schloss, 2016). After clustering, all singleton OTUs were removed from the analysis, and the remaining sequences within each OTU were used to compute a consensus taxonomy for each OTU.

2.6 Coverage analysis and diversity indices of target gene massive parallel sequencing samples

The sequencing coverage of each sample was checked by redundancy abundance-weighted coverage calculations using NonPareil software (Rodriguez-R & Konstantinidis, 2014a). The computations were done taking a 50% minimum overlap and a 95% minimum identity and 1000 sequences query set size, as standard parameters offered by the software (Rodriguez-R & Konstantinidis, 2014b). The α-diversity indices of Shannon and Simpson, were calculated using mothur.

2.7 Exploration of massive parallel sequencing samples OTU structure and composition of oligotypes of biofouling relevant OTUs

The reads of all massive parallel sequencing generated through the bioinformatics pipeline were taken for the similarity analysis of the samples studied, applying the statistical principles of compositional statistics (Bian et al., 2017; Gloor et al., 2017). For an exploration of the data, the OUT

tables and composition of oligotypess were treated using zComponents package implemented in R software, subjected to a Bayesian multiplicative replacement of zero values using the count zero multiplicative method. The treated data was then transformed by the centered log-ratio (clr) using CoDaPack software. The transformed data was subjected to a singular value decomposition (SVD) utilizing R in order to obtain differences among samples derived from their OTU variance. The results from the SVD were plotted in principal components analysis (PCA) manner using R. For quantitative analyses, the zero replacement and clr were conducted by generating a distribution using the data and computed by 128 Monte-Carlo replicates drawn from a Dirichlet distribution using ALDEx2 package implemented in R. The obtained data was then used for calculation of the expected effect size between biofouling and mixed liquor biomass for each salinity scenario.

2.8 Analysis of dissimilarity to determine OTUs important for biofouling

The structure of OTUs was analyzed in order to observe which OTUs contributed more to dissimilarity among samples. This was done by the means of SIMPER analysis, which was computed based on Bray-Curtis distance using PASTv3 software. The samples were clustered in 8 different groups, attending to influent maximum salinity (4.5, 6.5 or 8.5 mS cm^{-1}), salinity conditions (constant or variable) and biomass characteristics (membrane biofouling or mixed liquor).

2.9 Oligotyping analysis of OTUs of interest for biofouling

The OTUs of interest were defined as those with > 5% in at least one sample of biofouling at any given operational conditions and with > 1% dissimilarity contribution as per SIMPER analysis. For oligotyping, an analysis based on Shannon entropy was calculated for all aligned sequences within each OTU separately (Eren et al., 2014). Then, unraveling of the composition of oligotypes for each

of the OTUs was done based on Shannon entropy results and by iterative computation by increasing the number of highest entropy components for oligotypes structure generation until all oligotypes with > 100 sequences attained a total purity score > 0.90 (Okazaki et al., 2017). Removal of noise during the oligotyping process was set as: i) each oligotype had to appear in at least one sample; ii) each oligotype had to account for at least 1% relative abundance in at least one sample; iii) each oligotype had a substantive abundance of 30 (McLellan et al., 2014).

2.10 Multivariate redundancy analysis

The dominant OTUs in the global community were used to compute a multivariate redundancy analysis (RDA) in order to capture their susceptibility to environmental parameters of influent BOD_5, COD, TN and salinity loading, and to the performance of the bioreactors. For this purpose, the clr-escalated OTU community structure was taken. On the other hand, the values of environmental parameters were escalated to Log(variable+1) when needed. With both datasets, a multivariate redundancy analysis was done by 499 unconstrained Monte-Carlo simulations within a full permutation model using Canoco 4.5 for Windows (Gonzalez-Martinez et al., 2016b). Two RDA linking influent characteristics with OTUs were calculated in order to observe trends among HV, MV and LV scenarios, and between MV and MC scenarios, separately.

3. Results and discussion

3.1 Performance parameters of the bioreactors under different salinity conditions

The organic matter removal performance of the bioreactors under the four salinity conditions, measured as BOD_5 and COD, was efficient. The constant salinity scenario attained a performance of 98.09% and 88.55%, respectively. The scenarios of tidal-like variable salinity with peak salinity at

4.5, 6.5 and 8.5 mS cm^{-1} obtained, respectively, 99.37% and 80.44%, 99.51% and 88.64%, and 90.44% and 76.05% for BOD_5 and COD. The lower values obtained for the 8.5 mS cm^{-1} conditions and the similarities between the other scenarios could indicate that the hybrid MBBR-MBR was affected by saline influents at peak salinities higher than 6.5 mS cm^{-1}.

On the other hand, the removal of nitrogen was of poor efficiency. The variable salinity scenarios removed 59.59 ± 2.09% at 4.5 mS cm^{-1} peak, 30.85 ± 8.18% at 6.5 mS cm^{-1}, and 25.15 ± 2.01% for 8.5 mS cm^{-1} peak. For the constant 6.5 mS cm^{-1} salinity scenario the nitrogen removal was of 29.34 ± 7.00%. This trend showed that ammonium oxidation efficiency dropped dramatically when the peak salinity increased past the 4.5 mS cm^{-1}. Therefore, total nitrogen removal was affected when salinity higher than about 2.4 g L^{-1} was encountered in the bioreactor. It has been claimed that sharp increase in salinity could cause an inhibition of nitrification in hybrid MBBR-MBR systems (Leyva-Diaz et al., 2017).

In general, it has been shown that acclimatization of hybrid MBBRMBR systems to salinity after steady-state operation under regular-salinity wastewater allows for adaptation of biomass and thus yield efficient organic matter removal and nitrification (Di Trapani et al., 2014). In such case, COD removal and ammonium oxidation were of 81.20% and 63.20%, respectively, operating at 15 g L^{-1}. On the other hand, it has been proposed that start-up of the MBBR-MBR system under saline influent conditions results in lower COD elimination and NH_4^+ oxidation (Rodriguez-Sanchez et al., 2017a; Rodriguez-Sanchez et al., 2017b; Rodriguez-Sanchez et al., 2018).

The performance data collected under saline influent operation in this experiment suggested that there is a very important implication of maximum salinity values in the treatment of saline wastewater. Future implementation of full-scale saline wastewater treatment systems must take into account the maximum salinity variation in their influents in order to obtain good performances, especially in nitrogen removal.

3.2 Kinetic characterization of the bioreactors

The respirometric tests developed over the biomass in the systems showed differences between the salinity scenarios (constant 6.5, variable 6.5, variable 4.5 and variable 8.5 mS cm^{-1}) in terms of kinetic Monod growth model parameters (Table S2) and rate of substrate utilization (r_{su}) (Fig. 2). The r_{su} for both autrotrophic and heterotrophic biomass clearly differed between the constant salinity and variable salinity scenarios. Under the constant salinity scenario, the r_{su} remained constant regardless of the substrate added, while for the variable salinity conditions the biomass had faster kinetics with higher substrate concentrations. These results showed that the kinetics of the hybrid MBBR-MBR was affected by influent salinity conditions. This behavior could be caused by the changing conditions of the variable salinity scenarios, forcing the microbial biomass to adapt and therefore favoring those who had a marked r-strategist growth pattern. On the other hand, constant salinity would favor microbial phylotypes adapted to salinity conditions, which could develop under a k-strategist growth pattern.

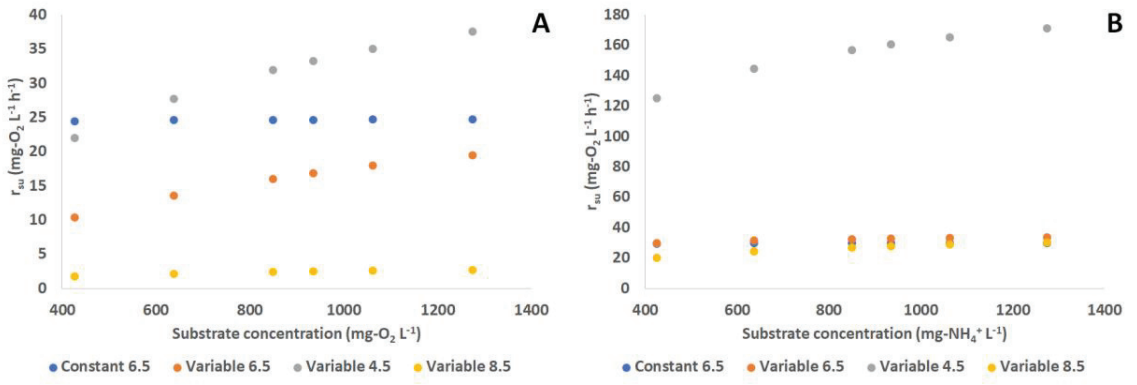

Figure 2 – Values of the rates of substrate utilization (r_{su}) of the hybrid MBBR-MBR under the four salinity conditions (constant 6.5, variable 6.5, variable 4.5 and variable 8.5 mS cm^{-1}) for the heterotrophic (A) and autotrophic (B) biomass.

Lower influent salinity concentrations were related to faster kinetics in both heterotrophic and autotrophic biomass. For heterotrophs and autotrophs, 4.5 mS cm^{-1} attained the fastest kinetics. On the other hand, 8.5 mS cm^{-1} attained the slowest kinetics in all cases. For heterotrophs, constant salinity conditions yielded faster kinetics at 6.5 mS cm^{-1}, and only the variable 8.5 mS cm^{-1} scenario showed significantly lower kinetics than all others. Interestingly, constant salinity conditions at 6.5 mS cm^{-1} yielded faster kinetics that variable conditions at 6.5 mS cm^{-1} scenario. In this sense, the heterotrophic kinetics showed that the biomass was more stressed under variable salinity than under constant salinity. In the case of autotrophs, the influent salinity concentration had a profound impact, with kinetics for salinities under 4.5 mS cm^{-1} reaching values 20-fold to 30-fold higher compared with the other scenarios. This was related to the higher TN removal performance of 4.5 mS cm^{-1} scenario with respect to the others. The slower kinetics for the 8.5 mS cm^{-1} scenario were related to its lower removal performance in terms of BOD_5, COD and TN. These results are linked to those obtained for performance, with faster kinetics being related to higher removal efficiencies.

The cell decay rate was 4-fold higher for the constant salinity conditions than for the variable salinity conditions. This result showed that influent salinity conditions pressure the microbial community in the hybrid MBBR-MBR and cause a much higher cell death than the variable salinity conditions.

The kinetics results demonstrated that the microbial communities had a different behavior for constant and variable salinity conditions. As well, lower microbial activity was found for higher peak salinities, which affected drastically the kinetics of autotrophic biomass. Slower kinetics for higher peak salinities suggested that operation of hybrid MBBR-MBR systems under saline wastewater should take into account this fact in order to develop tools for efficient treatment, such as increasing the hydraulic retention time at higher salinity peaks.

3.3 Metagenomic coverage of target gene massive parallel sequencing samples

The metagenomic coverage showed that all samples successfully captured the bacterial diversity of the ecosystems analyzed. This was highlighted by the high sequencing coverages (minimum of 99.67%), which suggested that contigs obtained by massive parallel sequencing offered a description of all bacterial species within the biological samples studied. The high actual sequencing efforts (that which was actually sequenced, with minimum of 21.07 Mbp) and the low expected required efforts for nearly-complete coverage (how much sequencing was expected to be needed to reach the limit of 100% coverage, which was greater than 0 only in LVFB1 sample) also suggested that massive parallel sequencing could determine all bacterial species in the biological samples (Table S3).

3.4 Diversity indices of target gene massive parallel sequencing samples

The α-diversity indices of all samples showed that all of them had high evenness and diversity, as determined by the values of Shannon (H) and inverse Simpson (1-D) indices. Overall, evenness was higher at constant salinity conditions, followed by 6.5 mS cm^{-1} tidal-like variable salinity. The lowest value was related to 4.5 mS cm^{-1} tidal-like variable salinity. With respect to diversity, as observed by Shannon index, the highest value corresponded to constant salinity conditions, followed by 8.5 mS cm^{-1} tidal-like variable scenario. In general, both biofouling and mixed liquor samples had similar evenness and diversities (Table S4). It has been reported that salinity build-up in MBR systems trended to increase the Shannon diversity index values, which was reported to be related to the growth of halotolerant bacteria replacing those that could not adapt to increasing salinity conditions (Luo et al., 2016). On the other hand, the higher evenness and diversity at constant salinity conditions suggested that tidal-like variable influent salinity was detrimental for the bacterial community as a whole, promoting fewer phylotypes that could adapt to the cycles of salinity/no-

salinity conditions. This result aimed that operation under variable salinity conditions create an environmental stress for bioreactor communities and thus leads to the necessity of a careful monitoring of such systems to achieve good performance.

The PCA plot showing the results from the singular value decomposition of clr escalated OTU table demonstrated that there was higher similarity among HV, MV and LV samples than among MC samples, with a clear grouping of samples with respect to influent salinity conditions (Fig. 3). This suggested that bacterial OTU diversity in the mixed liquor and biofouling at variable salinity scenarios was much similar than for constant salinity scenario. The similarity observed between attached biofilm and suspended biomass in tidal-like variable scenarios could be caused by difficult adaptation of the bacterial OTUs to variable salinity, reducing the diversity in the environments. The calculation of the effect size for the OTU tables of the four scenarios yielded many OTUs with statistically significant differences between the mixed liquor and the biofouling among the four salinity scenarios (> 1 effect size) (Fig. 4). This result is supported by previous literature in which it was shown that biological samples in MBR systems subjected to different salinity build-ups tend to cluster when salinity conditions were identical (Luo et al., 2016). In this sense, these results suggested that influent salinity conditions play a very important role in the development of bacterial communities in membrane-based technologies.

3.5 Exploration of massive parallel sequencing samples OTU structure

The PCA plot showing the results from the singular value decomposition of clr escalated OTU table demonstrated that there was higher similarity among HV, MV and LV samples than among MC samples, with a clear grouping of samples with respect to influent salinity conditions (Fig. 3). This suggested that bacterial OTU diversity in the mixed liquor and biofouling at variable salinity scenarios was much similar than for constant salinity scenario. The similarity observed between attached biofilm and suspended biomass in tidal-like variable scenarios could be caused by difficult

adaptation of the bacterial OTUs to variable salinity, reducing the diversity in the environments. The calculation of the effect size for the OTU tables of the four scenarios yielded many OTUs with statistically significant differences between the mixed liquor and the biofouling among the four salinity scenarios (> 1 effect size) (Fig. 4). This result is supported by previous literature in which it was shown that biological samples in MBR systems subjected to different salinity build-ups tend to cluster when salinity conditions were identical (Luo et al., 2016). In this sense, these results suggested that influent salinity conditions play a very important role in the development of bacterial communities in membrane-based technologies.

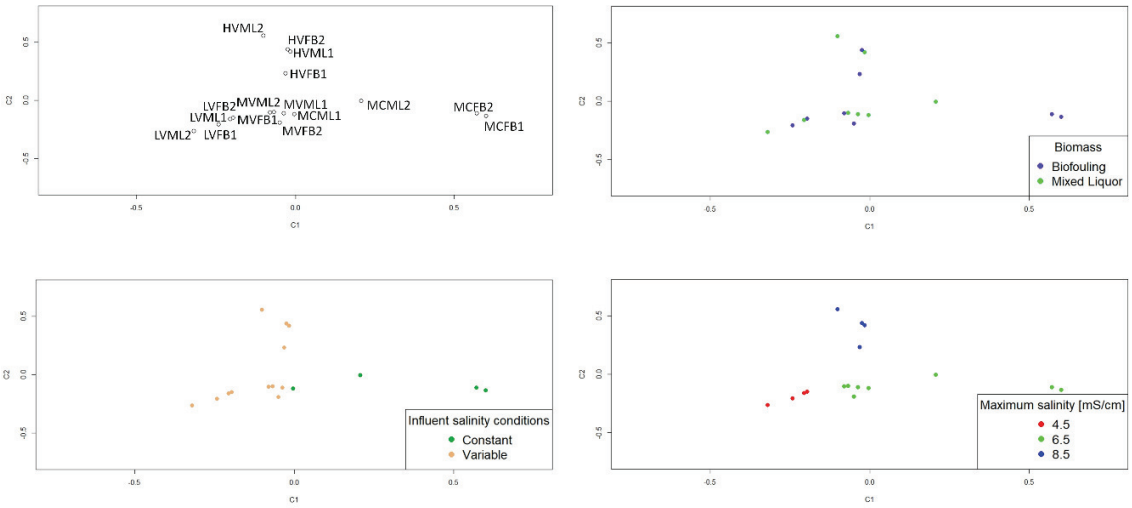

Figure 3 – Principal components analysis ordination plot of singular value decomposition of the clr-transformed OTU reads table for the massive parallel sequencing samples (HV: 8.5 mS cm^{-1} peak tidal-like variable salinity; LV: 4.5 mS cm^{-1} peak tidal-like variable salinity; MV: 6.5 mS cm^{-1} peak tidal-like variable salinity; MC: 6.5 mS cm^{-1} constant salinity; FB: Fixed Biofilm (Biofouling); ML: Mixed Liquor (Suspended Biomass))

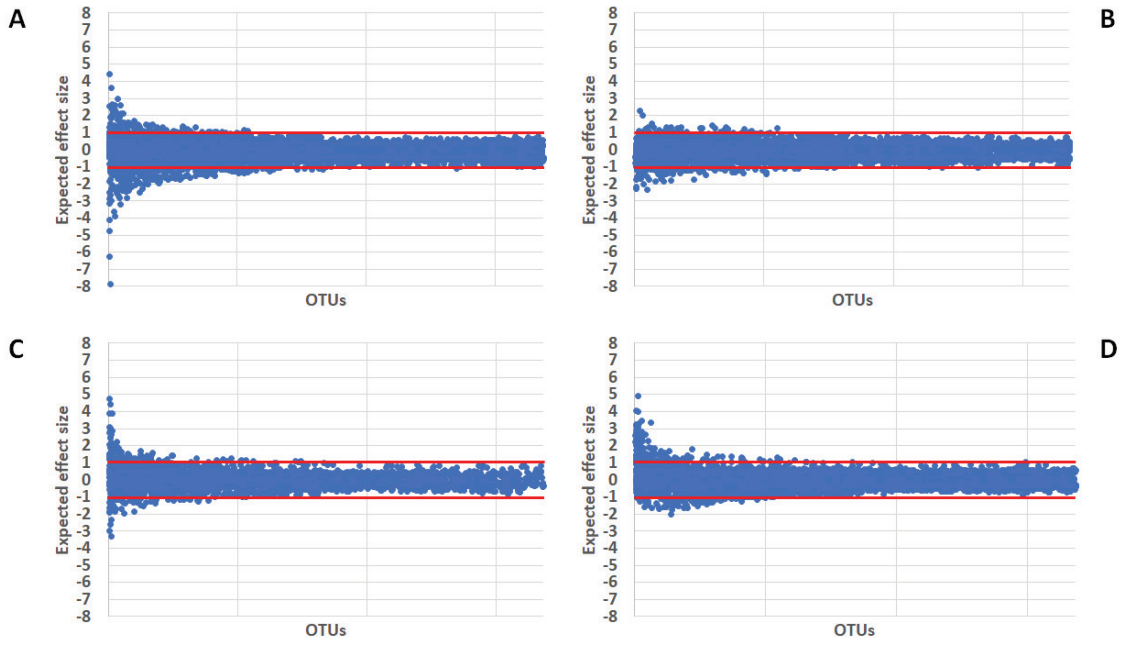

Figure 4 – Size effect of the OTU table comparing the biofouling and mixed liquor communities for the four salinity scenarios (A: HV - 8.5 mS cm^{-1} peak tidal-like variable salinity; B: LV - 4.5 mS cm^{-1} peak tidal-like variable salinity; C: MV - 6.5 mS cm^{-1} peak tidal-like variable salinity; D: MC - 6.5 mS cm^{-1} constant salinity)

3.6 Bacterial community structure of target gene massive parallel sequencing samples

3.6.1 OTUs of importance for biofouling

Among the dominant OTUs in 16S rRNA gene massive parallel sequencing samples, only 5 were considered as representative for biofouling (Fig. 5). BF_Otu000001 contributed to biofouling in all tidal-like variable scenarios, but was absent at constant salinity conditions. In the same manner, BF_Otu000002 and BF_Otu000015 were only important for HV, while BF_Otu000003 and BF_Otu000004 were present only at MV and LV scenarios, respectively. On the other hand, BF_Otu000009 was important only in the biofouling at MC. All these OTUs accounted for more than 1% dissimilarity contribution following the results of SIMPER analysis (Table S5). In this way, regardless of the similarities found in evenness, diversity and bacterial community structure as

shown by α-diversity and SVD/PCA analyses, OTUs causing biofouling were very dependent on the salinity conditions. This may indicate that biofouling process is caused by the presence of certain adapted OTUs with biofilm formation capacity that are unique for each set of conditions tested, therefore suggesting that biofouling is a more local-driven process in microbiological terms. It has been reported that influent wastewater salinity exerts an influence over the biofouling microbial communities, showing that influent wastewater salinity conditions dramatically change the bacterial communities in the membrane fouling of lab-scale MBR systems (Guo et al., 2015). This supports the results found in this study. Moreover, the presence of core microorganisms causing membrane biofouling, in contrast to the presence of randomly-selected biofouling related phylotypes, has also been reported elsewhere (Matar et al., 2017).

This also supports the results obtained in this study, in which different bacterial OTUs with different taxonomies were found to prevail in membrane biofouling under different salinity conditions.

BF_Otu000001, classified as a *Xanthomonadaceae* family member, showed to be important for biofouling at variable salinity conditions, and dominated biofouling at LV (2.56–33.00%). OTU BF_Otu000002 was also classified as *Xanthomonadaceae* family, attaining high abundance at HV (16.93–21.70%). The other biofouling-related OTU for HV conditions, BF_Otu000015 (1.32–5.33%), was classified as *Thermomonas* genus, which also belongs to *Xanthomonadaceae* family. Moreover, at MV conditions, the most important OTU in terms of biofouling, BF_Otu000003 (11.28–21.10%), was related to *Rhodanobacter* genus. At LV, OTU BF_Otu000004 (4.90–6.89%), affiliated to *Mizugakiibacter* genus, was also related to biofouling. Both *Rhodanobacter* genus and *Mizugakiibacter* genus are members of *Xanthomonadaceae* family. Thus, *Xanthomonadaceae* family was found to cause biofouling at all tidal-like variable conditions, highlighting its negative role on fouling in membrane processes *Rhodanobacter* genus has been found in MBBR-MBR systems (Leyva-Diaz et al., 2015a; Rodriguez-Sanchez et al., 2018) and its nitrite oxidation capacity in

autotrophic nitrogen removal systems has been reported (Gonzalez-Martinez et al., 2016a). *Rhodanobacter* genus, as well as *Mizugakiibacter* genus, can develop chemoautotrophic denitrification using ferrous iron (Wang et al., 2017). Nevertheless, metabolic capability of *Mizugakiibacter* also contained aerobic oxidation of multiple organic substrates (Kojima et al., 2017). The metabolic flexibility of *Rhodanobacter* and *Mizugakiibacter*, which can grow under both aerobic and anaerobic conditions, give them an ecological advantage for growth in both aerobic and anaerobic zones of biofouling. On the other hand, *Thermomonas* genus can oxidize ammonium fast and efficiently at high concentrations and utilize *N*-acetylglucosamine as organic carbon source under aerobic conditions (Wang et al., 2014; Ali et al., 2016; Rodriguez-Sanchez et al., 2017b). On the contrary, at MC conditions, *Xanthomonadaceae* family members did not appear as important biofouling OTUs, instead showing the presence of genus *Mycobacterium*-related bacteria in BF_Otu000009.

Among all salinity scenarios, expected effect size suggested that there were no significant differences for OTUs important in biofouling at LV and MC. In this sense, the results suggested that biofouling-related OTUs at LV and MC were not promoted in membrane biofilm with respect to mixed liquor. For the other scenarios: BF_Otu000003 for MV; and BF_Otu000001, BF_Otu000002, BF_Otu000015 for HV; were found to have significant different abundance in biofouling compared to mixed liquor. It is possible that certain biofouling-related OTUs in these salinity scenarios could find a relevant ecological niche in membrane biofilm, thus attachment to surfaces would promote their growth.

The results from the bacterial community structure of biofouling under the four salinity conditions tested demonstrated that salinity conditions greatly affected the dominant phylotypes in biofouling. This was shown in the high relative abundance of *Xanthomonadaceae* family at tidal-like variable conditions and its absence at constant salinity conditions. In addition, the proliferation of specialized

biofouling OTUs at all different conditions suggested that this process is driven by local, unique phylotypes that are not consistent at all conditions tested. This result suggested that control of biofouling by quorum sensing inhibitors (Dobretsov et al., 2009), which has been proposed as a plausible strategy for mitigation of biofouling (Siddiqui et al., 2015), is in practice more difficult to control in saline wastewater, since biofouling important OTUs (BF_Otu000001, BF_Otu000002, BF_Otu000003, BF_Otu000004, BF_Otu000009, BF_Otu000015) seemed to be very case-specific. In this way, more tests should be derived in order to elucidate the practical application of quorum sensing biofouling in membrane-based technologies.

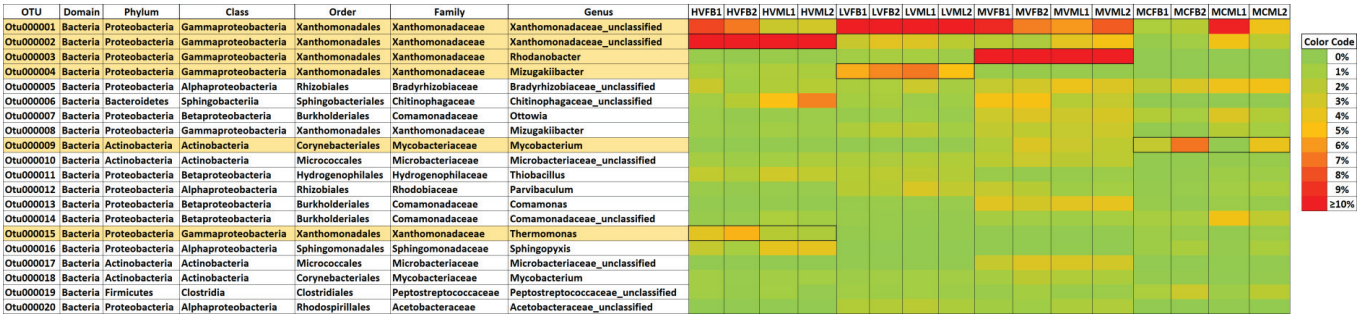

Figure 5 – Heat map of dominant OTUs. OTUs that were found important for biofouling at any given salinity scenario are highlighted (HV: 8.5 mS cm^{-1} peak tidal-like variable salinity; LV: 4.5 mS cm^{-1} peak tidal-like variable salinity; MV: 6.5 mS cm^{-1} peak tidal-like variable salinity; MC: 6.5 mS cm^{-1} constant salinity; FB: Fixed Biofilm (Biofouling); ML: Mixed Liquor (Suspended Biomass))

3.6.2 Dominant mixed liquor OTUs

Some of the biofouling-related OTUs were also dominant in the mixed liquor samples, such as BF_Otu000001 for MV and MC; BF_Otu000002 for HV, LV, MV and MC; BF_Otu000003 for MV; BF_Otu000004 for LV; or BF_Otu000009 for MC. Nevertheless, other OTUs were dominant members in the mixed liquor, such as BF_Otu000006 and BF_Otu000016 for HV; BF_Otu000012 for LV; BF_Otu000005 and BF_Otu000013 for MV; and BF_Otu000005, BF_Otu000007 and BF_Otu000014 for MC. Among these OTUs, all had a dissimilarity contribution higher than 1% as per SIMPER analysis except for BF_Otu000016 (0.9928%) and BF_Otu000014 (0.7108%), suggesting that they defined dissimilarity of biological samples (Table S5). All these OTUs were related to different phylogenies, namely *Chitinophagaceae* family, *Sphingopyxis* genus, *Parvibaculum* genus, *Bradyrhizobiaceae* family, *Comamonas* and *Ottowia* genera. *Ottowia* genus was found of importance in hybrid MBBR-MBR systems treating salinity wastewater due to their capability for complete heterotrophic conversion of NH^+ to N_2 and biofilm formation (Rodriguez-Sanchez et al., 2018). *Comamonas* genus has also been proposed as heterotrophic nitrifier (Gonzalez-Martinez et al., 2014). Many *Sphingopyxis* and *Parvibaculum* genera strains are heterotrophic and have been isolated from activated sludge or marine environments (Kämpfer et al., 2002; Rosario-Passapera et al., 2011; Lai et al., 2012). None of these were taxonomically related with *Xanthomonadaceae* family, which showed a phylogenetic differentiation between mixed liquor communities and biofouling important OTUs (BF_Otu000001, BF_Otu000002, BF_Otu000003, BF_Otu000004, BF_Otu000009, BF_Otu000015). In this way, it is possible that growth of biofouling in hybrid MBBR-MBR systems treating saline wastewater is essentially driven by *Xanthomonadaceae* family and thus controlling this taxonomic group could enhance the protection of this technology against biofouling when treating saline influents.

3.6.3 Autotrophic ammonium oxidizers and autotrophic nitrite oxidizers

It has been demonstrated that the presence of autotrophic ammonium and nitrite oxidizers (AOB and NOB, respectively) in MBR systems helps prevent its biofouling (Sepehri & Sarrafzadeh, 2018). The observed diversity of these phylotypes within the hybrid MBBR-MBR systems was specifically analyzed, showing 26 OTUs classified as *Nitrobacter* genus, 36 as unclassified *Nitrosomonadaceae* family members, 14 as *Nitrosomonas* genus, 18 as *Nitrosospira* genus and 2 as uncultured *Nitrosomonadaceae* family members. Their relative abundance was low in the hybrid MBBR-MBR systems at all salinity scenarios, with mean values between 0.01% and 0.70% (Fig. S3). There was a higher representation of AOB than NOB at all salinity scenarios in both biofouling and mixed liquor. Also, nitrite oxidizing *Nitrobacter* seemed to be affected by variable salinity conditions, since its relative abundance was more than threefold higher in the constant salinity scenario than in all others, which suggested a high inhibition of autotrophic nitrite oxidation under variable salinity conditions. The unclassified *Nitrosomonadaceae* family members were the prevalent members of AOB found and were more abundant at constant salinity conditions and at 8.5 mS cm^{-1} variable salinity conditions, which were the scenarios with higher salinity loadings. In this sense, it is possible that this unclassified *Nitrosomonadaceae* is a halophile AOB.

Compared to other MBBR-MBR systems treating regular urban wastewater, there was a significant difference in the total relative abundance of both AOB (up to 7% of total community under regular salinity) and NOB (up to 1% under regular salinity conditions) (Leyva-Diaz et al., 2015a). Moreover, for regular conditions the dominant AOB were *Nitrosospira* and *Nitrosomonas* genera, while an unclassified *Nitrosomonadaceae* family member outcompeted these genera at saline wastewater treatment. In this sense, the influent salinity conditions do have an effect over the diversity and relative abundance of AOB and NOB.

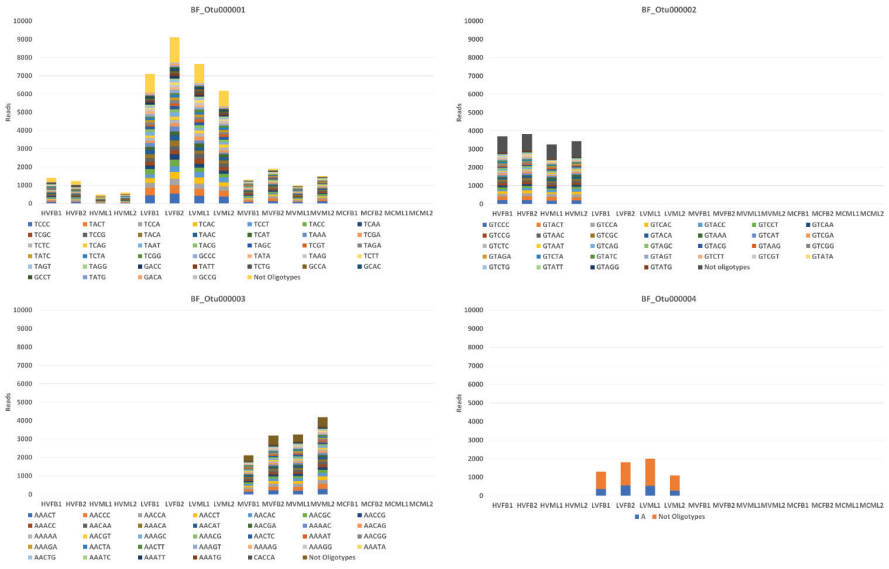

Figure 6 – Composition of oligotypes of OTUs important for biofouling (HV: 8.5 mS cm^{-1} peak tidal-like variable salinity; LV: 4.5 mS cm^{-1} peak tidal-like variable salinity; MV: 6.5 mS cm^{-1} peak tidal-like variable salinity; MC: 6.5 mS cm^{-1} constant salinity; FB: Fixed Biofilm (Biofouling); ML: Mixed Liquor (Suspended Biomass))

3.7 Oligotype structure of OTUs of interest in biofouling

The important OTUs in the biofouling (BF_Otu000001, BF_Otu000002, BF_Otu000003, BF_Otu000004, BF_Otu000009, BF_Otu000015) were subjected to an oligotyping analysis in order to check for certain oligotypes involved in the formation of biofouling (Fig. 6). Among these, OTUs BF_Otu000009 and BF_Otu000015 did not have any oligotypes meeting the criteria imposed during the analysis (≥1% relative abundance in at least one sample, substantive abundance ≥30). For BF_Otu000004, which was related to *Mizugakiibacter* genus, the composition of oligotypes showed only one oligotype, accounting for 25–30% of total OTU abundance. For the remaining OTUs BF_Otu000001, BF_Otu000002 and BF_Otu000003, the oligotype structure showed a myriad of oligotypes with similar abundance contribution at all samples were the OTU was found. In this sense, the dominant biofouling OTUs for the four salinity scenarios did not showed the predominance of a certain oligotype related with biofouling. A PCA analyses over the oligotype structure of the OTU BF_Otu000001 showed that variable salinity scenarios had more similar oligotypes structure (Fig. S2). Also, there was a differentiation between the fixed and suspended biomass with respect to composition of oligotypes for OTUs BF_Otu000002, BF_Otu000003 and BF_Otu000004. In this sense, the data showed that different salinity conditions and different biomass configurations affected the composition of oligotypess of biofouling-relevant OTUs in the experiment.

Thus, even though biofouling process could be related to certain OTUs that even shared phylogeny at family level in some cases, there were not preferred oligotypes in terms of biofouling, showing the capability of many different oligotypes to form biofilms over membranes. Furthermore, no differences in oligotypes structure were found between biofouling and mixed liquor samples, suggesting that biofouling-related composition of oligotypes was shared with mixed liquor. Therefore, OTU was the most detailed phylogenetic trait that defined the potential for biofouling,

and relative abundance of all oligotypes within an OTU was the only parameter discerning the importance of the OTU in biofouling.

3.8 Multivariate redundancy analysis

There was a clear linkage between several dominant OTUs in the bioreactors at different salinity scenarios and the removal efficiency of organic matter and nitrogen (Fig. 7A). Among these, OTUs BF_Otu000013, BF_Otu000007 and BF_Otu000003 were strongly correlated with COD and BOD_5 removal. These were dominant OTUs related to *Comamonas*, *Ottowia* and *Rhodanobacter* genera, respectively. These three genera have been reported from membrane-based systems treating saline wastewater, and their versatile metabolic capabilities for organic matter removal, nitrification and/or denitrification have been reported (Rodriguez-Sanchez et al., 2017a; 2017b; 2018). On the other hand, OTUs BF_Otu000001, BF_Otu000004 and BF_Otu000012, affiliated to *Xanthomonadaceae* family and *Mizugakiibacter* and *Parvibaculum* genera were strongly correlated with TN removal. In this sense, these three phylotypes could be of importance in nitrification and/or denitrification processes in hybrid MBBR-MBR systems treating saline wastewater. Accordingly, these three groups have been described for denitrifying metabolisms, such as autotrophic denitrification for *Xanthomonadaceae* family in bench-scale reactors treating synthetic wastewater (Xu et al., 2015), reduction of nitrate to nitrite in pure cultures of *Mizugakiibacter sediminis* strains (Kojima et al., 2017) and nitrite reduction in biological denitrifying processes related to *Parvibaculum* genus (Li & Lu, 2017). Moreover, *Mizugakiibacter* has been reported as denitrifier in membrane-based wastewater-treatment technologies (Rodriguez-Sanchez et al., 2018), as well as *Parvibaculum* (Sanchez, 2018).

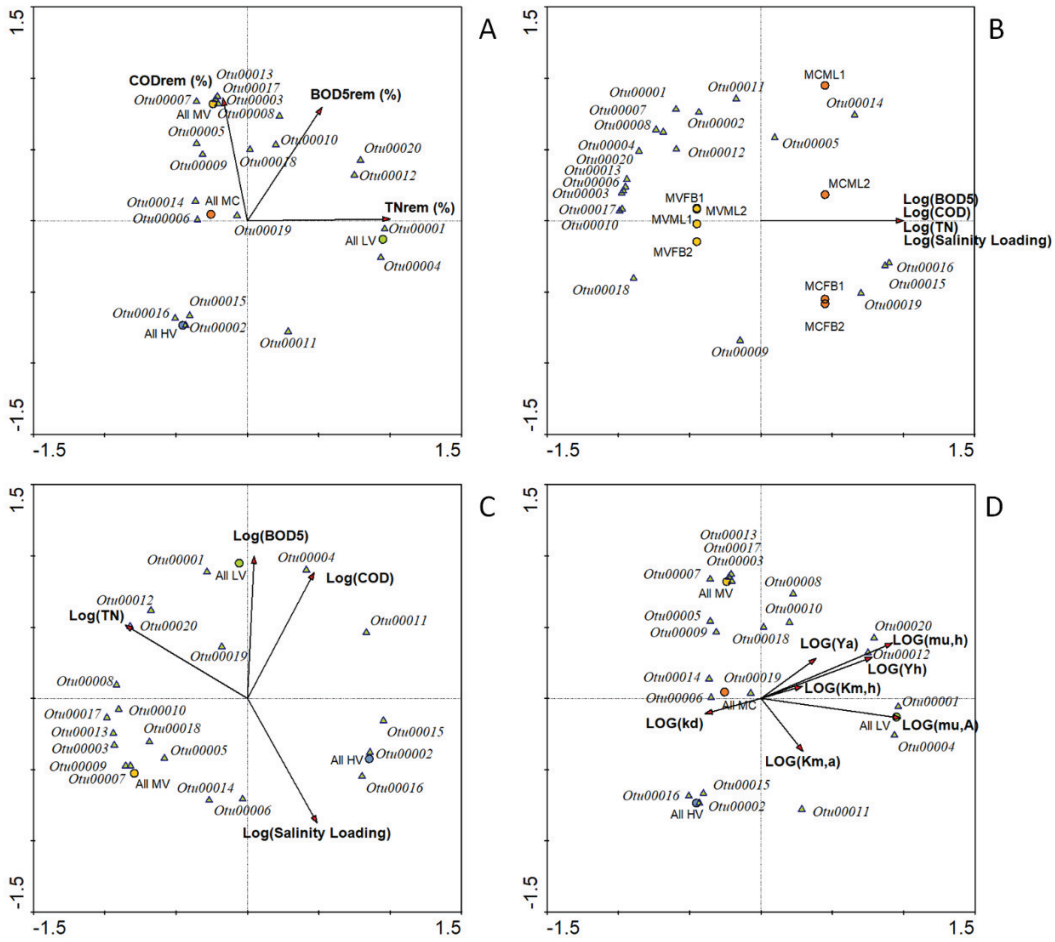

Figure 7 – Multivariate redundancy analyses linking removal efficiency (A), influent characteristics (B and C), and kinetic Monod parameters (D) with dominant OTUs in biofouling (HV: 8.5 mS cm^{-1} peak tidal-like variable salinity; LV: 4.5 mS cm^{-1} peak tidal-like variable salinity; MV: 6.5 mS cm^{-1} peak tidal-like variable salinity; MC: 6.5 mS cm^{-1} constant salinity; FB: Biofouling ML: Mixed Liquor)

The RDA comparing MC and MV scenarios showed that the majority of dominant OTUs were promoted at lower influent BOD_5, COD, TN and salinity loading (Fig. 7B). OTUs important for biofouling at these scenarios, such as BF_Otu000001, BF_Otu000003 or BF_Otu000009, were negatively correlated with these variables.

On the other hand, the OTUs important for biofouling for the tidalvariable salinity scenarios appeared to be influenced differently by organic matter, nitrogen and salinity in the influent (Fig.

7C). In this sense, OTUs BF_Otu000001 and BF_Otu000004 were positively correlated with influent organic matter and negatively with influent total nitrogen and salinity. The opposite occurred for OTUs BF_Otu000002, BF_Otu000006 and BF_Otu000015. Thus, the RDA for tidal-variable scenarios showed that important biofouling OTUs were indeed sensitive to influent conditions, but changes in these would trigger the apparition of different biofouling OTUs, thus not eliminating this operational problem. These findings have also been reported by previous research conducted over the microbial communities in membrane biofilm of membrane bioreactors operating under salinity shocks (Guo et al., 2015) and over the membrane biofilm of different full-scale membrane bioreactors (Matar et al., 2017). In light of this, different operational conditions did not offer better scenarios for mitigation of biofouling, but different ecological niches for biofouling-forming OTUs.

For microbial kinetics, OTUs BF_Otu00012 and BF_Otu00020 were strongly correlated with maximum growth rate for the heterotrophic fraction and BF_Otu00001 and BF_Otu00004 with maximum growth rate for the autotrophic fraction. These data suggested that *Xanthomonadaceae* family members were strongly correlated with ammonium oxidation activity, while *Parvibaculum* genus and an *Acetobacteraceae* family member were correlated with organic matter degradation in the system, showing an r-strategist behavior.

Other OTUs were strongly and negatively correlated with half saturation constant for autotrophs, classified as *Rhodanobacter*, *Ottowia* and *Comamonas* genera and a *Microbacteriaceae* family member. This suggested that these phylotypes were correlated with ammonium oxidation in the system, showing a k-strategist behavior. Three phylotypes were strongly and negatively correlated with half saturation constant for the heterotrophic fraction, namely *Thermomonas* genus, *Sphingopyxis* genus and a *Xanthomonadaceae* family member. Again, *Xanthomonadacae* family members were correlated with organic matter degradation, showing a k-strategist pattern.

In this way, this result suggested that *Xanthomonadaceae* family members have a beneficial effect over the hybrid MBBR-MBR system, in spite of their prevalence in biofouling. Thus, control of *Xanthomonadaceae* in order to reduce biofouling might impact the performance in ammonium oxidation and organic matter degradation of the bioreactor. More research is needed in order to discern the beneficial or detrimental control of *Xanthomonadaceae* family phylotypes in hybrid MBBR-MBR systems treating saline wastewater.

4. Conclusions

The investigation of the bacterial communities in the bioreactors showed that both mixed liquor and biofouling communities were more similar under variable salinity conditions than under constant salinity conditions, which could be attributed to low adaptability of wastewater bacteria to variable than to constant salinity regimes. Differences were observed in the relative abundance of dominant OTUs between biofouling and suspended biomass at all salinity scenarios, suggesting that biofouling was related to changes in relative abundance of biofouling-triggering OTUs. Variable salinity biofouling OTUs were related to several *Xanthomonadaceae* family members such as *Thermomonas* (4.54% relative abundance), *Rhodanobacter* (13.23%) or *Mizugakiibacter* (5.96%) genera; for the constant salinity conditions, *Mycobacterium* (4.60%) was the main biofouling-related OTU. Oligotyping analysis showed that OTUs important for biofouling had the same composition of oligotypes in attached and suspended biomass, and thus confirmed that biofouling differs from suspended biomass only in terms of relative abundance of certain biofouling-triggering OTUs (25.76–204.63% increase for biofouling-related OTUs). The effect of influent wastewater characteristics over biofouling communities was observed for the dominant OTUs, suggesting that variations in influent characteristics could promote different biofouling-related OTUs but would not stop the process. The results obtained aimed that operation of hybrid MBBRMBR under saline wastewater

conditions yields a performance very related to influent salinity conditions (maximum salinity and loading type), and prevention of its biofouling could be accomplished by targeting activity of a handful of phylotypes, and thus supporting the adequacy of quorum-sensing antibiofouling treatments.

Conflict of interests

The authors declare that no conflicts of interest arise from this work.

Acknowledgements

We would like to acknowledge the help given in this study by the Institute of Water Research and the Department of Civil Engineering at the University of Granada.

Appendix A. Supplementary data

Supplementary material related to this article can be found, in the online version, at doi:https://doi.org/10.1016/j.jwpe.2018.07.001.

References

Ali M, Chai LY, Min XB, Tang CJ, Afrin S, Liao Q, Wang HY, Peng C, Song Y-X, Zheng P (2016) Performance and characteristics of a nitritation air-lift reactor under long-term HRT shortening. Int Biodeterior Biodegrad 111 45–53.

American Public Health Association (APHA) (2012) Standard Methods for the Examination of Water and Wastewater, 22nd ed., American Public Health Association, Washington DC.

Bassin JP, Kleerebezem R, Muyzer G, Rosado AS, Van Loosdrecht MCM,

Dezotti M (2012) Effect of different salt adaptation strategies on the microbial diversity, activity, and settling of nitrifying sludge in sequencing batch reactors. Appl Microbiol Biotechnol 93: 1281–1294.

Bian G, Gloor GB, Gong A, Jia C, Zhang W, Hu J, Zhang H, Zhang Y, Zhou Z, Zhang J, Burton JP, Reid G, Xiao Y, Zeng Q, Yang K, Li J (2017) The gut microbiota of healthy aged Chinese is similar to that of the healthy young mSphere 2: e00327–17.

Cortes-Lorenzo C, Gonzalez-Martinez A, Smidt H, Gonzalez-Lopez J, Rodelas B (2012) Influence of salinity on fungal communities in a submerged fixed bed bioreactor for wastewater treatment. Chem Eng J 285: 562–572.

Di Trapani D, Di Bella G, Mannina G, Torregrossa M, Viviani G (2014) Comparison between moving bed-membrane bioreactor (MB-MBR) and membrane bioreactor (MBR) systems: influence of wastewater salinity variation. Bioresour Technol 162: 60–69.

Dobretsov S, Teplitski M, Paul V (2009) Mini-review: quorum sensing in the marine environment and its relationship to biofouling. Biofouling 25: 413–427.

Eren AM, Borisy GG, Huse SM, Mark Welch JL (2014) PNAS plus: from the cover: oligotyping analysis of the human oral microbiome. Proc Natl Acad Sci USA 111: E2875–E2884.

Fu C, Yue X, Shi X, Ng KK, Ng HY (2017) Membrane fouling between a membrane bioreactor and a moving bed membrane bioreactor: effects of solids retention time. Chem Eng J 309: 397–408.

Gloor GB, Macklaim JM, Pawlowsky-Glahn V, Egozcue JJ (2017) Microbiome datasets are compositional: and this is not optional. Front Microbiol 8: 1–6.

Gonzalez-Martinez A, Rodriguez-Sanchez A, Martinez-Toledo MV, Garcia- Ruiz MJ, Hontoria E, Osorio-Robles F, Gonzalez-Lopez J (2014) Effect of ciprofloxacin an- tibiotic on the partial-nitritation process and bacterial community structure of a submerged biofilter. Sci Total Environ 476–477: 276–287.

Gonzalez-Martinez A, Leyva-Díaz JC, Rodriguez-Sanchez A, Muñoz-Palazon B,

Rivadeneyra A, Poyatos JM, Rivadeneyra MA, Martinez-Toledo MV (2015) Isolation and metagenomic characterization of bacteria associated with calcium carbonate and struvite precipitation in a pure moving bed biofilm reactor-membrane bioreactor. Biofouling 31: 333–348.

Gonzalez-Martinez A, Rodriguez-Sanchez A, Garcia-Ruiz MJ, Muñoz-Palazon B,

Cortes-Lorenzo C, Osorio F, Vahala R (2016a) Performance and bacterial community dynamics of a CANON bioreactor acclimated from high to low operational temperatures, Chem Eng J 287: 557–567.

Gonzalez-Martinez A, Garcia-Ruiz MJ, Rodriguez-Sanchez A, Osorio F,

Gonzalez-Lopez J (2016b) Archaeal and bacterial community dynamics and bioprocess performance of a bench-scale two-stage anaerobic digester. Appl Microbiol Biotechnol 100: 6013–6033.

Guo X, Miao Y, Wu B, Ye L, Yu H, Liu S, Zhang XX (2015) Correlation between microbial community structure and biofouling as determined by analysis of microbial community dynamics. Bioresour Technol 197: 99–105.

Kämpfer P, Witzenberger R, Denner EBM, Busse H-J, Neef A (2002) Sphingopyxiswitflariensis sp. nov., isolated from activated sludge. Int J Syst Evol Microbiol 52: 2029–2034.

Kojima H, Tokizawa R, Fukui M (2017) Mizugakiibacter sediminis gen. nov., sp. nov., isolated from a freshwater lake. Int J Syst Evol Microbiol 64: 3983–3987.

Lai Q, Wang L, Liu Y, Yuan J, Sun F, Shao Z (2012) Parvibaculum indicum sp. nov., isolated from deep-sea water. Int J Syst Evol Microbiol 61: 271–274.

Leyva-Díaz JC, Calderón K, Rodríguez FA, González-López J (2013) Comparative kinetic study between moving bed biofilm reactor-membrane bioreactor and membrane bioreactor systems and their influence on organic matter and nutrients removal. Biochem Eng J 77: 28–40.

Leyva-Díaz JC, Martín-Pascual J, Muñío MM, González-López J, Hontoria E,

Poyatos JM (2014) Comparative kinetics of hybrid and pure moving bed reactor-membrane bioreactors. Ecol Eng 70: 227–234.

Leyva-Diaz JC, Lopez-Lopez C, Martin-Pascual J, Muñio MM, Poyatos JM (2015a) Kinetic study of the combined processes of a membrane bioreactor and a hybrid moving bed biofilm reactor-membrane bioreactor with advanced oxidation processes as a post-treatment stage for wastewater treatment. Chem Eng Process Process Intensif 91: 57–66.

Leyva-Díaz JC, González-martínez A, González-lópez J, Muñío MM,

Poyatos JM (2015b) Kinetic modeling and microbiological study of two-step nitrification in a membrane bioreactor and hybrid moving bed biofilm reactor – membrane bioreactor for wastewater treatment. Chem Eng J 259: 692–702.

Leyva-Díaz JC, Martín-Pascual J, Poyatos JM (2017) Moving bed biofilm reactor to treat wastewater. Int J Environ Sci Technol 14: 881–910.

Li E, Lu S (2017) Denitrification processes and microbial communities in a sequencing batch reactor treating nanofiltration (NF) concentrate from coking wastewater. Water Sci Technol 76: 3289–3298.

Luo W, Phan HV, Hai FI, Price WE, Guo W, Ngo HH, Yamamoto K,

Nghiem LD (2016) Effects of salinity build-up on the performance and bacterial com- munity structure of a membrane bioreactor. Bioresour Technol 200: 305–310.

Maharaja P, Mahesh M, Chitra C, Kalaivani D, Srividya R, Swarnalatha S, Sekaran G (2017) Sequential oxic-anoxic bio reactor for the treatment of tannery saline wastewater using halophilic and filamentous bacteria. J Water Process Eng 18: 47–57.

Matar GK, Bagchi S, Zhang K, Oerther DB, Saikaly PE (2017) Membrane biofilm communities in full-scale membrane bioreactors are not randomly assembled and consist of a core microbiome. Water Res 123: 124–133.

Mcilroy SJ, Kirkegaard RH, Mcilroy B, Nierychlo M, Kristensen JM, Karst SM (2017) MiDAS 2.0: an ecosystem-specific taxonomy and online database for the organisms of wastewater treatment systems expanded for anaerobic digester groups. Database 1: 1–9.

Mclellan SL, Newton RJ, Vandewalle JL, Shanks OC, Susan M, Eren AM, Sogin ML (2014) Sewage reflects the distribution of human faecal Lachnospiraceae. Environ Microbiol 15: 2213–2227.

Remmen K, Niewersch C, Wintgens T, Yüce S, Wessling M (2017) Effect of high salt concentration on phosphorus recovery from sewage sludge and dewatering properties. J Water Process Eng 19: 277–282.

Rodriguez-R LM, Konstantinidis KT (2014a) Nonpareil: a redundancy-based approach to assess the level of coverage in metagenomic datasets. Bioinformatics 30: 629–635.

Rodriguez-R LM, Konstantinidis KT (2014b) Estimating coverage in metagenomic data sets and why it matters. ISME J 8: 2349–2351.

Rodriguez-Sanchez A, Leyva-Díaz JC, Poyatos JM, González-López J (2017a) Performance and kinetics of membrane and hybrid moving bed biofilm-membrane bioreactors treating salinity wastewater. AIChE J 63: 3329–3342.

Rodriguez-Sanchez A, Leyva-Diaz JC, Gonzalez-Martinez A, Poyatos (2017b) Linkage of microbial kinetics and bacterial community structure of MBR and hybrid MBBR-MBR systems to treat salinity-amended urban wastewater. Biotechnol Progr 33: 1483–1495.

Rodriguez-Sanchez A, Leyva-Diaz JC, Gonzalez-Lopez J, Poyatos JM (2018) Membrane bioreactor and hybrid moving bed biofilm reactor-membrane bioreactor for the treatment of variable salinity wastewater: influence of biomass concentration and hydraulic retention time. Chem Eng J 336: 102–111.

Rognes T, Flouri T, Nichols B, Quince C, Mahé F (2016) VSEARCH: a versatile open source tool for metagenomics. PeerJ 4: e2584.

Rosario-Passapera R, Keddis R, Wong R, Lutz RA, Starovoytov V, Vetriani C (2011) Parvibaculumhydrocarboniclasticum sp. nov., a mesophilic, alkane-oxidizing alphaproteobacterium isolated from a deep-sea hydrothermal vent on the East Pacific rise. Int J Syst Evol Microbiol 62: 2921–2926.

Schloss PD, Westcott SL, Ryabin T, Hall JR, Hartmann M, Hollister EB, et al. (2009) Introducing mothur: Open-source, platform-independent, community-supported software for describing and com- paring microbial communities. Appl Environ Microbiol 75: 7537–7541.

Schloss PD (2016) Application of a database-independent approach to assess the quality of operational taxonomic unit picking methods. mSystems 1: 2–5.

Sánchez O (2018) Microbial diversity in biofilms from reverse osmosis membranes: a short review. J Memb Sci 545: 240–249.

Sepehri A, Sarrafzadeh M-H (2018) Effect of nitrifiers community on fouling mitigation and nitrification efficiency in a membrane bioreactor. Chem Eng Proc Process Int 128: 10–18.

Siddiqui MF, Rzechowicz M, Harvey W, Zularisam AW, Anthony GF (2015) Quorum sensing based membrane biofouling control for water treatment: a review. J Water Process Eng 7: 112–122.

Unno T (2015) Bioinformatic suggestions on MiSeq-based microbial community analysis. J Microbiol Biotechnol 25: 765–770.

Wang L, Zheng S, Wang D, Wang L, Wang G (2014) Thermomonascarbonis sp. nov., isolated from the soil of a coal mine. Int J Syst Evol Microbiol 64: 3631–3635.

Wang R, Yang C, Zhang M, Xu S-Y, Dai C-L, Liang L-Y, Zhao H-P, Zheng P (2017) Chemoautotrophic denitrification based on ferrous iron oxidation: reactor performance and sludge characteristics. Chem Eng J 313: 693–701.

Westcott SL, Schloss PD (2015) De novo clustering methods outperform reference-based methods for assigning 16S rRNA gene sequences to operational taxonomic units PeerJ 3: e1487.

Xu G, Peng J, Feng C, Fang F, Chen S, Xu Y, Wang X (2015) Evaluation of simultaneous autotrophic and heterotrophic denitrification processes and bacterial community structure analysis. Appl Microbiol Biotechnol 99: 6527–6536.

Yang J, Spanjers H, Jeison D, Van Lier JB (2013) Impact of Na1 on biological wastewater treatment and the potential of anoxic membrane bioreactors: a review. Crit Rev Environ Sci Technol 43: 2722–2746.

General Discussion

Given the fixed secondary objectives of this research, a general discussion about the effect of the operational variable over the parameters analyzed in each of these objectives is given, in order to better understand the global effect of start-up under saline influents and the effect of variable salinity over the MBR and MBBR-MBR technologies.

1) Study of the start-up of MBR and hybrid MBBR-MBR systems treating saline urban wastewater: effect over the performance, microbial kinetics and microbial communities

The results evaluating the effect of constant salinity on the start-up of a MBR and two hybrid MBBR-MBR systems with different configurations showed that 80 days were needed in order to achieve a solids concentration of 2500 mg L^{-1} when treating salinity-amended urban wastewater at 6.5 mS cm^{-1} electric conductivity (around 3.6 mg L^{-1} NaCl), which is similar to that observed for MBR and hybrid MBBR-MBR systems in the same configuration operating under regular-salinity urban wastewater (Leyva-Diaz & Poyatos, 2015). This result suggested that the capacity for the accumulation of biomass inside the MBR and hybrid MBBR-MBR is not influenced by the influent salinity.

However, the differences found for the attached biomass in the hybrid MBBR-MBR systems was significant. In this case, the attached biomass concentrations for the regular-salinity urban wastewater was found to be around 1570-1824 mg L^{-1} for the stationary phase (Leyva-Diaz & Poyatos, 2015), while this value became 17-21 mg L^{-1} for the constant salinity influent at 6.5 mS cm^{-1} electric conductivity. Moreover, the concentrations of attached biofilm in the hybrid MBBR-MBR systems treating variable salinity wastewater at 4.5, 6.5 and 8.5 mS cm^{-1} electric conductivity (2.4, 3.6 and 4.8 g L^{-1} NaCl, respectively) was lower than 50 mg L^{-1} in all operational cases. Therefore, one first interesting conclusion about the functioning of hybrid MBBR-MBR systems started-up and

operated under constant and variable salinity conditions is the difficulty for the formation of attached biomass.

It has been found that the biofilm formation capacity of many microorganisms, such as *Salmonella enterica*, *Vibrio sp.* and *Aeromonas hydrophila*, to mention a few, is detrimentally affected by NaCl (Jahid et al., 2015; Kim & Chong, 2017; Iliadis et al., 2018). Accordingly, the lack of biofilm formation over the carriers in the hybrid MBBR-MBR systems treating saline influents might be related to the inability of microorganisms present in urban wastewater to form biofilms under the NaCl concentrations in the influents during operation. Even though several researches have reported that biomass attached to carriers under treatment of regular-salinity urban wastewater can adapt to salinity, the loss in biofilm density after exposure to salinity was of 0.55 mg L^{-1} (about 40% of total attached biomass) (Di Trapani et al., 2014), which highlights the inability of microorganisms native to wastewater and wastewater treatment systems to grow in biofilms.

The results observed regarding the functioning of the hybrid MBBR-MBR treating saline influents suggested that the growth of biofilm attached to carriers is insufficient when the systems were started-up under these conditions, and therefore the hybrid MBBR-MBR systems operated as MBR in practice. This might be of importance for future implementations of hybrid MBBR-MBR systems for the treatment of wastewater with constant or variable salinity.

The influent salinity also had an effect over the performance of the MBR and hybrid MBBR-MBR during the start-up and steady-state phases. These differences were not marked for the parameters COD and BOD_5, which attained similar performances for the regular-salinity and 3.6 g L^{-1} NaCl (88-92% for COD, 97-99% for BOD_5) (Leyva-Diaz & Poyatos, 2015). However, the differences in total nitrogen removal were very high, with a range of 61-64% for the regular-salinity scenario (Leyva-Diaz & Poyatos, 2015) against a range of 22-30% for the 3.6 g L^{-1} NaCl scenario, both under steady-

state conditions. In this way, the removal of organic matter was efficient for the constant salinity scenario, but the removal of nitrogen was very limited by salinity.

The dominant bacterial communities for the MBR and hybrid MBBR-MBR operating under regular-salinity and 3.5 g L^{-1} salinity conditions were very different, suggesting that salinity exert a great influence over the development of microbial communities within the bioreactors. Autotrophic ammonium oxidizers such as *Nitrosomonas* or *Nitrosospira* were only found under the regular-salinity conditions, while no known autotrophic ammonium oxidizers were found for the 3.5 g L^{-1} salinity conditions. Surely this could be linked with the lower total nitrogen removal capacity observed between the two salinity scenarios.

2) Analyze of the performance, microbial kinetics and microbial communities of MBR and hybrid MBBR-MBR systems treating variable-salinity urban wastewater: effect of maximum influent salinity, hydraulic retention time and total solids concentration

As per the removal of organic matter, the MBR and MBBR-MBR systems had high removal performances for BOD_5 and COD under the 2.4 and 3.6 g L^{-1} NaCl scenarios (97-99% for BOD_5 and 71-99% for COD in both cases). However, these values were slightly lower for the BOD_5 in the scenario at 4.8 g L^{-1} NaCl, with values ranging 83-98%. On the other hand, the values for COD were in the range of 74-99%. For the three scenarios, the removal of BOD_5 and COD was higher at higher solids concentrations and at longer HRT.

The values obtained for MBR and hybrid MBBR-MBR treating regular-salinity urban wastewater reported similar removal efficiencies of BOD_5 and COD, in the range of 98-99% for BOD_5 and even lower for COD, in the range of 86-92% (Leyva-Diaz et al., 2013; Leyva-Diaz et al., 2015a). In this sense, it can be said that the removal of organic matter in the MBR and hybrid MBBR-MBR systems

did not significantly decrease with the influent variable salinity. For this reason, the MBR and hybrid MBBR-MBR technologies are robust bioprocesses to treat organic matter contamination in saline effluents and wastewater treatment systems with seawater intrusion issues.

Nevertheless, the results obtained for total nitrogen removal were completely different than those found for organic matter. According to the performance in total nitrogen removal, the salinity scenarios at 2.4, 3.6 and 4.8 g L^{-1} reported a value range of 27-85%, 15-50% and 24-38%. In this case, the maximum salinity for cyclical salinity loading had a substantial effect over the nutrient removal in the bioreactors. The behavior of the systems seemed to be an accumulation of ammonium, which was evidenced by removal rates of this substance in the range of 53-85% for 2.4 g L^{-1} NaCl and 25-38 for the 4.8 g L^{-1} NaCl. In this way, the results suggested that higher maximum salinities for the cyclical salinity loading decrease the capacity of the bioreactors to oxidize ammonium thus reducing the capacity for nitrogen removal.

For the case of MBR and hybrid MBBR-MBR systems treating regular-salinity urban wastewater, the results showed a total nitrogen removal of 56-64% (Leyva-Diaz et al., 2013; Leyva-Diaz et al., 2015a). These results are comparable to the systems treating variable salinity wastewater at 2.4 g L^{-1} NaCl, thus it can be stated that maximum salinities higher than 2.4 g L^{-1} NaCl have a detrimental effect over the removal performance of total nitrogen in MBR and hybrid MBBR-MBR systems. The data showed that these technologies are not sufficiently capable of assure efficient removal of total nitrogen under the operational parameters tested.

The microbial kinetics for both heterotrophic and autotrophic biomass also showed to be influenced by the maximum salinity in the influent. For the heterotrophic biomass, values were higher for the 2.4 g L^{-1} NaCl scenario, followed by the 3.6 and 4.8 g L^{-1} NaCl. Overall, the hybrid MBBR-MBR with carriers in all chambers seemed to have the lowest values of rate of substrate (r_{su}) utilization among

the three configurations used in the experiments, while the MBR had the highest values for the 2500 mg L^{-1} solids concentration and the hybrid MBBR-MBR without carriers in the anoxic chamber had the fastest kinetics for the 3500 mg L^{-1} concentration. In general, solids concentrations at operation impacted the heterotrophic kinetics in such a way that higher solids concentrations minimized the differences in r_{su} among technologies and maximum influent salinities. Also, higher HRTs showed to minimize the effect of influent organic matter concentration over the r_{su} of the heterotrophic biomass.

However, the kinetics of the autotrophic biomass showed faster r_{su} for the 3.6 g L^{-1} scenario than for the 2.4 and 4.8 g L^{-1} scenarios. In these cases, the MBR was overall the configuration with slowest autotrophic kinetics at all operational conditions and salinity scenarios, with the two hybrid MBBR-MBR systems being close in terms of autotrophic r_{su} values. As occurred for heterotrophic kinetics, higher solids at operation yielded in general lower r_{su}, and longer HRTs decreased the influence of substrate concentrations over the autotrophic r_{su}.

These results showed that the maximum influent salinity and operational conditions played a role over the kinetics of autotrophic and heterotrophic biomass. Similar values for the heterotrophic kinetics at all operational conditions suggested that kinetic behavior of this fraction of the biomass did not have an influence over the removal performances of the bioreactors, and thus the elimination of organic matter in the systems was more influenced by other parameters. The same could be stated for the autotrophic biomass.

The bacterial communities of the three bioreactors showed differences when operating under the three salinity scenarios tested. It was demonstrated that the most important parameter driving the bacterial community composition of the bioreactors treating variable salinity wastewater was the maximum influent salinity, followed by the solids concentration at operation and the HRT, with the

technological configuration not affecting much to it. In this sense, the similarities among the MBR and the hybrid MBBR-MBR systems under the same salinity scenario and operational conditions were very high. This result suggested that the technological configuration did not affect the bacterial community thriving in the membrane-based technologies, which may be influenced by the fact that a very small attachment of biomass to carriers occurred. In fact, the bacterial communities in the carriers were remarkably similar than the mixed liquor communities in the hybrid MBBR-MBR systems at all conditions tested. This result is contrary to the findings under operation with regular-salinity urban wastewater, in which the bacterial communities in the carriers were enriched in different phylotypes of nitrifying genera (Leyva-Diaz et al., 2015a; Leyva-Diaz et al., 2015b). From a microbiological point of view, the difference between the MBR and hybrid MBBR-MBR systems was small for the treatment of variable salinity influent in comparison with the treatment of regular-salinity wastewater.

In spite of these differences, it was found that a few of bacterial genera were present at all salinity scenarios and operational conditions. These were related to *Rhodanobacter*, *Nitrobacter* and *Mizugakiibacter*. It was proposed that *Rhodanobacter* could be related to oxidation of nitrite in the MBR and hybrid MBBR-MBR, as previously reported in membrane-based bioprocess and other wastewater treatment technologies (Leyva-Diaz et al., 2015a; Gonzalez-Martinez et al., 2015a). The metabolism of *Nitrobacter* is autotrophic oxidation of nitrite (Leyva-Diaz et al., 2015a; Leyva-Diaz et al., 2015b), which suggested that *Rhodanobacter* and *Nitrobacter* could compete for the same substrate in the MBR and hybrid MBBR-MBR systems treating variable salinity wastewater. On the other hand, *Mizugakiibacter* is a novel discovered bacterial genus isolated from freshwater, not identified many times as important member of a bioreactor community, which has been related to aerobic, heterotrophic degradation of organic matter and heterotrophic and chemoautotrophic

denitrification (Kojima et al., 2014; Wang et al., 2017). These two genera might even be involved in a syntrophic relationship around generation-consumption of nitrate.

There were more bacterial phylotypes identified which were also of importance for the bacterial community structure of the MBR and hybrid MBBR-MBR treating variable salinity wastewater. Among these, *Ottowia* and *Gemmatimonadaceae* members were predominant. It was found that *Gemmatimonadaceae* members were favored under 3500 mg L^{-1} solids and at lower maximum influent salinities. The metabolic capabilities of *Gemmatimonadaceae* members are related to aerobic heterotrophy, and their high resistance to toxics has been reported (Zhang et al., 2003; Wang et al., 2014). On the contrary, *Ottowia* seemed to be favored at 2500 mg L^{-1} solids. This genus has been reported in bioreactors for heterotrophic nitrification and reduction of nitrate and nitrite (Liu et al., 2017).

The results obtained might be used to picture the ecological relevance of these phylotypes, with importance of *Nitrobacter* and *Rhodanobacter* for nitrite oxidation, of *Ottowia* for ammonium oxidation, of *Mizugakiibacter* and *Ottowia* for denitrification, and of *Gemmatimonadaceae* members, *Mizugakiibacter* and *Ottowia* for organic matter degradation. Still, these is just a hypothesis that should be further investigated. The results highlighted the lack of knowledge over the ecological role of dominant phylotypes in bioreactors treating variable salinity wastewater and aimed to develop more research regarding this topic in the future.

The presence of not known autotrophic ammonium oxidizing bacteria is in contrast with the results observed for MBR and hybrid MBBR-MBR systems operating under regular-salinity urban wastewater. In that case, *Nitrosomonas* was the dominant ammonium oxidizing bacteria (Leyva-Diaz et al., 2015a; Leyva-Diaz et al., 2015b). However, no autotrophic ammonium oxidizing bacteria was found in the membrane-based bioprocess under the treatment of variable salinity wastewater.

Instead, the genera that could be related to ammonium oxidation were identified as heterotrophic nitrifiers *Ottowia*, *Comamonas*, *Azoarcus* or *Blastocatella*. The absence of autotrophic ammonium oxidizers might be related with the inefficiency of ammonium oxidation in the bioreactors that led to poor nitrogen removal performances in comparison with regular-salinity scenario.

3) Analyze of the biofouling communities of hybrid MBBR-MBR systems treating constant- and variable-salinity urban wastewater: effect of maximum influent salinity

4) Analyze of the biomineralization capacity of bacterial strains isolated from biofouling of MBR and hybrid MBBR-MBR systems treating constant- and variable-salinity urban wastewater: effect of maximum influent salinity

The results suggested that the influent salinity conditions drove the bacterial communities in the biofouling of the hybrid MBBR-MBR systems. In this case, the bacterial communities in biofouling under 2.4, 3.6 and 4.8 g L^{-1} variable salinity scenarios were more similar among them than with respect to those found at the 3.6 g L^{-1} constant salinity conditions. Similar results have been found previously that MBR communities were more similar for similar scenarios of salinity scale-up (Luo et al., 2016). This fact highlights the sensitivity of bacterial communities in membrane biofouling to the influent salinity conditions.

All the dominant phylotypes in biofouling for variable salinity conditions were related with *Xanthomonadaceae* family, among which *Thermomonas* and *Rhodanobacter* genera were found. Moreover, the dominance of these *Xanthomonadaceae* genera was related to the maximum influent salinity concentration, suggesting a different dominant phylotype in the biofouling for each of the 2.4, 3.6 and 4.8 g L^{-1} variable salinity scenarios. On the other hand, the most important genera found for biofouling in the 3.6 g L^{-1} constant salinity scenario was related to *Mycobacterium* genus

of the *Mycobacteriaceae* family. A comparison of these results with those obtained from fouling communities in a MBBR-MBR system treating regular-salinity urban wastewater showed that dominant phylotypes were very different, being for this case dominant the genera *Simplicispira*, *Acidovorax*, *Comamonas* and *Rhodobacter* (Gonzalez-Martinez et al., 2015b). Therefore, the results suggested that dominant phylotypes in biofouling are very dependent on the influent wastewater salinity conditions.

The specialization of bacterial communities in biofouling was also reflected in the nature of mineralization-mediating bacterial strains but not in the morphology and composition of minerals formed. Strains capable for mediating formation of minerals were isolated from both calcium and magnesium media for all four salinity conditions. The minerals obtained from the calcium medium had the same elemental composition regardless of the salinity condition at operation, showing a major importance of Ca element. Likewise, the morphology of all biominerals extracted from the calcium media was similar regardless of the salinity conditions exerted over the fouling biomass. The elemental composition and morphology of calcium crystals was similar to that found for the fouling biomass of a pure MBBR-MBR system treating regular-salinity urban wastewater (Gonzalez-Martinez et al., 2015b).

On the other hand, the composition of the minerals extracted from the magnesium medium showed different elemental composition for the salinity scenarios. In those of 2.4 g L^{-1}, 3.6 g L^{-1} variable and 3.6 g L^{-1} constant, the composition was conformed mainly by P and Mg elements, while for the 4.8 g L^{-1} variable the composition was formed by Ca and P elements. The morphology of the crystals formed in the magnesium medium was different for the salinity conditions. Compared to the magnesium minerals formed by fouling biomass of regular-salinity urban wastewater treating MBBR-MBR, the elemental composition was similar but not the crystal morphology (Gonzalez-Martinez et al., 2015b). In a similar fashion to the results described, different salinity concentrations

in *Microbacterium marinum sp. nov. H207* culture medium have been proven to influence the time of mineralization and the morphology of the magnesium phosphate crystals formed (Zhao et al., 2019). In such case, the morphology of calcium minerals was similar to those found for the four salinity scenarios, while the morphology of the magnesium minerals was

Only one bacterial strain capable to mediate the precipitation of calcium minerals was found for each salinity scenario, suggesting a specialization linked to the salinity conditions. Thus, for the 3.6 g L^{-1} constant salinity scenario and for the 2.4, 3.6 and 4.8 g L^{-1} variable salinity scenarios the identified strains were *Citrobacter freundii*, *Brevibacterium linens*, *Bacillus stratosphericus* and *Bacillus toyonensis*, respectively. The diversity of magnesium precipitating bacteria was slightly higher, accounting for: *Citrobacter freundii*, *Bacillus licheniformis* and *Bacillus pumilus* for the 3.6 g L^{-1} constant salinity scenario; *Bacillus stratosphericus* for the 2.4 g L^{-1} variable salinity scenario; *Bacillus licheniformis* for the 3.6 g L^{-1} variable salinity scenario; and *Bacillus stratosphericus*, *Comamonas testosteroni*, *Janibacter melonis* and *Microbacterium esteraromaticum* for the 4.8 g L^{-1} variable salinity scenario.

The bacterial strains isolated from the biofouling of a MBBR-MBR treating regular-salinity urban wastewater that were capable to mediate the formation of calcium and magnesium minerals were *Bacillus subtilis, Bacillus thuringensis* and *Comamonas terrigena* for calcium minerals, and *Bacillus pumilus*, *Lysinibacillus fusiformis* and *Trichococcus floculiformis* for magnesium minerals (Gonzalez-Martinez et al., 2015b). A comparison of the isolates from all different influent salinity conditions showed that *Bacillus* was the only genus found to mediate precipitation at all salinities.

References

Di Trapani D, Di Bella G, Mannina G, Torregrossa M, Viviani G. (2014). Comparison between moving bed-membrane bioreactor (MB-MBR) and membrane bioreactor (MBR) systems: Influence of wastewater salinity variation. Bioresour Technol 162: 60–69.

Gonzalez-Martinez a, Leyva-Díaz JC, Rodriguez-Sanchez A, Muñoz-Palazon B, Rivadeneyra A, Poyatos JM, et al. (2015). Isolation and metagenomic characterization of bacteria associated with calcium carbonate and struvite precipitation in a pure moving bed biofilm reactor-membrane bioreactor. Biofouling 31: 333–348.

Gonzalez-Martinez A, Rodriguez-Sanchez A, Garcia-Ruiz MJ, Muñoz-Palazon B, Cortes-Lorenzo C, Osorio F, et al. (2016). Performance and bacterial community dynamics of a CANON bioreactor acclimated from high to low operational temperatures. Chem Eng J 287: 557–567.

Iliadis I, Daskalopoulou A, Simões M, Giaouris E. (2018). Integrated combined effects of temperature, pH and sodium chloride concentration on biofilm formation by Salmonella enterica ser. Enteritidis and Typhimurium under low nutrient food-related conditions. Food Res Int 107: 10–18.

Kabir I, Rahaman F, Ha AJ, Ha S. (2015). Effect of salinity and incubation time of planktonic cells on bio film formation, motility, exoprotease production, and quorum sensing of Aeromonas hydrophila. Food Microbiol 49: 142–151.

Kim LH, Chong TH. (2017). Physiological Responses of Salinity-Stressed Vibrio sp. and the E ffect on the Biofilm Formation on a Nano filtration Membrane. Environ Sci Technol 51: 1249-1258, doi: 10.1021/acs.est.6b02904.

Kojima H, Tokizawa R, Fukui M. (2018). Mizugakiibacter sedimins gen. nov., sp. nov., isolated from a freshwater lake. Int J System Evol Microbiol 64: 3983–3987.

Leyva-Diaz JC, Gonzalez-Martinez A, Gonzalez-Lopez J, Muñio MM, Poyatos JM. (2015). Kinetic modeling and microbiological study of two-step nitrification in a membrane bioreactor and hybrid moving bed biofilm reactor-membrane bioreactor for wastewater treatment. Chem Eng J 259: 692–702.

Leyva-Diaz JC, Calderon K, Rodriguez FA, Gonzalez-Lopez J. (2013). Comparative kinetic study between moving bed biofilm reactor-membrane bioreactor and membrane bioreactor systems and their influence on organic matter and nutrients removal. Biochem Eng J 77: 28–40.

Leyva-Diaz JC, Gonzalez-Martinez A, Gonzalez-Lopez J, Muñio MM, Poyatos JM. (2015). Kinetic modeling and microbiological study of two-step nitrification in a membrane bioreactor and hybrid moving bed biofilm reactor – membrane bioreactor for wastewater treatment. Chem Eng J 259: 692–702.

Leyva-Diaz JC, Poyatos JM. (2018). Start-up of membrane bioreactor and hybrid moving bed biofilm reactor – membrane bioreactor: kinetic study. Water Sci Technol 72: 1948–1953.

Liu T, Mao Y, Shi Y, Quan X. (2017). Start-up and bacterial community compositions of partial nitrification in moving bed biofilm reactor. Appl Microbiol Biotechnol 101: 2563–2574.

Luo W, Phan H V., Hai FI, Price WE, Guo W, Ngo HH, et al. (2016). Effects of salinity build-up on the performance and bacterial community structure of a membrane bioreactor. Bioresour Technol 200: 305–310.

Wang R, Yang C, Zhang M, Xu S, Dai C, Liang L, et al. (2017). Chemoautotrophic denitrification based on ferrous iron oxidation: Reactor performance and sludge characteristics. Chem Eng J 313: 693–701.

Wang Z, Huang F, Mei X, Wang Q, Song H, Zhu C, et al. (2014). Long-term operation of an MBR in the presence of zinc oxide nanoparticles reveals no significant adverse effects on its performance. J Memb Sci 471: 258–264.

Zhang H, Sekiguchi Y, Hanada S, Hugenholtz P, Kim H, Kamagata Y, et al. (2018). Gemmatimonas aurantiaca gen. nov., sp. nov., a Gram-negative, aerobic, polyphosphate accumulating micro-organism, the first cultured representative of the new bacterial phylum. Int J System Evol Microbiol 53: 1155–1163.

Zhao T, Li H, Huang Y, Yao Q, Huang Y, Zhou G. (2019). Microbial mineralization of struvite: Salinity effect and its implication for phosphorus removal and recovery. Chem Eng J 358: 1324–1331.

Conclusions

Based in the results obtained in this research project, the conclusions that can be drawn from the previous general discussion sections are the following:

1. The start-up of the MBR and hybrid MBBR-MBR systems under constant 6.5 mS cm^{-1} electric conductivity salinity influent at 6 h HRT resulted in: the bioreactors reaching steady-state conditions in a similar fashion than under regular-salinity influent, however showing lower total nitrogen removal; and the hybrid MBBR-MBR systems showing very poor formation of attached biofilm over the carriers compared to the attached biofilm formed treating regular-salinity wastewater

2. The performance of the MBR and hybrid MBBR-MBR systems treating variable-salinity influent wastewater at 4.5, 6.5 and 8.5 mS cm^{-1} electric conductivity and under 6, 9.5 and 12 h HRT and 2500 and 3500 mg L^{-1} total solids was similar in terms of organic matter but increasing salinity impacted negatively the ammonium oxidation and total nitrogen removal in all technologies systems. The performance was higher for both organic matter and nitrogen with increasing hydraulic retention time and total solids at operation, and was very similar for the three technological configurations under the same influent and operational conditions
3. The microbial kinetics of the MBR and hybrid MBBR-MBR systems treating variable-salinity influent wastewater at 4.5, 6.5 and 8.5 mS cm^{-1} electric conductivity and under 6, 9.5 and 12 h HRT and 2500 and 3500 mg L^{-1} total solids were faster for lower influent maximum salinity, lower hydraulic retention times and lower total solids at operation, and were very similar in value for the three technological configurations under the same influent and operational conditions
4. The bacterial communities in the MBR and hybrid MBBR-MBR systems treating variable-salinity influent wastewater at 4.5, 6.5 and 8.5 mS cm^{-1} electric conductivity and under 6, 9.5 and 12 h HRT and 2500 and 3500 mg L^{-1} total solids were driven primarily by maximum influent salinity, then by hydraulic retention time, total solids at operation and in the lowest proportion by technological configuration. The dominant bacterial phylotypes were related to *Nitrobacter*, *Rhodanobacter*, *Mizugakiibacter* and *Ottowia* genera and *Gemmatinonadaceae* family, and the communities in the attached biofilm and the mixed liquor in the hybrid MBBR-MBR systems were very similar under the same influent and operational conditions

5. Biofouling bacterial communities in the hybrid MBBR-MBR technology for constant salinity at 6.5 mS cm^{-1} and variable salinity at 4.5, 6.5 and 8.5 mS cm^{-1} electric conductivity under 6 h HRT and 2500 mg L^{-1} total solids were mainly driven by the influent salinity conditions: constant vs variable salinity loading, maximum salinity. However, the dominant phylotype in biofouling at variable salinity conditions was the family *Xanthomonadaceae*. The bacterial strains identified for their capacity to mediate calcium and/or magnesium mineral formation were very different with respect to the influent salinity conditions, however *Bacillus* genus had representatives in all salinity scenarios

Tomando como base los resultados obtenidos en esta investigación, las conclusiones que pueden extraerse de los diferentes puntos de la discusión general previa son las siguientes:

1. La puesta en marcha de los sistemas MBR y MBBR-MBR híbridos bajo influente de salinidad constante de 6.5 mS cm^{-1} de conductividad eléctrica y TRH de 6 h resultó en: que los biorreactores alcanzaron condiciones de estado estacionario de forma similar a los mismos sistemas cuando trataron agua residual de salinidad normal, sin embargo mostrando peor eliminación de nitrógeno; y que los sistemas MBBR-MBR híbridos mostraron muy pobre formación de biopelícula adherida a los carriers en comparación con la biopelícula adherida formada cuando se trató agua residual con salinidad normal.

2. El rendimiento de eliminación de los MBR y MBBR-MBR híbridos tratando agua residual de salinidad variable para 4.5, 6.5 y 8.5 mS cm^{-1} de conductividad eléctrica, bajo 6, 9.5 y 12 h de TRH y 2500 y 3500 mg L^{-1} de sólidos totales, fue similar para materia orgánica pero mayores salinidades afectaron negativamente la oxidación de amonio y nitrógeno total en todas las tecnologías. El rendimiento de eliminación fue mayor para materia orgánica y nitrógeno para mayores tiempos de retención hidráulico y sólidos totales, a la vez que muy similar para las tres tecnologías bajo las mismas condiciones de influente y operación.
3. La cinética microbiana de los MBR y MBBR-MBR híbridos tratando agua residual de salinidad variable para 4.5, 6.5 y 8.5 mS cm^{-1} de conductividad eléctrica, bajo 6, 9.5 y 12 h de TRH y 2500 y 3500 mg L^{-1} fue más rápida para menores salinidades máximas en el influente, menores tiempos de retención hidráulica y menores sólidos totales, a la vez que fue muy similar para las tres tecnologías bajo las mismas condiciones de influente y operación
4. Las comunidades bacterianas de los MBR y MBBR-MBR híbridos tratando agua residual de salinidad variable para 4.5, 6.5 y 8.5 mS cm^{-1} de conductividad eléctrica, bajo 6, 9.5 y 12 h de TRH y 2500 y 3500 mg L^{-1} fueron principalmente determinadas por la salinidad máxima en el influente, seguida del tiempo de retención hidráulico, luego por los sólidos totales y en la menor proporción por la tecnología. Los filotipos bacterianos dominantes fueron identificados como miembros de los géneros *Nitrobacter*, *Rhodanobacter*, *Mizugakiibacter* y *Ottowia* y miembros de la familia *Gemmatimonadaceae*, a la vez que las comunidades en la biopelícula fija y en el licor mezcla de los MBBR-MBR híbridos fueron muy similares bajos las mismas condiciones de influente y operación

5. Las comunidades bacterianas del biofouling en la tecnología MBBR-MBR híbrido para salinidad constante de 6.5 mS cm^{-1} y salinidad variable de 4.5, 6.5 y 8.5 mS cm^{-1} de conductividad eléctrica, bajo 6 h de TRH y 2500 mg L^{-1}, fue principalmente determinada por las condiciones de salinidad en el influente: carga salina constante frente a variable y salinidad máxima. Sin embargo, la familia *Xanthomonadaceae* fue dominante en el biofouling bajo todas las condiciones de salinidad variable. Las cepas bacterianas identificadas por su capacidad de mediar la formación de minerales de calcio y/o magnesio fueron muy diferentes con respecto a las condiciones de salinidad del influente, pero sin embargo el género *Bacillus* tuvo representantes en todos los escenarios de salinidad

Engineering Applications and Future Prospects

Engineering applications of the conclusions

1. The hybrid MBBR-MBR systems did now show growth of attached biofilm over the carriers operating under all operational scenarios tested in the research, thus the hybrid MBBR-MBR operated basically as a MBR system. This result suggests that the advantage of attached biofilm in the MBBR-MBR systems is not achieved when treating saline influents, and therefore the hybrid MBBR-MBR would not have a technological advantage over the MBR systems for the treatment of saline influents
2. MBR and hybrid MBBR-MBR systems could efficiently treat constant-salinity and variable salinity urban wastewater, proving the feasibility of these technologies for this purpose. Membrane technologies should be considered as viable option in the design process of treatment trains for saline wastewater
3. From an operational point of view, saline influents affected greatly the nitrogen removal, the kinetics of the autotrophic communities, and reduced the presence of autotrophic ammonium oxidizing bacteria. This result suggested that saline wastewater treatment should put more attention on ammonium oxidation processes. Nitrogen removal could be improved by exhaustively controlling the operational variables in membrane-based technologies treating saline wastewater
4. The dominant phylotypes in biofouling for variable salinity influents were related to *Xanthomonadaceae* family. In this regard, quorum quenching methodologies for mitigation of biofouling under such conditions should target for *Xanthomonadaceae* members

Future prospects

1. A new research line should consider the economic aspects of membrane technologies for the treatment of saline influents and its advantages or disadvantages from a cost point of view with respect to other technologies
2. The scale-up from laboratory scale to bench-scale and full-scale should be explored in the future
3. The treatment of industrial variable salinity influents should be investigated in addition to saline urban wastewater treatment
4. The effect of a more realistic salinity variation observed for seawater intrusion in coastal wastewater treatment systems should be considered, first by measuring of salinity across a long experimentation time and reproducing it in the laboratory instead of using constant-peak salinity cycles
5. Quorum quenching mechanisms to hinder the biofouling capacity of *Xanthomonadaceae* family members should be explored as means of biofouling mitigation in salinity membrane bioreactors
6. The members of *Eukarya* domain and their ecological roles should be more investigated in saline wastewater treatment systems

Aplicaciones de las conclusiones obtenidas para la práctica en ingeniería

1. Los sistemas MBBR-MBR híbridos no mostraron crecimiento de biopelícula fija sobre los carriers bajo ninguna de las condiciones operacionales probadas en esta investigación, por lo que los MBBR-MBR híbridos operaron en la práctica como sistemas MBR. Este resultado sugiere que la ventaja de presencia de biopelícula fija en los sistemas MBBR-MBR no se consigue cuando se trata agua residual salina, y por lo tanto los sistemas MBBR-MBR híbridos no presentaron ninguna ventaja sobre los sistemas MBR para el tratamiento de estas aguas residuales
2. Los sistemas MBR y MBBR-MBR híbridos se mostraron como tecnologías eficientes para el tratamiento de agua residual urbana con salinidad constante y variable, demostrando su capacidad para cumplir este propósito. Las tecnologías de membrana deberían ser consideradas como una opción viable en los procesos de diseño de tratamiento de agua residual salina
3. Desde el punto de vista operacional, los influentes salinos afectaron sustancialmente la eliminación de nitrógeno y la cinética de las comunidades autotróficas, así como redujeron la abundancia de bacteria autotróficas oxidadoras de amonio. Este resultado sugiere que el proceso de oxidación de amonio debería monitorizarse cuidadosamente en procesos de tratamiento de agua residual salina. Un exhaustivo control mediante cambios en las variables operacionales dentro de los límites de operación permitirá obtener mejores eliminaciones de nitrógeno en procesos de membrana en condiciones salinas
4. Los filotipos dominantes en el biofouling para influentes de salinidad variable estuvieron relacionados con miembros de la familia *Xanthomonadaceae*. En este sentido, métodos de control de biofouling basados en quorum quenching deberían hacer objetivo a estos microorganismos

Investigaciones futuras

1. Nuevas investigaciones deberían realizarse para tener en cuenta los aspectos económicos de las tecnologías de membrana en el tratamiento de influentes salinos así como sus ventajas y desventajas con respecto a otras tecnologías desde un enfoque de costes
2. El escalado desde laboratorio hasta escala real debería explorarse en el futuro
3. Además del tratamiento de influentes urbanos de salinidad variable, el tratamiento de influentes industriales de salinidad variable debería ser investigado
4. El efecto de una variación de salinidad más realista observada en intrusión de agua marina en sistemas de tratamiento de agua residual costeros debería considerarse, primerio midiendo la salinidad en los mismos durante un largo período de experimentación y luego reproduciendo este patrón en el laboratorio en lugar de usar ciclos con picos de salinidad constantes
5. Los mecanismos de quorum quenching para evitar la capacidad de producir biofouling de miembros de la familia *Xanthomonadaceae* deberían explorarse como medios para mitigar el biofouling en bioreactors de membrana bajo salinidad
6. Los miembros del dominio *Eukarya* y sus roles ecológicos en sistemas de tratamiento de agua residual salina deberían ser más ampliamente estudiados

Research Completed Outside of The Ph.D. Thesis

At the same time that the Ph.D. candidate was involved in the experimentation and analysis of the results concerning this Ph.D. thesis, he also developed collaborations in other researches which concluded in his co-authorship of these. A list of such papers is given below:

1. Title: Application of microbial fuel cell technology for wastewater treatment and electricity generation under Nordic countries climate conditions: Study of performance and microbial communities
Journal: Bioresource Technology
Year: 2018
Volume: 270
Issue:
Initial Page: 1
Final Page: 10
Authors: Gonzalez-Martinez, Alejandro; Chengyuan, Su; **Rodriguez-Sanchez, Alejandro**; Pozo-Llorente, Clementina; Vahala, Riku
Impact Factor (ISI): 5.807
Impact Factor (SCImago): 2.029
Quartile (SCImago): Q1

2. Title: Pollutants degradation performance and microbial community structure of aerobic granular sludge systems using inoculums adapted at mild and low temperature
Journal: Chemosphere
Year: 2018
Volume: 204
Issue:
Initial Page: 431
Final Page: 441
Authors: Muñoz-Palazon, Barbara; Pesciaroli-, Chiara; **Rodriguez-Sanchez, Alejandro**; Gonzalez-Lopez, Jesus; Gonzalez-Martinez, Alejandro
Impact Factor (ISI): 4.427
Impact Factor (SCImago): 1.435
Quartile (SCImago): Q1

3. Title: Performance and microbial community structure of a polar Arctic Circle aerobic granular sludge system operating at low temperature
Journal: Bioresource Technology
Year: 2018
Volume: 256
Issue:
Initial Page: 22
Final Page: 29
Authors: Gonzalez-Martinez, Alejandro; Muñoz-Palazon, Barbara; Maza, Paula; **Rodriguez-Sanchez, Alejandro**; Gonzalez-Lopez, Jesus; Vahala, Riku
Impact Factor (ISI): 5.807

Impact Factor (SCImago): 2.029
Quartile (SCImago): Q1

4. Title: Linking the Effect of Antibiotics on Partial-Nitritation Biofilters: Performance, Microbial Communities and Microbial Activities
Journal: Frontiers in Microbiology
Year: 2018
Volume: 9
Issue:
Initial Page: 354
Final Page:
Authors: Gonzalez-Martinez, Alejandro; Margareto, Alejandro; **Rodriguez-Sanchez, Alejandro**; Pesciaroli, Chiara; Diaz-cruz, Silvia; Barcelo, Damia; Vahala, Riku
Impact Factor (ISI): 4.019
Impact Factor (SCImago):
Quartile (SCImago):

5. Title: New concepts in anammox processes for wastewater nitrogen removal: recent advances and future prospects
Journal: FEMS Microbiology Letters
Year: 2018
Volume: 365
Issue: 6
Initial Page: fny031
Final Page:
Authors: Gonzalez-Martinez, Alejandro; Muñoz-Palazon, Barbara; **Rodriguez-Sanchez, Alejandro**; Gonzalez-Lopez, Jesus
Impact Factor (ISI): 1.735
Impact Factor (SCImago): 0.790
Quartile (SCImago): Q3

6. Title: Microbial ecology of full-scale wastewater treatment systems in the Polar Arctic Circle: Archaea, Bacteria and Fungi
Journal: Scientific Reports
Year: 2018
Volume: 8
Issue: 1
Initial Page: 2208
Final Page:
Authors: Gonzalez-Martinez, Alejandro; Sihvonen, Maija; Muñoz-Palazon, Barbara; **Rodriguez-Sanchez, Alejandro**; Mikola, Anna; Vahala, Riku
Impact Factor (ISI): 4.122
Impact Factor (SCImago): 1.533
Quartile (SCImago): Q1

7. Title: Quantitative and qualitative studies of microorganisms involved in full-scale autotrophic nitrogen removal performance

Journal: AIChE Journal
Year: 2018
Volume: 64
Issue: 2
Initial Page: 457
Final Page: 467
Authors: Muñoz-Palazon, Barbara; **Rodriguez-Sanchez, Alejandro**; Castellano, Antonio; Gonzalez-Lopez, Jesus; Van Loosdrecht, Mark; Vahala, Riku; Gonzalez-Martinez, Alejandro
Impact Factor (ISI): 3.326
Impact Factor (SCImago): 1.015
Quartile (SCImago): Q1

8. Title: Insight on the bacterial ecology in membrane bioreactor: operational conditions effect over dominant ecological players
Journal: AIChE Journal
Year: 2018
Volume:
Issue:
Initial Page:
Final Page:
Authors: **Rodriguez-Sanchez, Alejandro**; Calero-Diaz, Gustavo; Martin-Pascual, Jaime; Lopez-Lopez, Cristina; Torres, Juan Carlos; Poyatos-Capilla, Jose Manuel
Impact Factor (ISI): 3.326
Impact Factor (SCImago): 1.015
Quartile (SCImago): Q1

9. Title: Effect of salinity variation on the autotrophic kinetics of the start-up of a membrane bioreactor and hybrid moving bed biofilm reactor-membrane bioreactor at low hydraulic retention time
Journal: Water Science and Technology
Year: 2018
Volume: 77
Issue: 3
Initial Page: 714
Final Page: 720
Authors: Leyva-Díaz, Juan Carlos; **Rodriguez-Sanchez, Alejandro**; Gonzalez-Lopez, Jesus; Poyatos-Capilla, Jose Manuel
Impact Factor (ISI): 1.247
Impact Factor (SCImago): 0.429
Quartile (SCImago): Q3

10. Title: Performance and bacterial community structure of a granular autotrophic nitrogen removal bioreactor amended with high antibiotic concentrations
Journal: Chemical Engineering Journal
Year: 2017
Volume: 325

Issue:
Initial Page: 257
Final Page: 259
Authors: **Rodriguez-Sanchez, Alejandro**; Margareto, Alejandro; Robledo-Mahón, Tatiana; Elisabet Aranda Ballesteros; Díaz-Cruz, Silvia; Gonzalez-Lopez, Jesus; Barcelo, Damià; Vahala, Riku; Gonzalez-Martinez, Alejandro
Impact Factor (ISI): 6.735
Impact Factor (SCImago): 1.863
Quartile (SCImago): Q1

11. Title: 16S rRNA gene-based characterization of bacteria potentially associated with phosphate and carbonate precipitation from a granular autotrophic nitrogen removal bioreactor
Journal: Applied Microbiology and Biotechnology
Year: 2017
Volume: 101
Issue:
Initial Page: 817
Final Page: 829
Authors: Gonzalez-Martinez, Alejandro; **Rodriguez-Sanchez, Alejandro**; Rivadeneira-Ruiz, Maria Angustias; Rivadeneyra-Torres, Almudena; Martín-Ramos, Daniel; Vahala, Riku; Gonzalez-Lopez, Jesus
Impact Factor (ISI): 3.340
Impact Factor (SCImago): 1.182
Quartile (SCImago): Q1

12. Title: Impact of methionine on a partial-nitritation biofilter
Journal: Environmental Science and Pollution Research
Year: 2016
Volume: 23
Issue: 7
Initial Page: 6651
Final Page: 6660
Authors: Gonzalez-Martinez, Alejandro; **Rodriguez-Sanchez, Alejandro**; Garcia-Ruiz, Maria Jesus; Osorio-Robles, Francisco; Gonzalez-Lopez, Jesus
Impact Factor (ISI): 2.741
Impact Factor (SCImago): 0.813
Quartile (SCImago): Q2

13. Title: Detection of comammox bacteria in full-scale wastewater treatment bioreactors using tag-454-pyrosequencing
Journal: Environmental Science and Pollution Research
Year: 2016
Volume: 23
Issue: 24
Initial Page: 25501
Final Page: 25511
Authors: Gonzalez-Martinez, Alejandro; **Rodriguez-Sanchez, Alejandro**; Van Loosdrecht, Mark; Gonzalez-Lopez, Jesus; Vahala, Riku

Impact Factor (ISI): 2.741
Impact Factor (SCImago): 0.813
Quartile (SCImago): Q2

14. Title: Distribution and microbial community structure analysis of a single-stage partial nitritation/anammox granular sludge bioreactor operating at low temperature
Journal: Environmental Technology
Year: 2016
Volume: 37
Issue: 18
Initial Page: 2281
Final Page: 2291
Authors: **Rodriguez-Sanchez, Alejandro**; Purswani, Jessica; Lotti, Tommaso; Maza, Paula; Van Loosdrecht, Mark; Vahala, Riku; Gonzalez-Martinez, Alejandro
Impact Factor (ISI): 1.751
Impact Factor (SCImago): 0.528
Quartile (SCImago): Q3

15. Title: Archaeal and bacterial community dynamics and bioprocess performance of a bench-scale two-stage anaerobic digester
Journal: Applied Microbiology and Biotechnology
Year: 2016
Volume: 100
Issue: 13
Initial Page: 6013
Final Page: 6033
Authors: Gonzalez-Martinez, Alejandro; Garcia-Ruiz, Maria Jesus; **Rodriguez-Sanchez, Alejandro**; Osorio-Robles, Francisco; Gonzalez-Lopez, Jesus
Impact Factor (ISI): 3.420
Impact Factor (SCImago): 1.177
Quartile (SCImago): Q1

16. Title: Comparison of bacterial communities of conventional and A-stage activated sludge systems
Journal: Scientific Reports
Year: 2016
Volume: 6
Issue: 18786
Initial Page:
Final Page:
Authors: Gonzalez-Martinez, Alejandro; **Rodriguez-Sanchez, Alejandro**; Lotti, Tommaso; Garcia-Ruiz, Maria Jesus; Osorio-Robles, Francisco; Gonzalez-Lopez, Jesus; Van Loosdrecht, Mark
Impact Factor (ISI): 4.259
Impact Factor (SCImago): 1.625
Quartile (SCImago): Q1

17. Title: Performance and bacterial community dynamics of a CANON bioreactor acclimated from high to low operational temperatures

Journal: Chemical Engineering Journal
Year: 2016
Volume: 287
Issue:
Initial Page: 557
Final Page: 567
Authors: Gonzalez-Martinez, Alejandro; **Rodriguez-Sanchez, Alejandro**; Garcia-Ruiz, Maria Jesus; Muñoz-Palazon, Barbara; Cortés-Lorenzo, Carmen; Osorio-Robles, Francisco; Vahala, Riku
Impact Factor (ISI): 6.216
Impact Factor (SCImago): 1.745
Quartile (SCImago): Q1

18. Title: Process performance and bacterial community dynamics of partial¿nitritation biofilters subjected to different concentrations of cysteine amino acid
Journal: Biotechnology Progress
Year: 2016
Volume: 32
Issue: 5
Initial Page: 1254
Final Page: 1263
Authors: **Rodriguez-Sanchez, Alejandro**; Muñoz-Palazon, Barbara; Maza, Paula; Gonzalez-Lopez, Jesus; Vahala, Riku; Gonzalez-Martinez, Alejandro
Impact Factor (ISI): 1.986
Impact Factor (SCImago): 0.668
Quartile (SCImago): Q2

19. Title: Performance and bacterial community structure of a submerged biofilter subjected to high ammonium and high organic carbon concentrations
Journal: International Biodeterioration & Biodegradation
Year: 2016
Volume: 115
Issue: -
Initial Page: 224
Final Page: 233
Authors: **Rodriguez-Sanchez, Alejandro**; Mikola, Anna; Muñoz-Palazon, Barbara; Vahala, Riku; Gonzalez-Martinez, Alejandro
Impact Factor (ISI): 2.962
Impact Factor (SCImago): 1.033
Quartile (SCImago): Q1

20. Title: Comparison of bacterial diversity in full scale anammox bioreactors operated under different conditions
Journal: Biotechnology Progress
Year: 2015
Volume: 31
Issue: 6
Initial Page: 1464
Final Page: 1472

Authors: Gonzalez-Martinez, Alejandro; Osorio-Robles, Francisco; Morillo, Jose; **Rodriguez-Sanchez, Alejandro**; Gonzalez-Lopez, Jesus; Abbas, Ben; Van Loosdrecht, Mark
Impact Factor (ISI): 2.167
Impact Factor (SCImago): 0.736
Quartile (SCImago): Q2

21. Title: Effect of methionine amino acid over the performance process and bacterial community structure of a partial bench-scale nitritation biofilter
Journal: Amino Acids
Year: 2015
Volume: 47
Issue: 8
Initial Page: 1691
Final Page: 1691
Authors: Gonzalez-Martinez, Alejandro; **Rodriguez-Sanchez, Alejandro**; Garcia-Ruiz, Maria Jesus; Osorio-Robles, Francisco; Rivadeneira-Ruiz, Maria Angustias; Gonzalez-Lopez, Jesus
Impact Factor (ISI): 3.196
Impact Factor (SCImago): 1.362
Quartile (SCImago): Q2

22. Title: Bacterial community structure of a lab-scale anammox membrane bioreactor
Journal: Biotechnology Progress
Year: 2015
Volume: 31
Issue: 1
Initial Page: 186
Final Page: 193
Authors: Gonzalez-Martinez, Alejandro; Osorio-Robles, Francisco; **Rodriguez-Sanchez, Alejandro**; Martinez-Toledo, Maria Victoria; Gonzalez-Lopez, Jesus; Lotti, Tommaso; Van Loosdrecht, Mark
Impact Factor (ISI): 2.167
Impact Factor (SCImago): 0.736
Quartile (SCImago): Q2

23. Title: Isolation and metagenomic characterization of bacteria associated with calcium carbonate and struvite precipitation in a pure moving bed biofilm reactor-membrane bioreactor
Journal: Biofouling
Year: 2015
Volume: 31
Issue: -
Initial Page: 333
Final Page: 348
Authors: Gonzalez-Martinez, Alejandro; Leyva-Díaz, Juan Carlos; **Rodriguez-Sanchez, Alejandro**; Muñoz-Palazon, Barbara; Rivadeneyra-Torres, Almudena; Poyatos-Capilla, Jose Manuel
Impact Factor (ISI): 3
Impact Factor (SCImago): 1.219
Quartile (SCImago): Q1

24. Title: Microbial community analysis of a full-scale DEMON bioreactor

Journal: Bioprocess and Biosystems Engineering
Year: 2015
Volume: 38
Issue: -
Initial Page: 499
Final Page: 508
Authors: Gonzalez-Martinez, Alejandro; **Rodriguez-Sanchez, Alejandro**; Muñoz-Palazon, Barbara; Garcia-Ruiz, Maria Jesus; Osorio-Robles, Francisco; Van-Loosdrecth, Mark; Gonzalez-Lopez, Jesus
Impact Factor (ISI): 1.901
Impact Factor (SCImago): 0.7
Quartile (SCImago): Q2

25. Title: 454-pyrosequencing analysis of bacterial communities from autotrophic nitrogen removal bioreactors utilizing universal primers: effect of annealing temperature
Journal: BioMed Research International
Year: 2015
Volume: 2015
Issue:
Initial Page: 1
Final Page: 12
Authors: Gonzalez-Martinez, Alejandro; **Rodriguez-Sanchez, Alejandro**; Abbas, Ben; Martinez-Toledo, Maria Victoria; Van Loosdrecht, Mark; Osorio-Robles, Francisco; Gonzalez-Lopez, Jesus
Impact Factor (ISI): 2.134
Impact Factor (SCImago): 0.725
Quartile (SCImago): Q2

26. Title: The effect of influent characteristics and operational conditions over the performance and microbial community structure of partial nitritation reactors
Journal: Water
Year: 2014
Volume: 6
Issue: 7
Initial Page: 1905
Final Page: 1924
Authors: **Rodriguez-Sanchez, Alejandro**; Gonzalez-Martinez, Alejandro; Martinez-Toledo, Maria Victoria; Garcia-Ruiz, Maria Jesus; Osorio-Robles, Francisco; Gonzalez-Lopez, Jesus
Impact Factor (ISI): 1.428
Impact Factor (SCImago): 0.5
Quartile (SCImago): Q3

27. Title: Effect of ciprofloxacin antibiotic on the partial-nitritation process and bacterial community structure of a submerged biofilter
Journal: Science of the Total Environment
Year: 2014
Volume: 476-477
Issue:
Initial Page: 276
Final Page: 287

Authors: Gonzalez-Martinez, Alejandro; **Rodriguez-Sanchez, Alejandro**; Martinez-Toledo, Maria Victoria; Garcia-Ruiz, Maria Jesus; Hontoria-Garcia, Ernesto; Osorio-Robles, Francisco; Gonzalez-Lopez, Jesus
Impact Factor (ISI): 4.099
Impact Factor (SCImago): 1.658
Quartile (SCImago): Q1